12-2016

Investigating Materials that Promote New Organic Methodology and Remediation of Volatile Organic Compounds

McKenzie Louise Campbell

INVESTIGATING MATERIALS THAT PROMOTE NEW ORGANIC METHODOLOGY AND REMEDIATION OF VOLATILE ORGANIC COMPOUNDS

A Dissertation
Presented to
the Graduate School of
Clemson University

In Partial Fulfillment
of the Requirements for the Degree
Doctor of Philosophy
Chemistry

---

by
McKenzie Louise Campbell
December 2016

Accepted by:
Dr. Daniel C. Whitehead, Committee Chair
Dr. Leah Casabianca
Dr. Shiou-Jyh Hwu
Dr. Modi Wetzler

ABSTRACT

The need for environmentally safe reagents for the promotion of organic transformations is critical in order to reduce hazardous waste and byproducts associated with industrial-scale chemical processes. We have developed two practical methods that obviate the need for harsh oxidative and toxic brominating reagents in electrophilic halogenation reactions.

In our hands, a catalytic loading of the inexpensive, commercially available V_2O_5 (~$0.25/g) promotes the bromolactonization of a series of substituted alkenoic acids in isolated yields up to 97% by means of the *in situ* generation of bromenium (Br^+) from bromide (Br^-) at room temperature. This process obviates the need for molecular bromine (Br_2), known for its potent toxicity and threat to the human nervous system, instead relying on the use of less toxic bromide salts, such as ammonium bromide (NH_4Br). The oxidation of halides to halenium equivalents has previously relied on the use of harsh oxidants like lead acetate or Oxone®. The system used by our group is promoted by the mild organic oxidant, urea-hydrogen peroxide (UHP), thereby making this process more environmentally benign. The methodology can be extended to afford high yields of α-brominated β-diketones.

Our group's interest in vanadium catalysis through next turned to an investigation of polyoxometalates. Specifically, highly functional, anionic polyoxovanadates (POVs) developed in the Hwu laboratory posed a particular interest as possible catalysts for organic oxidations. A room temperature

oxidation of alcohols using reduced polyoxovanadates $Cs_5(V_{14}As_8O_{42}Cl)$ (**III**-**2**) and $Cs_{11}Na_3(V_{15}O_{36}Cl)Cl_5$ (**III**-**3**) was explored. The selective oxidation of various substituted secondary benzylic alcohols were promoted in good to quantitative yields using only 2 mol % of catalyst **III**-**2** in the presence of the terminal co-oxidant *tert*-butyl hydrogen peroxide (*t*-BuOOH). Further investigation has focused on kinetic studies of the transformation.

In a separate focus area, our group, in collaboration with the Alexis laboratory developed the preparation of nanoparticles comprised of a Poly(D,L-lactic acid)-poly(ethylene glycol)-poly(ethyleneimine) (*i.e.* PDLLA-PEG-PEI) tri-block co-polymer. These nanoparticles are capable of selectively capturing environmental contaminants of broad concern bearing aldehyde and carboxylic acid functional groups in the gas phase. These materials effected greater than 80% and 76% reduction of aldehyde and carboxylic acid vapors, respectively, with reductions of up to 98% in some cases. Further, we demonstrated the functionalization of kaolinite and montmorillonite clays with PEI on a multi-gram scale using wet impregnation preparative methods. The synthesized amino-kaolinite clay revealed significant efficiency in capturing volatile aldehydes, carboxylic acids, and sulfides with most of these assays showing 100% reduction of these vapors. Future studies will focus on similar evaluation of the remediation capabilites, with the MMT and MMT-PEI clay minerals.

DEDICATION

I dedicate this dissertation to my brothers and sisters: Creed, Carlee, McCrae, and Cayden. Having you all in my life has been the driving force for me to never give up. Just know that if I can do this, you all can change the world. I also want to dedicate this work to my parents, grandparents, and Dr. Bradley Stadelman. Without their continuous love and encouragement, achieving my goals would not have been possible. Thank you all.

ACKNOWLEDGMENTS

First and foremost, I would like to thank Dr. Daniel C. Whitehead for his guidance and support while learning and investigating exciting aspects of organic synthesis. His mentorship and encouragement has allowed me to develop as an individual thinker and chemist.

I would also like to thank Kim Ivey for her assistance on numerous TGA and FTIR characterizations. Her open door policy and expedient data collection was much appreciated and crucial in manuscript preparation. I would like to acknowledge the synthetic work that our collaborators in the Alexis and Hwu laboratories have completed in pursuit of our shared goals. Thank you all for the hard work and communication during this process.

I would especially like to thank Dr. Bradley Stadelman without whom I would not have been able to complete my degree. Your love and support have gotten me through the impossible times. To Dr. Tiffany Hayden, I would like to give special acknowledgement. Without her mentorship I would not have gone to graduate school. And lastly, I would like to give acknowledgement to my group members: Maria Swasy, Timothy Lex, Heeren Gordhan, Anthony Santilli, Beau Brummel, and Chandima Narangoda. Thank you for all the laughs and support you all have given over the last five years.

TABLE OF CONTENTS

Page

Table of Contents (Continued) **Page**

II. VANADIUM(V) OXIDE MEDIATED HALOLACTONIZATION OF ALKENOIC ACIDS

Table of Contents (Continued) **Page**

Table of Contents (Continued) **Page**

Table of Contents (Continued) **Page**

LIST OF TABLES

LIST OF FIGURES

List of Figures (Continued) **Page**

List of Figures (Continued) **Page**

List of Figures (Continued) **Page**

List of Figures (Continued) **Page**

List of Figures (Continued) **Page**

LIST OF SCHEMES

Scheme **Page**

List of Schemes (Continued) **Page**

CHAPTER ONE

A BRIEF OVERVIEW OF VANADIUM(V) OXIDE AND VANADIUM-COMPLEXES AS CATALYSTS FOR ORGANIC REACTIONS

1.1 Introduction

This chapter focuses on vanadium catalysts responsible for a large number of organic oxidation reactions. Due to the rich chemistry of vanadium and its corresponding oxides, numerous vanadium complexes have been explored.[1-3] Oxidation reactions mediated by vanadium complexes are the most broadly investigated. Reasons for this lie in vanadium's ability to easily interconvert between its different oxidation states (*i.e.* +2, +3, +4, and +5) and easily accessible higher oxidation states with the +4 and +5 states being the most stable under aerobic conditions.[3,4] The metal center also has a high affinity for oxygen and behaves as a Lewis acid.[5] All of these factors contribute to vanadium complexes being used as catalysts in redox and Lewis acid mediated oxidation reactions.[4]

Scientists first realized the unique properties of the vanadium atom from examining its various oxides.[3] Under ambient conditions the most predominate oxide is vanadium(V) oxide, *i.e.* V_2O_5 or vanadium pentoxide.[2] Research investigating the surface morphology of bulk V_2O_5 as it relates to the crystalline faces undergoing reaction has been extensively detailed by Haber *et al.* using EPR and IR spectroscopy.[2,3] When using vanadium(V) oxide as a catalyst, the

exposed crystal faces involved in the reaction possess one of two types of atoms. Exposed saturated atoms include the vanadium metal cation with non-bonding d-orbitals pointing out away from the surface leading to potential electron acceptor sites as the LUMOs (Figure 1.1).[2] There are also saturated oxygen ions that bridge the vanadium-oxygen lattice and their lone pairs perpendicular to the surface are the oxides' HOMOs acting as Lewis basic sites shown in Figure 1.1. The second type of exposed atom includes unsaturated atoms, such as the vanadyl group (V=O) (Figure 1.1), that cause a subsequent energetic potential difference along the surface. These sites either remain as

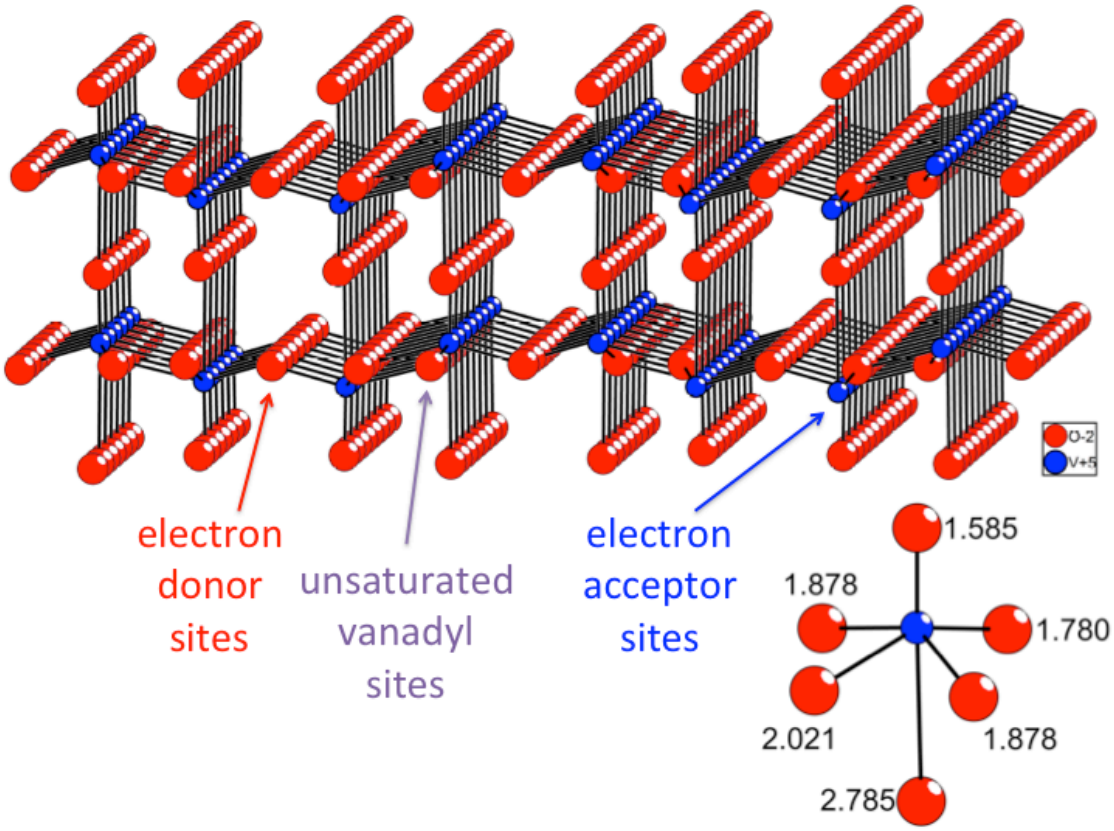

Figure 1.1. View of orthorombic vanadium pentoxide crystal lattice and oxygen coordination around vanadium atom

vanadyl or, depending on pH or aqueous environment, undergo hydroxylation to become active sites through Brønsted acid-base interactions.[2,3]

Of particular interest to researchers is the vanadyl functionality that arises in many catalytic vanadium complexes as seen in the vanadium(V) pentoxide lattice. It is generally assumed that the V=O bond plays the most critical role in catalytic oxidations due to two possible modes of activation.[6-17] First, activation can occur when molecules involved in the oxidation adsorb at these metal centers.[10,12,16,17] The second mode of activation involves the V=O unsaturated bond as an essential role for the electrical and catalytic properties of V_2O_5.[6,7,11] The increased electronic density of the oxygen atom in resonance can act as a Lewis base in proton abstraction in organic substrate oxidation.

Today, many reagents are used in conjunction with V_2O_5 to promote oxidative transformations for a variety of organic substrates. This chapter will focus on catalysts that utilize peroxovanadium complexes to facilitate the organic transformation. Oxovanadium complexes may vary based on the ligands coordinated to the metal center, but for the context of this discussion there will always be a vanadyl moiety present as an oxovanadium(IV/V) center (Figure 1.2). Peroxovanadium complexes are formed when hydrogen peroxide or alkyl

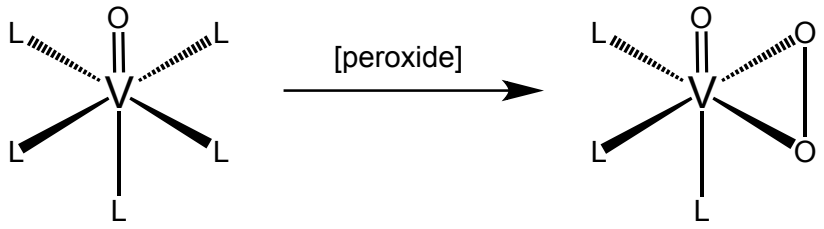

Figure 1.2. General oxidative formation of peroxovanadium complex

peroxides are used as the co-oxidant. While these derivatives also contain the vanadyl group, there is also a coordinated peroxide functionality; the generic structure for which is shown in Figure 1.2.

1.2 Oxovanadium and peroxovanadium complexes as catalysts for organic transformations

Oxovanadium complexes are broadly used in oxidation catalysis, specifically complexes featuring the higher, more stable oxidization states of +4 and +5.[5,18-20] A brief review of the use of oxovanadium complexes as catalysts in organic oxidations follows.

1.2.1 Oxidation reactions for alkanes and alkylaromatics

Oxovanadium complexes are efficient as both catalysts and catalyst precursors the promotion alkane oxidations.[4] The functionalization of alkanes, especially selective functionalization, is rare due to the relative inertness of saturated C-H bonds. Featured in this chapter are oxidation reactions including peroxidative oxygenations to produce alcohols, aldehydes and ketones. Additionally, carboxylation to form carboxylic acids and halogenation to give organohalides will be the final two organic transformations highlighted here.[4]

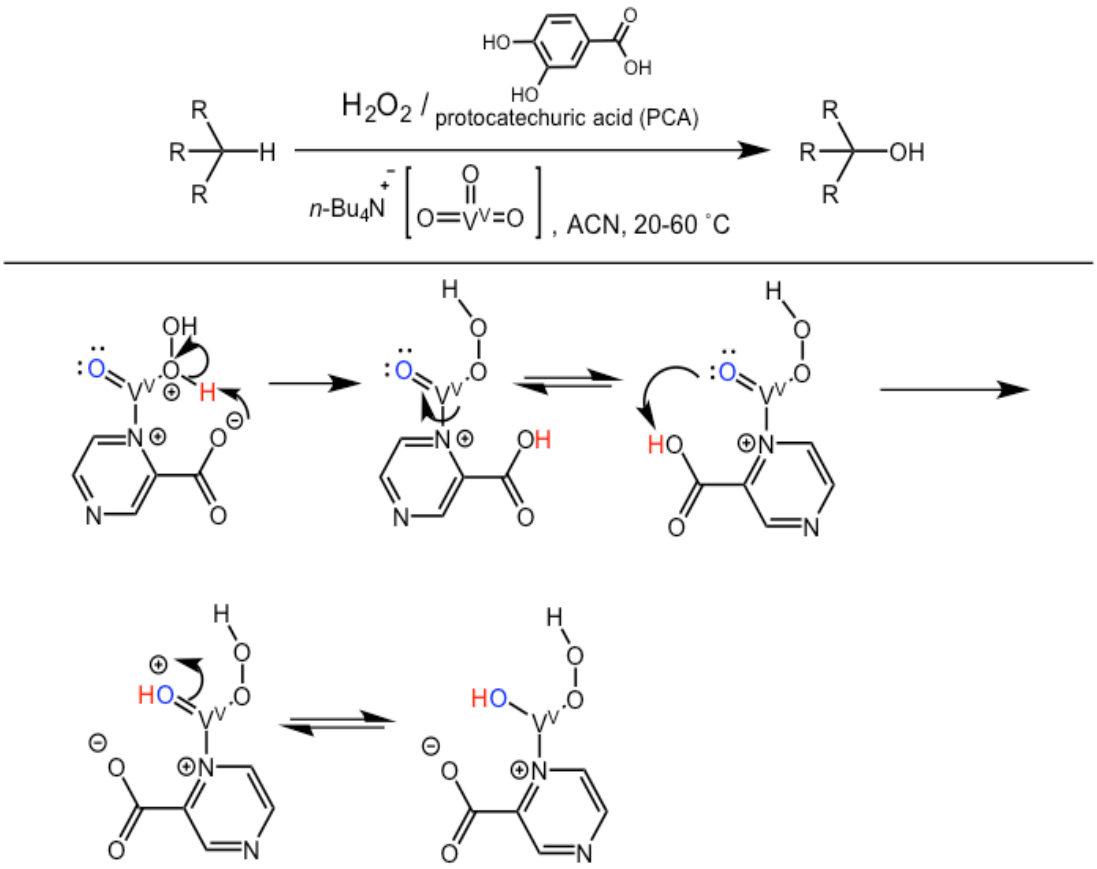

Figure 1.3. PCA promoted proton migration from coordinated H_2O_2 through "robot arm" mechanism

The vanadate salt (*n*-Bu_4N)[VO_3] in the presence of an acid co-catalyst (*e.g.*, 2-pyrazinecarboxylic acid (PCA), nitric, sulfuric, or oxalic acid) facilitates the oxidation of alkanes, arenes, and alcohols with hydrogen peroxide (H_2O_2) in acetonitrile at 20-60 ˚C (Figure 1.3).[21] Extension of this methodology to both liquid and gaseous alkane oxidations proved effective with PCA as the acid co-catalyst in the presence of vanadium compounds.[22-26] Using PCA as the promoter has a pronounced efficiency for alkane oxidation as compared to the other acids investigated due to accelerated proton transfer with the PCA moiety

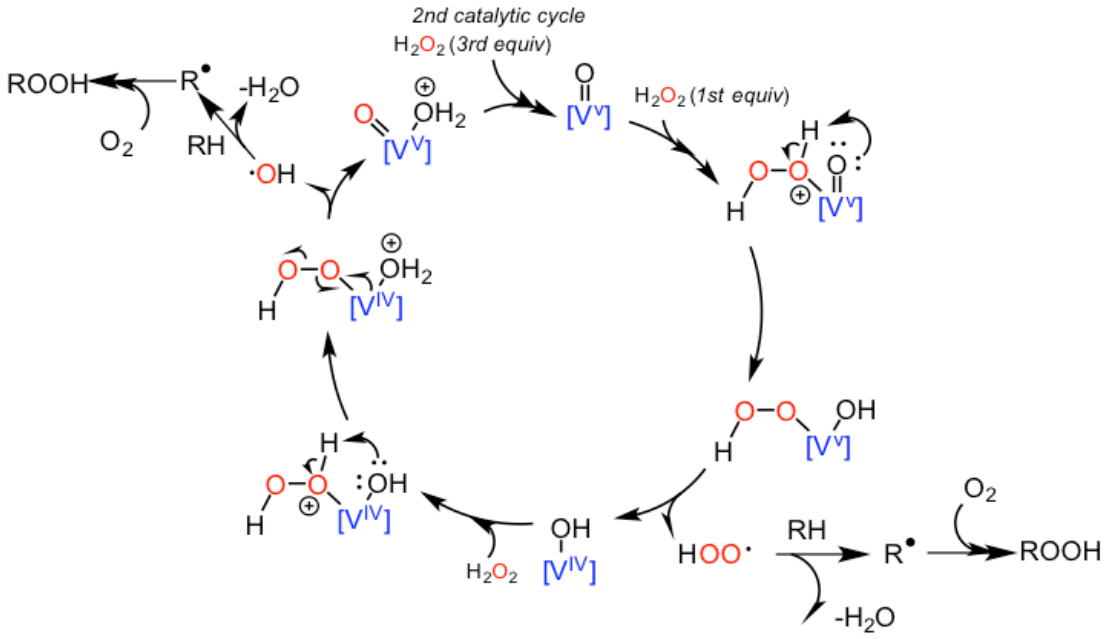

Figure 1.4. Proposed catalytic cycle for vanadium(V) catalyzed hydroxyl radical generation

facilitating proton migration from a coordinated hydrogen peroxide molecule to the vanadyl oxygen, which is proposed to proceed via a 7-membered transition state.[27-31] Through kinetic studies and DFT investigations as well as selectivity studies, Pombeiro and Shul'pin propose a radical mechanism that proceeds by the formation of hydroxyl and peroxide radicals (HO• and HOO•) through hydroperoxy-vanadium complexes (Figure 1.4). These radicals then abstract hydrogen atoms from the alkane (RH) to form an alkyl radical (R•).[21,26-34] Excess concentrations of the reactive HO• and HOO• reagents then undergo radical coupling to alkyl radicals to give the oxidized organic product.[35,36]

Briefly, Figure 1.5 shows a series of complexes (**I-1 to I-7**) that catalyze carboxylation of methane and ethane to yield acetic acid and propanoic acid,

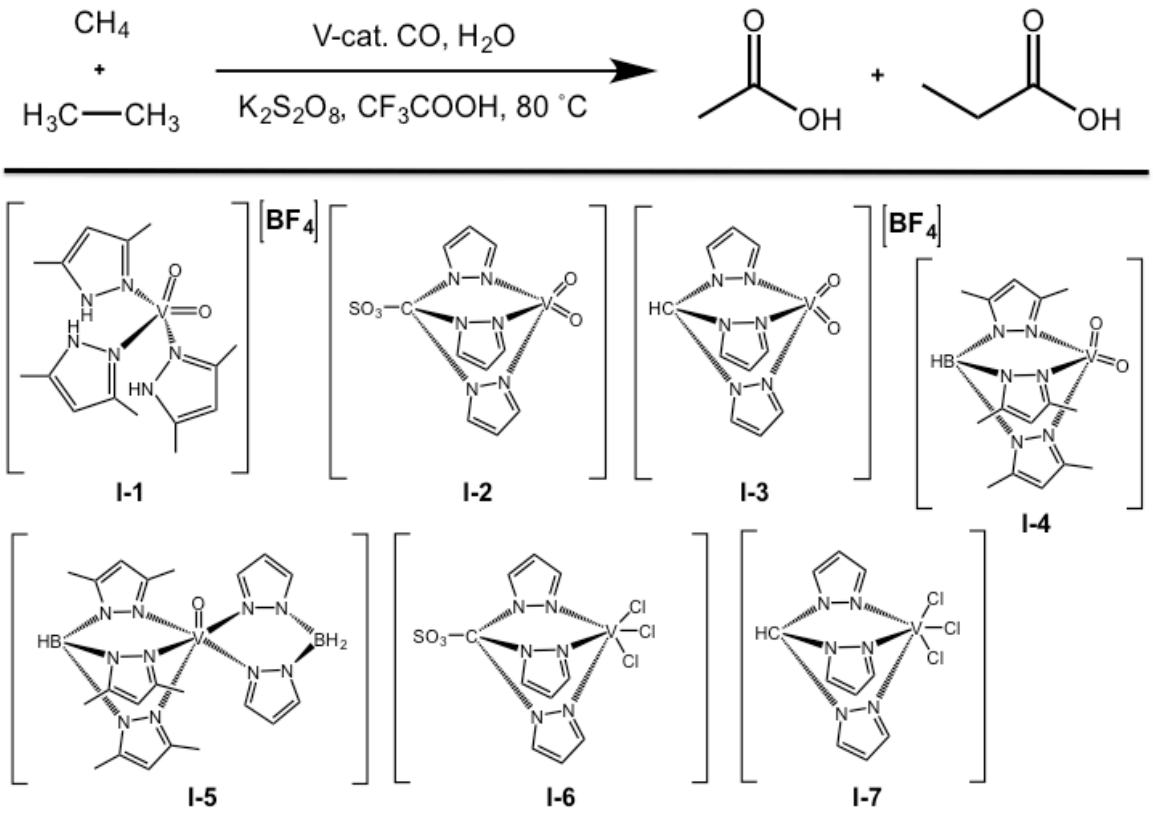

Figure 1.5. Carboxylation of methane to acetic acid and ethane to propanoic acid using oxovanadium complexes **I-1** through **I-7**

respectively. Optimal conditions were established in the presence of carbon monoxide, peroxodisulfate as a co-oxidant, and concentrated TFA at 80 ˚C.

Catalytic loadings of hydroxyquinoline derivatives of oxovanadium(IV) complexes (Scheme 1.1, catalysts **I-8** to **I-11**) promote the oxidation of ethylbenzene using molecular oxygen as the oxidant in benzonitrile solvent with N-hydroxyphthalimide (NHPI) as the co-catalyst at 90 ˚C.[37] The major products recovered include acetophenone, 1-phenylethanol and 1-phenylethane with the established reaction conditions returning 69% conversion of the starting material with 97% selectivity for acetophenone.

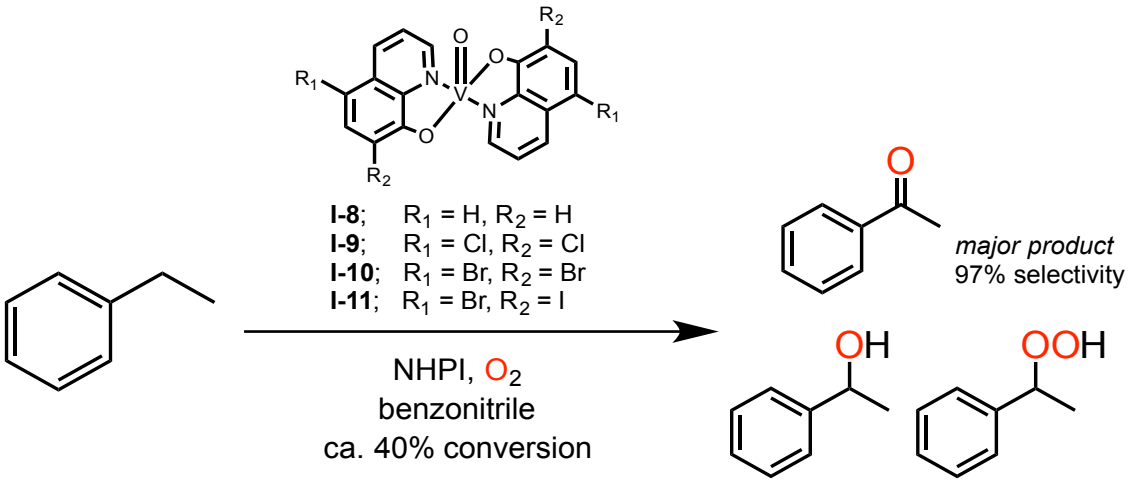

Scheme 1.1. Oxidation of ethylbenzene using vanadium complexes **I-8** through **I-11**

1.2.2 Alcohol oxidations

One of the most important organic transformations is the oxidation of alcohols. Catalytic transformations employing vanadium complexes in the presence of molecular oxygen or air as the terminal oxidant represent an attractive class of environmentally benign transformations for the synthesis of these compounds even at industrial scales.[38,39]

Initially, peroxovanadium(V) complexes were investigated for the catalytic oxidations of ethanol and 2-propanol.[40,41] Reactive alkoxo oxomonoperoxo species (Figure 1.6) can be generated *in situ* from H_2O_2, and in turn promote radical mediated catalytic oxidations of alcohols. For the oxidation of 2-propanol, a linear increase in acetone production was observed with an increasing concentration of hydrogen peroxide equivalency.[40,41]

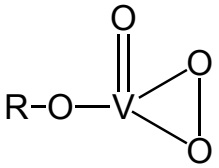

Figure 1.6. Alkoxo oxomonoperoxo species

Along with ethanol and 2-propanol, cyclohexanol and benzyl alcohol were also oxidized in the presence of catalytic Bu_4NVO_3 in the presence of a pyrazine 2-carboxylic acid co-catalyst and hydrogen peroxide acting as the terminal oxidant.[42] The reaction was carried out at 50 ˚C with the starting alcohols serving as the solvent and the reactive intermediate being a monoperoxovanadium(V) complex that features one pyrazine 2-carboxylic acid anion as previously discussed in the oxidation of alkanes (*cf.* Figure 1.3).

1.2.2.1 Oxidation of primary and secondary alcohols

Over the years, researchers have focused on improving the selectivity and understanding mechanistic implications of the oxidation of alcohols mediated by vanadium species. Oxovanadium(IV or V), or a mixed-valent complex, can facilitate catalytic the oxidation of both primary and secondary alcohols shown in Scheme 1.2.[42-44]

Vanadium complexes utilizing bypyridyl and phenanthryl ligands shown in Figure 1.7 are all catalysts formed from $VOSO_4$ as the metal containing catalytic

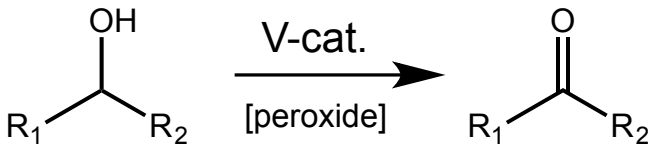

R_1 = alkyl, aryl

R_2 = H, aryl

Scheme 1.2. General representation of primary and secondary alcohol oxidations using vanadium catalysts

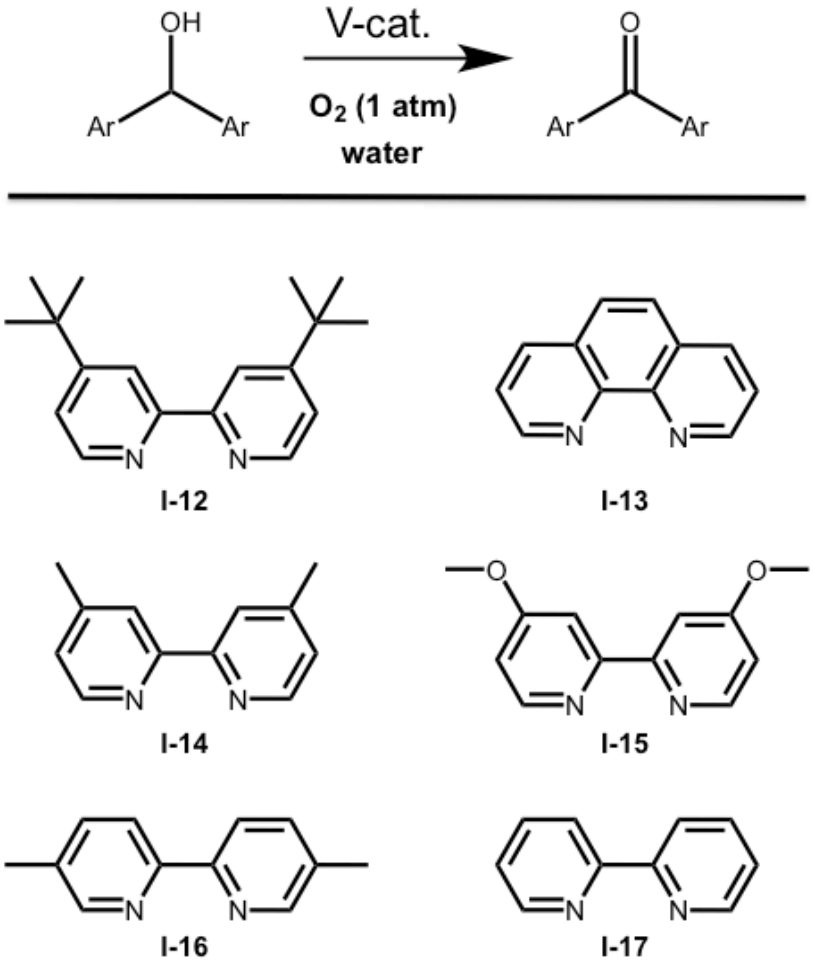

Figure 1.7. Bipyridyl ligands screened for oxovanadium(IV) complexes in the oxidation of activated secondary alcohols at 90 ˚C

precursor. These catalysts are known to promote the oxidation of benzhydrols to benzophenones in good yields in aqueous solution at near reflux under atmospheric O_2.[43] Regardless of the electron-donating or electron-withdrawing character of the benzhydrol substituent (**I-12** – **I-17**), successful oxidation using catalytic amounts of $VOSO_4$ and 4,4-di-*tert*-butyl-2,2,-bipyridyl (4,4-*t*Bubpy) as the ligand was realized, and proved to be the most successful catalytic combination investigated. Unfortunately, the complex was not amenable for the

oxidation of 1-phenylethanol, as only trace amounts of acetophenone were observed. [43]

Vanadium(V) complexes **I-18** through **I-24** with 8-hydroxyquinolinato ligands (formula $[(HQ)_2V(O)(OR)]$*i*Pr) promote the oxidation of benzylic, allylic, and propargylic alcohols using molecular oxygen as the terminal co-oxidant (Figure 1.8).[39,44] Extension of the process to the aerobic oxidation of 4-methoxybenzyl alcohol to its corresponding benzaldehyde proceeded similarly with only 2 mol% of the catalyst **I-18** (Figure 1.9).[44] An elevated reaction temperature of 60 ˚C was required for the 24 h reaction period; however, the transformation is compatible with a number of solvents including: tetrahydrofuran (THF), ethyl acetate (EtOAc), acetonitrile (ACN), 1,2-dichloroethane, 1,2-dichlorobenzene, and 2-methyltetrahydrofuran returning products in uniformly excellent yields of >99%. In doing a thorough substrate evaluation using 1,2-dichloroethane as the solvent and triethylamine (Et_3N) as an additive, excellent yields of 90 to 96% were isolated for the oxidation of a variety of benzylic

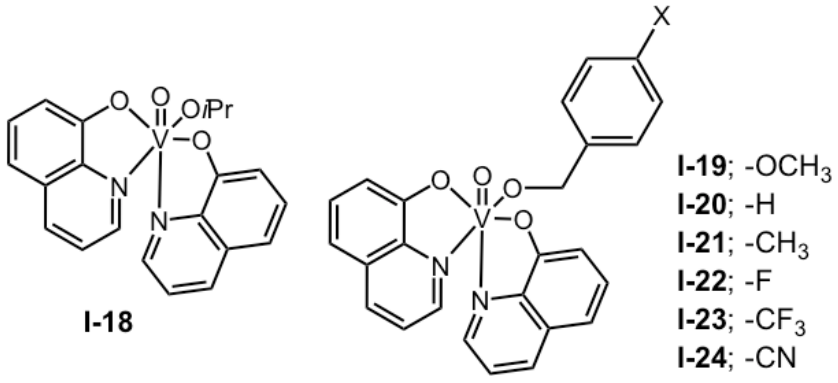

Figure 1.8. Vanadium(V) complexes using 8-hydroxoquinolinato (HQ) ligands

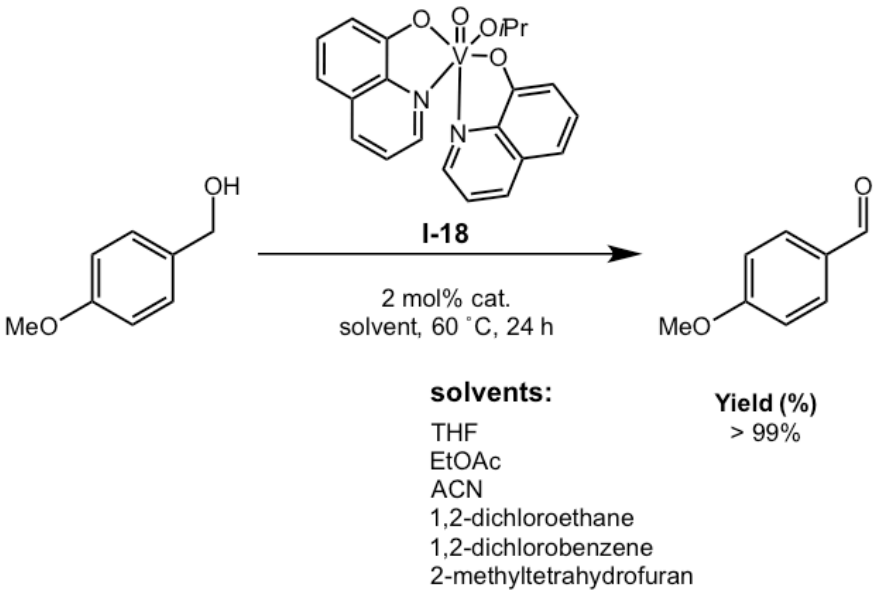

Figure 1.9. Vanadium catalyzed oxidation of 4-methoxybenzyl alcohol

alcohols to their corresponding aldehydes and ketones.[44] Cinnamyl alcohol, 3-methyl-2-cyclohexen-1-ol, 5-hydroxymethylfurfural, and 2-hydroxymethylpyridine returned the corresponding aldehyde or ketone products in excellent yields (94–98%). The secondary propargylic alcohol, 4-phenyl-3-butyn-2-ol, was also oxidized in high yield (96%). The primary propargylic alcohols, 3-phenyl-2-propyn-1-ol and 2-decyn-1-ol, were oxidized to their corresponding aldehydes in good yields of 80% and 60%, respectively. Unfortunately, steric bulk retarded the reaction with α-isopropyl- and α-*tert*-butyl benzyl alcohols returning 20% and 0% yields. The terminal alkyne, 1-phenyl-2-propyn-1-ol, underwent non-selective oxidation, whereby only 38% of the desired ketone product was recovered.[44] Finally, primary and secondary aliphatic alcohols were unreactive under the optimized conditions.

The cheap and efficient catalyst, vanadium pentoxide (V_2O_5), promotes the oxidation of 1˚ alcohols to their carboxylic acids, and 2˚ alcohols to ketones in a dilute aqueous *tert*-butyl hydrogen peroxide (*t*BuOOH) solution.[45] As with the previous vanadium catalysts in the presence of peroxide, the reactive intermediate responsible for the oxidation is either a mono or diperoxovanadium(V) complex. The determination of which complex will under go reaction depends on the concentration of *t*BuOOH in solution. Specifically, the more peroxide, the higher concentration for the diperoxovanadium(V) complex. Benzyl alcohol and benzylic alcohols containing electron-donating substituents, such as *p*-methoxybenzyl alcohol, 3,4-dimethoxybenzyl alcohol, and *p*-methylbenzyl alcohol are oxidized to their corresponding acids in high yields of 95%, 99%, 98%, and 74%, respectively.[45] The co-oxidant *t*BuOOH is also used in the vanadium-catalyzed oxidation in which secondary alcohols are converted to ketones in benzene at 80 ˚C (Scheme 1.3).[44] The $VO(acac)_2$ catalyst successfully promoted the formation of ketone products in upwards of 96% yield, while primary alcohols returned their corresponding aldehydes in poor yields.

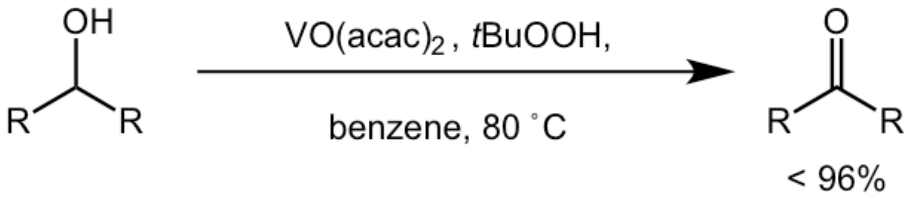

Scheme 1.3. Secondary alcohol oxidation using $VO(acac)_2$ as the catalyst

1.2.2.2 Oxidation of α-hydroxy ketones

The complexes shown in Figure 1.10A (*i.e.* **I-25** to **I-36**) are made from the combination of vanadyl sulfate and 3,5-disubstituted-*N*-salicylidene-1-*tert*-butylglycines to form chiral oxovanadium(V) methoxides. In the presence of air-saturated methanol, these compounds proved to be efficient enantioselective catalysts for the kinetic resolution of racemic α-hydroxyketones by means of aerobic oxidation in toluene or *tert*-butyl methyl ether (TBME) solvents (Figure 1.10B).[46]

The selective oxidation of benzoin to benzil proved difficult for

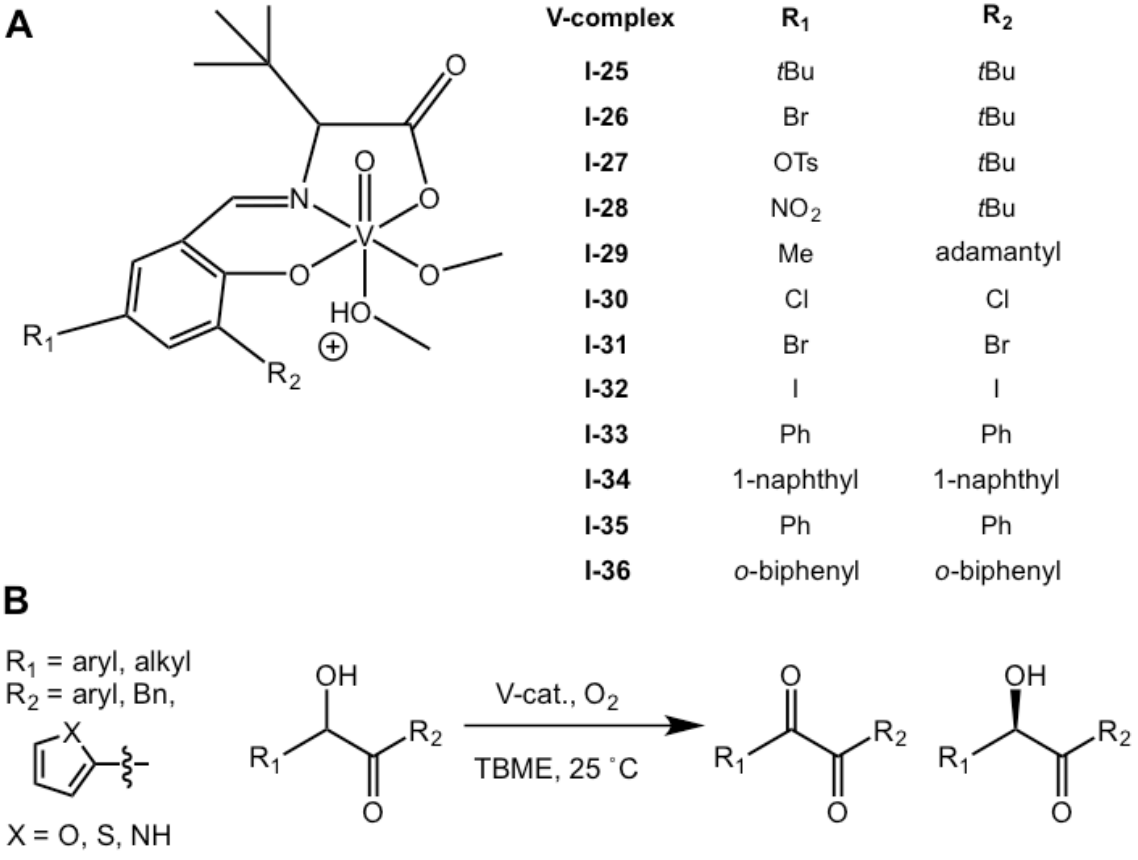

V-complex	R_1	R_2
I-25	*t*Bu	*t*Bu
I-26	Br	*t*Bu
I-27	OTs	*t*Bu
I-28	NO_2	*t*Bu
I-29	Me	adamantyl
I-30	Cl	Cl
I-31	Br	Br
I-32	I	I
I-33	Ph	Ph
I-34	1-naphthyl	1-naphthyl
I-35	Ph	Ph
I-36	*o*-biphenyl	*o*-biphenyl

Figure 1.10. Variations for vanadium complexes as catalysts for asymmetric aerobic oxidation

conventional oxidizing methods with major isolates being benzaldehyde and/or benzoic acid and lesser amount of benzil.[47] Using a series of oxovanadium(IV) Schiff base complexes with H_2O_2 as the co-oxidant in acetonitrile solvent, the fully selective oxidation (*ca.* 100%) with a greater than 99% conversion to benzil after only 2 h was realized using catalyst **I-40** (Figure 1.11). [47]

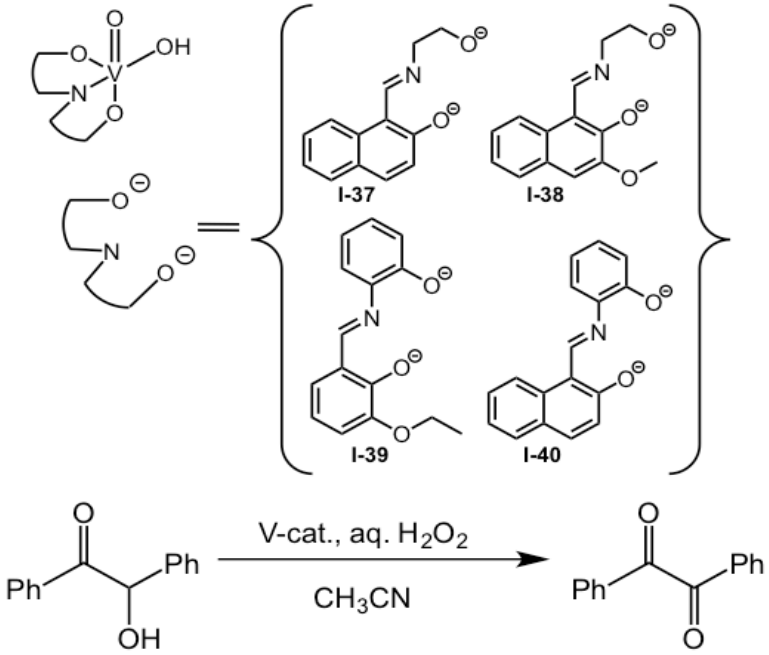

Figure 1.11. Vanadium complexes **I-37** through **I-40** catalyze the oxidation of benzil to benzoin

1.2.3 Oxidative cleavage of styrenes

The oxidative cleavage of styrene and several derivatives to their corresponding benzaldehydes is known using catalytic vanadyl acetate ($VO(OAc)_2$). The reaction is conducted in the presence of acetic acid and aqueous H_2O_2 at 70 ˚C (Scheme 1.4).[48,49] While some substituent effects are

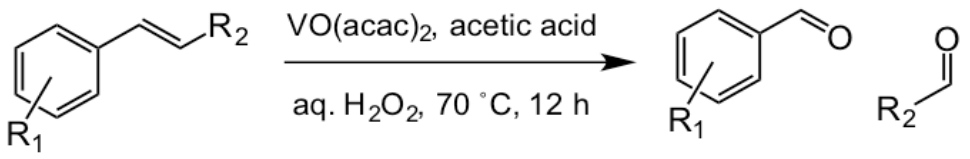

Scheme 1.4. Vanadium catalyzed oxidation of styrene derivatives to their corresponding benzaldehyde

evident, substituted styrenes were oxidized in good to excellent yields of 85 to 95%. Stilbene was not as effective a substrate, returning a maxiumum of 58% yield of the desired product. The responsible reactive intermediate in facilitating oxidation is the monoperoxovanadium with acetate molecules coordinated to the vanadium center. [48,49]

1.2.4 Epoxidation of alkenes

Epoxidation of alkenes using vanadium complexes has been known for some time.[50-52] The activated vanadium complex that mediates these tranformations is understood to be a peroxovanadium species, but the overall mechanism for the epoxidation event, regardless of the initial co-oxidant employed (*t*BuOOH or H_2O_2), remains unclear.[20] Several reviews and a large number of articles are dedicated to the discussion of the mechanistic nuances relevant to the vanadium promoted epoxidation of alkenes.[20,53-56] Selectivity for epoxide formation using aqueous solutions of *t*BuOOH in dioxane or dioxane-ethanol solvent systemes returned better results than those reactions employing H_2O_2 as the co-oxidant.[57-59] When subjecting cyclohexene to the reaction system with *t*BuOOH as the co-oxidant, the epoxide was recovered in quantitative yield. In comparison, reactions using H_2O_2 resulted in a mixture of allylic oxidation

products and the desired epoxide.[58,59] Evidence from these experimental observations indicates a reduced selectivity for epoxide formation when using H_2O_2, yet researchers agree that a peroxovanadium reactive intermediate is common regardless of the nature of the terminal co-oxidant. Therefore, it is clear that nuances of the mechanism for the oxidation must account for the divergence in experimental outcomes.

The epoxidation of cylcooctene is facilitated by several vanadium complexes using either H_2O_2 or *t*BuOOH as the terminal co-oxidant at elevated reaction temperatures.[55-57,60] First, the tridentate Schiff base salicylideneaminophenol ($SAPH_2$) forms an oxo-bridged dinuclear oxovanadium(V) complex, $[VO(SAP)]_2O$ (**I-41**) that promotes the epoxidation of cyclooctene in the presence of aqueous *t*BuOOH without added solvent at 80 ˚C (Figure 1.12).[61] The selectivity for epoxide formation was 83% with a 94%

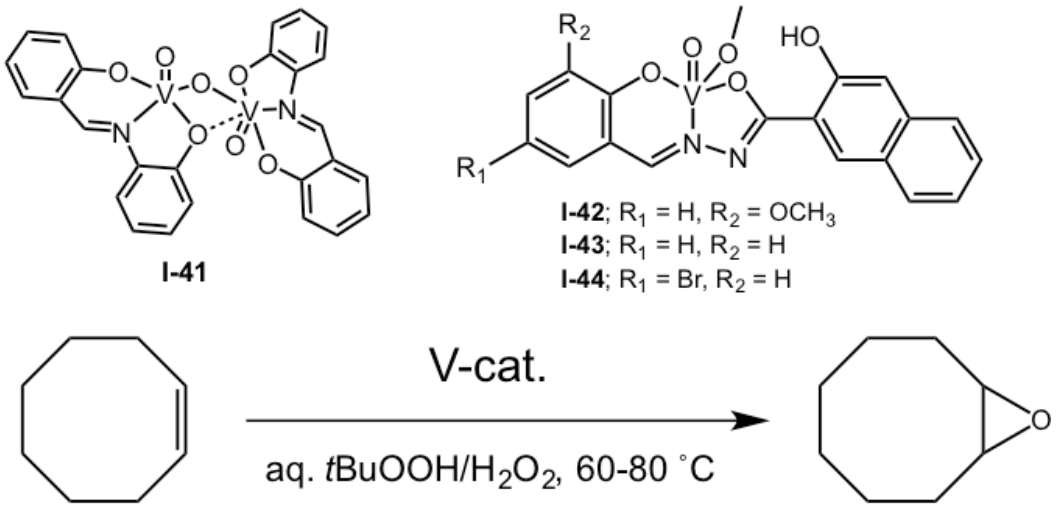

Figure 1.12. Vanadium catalyzed epoxidation of cylcooctene using benign H_2O_2 or *t*BuOOH co-oxidants

conversion of cyclooctene after only 5.5 h. Additionally, the use of tridentate Schiff base ligands in a series of three oxovanadium(V) complexes with the structures [VO(OMe)L^1] (**I-42**), [VO(OMe)L^2] (**I-43**), and [VO(OMe)L^3] (**I-44**) catalyzed the epoxidation of cyclooctene using H_2O_2 as the oxidant at 60 ˚C for 5 h in 100% selectivity.

Other olefins including cyclohexene, norbornene, and α-methylstyrene were also oxidized with conversions greater than 90% using catalyst **I-44** in acetonitrile with H_2O_2 as the oxidant.[62] As with the previous catalytic system, the selectivity for epoxide formation was 100% when cyclooctene was used as the substrate. The oxidation of cyclohexene gave a minimal 29% of the cyclohexene oxide, with the major product being 55% 2-cyclohexenol along with an 8% yield of 2-cyclohexenone.[62]

1.2.5 Epoxidation of allylic alcohols

Figure 1.13 shows the oxovanadium(IV) pyrone complexes responsible for the epoxidation of geraniol under ambient conditions in dichloromethane (DCM) with *t*BuOOH as the oxidant (**I-45** – **I-54**).[63] Geraniol conversion using these catalysts was quantitative with high selectivity for the 2,3-epoxygeraniol product in yields greater than 86%. The reactivity of these oxovanadium(IV) pyrone complexes is comparable to that of the established oxovanadium(IV) acetylacetonate (*i.e.* [VO(acac)$_2$] (**I-55**)) protocol.[63-65]

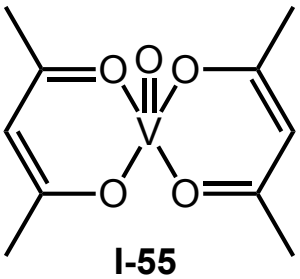

I-55

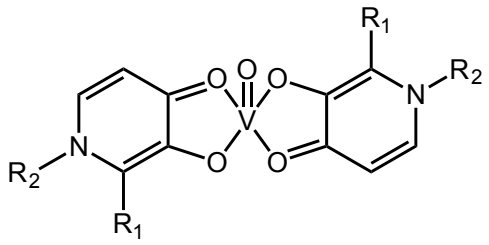

V-complex	R_1	R_2
I-45	Me	H
I-46	Et	H
I-47	Me	Me
I-48	Me	Et
I-49	Et	Me
I-50	Et	Et
I-51	Et	EtOH
I-52	Me	Ph
I-53	Et	Ph
I-54	Me	Ph-$(CH_2)_2CH_3$

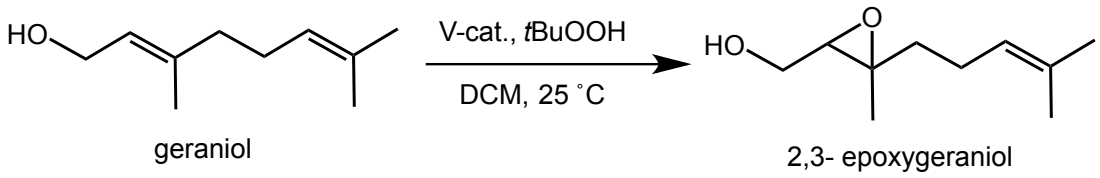

geraniol

2,3- epoxygeraniol

Figure 1.13. Epoxidation of geraniol using vanadium pyrone complexes

While the acetylacetate ligands are better catalysts than the pyrones, the significance of a ligand effect was observed with acetylacetonate having the best catalytic activity and pyrone followed by pyridinone respectively following in efficiency.[65]

Initial electrophilic oxidation methods for the epoxidation of allylic alcohols utilized strongly electrophilic organic peracids due to the decreased nucleophilic character of the double bond of the allylic alcohol substrate.[5,66] It was List and Kuhnen in 1967,[67] Sheng and Zajacek in 1970,[68] and most notably Sharpless and Michaelson in 1973 who established oxovanadium$(acac)_2$ complexes as the catalyst of choice for the epoxidation for allylic alcohols in the presence of *t*BuOOH in non-polar solvents such as toluene or dichloroethane.[69-71] Yields do vary depending on the electronic nature of the starting allylic alcohol; however,

the yields are usually high.[65,72-75] While the mechanism for peroxide assisted oxidation of the $VO(acac)_2$ to the V(V) oxo derivative is a one-electron process in which the acetylacetonato ligand is removed from the metal center to accommodate the bidentate alkylperoxide coordination to the vanadium, no radical propagation or decomposition of the *t*BuOOH oxidant is observed.[73,74] After the allylic alcohol is introduced, an alkoxo-alkylperoxovanadium complex facilitates the intramolecular oxygen transfer, thus forming the epoxide product in good yields.[65,76]

The ability to selectively oxidize allylic alcohols to optically active expoxyalcohols was realized using chiral ligands complexed to vanadium.[69-71] An efficient synthesis of florfenicol (*i.e.* 37%) was achieved in 91% enantiomeric excess (*ee*) using the bis(hydroxamate) complexes **I-56** – **I-58** (Figure 1.14).[77,78]

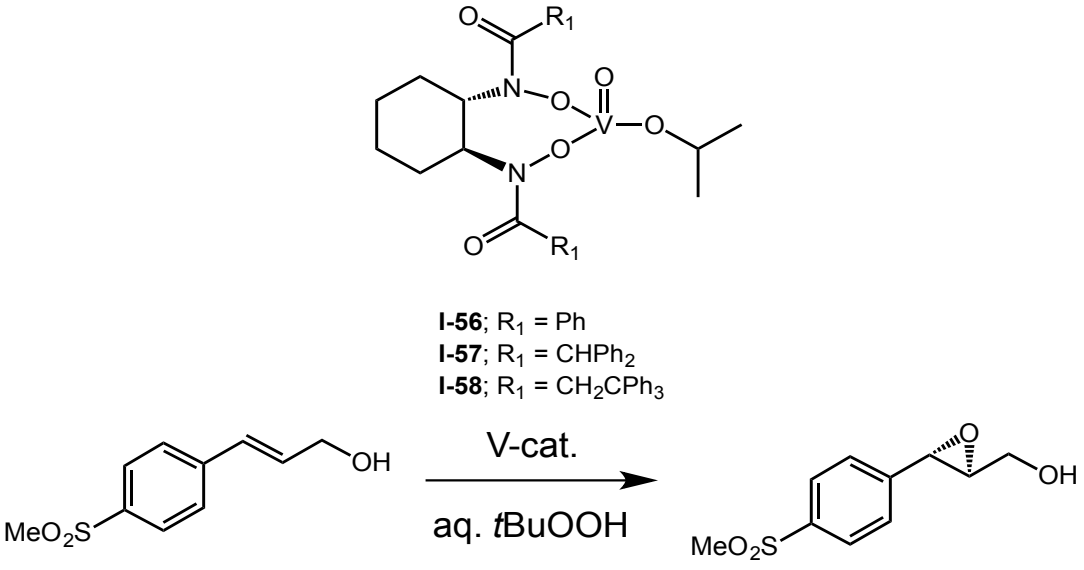

Figure 1.14. Vanadium-catalyzed asymmetric epoxidation

These complexes are used in conjunction with the commercial 4-methylthiobenzaldehyde to facilitate a crucial enantioselective step in the total synthesis of the natural product.[77,78]

1.2.6 Sulfoxidation

The synthesis of chiral sulfoxides is a significant endeavor owing to the rich chemistry associated with this class of chiral organosulfur compounds. These molecules are known for their important biological activities, including antimicrobial properties,[79] inhibition of the biosynthesis for uracid,[80] and regulation of stomach acids and cholesterol catabolism.[81-84] While there are chemical and biological processes for synthesizing chiral sulfoxides, it is the metal-catalyzed enantioselective oxidation of prochiral sulfides that remains the most efficient and economical route for the generation of optically pure sulfoxides.[85]

Examples of asymmetric vanadium-catalyzed oxidations of sulfides have been reported. Some of the first disclosures utilize an excess of optically active alcohols (*e.g.* (-)-2-octanol, (-)-menthol, (-)-borneol) as chiral ligands in the presence of $VO(acac)_2$ and *t*BuOOH in a 12% benzene/toluene solvent solution. The resulting chiral peroxo complex then promotes catalytic oxidization of both methylphenyl and methyl-*p*-tolylsulfide substrates.[86,87] While the enantioselectivity of the early protocols were low (<10% *ee*), these initial results

suggested that the optically active alcohols were acting as chiral ligands and not just chiral solvating agents.

Significantly higher enantioselectivities were realized using chiral Schiff base ligands **I-59**,[88,89] **I-60**,[88,89] **I-61,**[90-92] and **I-62** along with $VO(acac)_2$ as the precatalyst (Figure 1.15).[93] These complexes are formed *in situ* by first mixing the vanadium precatalyst, the chiral ligand, and thioanisole (**I-63**) at room temperature in dichloromethane (DCM). Hydrogen peroxide is then added dropwise to afford moderate to good yields of the chiral sulfoxide (**I-64**) with enantioselectivities ranging from 50 to 85% *ee*. The best enantioselectivity was achieved using $VO(acac)_2$, chiral ligand **I-62**, and H_2O_2 in a 1:1.5:110 ratio (Figure 1.15).[93]

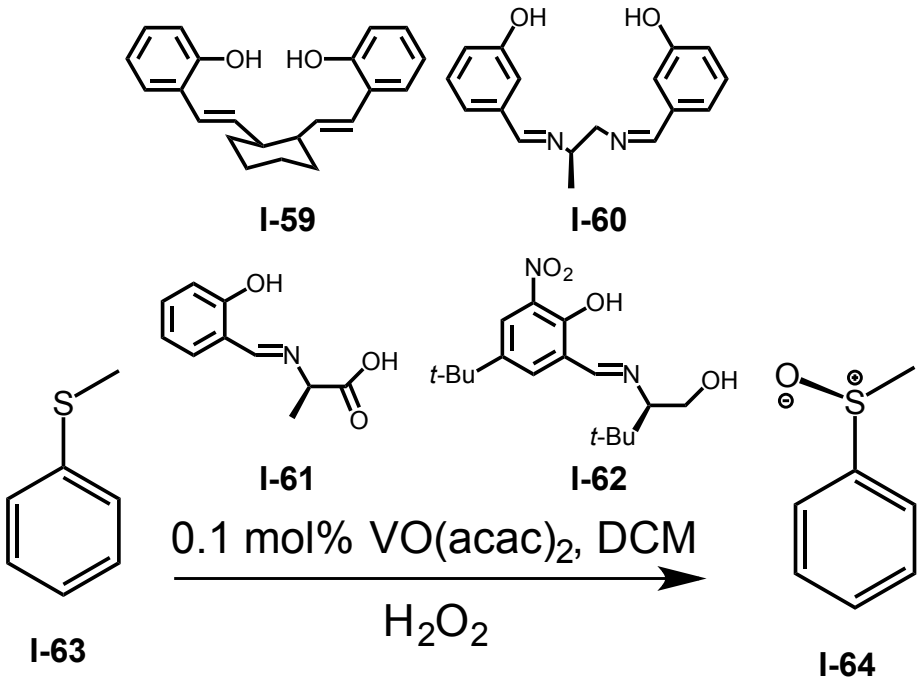

Figure 1.15. Catalytic enantioselective oxidation of sulfide **I-63**

1.3 Polyoxometalates as catalysts for organic transformations

As highlighted in the previous sections, numerous catalytic oxidations can be promoted by vanadium complexes as catalysts. Indeed, the selection of reactions described above are merely a sampling of reports in literature, and by no means exhaustive. More recently, polyoxometalates (POMs) have emerged as an interesting class of macromolecules. Over the last thirty years these complexes have developed into a thriving avenue for catalytic oxidation reactions.[94-98] While the most commonly synthesized POMs include polyoxomolybdates, tungstates and hetero-transition metal frameworks,[99-108] POMs having exclusively vanadium-substituted scaffolds are relatively under-explored.

Polyoxometalates have been known since the early 1800s.[109] But with the development of X-ray crystallographic techniques during the early 1900s, interest surrounding the structures of POMs and their possible applications encouraged new investigations on the topic. POMs consist of a polyatomic anion featuring early transition metal (*e.g.* Mo, W, V, Nb, Ta) oxyanions linked together through shared oxygen atoms to assemble 3-dimensional (3D) anionic frameworks. Tungsten (W) and molybdenum (Mo) metals predominately form Keggin ions as 3D conformations and commonly incorporate atoms such as phosphorous (P) or silicon (Si) into the center of the framework forming heteroatom-POM anion clusters which helps stabilize the overall molecule (Figure 1.16A).[110]

Vanadium substitution into polyoxomolybdates and tungstates is known and the element is considered one of the most intriguing early transition metals to use in that its biological presence could result in medicinal therapeutic applications.[111] Commonly, vanadium-substituted POMs (V-POMs) are generated by doping polyoxomolybdates or tungstates with vanadium in order to exploit increased catalytic efficiency for oxidative organic reactions. Vanadium substitution into the framework of these POMs typically results in vanadium centers with a distorted square bipyramidal or octahedral geometry. For other POMs, the geometry of the metal centers for the resulting POM cluster depends on the type and number of atoms distributed throughout the framework. Keggin and Wells-Dawson structures usually consisting of P, Si and As hetero-atoms exhibit a four coordinate tetrahedral geometry (Figure 1.16A and 1.16B). In comparison, substituting Al or Te as the heteroatoms results in a 6-coordinate

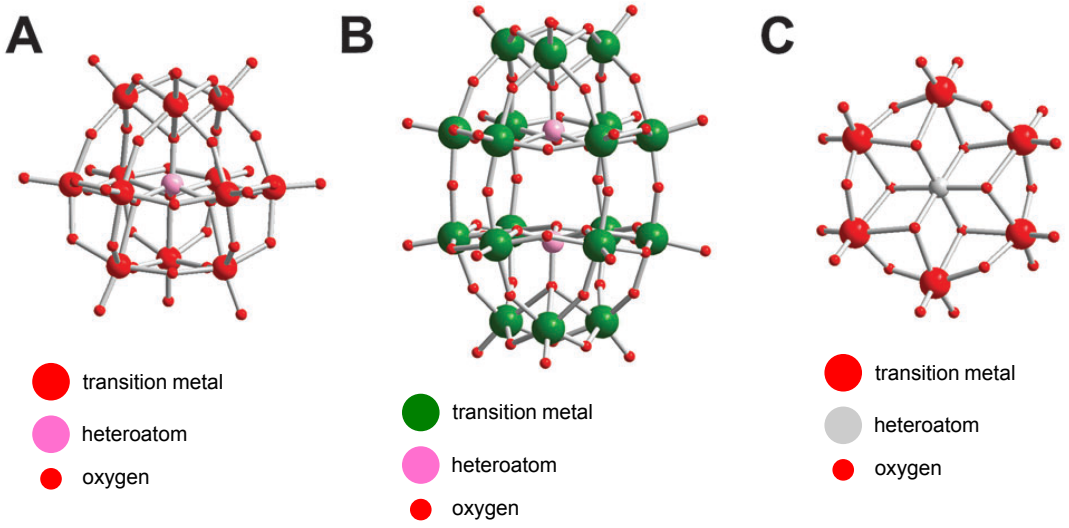

Figure 1.16. Structures for A) Keggin B) Wells-Dawson and C) Anderson type polyoxometalates

octahedral system referred to as an Anderson structure (Figure 1.16C). The heteroatom may also reside within the center of the 3D anionic sphere, as with Keggin and Dawson structures.

Traditional oxidative processes usually engage strong oxidants such as nitric acid (HNO_3) and hypochlorous acid (HClO) which produce large amounts of wastes.[112-114] POMs have been investigated as catalysts for a number of organic oxidations due to their notable redox properties, strong persistence against oxidants, and environmental compatibility. The combination of POM catalysts and environmentally conscious oxidants has been exploited in order to oxygenate carbons in alkenes, aromatic rings, and even inert alkanes. Over the last thirty years the catalytic application of POMs has been well investigated.[94-98] In this chapter, the discussion will be restricted to transformations promoted by POMs containing vanadium (V-POMs).

1.3.1 Oxidation of alkanes

Selective oxidation of alkanes to provide alcohols or alkenes affords an attractive route for the utilization of abundant alkanes as a chemical feedstock.[115] Although intensive efforts have been made in this field, the selective oxidation of C1−C4 alkanes still remains a challenge, except for the conversion of *n*-butane to maleic anhydride.[116-120] The main reason for this lies in the high activation energy required to promote alkane oxidation, and generally requires relatively harsh conditions due to the inertia of the C−H bond. Such conditions often suffer from

over oxidation of the target products.[121,122] Consequently, a high degree selectivity for generation of desired products at reasonably high conversions is often unattainable under these conditions. Therefore, developing catalysts that efficiently promote oxidation under mild conditions is a large area of interest in the synthetic community. In view of the remarkable redox properties of POM catalysts and their general stability, they have received considerable attention as potential alternatives to conventional redox methods.[117]

The V-substituted heteropolyacid (HPA) catalysts $H_4VPMo_{11}O_{40}$ (**I-65**), $H_5V_2PMo_{10}O_{40}$ (**I-66**), and $H_6V_3PMo_9O_{40}$ (**I-67**) are effective promoters of the oxidation of adamantane with 1 atm of O_2 as the sole oxidant (Scheme 1.5).[123] V atoms release from the surface framework in the form of monomeric vanadium species $V^{V}O^{2+}$ and $V^{IV}O^{2+}$ during the reaction.[123] The free vanadium species initially abstracts a hydrogen from adamantane to form an adamantyl radical and reduced vanadium species.[123] The adamantyl radical then initiates successive formation of more adamantly radical and hydroperoxide species to propagate oxidation. Poor selectivity of product formation was observed as shown by the

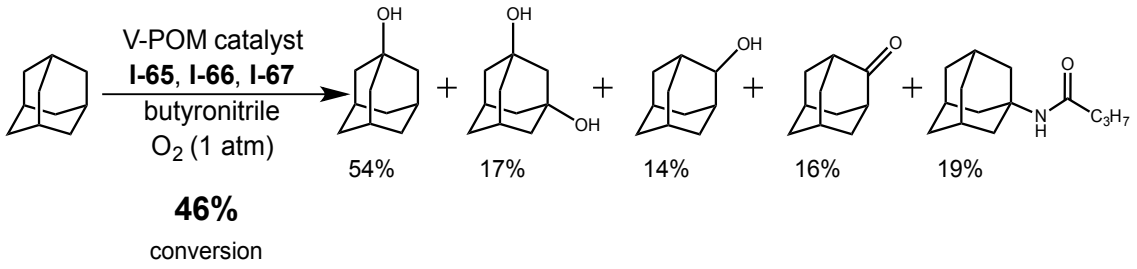

Scheme 1.5. Adamantane hydroxylation using vanadium-substituted POMs as catalysts **I-65**, **I-66**, and **I-67**

five different oxidized adamantyl derivatives shown in Scheme 1.5.

The bulky bis(μ-hydroxo) di-V-substituted phosphotungstate [γ-$H_2V_2PW_{10}O_{40}]^{3-}$ (**I-68**), also successfully promoted the oxidation of alkanes.[124] In H_2O_2-initiated alkane oxidation, high steric hindrance of the strongly electrophilic oxidant leads to high selectivities for alcohols (>56%) (Table 1.1). All the reactions are completed in less than 4 hours at a temperature of 60 or 70 ˚C. The bulky framework of the catalyst makes the oxidation of the secondary C−H bond

Table 1.1. Hydroxylation of alkanes with $TBA_3(H_2V_2PW_{10}O_{40})$

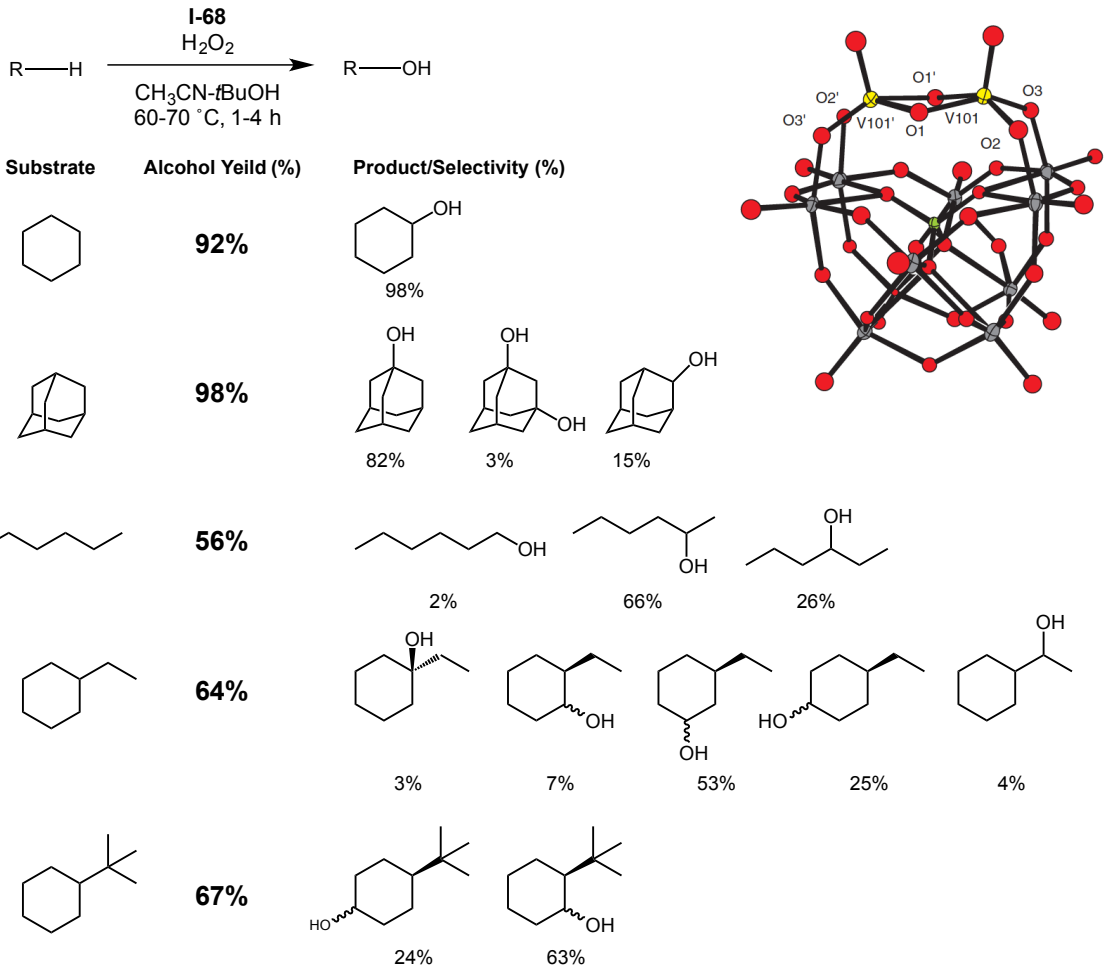

easier than that of the more sterically hindered tertiary C−H bonds resulting in secondary alcohols as the main products using catalyst **I-68**.

1.3.2 Oxidation of alkenes to epoxides

In the early years of research on POM catalysis, epoxidation reactions with alkenes employing O_2 as the oxygen donor were also published.[99] In these systems, aldehydes are usually needed as sacrificial agents because of the relatively low reactivity of O_2. The aldehydes initially react with O_2 to form peroxyacids and are reduced to carboxylic acids at the end of the reactions. Although such systems are effective for alkene oxidation, they are not widely used because of the following disadvantages. First, aldehydes are used as sacrificial agents, which detracts somewhat from the advantage of using O_2 as the terminal oxidant. The requirement of the aldehyde for catalytic activity lowers atom economy of the reaction. Secondly, the reactions proceed through a free radical mechanism which can generate complicating byproducts that may require tedious purification steps.

Substituting vanadium into the POM skeleton can greatly change the reaction pathway and improve the oxidant utilization efficiency. The bis(μ-hydroxo)-bridged di-V-substituted POM $TBA_4(\gamma\text{-}V_2SiW_{10})$ (**I-69**) is an exemplary compound as it exhibits high catalytic activity in the epoxidation of a diverse range of alkenes (Table 1.2).[125,126] Notably, the system with $TBA_4(\gamma\text{-}V_2SiW_{10})$ shows unique stereospecificity, diastereoselectivity, and regioselectivity that are

different from those reported for the epoxidation systems with the related catalyst $TBA_4(\gamma\text{-}H_4SiW_{10})$ that lacks vanadium substitution. In the case of non-conjugated dienes, the more accessible, but less nucleophilic double bonds are oxidized preferentially (*e.g.* Table 1.2, entry 4). Employing optimized reaction conditions, the amounts of allylic oxidation products and glycols produced by hydrolysis are

Table 1.2. Alkene epoxidation using silicotungstate **I-69**

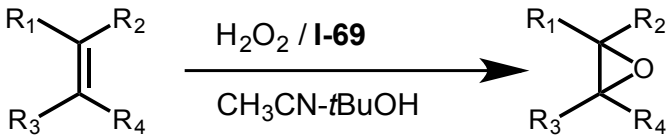

Entry	Alkene	Yield (%)	Product
1		87%	
2		91%	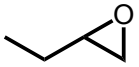
3	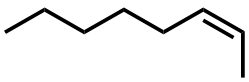	90%	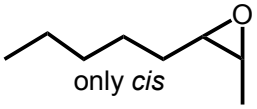 only *cis*
4	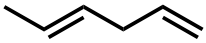	90%	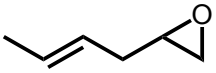
5	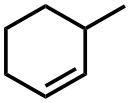	91%	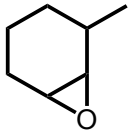 *syn:anti* = 5:95
6	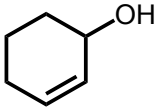	87%	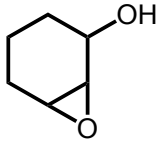 *syn:anti* = 12:88
7	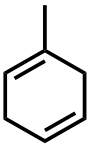	76%	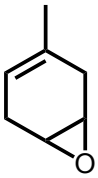

negligible for all cases indicating selective epoxidation with little accompanying over-oxidation.

1.3.3 Oxidation of arenes and arene derivatives

The POM promoted oxidation of arenes and their derivatives represents a practical way to acquire phenols, quinones, and a variety of related derivatives. In the presence of $H_5V_2PMo_{10}O_{40}$ (**I-70**) and 1 atm of O_2, the selective oxidation (>99%) of anthracene to anthraquinone is achieved at 60 ˚C after 18 h (Scheme 1.6).[127] It has been previously documented that $H_5V_2PMo_{10}O_{40}$ activates arenes such as anthracene and 4-methoxytoluene. The mechanism proceeds through extraction of an electron from the hydrocarbon forming a radical organic species, which is directly followed by an oxygen atom transfer from the POM anion to the substrate to form the corresponding oxidized product.[127-129]

To acquire phenols, Fe- and V-substituted POM catalysts have been investigated for the oxidative hydroxylation of benzene.[130-136] These catalysts show remarkable activity; however, selective hydroxylation of substituted arenes

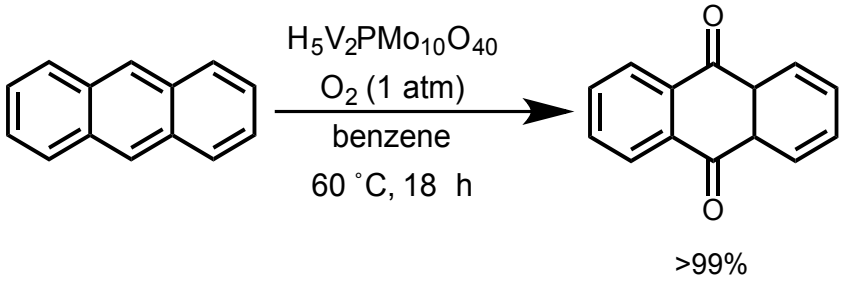

Scheme 1.6. Oxidation of anthracene to antraquinone using $H_5V_2PMo_{10}O_{40}$

is still a limiting aspect for POM catalysts. A confounding factor for these transformations is the fact that the product phenols are often more oxidatively labile than their arene congeners. As a result, this process is often accompanied by the formation of undesirable products including regioisomers, polyhydroxylated arenes, quinones, and intractable tars.[137] Nickel (Ni) substituted oxovanadium $K_7NiV_{13}O_{38}\cdot 16H_2O$ (**I-71**) promotes the hydroxylation of aromatics bearing an electron-withdrawing group using 30% H_2O_2 as the oxygen donor with acetic acid (HOAc) as an acidic additive.[138] For methyl benzoate, the yield of hydroxylated products reaches up to 73%. The ratio of *o*-, *m*-, and *p*–OH isomers is 70:20:10 (Scheme 1.7).

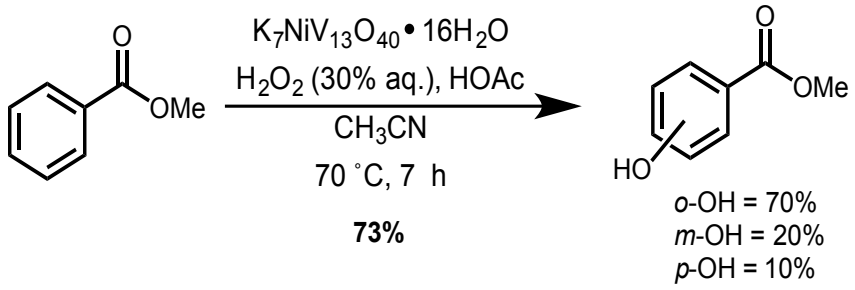

Scheme 1.7. Nickel-substituted oxovanadium complex for catalytic hydroxylation with H_2O_2

Usually, the oxidation of alkylarenes occurs preferentially at the benzylic position rather than the aromatic ring sp^2 C−H bonds because the bond dissociation energies of the $ArCR_2$−H bonds are much lower than those of the Ar−H bonds.[139,140] Therefore, it is difficult to obtain alkylphenols selectively by direct oxidation of alkylarenes. Nevertheless, chemo- and regioselective direct hydroxylation of structurally variant arenes including alkylarenes with reactive

Table 1.3. Chemo- and regioselective hydroxylation of arenes with $TBA_3(V_2PW_{10})$

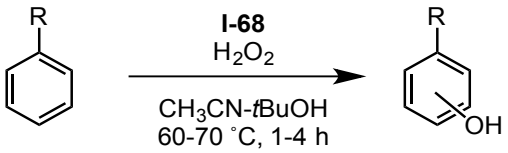

Substrate	Alcohol Yeild (%)	Product/Selectivity (%)
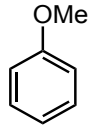	**85%**	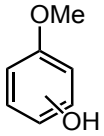 **>99%** ***o*:*m*:*p* = 5:<1:95**
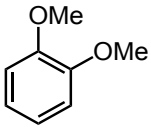	**78%**	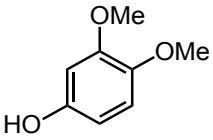 **>99%**
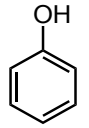	**86%**	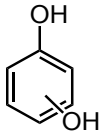 **85%** ***o*:*m*:*p* = 5:<1:95**
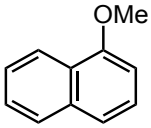	**63%**	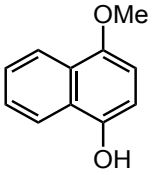 **>99%**
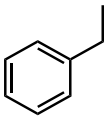	**66%**	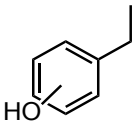 **77%** ***o*:*m*:*p* = 5:20:75**
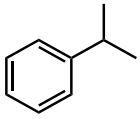	**55%**	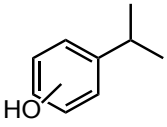 **88%** ***o*:*m*:*p* = 2:20:77**
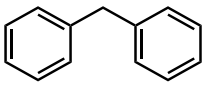	**47%**	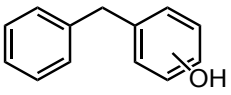 **97%** ***o*:*m*:*p* = 9:20:71**
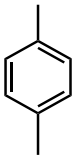	**98%**	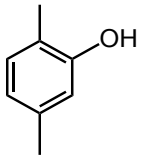 **45%**

alkyl side chains can be achieved using the di-V-substituted phosphotungstate γ-V_2PW_{10} (**I-68**) and H_2O_2 as the terminal oxidant (Table 1.3).[141] The system shows a unique preference for the formation of *p*-substituted phenols in lieu of side-chain oxygenated products. As for anisole, the oxidative demethylation is also successfully suppressed. Thus, the *para*-hydroxylation of anisole proceeded with an 85% yield. The *ortho*-, *meta*-, and *para*-isomer ratio is 5:<1:95 compared with 100:0:0 with the Ni polyoxovanadate, $K_7NiV_{13}O_{38} \cdot 16H_2O$ (**I-71**). As for toluene, 86% selectivity for hydroxylated products with the ratio of *o*- , *m*- , and *p*–OH isomers equivalent to 7:16:77 was determined.

1.4 Conclusions

In conclusion, vanadium complexes that form peroxovanadium species in the oxidation of organic compounds represent a widely applicable catalytic system using environmentally conscious terminal oxidant sources such as H_2O_2 and O_2 to promote selective and often quantitative organic oxidations. Vanadium pentoxide has been a valuable contributor in both the early years of its catalytic utilization and still remains an area of interest for many organic chemists owing to vanadium's unique chemical properties.

Vanadium-substituted polyoxometalates have also been utilized as catalysts in organic oxidation reactions over the last thirty years. Their unique redox reactivity has been exploited to promote a large volume of reactions, a selection of which were presented here. The high thermal and oxidative stability

of these materials is a key feature that allows for their superior stability under peroxidative conditions as compared to more conventional organometallic catalysts. The high regio-, stereo-, and diastereomeric selectivity that V-POMs exhibit versus other POMs is one of the contributing factors for its extended use in catalytic oxidations.

1.5 References

(1) Haber, J. *ACS Symp. Ser.* **1985**, *279*, 3-21.

(2) Haber, J.; Witko, M.; Tokarz, R. *Appl. Catal., A* **1997**, *157*, 3-22.

(3) Haber, J. *Catal. Today* **2009**, *142*, 100-113.

(4) Sutradhar, M.; Martins, L. M. D. R. S.; Guedes da Silva, M. F. C.; Pombeiro, A. J. L. *Coord. Chem. Rev.* **2015**, *301-302*, 200-239.

(5) da Silva, J. A. L.; da Silva, J. J. R. F.; Pombeiro, A. J. L. *Coordination Chemistry Reviews* **2011**, *255*, 2232-2248.

(6) Lambrecht, W.; Djafari-Rouhani, B.; Vennik, J. *Surf. Sci.* **1983**, *126*, 558-564.

(7) Lambrecht, W.; Djafari-Rouhani, B.; Vennik, J. *Solid State Commun.* **1981**, *39*, 257-261.

(8) Fiermans, L.; Vennik, J. *Surface Sci.* **1968**, *9*, 187-197.

(9) Andersson, A. *J. Solid State Chem.* **1982**, *42*, 263-275.

(10) Che, M.; Bond, G. C. *Adsorption and catalysis on oxide surfaces*; Elsevier, 1985; Vol. 21.

(11) Gillis, E.; Boesman, E. *Phys. Status Solidi* **1966**, *14*, 337-347.

(12) Tarama, K.; Yoshida, S.; Ishida, S.; Kakioka, H. *Bull. Chem. Soc. Jap.* **1968**, *41*, 2840-2845.

(13) Inomata, M.; Miyamoto, A.; Murakami, Y. *J. Catal.* **1980**, *62*, 140-148.

(14) Hirota, K.; Kera, Y.; Teratani, S. *J. Phys. Chem.* **1968**, *72*, 3133-3141.

(15) Inomata, M.; Miyamoto, A.; Murakami, Y. *Chem. Lett.* **1978**, 799-802.

(16) Ramirez, R.; Casal, B.; Utrera, L.; Ruiz-Hitzky, E. *J. Phys. Chem.* **1990**, *94*, 8960-8965.

(17) Miyamoto, A.; Yamazaki, Y.; Inomata, M.; Murakami, Y. *J. Phys. Chem.* **1981**, *85*, 2366-2372.

(18) Conte, V.; Floris, B. *Dalton Transactions* **2011**, *40*, 1419-1436.

(19) da Silva, J. A. L.; Frausto da Silva, J. J. R.; Pombeiro, A. J. L. *Coord. Chem. Rev.* **2011**, *255*, 2232-2248.

(20) Licini, G.; Conte, V.; Coletti, A.; Mba, M.; Zonta, C. *Coordination Chemistry Reviews* **2011**, *255*, 2345-2357.

(21) Shul'pin, G. B.; Attanasio, D.; Suber, L. *J. Catal.* **1993**, *142*, 147-152.

(22) Sutradhar, M.; Shvydkiy, N. V.; Guedes da Silva, M. F. C.; Kirillova, M. V.; Kozlov, Y. N.; Pombeiro, A. J. L.; Shul'pin, G. B. *Dalton Transactions* **2013**, *42*, 11791-11803.

(23) Sutradhar, M.; Kirillova, M. V.; Guedes da Silva, M. F. C.; Martins, L. M. D. R. S.; Pombeiro, A. J. L. *Inorganic Chemistry* **2012**, *51*, 11229-11231.

(24) Buehl, M.; Schurhammer, R.; Imhof, P. *J. Am. Chem. Soc.* **2004**, *126*, 3310-3320.

(25) Shul'pin, G. B. *Dalton Transactions* **2013**, *42*, 12794-12818.

(26) Fernandes, R. R.; Lasri, J.; da Silva, M. F. C. G.; da Silva, J. A. L.; Fraústo da Silva, J. J. R.; Pombeiro, A. J. L. *Applied Catalysis A: General* **2011**, *402*, 110-120.

(27) Shul'pin, G. B.; Wiley-VCH Verlag GmbH & Co. KGaA: 2004; Vol. 2, p 215-241.

(28) Shul'pin, G. B. *Mini-Rev. Org. Chem.* **2009**, *6*, 95-104.

(29) Shul'pin, G. B.; Kozlov, Y. N.; Nizova, G. V.; Suss-Fink, G.; Stanislas, S.; Kitaygorodskiy, A.; Kulikova, V. S. *J. Chem. Soc., Perkin Trans. 2* **2001**, 1351-1371.

(30) Shul'pin, G. B. *Dalton Trans.* **2013**, *42*, 12794-12818.

(31) Kuznetsov, M. L.; Pombeiro, A. J. L. *Inorganic Chemistry* **2009**, *48*, 307-318.

(32) Silva, T. F. S.; Alegria, E. C. B. A.; Martins, L. M. D. R. S.; Pombeiro, A. J. L. *Adv. Synth. Catal.* **2008**, *350*, 706-716.

(33) Shul'pina, L. S.; Kirillova, M. V.; Pombeiro, A. J. L.; Shul'pin, G. B. *Tetrahedron* **2009**, *65*, 2424-2429.

(34) Gupta, S.; Kirillova, M. V.; Guedes da Silva, M. F. C.; Pombeiro, A. J. L.; Kirillov, A. M. *Inorganic Chemistry* **2013**, *52*, 8601-8611.

(35) Kirillova, M. V.; Kuznetsov, M. L.; Romakh, V. B.; Shul'pina, L. S.; Frausto da Silva, J. J. R.; Pombeiro, A. J. L.; Shul'pin, G. B. *J. Catal.* **2009**, *267*, 140-157.

(36) Kuznetsov, M. L.; Pombeiro, A. J. L. *Inorg. Chem.* **2009**, *48*, 307-318.

(37) Qin, J.; Fu, Z.; Liu, Y.; He, X.; Zhang, D.; Wu, W.; Wang, Y.; Gong, X.; Deng, X.; Wu, H.; Zou, Y.; Yu, N.; Yin, D. *Cuihua Xuebao* **2011**, *32*, 1342-1348.

(38) Conte, V.; Floris, B. *Dalton Trans.* **2011**, *40*, 1419-1436.

(39) Wigington, B. N.; Drummond, M. L.; Cundari, T. R.; Thorn, D. L.; Hanson, S. K.; Scott, S. L. *Chem. - Eur. J.* **2012**, *18*, 14981-14988, S14981/14981-S14981/14983.

(40) Campestrini, S.; Di Furia, F.; Modena, G.; Novello, F. *Stud. Surf. Sci. Catal.* **1991**, *66*, 375-384.

(41) Conte, V.; Di Furia, F.; Modena, G. *J. Org. Chem.* **1988**, *53*, 1665-1669.

(42) Chen, B.; Huang, X.; Wang, B.; Lin, Z.; Hu, J.; Chi, Y.; Hu, C. *Chem. - Eur. J.* **2013**, *19*, 4408-4413.

(43) Kodama, S.; Hashidate, S.; Nomoto, A.; Yano, S.; Ueshima, M.; Ogawa, A. *Chem. Lett.* **2011**, *40*, 495-497.

(44) Hanson, S. K.; Wu, R.; Silks, L. A. P. *Organic Letters* **2011**, *13*, 1908-1911.

(45) Alagiri, K.; Prabhu, K. R. *Tetrahedron* **2011**, *67*, 8544-8551.

(46) Chen, C. M.; Macwan, A.; Rupe, J. *IEEE Communications Magazine* **2011**, *49*, 26-27.

(47) Alsalim, T. A.; Hadi, J. S.; Ali, O. N.; Abbo, H. S.; Titinchi, S. J. *Chemistry Central Journal* **2013**, *7*, 1-8.

(48) Adão, P.; Costa Pessoa, J.; Henriques, R. T.; Kuznetsov, M. L.; Avecilla, F.; Maurya, M. R.; Kumar, U.; Correia, I. *Inorganic Chemistry* **2009**, *48*, 3542-3561.

(49) Xia, Q. H.; Ge, H. Q.; Ye, C. P.; Liu, Z. M.; Su, K. X. *Chem. Rev. (Washington, DC, U. S.)* **2005**, *105*, 1603-1662.

(50) Sutradhar, M.; Mukherjee, G.; Drew, M. G. B.; Ghosh, S. *Inorg. Chem.* **2007**, *46*, 5069-5075.

(51) Sutradhar, M.; Roy Barman, T.; Ghosh, S.; Drew, M. G. B. *Journal of Molecular Structure* **2012**, *1020*, 148-152.

(52) Sutradhar, M.; Kirillova, M. V.; Guedes da Silva, M. F. C.; Liu, C.-M.; Pombeiro, A. J. L. *Dalton Transactions* **2013**, *42*, 16578-16587.

(53) Maurya, M. R.; Kumar, A.; Costa Pessoa, J. *Coordination Chemistry Reviews* **2011**, *255*, 2315-2344.

(54) Bolm, C. *Coordination Chemistry Reviews* **2003**, *237*, 245-256.

(55) Trivedi, M.; Nagarajan, R.; Kumar, A.; Rath, N. P. *Journal of Organometallic Chemistry* **2010**, *695*, 1722-1728.

(56) Rahchamani, J.; Behzad, M.; Bezaatpour, A.; Jahed, V.; Dutkiewicz, G.; Kubicki, M.; Salehi, M. *Polyhedron* **2011**, *30*, 2611-2618.

(57) Ghaffari, A.; Behzad, M.; Dutkiewicz, G.; Kubicki, M.; Salehi, M. *J. Coord. Chem.* **2012**, *65*, 840-855.

(58) Kirillova, M. V.; Kuznetsov, M. L.; da Silva, J. A. L.; Guedes da Silva, M. F. C.; Frausto da Silva, J. J. R.; Pombeiro, A. J. L. *Chem. - Eur. J.* **2008**, *14*, 1828-1842.

(59) Kirillova, M. V.; Kuznetsov, M. L.; Reis, P. M.; da Silva, J. A. L.; Frausto da Silva, J. J. R.; Pombeiro, A. J. L. *J. Am. Chem. Soc.* **2007**, *129*, 10531-10545.

(60) Cordell, C. L.; Schubkegel, T.; Light, T. R.; Ahmad, F. *Journal of Hand Surgery*, *35*, 144-146.

(61) Cordelle, C.; Agustin, D.; Daran, J.-C.; Poli, R. *Inorg. Chim. Acta* **2010**, *364*, 144-149.

(62) Monfared, H. H.; Bikas, R.; Mayer, P. *Inorg. Chim. Acta* **2010**, *363*, 2574-2583.

(63) Pereira, C.; Leite, A.; Nunes, A.; Rebelo, S. L. H.; Rangel, M.; Freire, C. *Catalysis Letters* **2010**, *135*, 98-104.

(64) Dorbes, S.; Pereira, C.; Andrade, M.; Barros, D.; Pereira, A. M.; Rebelo, S. L. H.; Araujo, J. P.; Pires, J.; Carvalho, A. P.; Freire, C. *Microporous Mesoporous Mater.* **2012**, *160*, 67-74.

(65) Bortolini, O.; Di Furia, F.; Modena, G.; Scrimin, P. *J. Mol. Catal.* **1980**, *9*, 323-334.

(66) Hirao, T. *Chemical Reviews* **1997**, *97*, 2707-2724.

(67) Kuhnen, L.; List, F.; Vangermain, E.; Chemische Werke Huels A.-G. . 1966, p 3 pp.

(68) Sheng, M. N.; Zajacek, J. G. *J. Org. Chem.* **1970**, *35*, 1839-1843.

(69) Rossiter, B. E.; Verhoeven, T. R.; Sharpless, K. B. *Tetrahedron Lett.* **1979**, 4733-4736.

(70) Tanaka, S.; Yamamoto, H.; Nozaki, H.; Sharpless, K. B.; Michaelson, R. C.; Cutting, J. D. *J. Am. Chem. Soc.* **1974**, *96*, 5254-5255.

(71) Sharpless, K. B.; Michaelson, R. C. *J. Amer. Chem. Soc.* **1973**, *95*, 6136-6137.

(72) Johnson, R. A.; Sharpless, K. B.; Ojima, I. *VCH, New York* **1993**, 227-272.

(73) Curci, R.; Di Furia, F.; Testi, R.; Modena, G. *J. Chem. Soc., Perkin Trans. 2* **1974**, 752-757.

(74) Cenci, S.; Di Furia, F.; Modena, G.; Curci, R.; Edwards, J. O. *J. Chem. Soc., Perkin Trans. 2* **1978**, 979-984.

(75) Chong, A. O.; Sharpless, K. B. *J. Org. Chem.* **1977**, *42*, 1587-1590.

(76) Conte, V.; Di Furia, F.; Licini, G. *Appl. Catal., A* **1997**, *157*, 335-361.

(77) Li, Z.; Zhang, W.; Yamamoto, H. *Angew. Chem., Int. Ed.* **2008**, *47*, 7520-7522.

(78) Li, F.; Wang, Z.-H.; Zhao, L.; Xiong, F.-J.; He, Q.-Q.; Chen, F.-E. *Tetrahedron: Asymmetry* **2011**, *22*, 1337-1341.

(79) Kyung, K. H.; Han, D. C.; Fleming, H. P. *J. Food Sci.* **1997**, *62*, 406-409.

(80) Naito, S.; Nishimura, M. *YAKUGAKU ZASSHI* **2001**, *121*, 989-994.

(81) Cotton, H.; Elebring, T.; Larsson, M.; Li, L.; Sörensen, H.; von Unge, S. *Tetrahedron: Asymmetry* **2000**, *11*, 3819-3825.

(82) Komatsu, W.; Miura, Y.; Yagasaki, K. *Lipids* **1998**, *33*, 499-503.

(83) Kagan, H. B. In *Organosulfur Chemistry in Asymmetric Synthesis*; Wiley-VCH Verlag GmbH & Co. KGaA: 2009, p 1-29.

(84) Zeng, Q.; Gao, Y.; Dong, J.; Weng, W.; Zhao, Y. *Tetrahedron: Asymmetry* **2011**, *22*, 717-721.

(85) Romanowski, G.; Kira, J. *Polyhedron* **2013**, *53*, 172-178.

(86) Di Furia, F.; Modena, G.; Curci, R. *Tetrahedron Lett.* **1976**, 4637-4638.

(87) Curci, R.; Di Furia, F.; Edwards, J. O.; Modena, G. *Chim. Ind. (Milan)* **1978**, *60*, 595-597.

(88) Nakajima, K.; Kojima, M.; Fujita, J. *Chem. Lett.* **1986**, 1483-1486.

(89) Nakajima, K.; Kojima, K.; Kojima, M.; Fujita, J. *Bull. Chem. Soc. Jpn.* **1990**, *63*, 2620-2630.

(90) Nakajima, K.; Kojima, M.; Toriumi, K.; Saito, K.; Fujita, J. *Bull. Chem. Soc. Jpn.* **1989**, *62*, 760-767.

(91) Casella, L.; Gullotti, M.; Pintar, A.; Colonna, S.; Manfredi, A. *Inorg. Chim. Acta* **1988**, *144*, 89-97.

(92) Colonna, S.; Manfredi, A.; Spadoni, M.; Casella, L.; Gullotti, M. *J. Chem. Soc., Perkin Trans. 1* **1987**, 71-73.

(93) Bolm, C.; Bienewald, F. *Angew. Chem., Int. Ed. Engl.* **1996**, *34*, 2640-2642.

(94) Kozhevnikov, I. V.; Taraban'ko, V. E.; Matveev, K. I. *Dokl. Akad. Nauk SSSR* **1977**, *235*, 1347-1349 [Phys. Chem.].

(95) Nomiya, K.; Sugie, Y.; Miyazaki, T.; Miwa, M. *Polyhedron* **1986**, *5*, 1267-1271.

(96) Neumann, R.; Khenkin, A. M.; Juwiler, D.; Miller, H.; Gara, M. *Journal of Molecular Catalysis A: Chemical* **1997**, *117*, 169-183.

(97) Firouzabadi, H.; Iranpoor, N.; Amani, K. *Synthesis* **2003**, *2003*, 0408-0412.

(98) Leng, Y.; Zhao, P.; Zhang, M.; Wang, J. *Journal of Molecular Catalysis A: Chemical* **2012**, *358*, 67-72.

(99) Kozhevnikov, I. V. *Chemical Reviews* **1998**, *98*, 171-198.

(100) Ding, Y.; Zhao, W.; Zhang, Y.; Ma, B.; Qiu, W. *Reaction Kinetics, Mechanisms and Catalysis* **2011**, *102*, 85-92.

(101) Farsani, M. R.; Assady, E.; Jalilian, F.; Yadollahi, B.; Rudbari, H. A. *Journal of the Iranian Chemical Society* **2015**, *12*, 1207-1212.

(102) Farsani, M. R.; Yadollahi, B. *Journal of Molecular Catalysis A: Chemical* **2014**, *392*, 8-15.

(103) Chen, Y.; Tan, R.; Zheng, W.; Zhang, Y.; Zhao, G.; Yin, D. *Catal. Sci. Technol.* **2014**, *4*, 4084-4092.

(104) Misono, M. *Chemical Communications* **2001**, 1141-1152.

(105) Ben-Daniel, R.; Neumann, R. *Angewandte Chemie International Edition* **2003**, *42*, 92-95.

(106) Ben-Daniel, R.; Alsters, P.; Neumann, R. *J. Org. Chem.* **2001**, *66*, 8650-8653.

(107) Dornan, L. M.; Muldoon, M. J. *Catalysis Science & Technology* **2015**, *5*, 1428-1432.

(108) Huang, X.; Zhang, X.; Zhang, D.; Yang, S.; Feng, X.; Li, J.; Lin, Z.; Cao, J.; Pan, R.; Chi, Y.; Wang, B.; Hu, C. *Chem. - Eur. J.* **2014**, *20*, 2557-2564.

(109) Baffert, C.; Boas, J. F.; Bond, A. M.; Koegerler, P.; Long, D.-L.; Pilbrow, J. R.; Cronin, L. *Chem. - Eur. J.* **2006**, *12*, 8472-8483.

(110) Housecroft, C.; Sharpe, A.; Prentice Hall, New York, USA.

(111) Rhule, J. T.; Hill, C. L.; Judd, D. A.; Schinazi, R. F. *Chem. Rev. (Washington, D. C.)* **1998**, *98*, 327-357.

(112) van Woezik, B. A. A.; Westerterp, K. R. *Chem. Eng. Process.* **2000**, *39*, 521-537.

(113) Rice, R. G.; Gomez-Taylor, M. *Environmental health perspectives* **1986**, *69*, 31.

(114) Westerhoff, P.; Aiken, G.; Amy, G.; Debroux, J. *Water Res.* **1999**, *33*, 2265-2276.

(115) Cavani, F.; Ballarini, N.; Cericola, A. *Catal. Today* **2007**, *127*, 113-131.

(116) Li, D.; Chen, G.; Qi, H.; Tianjin Tianhuan Fine Chemical Research Institute, Peop. Rep. China . 2016, p 5pp.

(117) Iwasaka, H. *Fain Kemikaru* **2015**, *44*, 46-52.

(118) Ballarini, N.; Cavani, F.; Cortelli, C.; Ligi, S.; Pierelli, F.; Trifiro, F.; Fumagalli, C.; Mazzoni, G.; Monti, T. *Top. Catal.* **2006**, *38*, 147-156.

(119) Contractor, R. M.; Garnett, D. I.; Horowitz, H. S.; Bergna, H. E.; Patience, G. S.; Schwartz, J. T.; Sisler, G. M. *Stud. Surf. Sci. Catal.* **1994**, *82*, 233-242.

(120) Agaskar, P. A.; DeCaul, L.; Grasselli, R. K. *Catal. Lett.* **1994**, *23*, 339-351.

(121) Lin, M.; Sen, A. *Nature (London)* **1994**, *368*, 613-615.

(122) Periana, R. A.; Mironov, O.; Taube, D.; Bhalla, G.; Jones, C. J. *Science (Washington, DC, U. S.)* **2003**, *301*, 814-818.

(123) Shinachi, S.; Matsushita, M.; Yamaguchi, K.; Mizuno, N. *J. Catal.* **2005**, *233*, 81-89.

(124) Kamata, K.; Yonehara, K.; Nakagawa, Y.; Uehara, K.; Mizuno, N. *Nat. Chem.* **2010**, *2*, 478-483.

(125) Nakagawa, Y.; Mizuno, N. *Inorg. Chem.* **2007**, *46*, 1727-1736.

(126) Nakagawa, Y.; Kamata, K.; Kotani, M.; Yamaguchi, K.; Mizuno, N. *Angew. Chem., Int. Ed.* **2005**, *44*, 5136-5141.

(127) Khenkin, A. M.; Neumann, R. *Angew. Chem., Int. Ed.* **2000**, *39*, 4088-4090.

(128) Khenkin, A. M.; Weiner, L.; Wang, Y.; Neumann, R. *J Am Chem Soc* **2001**, *123*, 8531-8542.

(129) Bordoloi, A.; Lefebvre, F.; Halligudi, S. B. *J. Catal.* **2007**, *247*, 166-175.

(130) Kuznetsova, L. I.; Detusheva, L. G.; Fedotov, M. A.; Likholobov, V. A. *J. Mol. Catal. A: Chem.* **1996**, *111*, 81-90.

(131) Nomiya, K.; Yanagibayashi, H.; Nozaki, C.; Kondoh, K.; Hiramatsu, E.; Shimizu, Y. *J. Mol. Catal. A: Chem.* **1996**, *114*, 181-190.

(132) Passoni, L. C.; Cruz, A. T.; Buffon, R.; Schuchardt, U. *J. Mol. Catal. A: Chem.* **1997**, *120*, 117-123.

(133) Nomiya, K.; Nemoto, Y.; Hasegawa, T.; Matsuoka, S. *J. Mol. Catal. A: Chem.* **2000**, *152*, 55-68.

(134) Tani, M.; Sakamoto, T.; Mita, S.; Sakaguchi, S.; Ishii, Y. *Angew. Chem., Int. Ed.* **2005**, *44*, 2586-2588.

(135) Sumimoto, S.; Tanaka, C.; Yamaguchi, S.-t.; Ichihashi, Y.; Nishiyama, S.; Tsuruya, S. *Ind. Eng. Chem. Res.* **2006**, *45*, 7444-7450.

(136) Yang, H.; Wu, Q.; Li, J.; Dai, W.; Zhang, H.; Lu, D.; Gao, S.; You, W. *Appl. Catal., A* **2013**, *457*, 21-25.

(137) Panov, G. I.; Uriarte, A. K.; Rodkin, M. A.; Sobolev, V. I. *Catal. Today* **1998**, *41*, 365-385.

(138) Gao, F.; Hua, R. *Appl. Catal., A* **2004**, *270*, 223-226.

(139) Warren, J. J.; Tronic, T. A.; Mayer, J. M. *Chem. Rev. (Washington, DC, U. S.)* **2010**, *110*, 6961-7001.

(140) Blanksby, S. J.; Ellison, G. B. *Acc. Chem. Res.* **2003**, *36*, 255-263.

(141) Kamata, K.; Yamaura, T.; Mizuno, N. *Angew. Chem., Int. Ed.* **2012**, *51*, 7275-7278.

CHAPTER TWO

VANADIUM(V) OXIDE MEDIATED HALOLACTONIZATION OF ALKENOIC ACIDS

2.1 INTRODUCTION

2.1.1 Specific Aims

This chapter describes the development of methodology for the vanadium (V) oxide catalyzed halolactonization of substituted aryl alkenoic acids.[1,2] The goal for this project was the development of a safe and facile catalytic process for the *in situ* oxidation of bromide (Br^-) to its halenium counterpart through the generation of bromenium equivalents (Br^+). This reactive intermediate leads to the bromo-functionalization of various reactive organic substrates needed for further synthetic gain; as in precursor of various natural products, drug candidates, imaging compounds, etc. The methodology hinges on the oxidation of halide ions in the presence of a peroxovanadium(V) activated species similar to the peroxovanadium complexes responsible for organic transformation discussed in chapter one.

In chapter two, the discussion will focus on first, the role of vanadium-dependent haloperoxidases in the oxidation of halide ions to halenium equivalents in Nature and second, how this biosynthetic strategy for the bromination of organic compounds inspired our exploration into the bromolactonization of alkenoic acids. The last forty years of research had been

devoted to understanding the mechanistic role of the enzyme active site for these types of metalloenzymes. During that time, enzymes with similar reactivity have been isolated from Nature and functional mimics for these biomolecules have been critical in uncovering the mechanism of halide oxidation for which a detailed mechanism is still unclear.

The methodology introduced by our group has optimized conditions that employ a 5 mol % loading of V_2O_5, 3.0 equivalents of urea-H_2O_2 as the terminal co-oxidant, and ammonium bromide as the bromide source in a solvent system comprised of a 6:1 ratio of acetone and H_2O at room temperature (Scheme 2.1). These conductions cleanly generate the desired bromolactone products, which are conveniently purified by a simple acid/base extraction without recourse to column chromatography. As an illustrative example, these optimized conditions allowed for the conversion of alkenoic acid **II-1** to γ-bromolactone **II-2** in a 93 % isolated yield. This chapter will detail the discovery, optimization and substrate scope of this reaction.

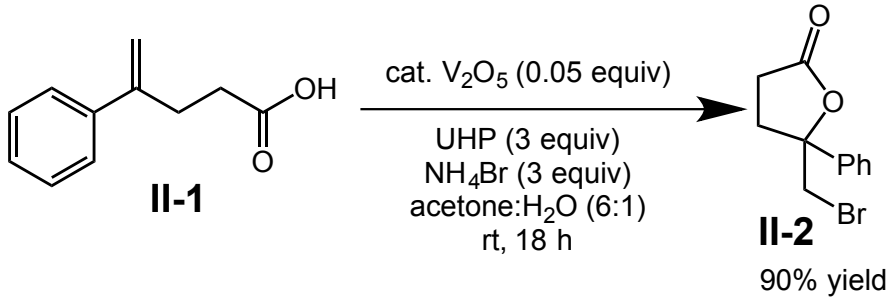

Scheme 2.1. Our established bromolactonization reaction conditions

2.1.2 Vanadium-dependent haloperoxidases as catalysts for halogenation of organic substrates

Halogenation of organic compounds is a vital chemical process in the synthesis of biologically active natural products. Selected examples of these secondary metabolites are shown in Figure 2.1, and highlight the stereochemical complexity and variety of functional groups common to these materials. These natural products serve numerous purposes including antibacterial, antifungal, anti-inflammatory, and antiviral properties that are potentially valuable as pharmaceuticals.[3-6] These compounds also represent vital role in the survival of living organisms from which they originate.[7] For marine organisms, the evolution of enzymatic pathways to said secondary metabolites serves as a self-defense mechanism against predators. The halofunctionalized materials range from phenol derivatives, known also for their antimicrobial properties to small

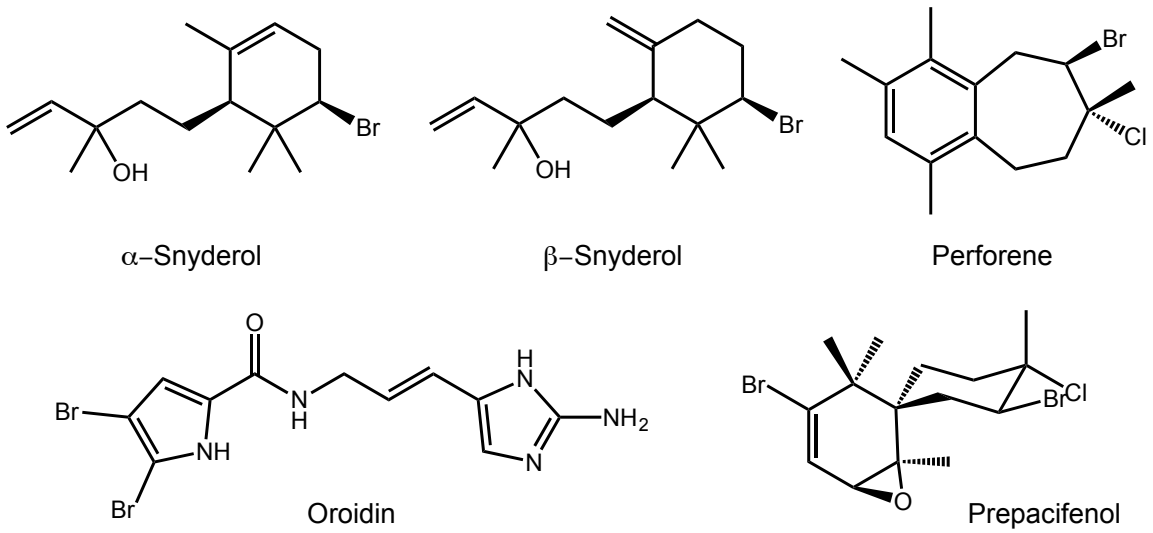

Figure 2.1. Natural products known as common secondary metabolites for marine organisms

molecules such as bromoform, dibromomethane, and other volatile halohydrocarbons.[8-12] Many of the biogenic halogenated compounds isolated from marine environments originate from macroalgae (*e.g.*, Rhodophyta, Phaeophyta, Chlorophyta, *etc.*).[8,13] These metabolites are typically halogenated by action of haloperoxidase enzymes which facilitate the oxidation of halide anions (X-) to halenium equivalents (X+) in oceanic environments where the concentrations of halogen ions are approximately 0.5 M in chloride, 1.0 mM in bromide, and 1.0 μM in iodide.[8] With an abundance of halide ions present for reaction, these enzymes are attributed to the synthesis for a majority of halogenated biocompounds necessary for the protection for marine life.[8,9]

Metal-free and iron-heme-dependent haloperoxidases are known to facilitate halide oxidation and subsequent halo-functionalization of organic substrates.[14-19] Given our group's interest in vanadium materials as catalysts,[20] the vanadium-dependent haloperoxidase activity towards similar transformations served as inspiration for methodology developed by our group and is therefore the focus of the initial discussion for this chapter. The isolation of the vanadium bromoperoxidase (VBrPO) from the marine alga *Ascophyllum nodosum* in 1984 represents the first example of a vanadium-dependent haloperoxidase.[21] Since this seminal disclosure, VBrPOs are now known to be common to most marine algae, seaweeds, and some lichens. These enzymes are classified based on the most electronegative halogen that the enzyme is capable of oxidizing (*i.e.* chloroperoxidase oxidizes chlorine, bromine, and iodide; bromoperoxidase

oxidizes bromine and iodine).[8,13,22] Enzyme-mediated halide oxidation and subsequent organic halogenation was first investigated with monochlorodimedone (2-chloro-5,5-dimethyl-1,3-dimedone; MCD) as the organic substrate used by both the Butler and Wever groups to elucidate the haloperoxidase oxidative mechanism. Their steady state kinetic and NMR evaluations revealed coordination of peroxide first to the vanadium metal of dihydrovanadate, the presumed activate site of the enzyme.[8,9,23-25] This reaction proceeds in an exothermic fashion facilitated by the hydrogen bonding of water molecules locked in a supramolecular array with the active site of the enzyme (*i.e.* vanadium metal center) (Figure 2.2).[26]

Once the peroxovanadate-activated species is revealed, two-electron oxidation of halide ions (X^-) forming halenium (X^+) equivalents affords the reactive intermediate available for organic halogenation (Figure 2.2). Wishchang,

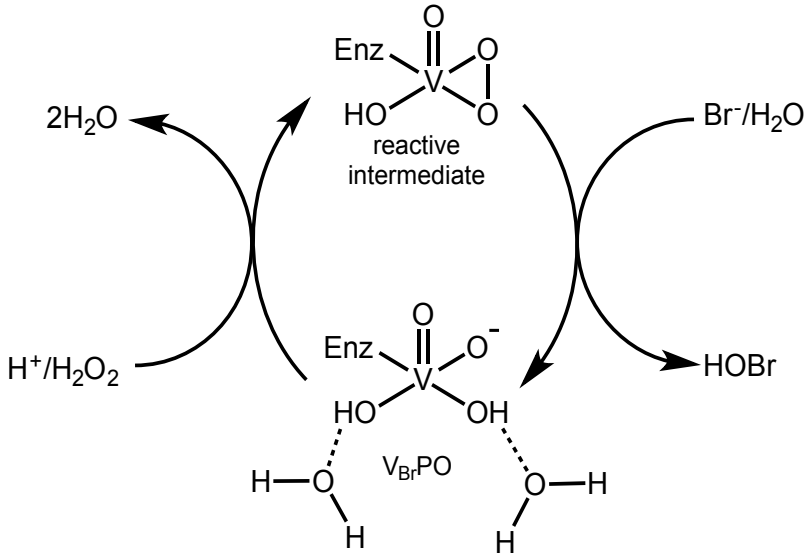

Figure 2.2. Major steps in bromide oxidation using H_2O_2 in vanadium bromoperoxidase ($V_{Br}PO$)-catalyzed reactions; Enz = enzyme

Radlow, and Hartung's in-depth discussion of steady state kinetic evidence for possible brominating intermediates gave focus to three possible agents present in equilibrium at physiological conditions.[24] Their analysis shows bromine being the effective brominating agent with alternative reagents, such as hypobromous acid and tribromide, being non-competitive due to the pronounced electrophilicity of bromine. In previous studies Butler, Wever, and Vilter, all include bromine bound enzymatic intermediates (*e.g.*, Enz-Br, Enz-OBr) as possible bromenium ion-type species; however, evidence for these types of materials is difficult to obtain because of their sensitivity to reaction conditions (*e.g.*, pH, substrate concentration, peroxide concentration, *etc.*).[9]

Through preliminary analysis using VBrPO to promote halogenation of MCD in the presence of hydrogen peroxide and bromide, a competitive catalytic reaction was observed having a relatively comparable rate in the absence of an organic substrate to react upon. This side reaction is the bromide-assisted disproportionation of peroxide to form dioxygen and occurs in a stoichiometric fashion to peroxide concentration.[3,27] This indicates that both organic halogenation and disproportionation of peroxide proceed through a common intermediate and the formation of said species is rate limiting.[3,9,27]

Due to the intensive isolation process for VBrPO in the late 1980s, obtaining enough material to run extensive kinetic evaluations was not effective.[8] Further, issues with limitations in spectroscopic analysis available for monitoring the metal center in complex biological compounds prompted researchers to use

model compounds to address the role of vanadium in catalyzing halide oxidation and subsequent organic halogenation.[28] The Butler group at UC Santa Barbara was the first to use functional mimics to investigate mechanistic considerations for the active site of VBrPO by using *cis*-dioxovanadium(V) as the enzymatic peroxidase catalyst for the bromination of trimethoxybenzene (TMB) in acidic aqueous solution.[28] As with the VBrPO catalyzed bromination of MCD by the group earlier,[27,29] hydrogen peroxide coordinates to dioxovanadium(V) site forming both mono- and diperoxovanadium species whose ratios are dependent on both the acid and hydrogen peroxide concentration in solution.[28,30] GC monitoring of Br-TMB production in an excess of the starting TMB revealed a stoichiometric dependence of 1 equiv of H_2O_2 and 1 equiv of bromide per equivalent of Br-TMB observed. While monitoring the reaction via ^{51}V NMR, the group was also successful in identifying chemical shifts that were attributed to mono- and diperoxovanadium species. Either of these two species could in principle oxidize the halide *in situ*, however, their results indicated that diperoxovanadium(V) oxidizes bromide faster than monoperoxovanadium(V).[30] This phenomenon then resulted in either bromide-assisted dioxygen formation or TMB bromination.[28] Without the presence of an appropriate organic substrate, the bromide-assisted disproportionation of hydrogen peroxide predominates via the release of singlet oxygen ($^1O_2$).[3,27] Just one year later, the group published an extension of TMB bromination in non-acidic aqueous and aqueous/ethanol solutions.[31] Extensive ^{51}V NMR and UV/Vis Spectroscopy lead to their conclusion

that tribromide is initially formed and quickly undergoes equilibration to bromine and bromide to brominate TMB.[8,28,30,31]

Based on their extensive kinetic and spectroscopic work with *cis*-diperoxovanadium(V), they proposed that halide oxidation was mediated by a binuclear, oxotriperoxodivanadium(V) species. The surmised that material was in turn formed from the dimerization of oxomono- and oxodiperoxovanadium(V) compounds whose concentrations were dependent upon the initial concentration of hydrogen peroxide.[30] The rate of the halogenation reaction increased when ethanol was used as the solvent by increasing the formation of the vanadium(V) dimer whereas water readily coordinated to the vanadium center reducing dimerization.[30,32]

Pecoraro *et. al*. have also made significant contributions in mechanistic insight for the process, focusing specifically on the activation of the oxovanadium

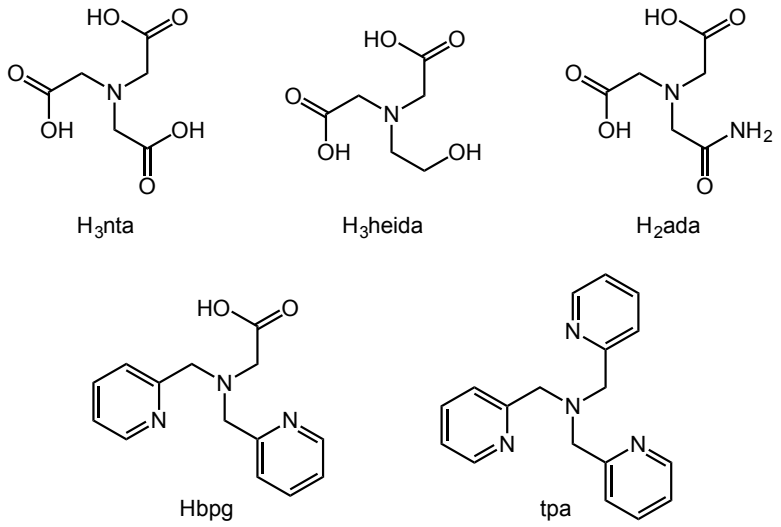

Figure 2.3. Structures for a series of tripodal-amine and aminocarboxylic ligands

metal centers that mimick the VBrPO enzymatic active site.[22,33,34] They synthesized derivatized oxoperoxovanadium(V) complexes bearing tripodal-amine chelates or aminocarboxylic acid ligands (Figure 2.3). The structure of these catalysts was verified via X-ray crystallography. X-ray analysis revealed a side-on bound peroxide that only promoted halide oxidation in the presence of stoichiometric equivalents of acid relative to bromide concentrations.[22,35] DFT calculations and spectroscopic studies later revealed that a protonation is critical for the activation of the vanadate species towards hydrogen peroxide coordination.[36-38] These experiments were critical in determining that the oxygen atoms of the vanadate oxygens resident in the enzymatic active site were most likely doubly protonated in order to facilitate the exothermic coordination of peroxide to the vanadium metal center (*cf.* Figure 2.2).[13,24]

The largest limitations associated with the VBrPO and the biomimetic dioxovanadium(V) system for halide oxidation are the rate of catalysis and the pH dependency of the system.[9] An acidic pH is required for early aqueous investigations and the turnover rates are marginal in comparison to the VBrPO system (15 mol Br-TMB/(mol of V)h^{-1} vs 4.7 x10^5 mol of Br product/(mol of enzyme) h^{-1}).[28,30] Butler established that in aqueous solution bromide oxidation by hydrogen peroxide is only feasible under neutral to acidic conditions and the role of the acid is to neutralize hydroxide anions released from the vanadium center once peroxide coordination occurs.[9,13]

2.1.3 Haloperoxidase inspired methodology using peroxovanadium(V) catalysts in the presence of bromide (Br^-)

Current bromofunctionalization protocols often employ hazardous and toxic brominating reagents (*e.g.* molecular bromine, Br_2). Concerns over both safety and environmental impact have encouraged research towards employing methodology that obviates the use of highly reactive brominating reagents. Presented below are several bromination reactions facilitated by mild oxidants such as hydrogen peroxide (H_2O_2), molecular oxygen (O_2), or alkylperoxide (ROOH) in the presence of vanadium pentoxide. In these transformations, V_2O_5 acts as a catalyst to promote the oxidation of bromide to its bromenium equivalent (Br^+) similar to the activity of the vanadium bromoperoxidase enzymes described above.

2.1.3.1 Bromination of aromatic compounds

Research focusing on the bromination of aromatic compounds has been a significant area of study owing to the numerous uses of these halogenated compounds. Many of them exhibit a range of biological activity serving as potent antitumor, antibacterial, antifungal, antineoplastic, and antiviral agents. Further, the importance of halogenated arenes as synthetic intermediates en route to specialty chemicals, pharmaceuticals, and agrochemicals cannot be ignored.[5,31,39]

Khan, Patel, and co-workers have established a series vanadium(V) oxide catalyzed bromination reactions using ammonium bromide salts as the halogen source (Scheme 2.2). Some of their initial investigations focused on the synthesis of organic ammonium tribromide compounds, which were in turn used as brominating agents in aqueous solution for the halogenation of activated aromatics.[39] Khan suggested that the tribromide salt acts as the initial precursor to the reactive brominating agent,[39] which likely arises from the equilibrium established in solution between the tribromide anion and Br_2 and bromide (Br^-). The in situ generation of Br_2 then effected the bromination of reactive organic substrates.[24,39] Their conditions employing ammonium tribromide salts facilitated the bromination of a number of aromatic compounds imidazoles, aniline derivatives, cresol isomers, and phenols.[5,39] The benign haloperoxidase-inspired methodology was then extended to the synthesis of natural products in the

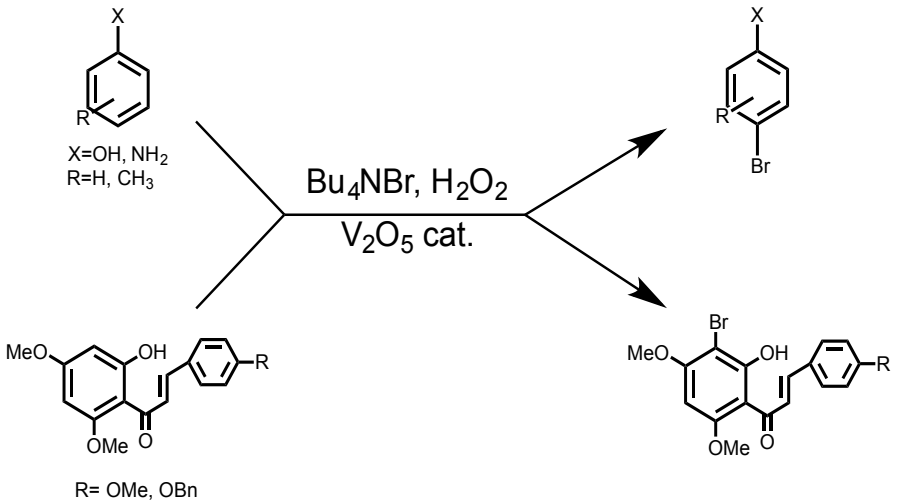

Scheme 2.2. Regioselective bromination of organic substrates mediated by the V_2O_5 catalyzed oxidation of bromide

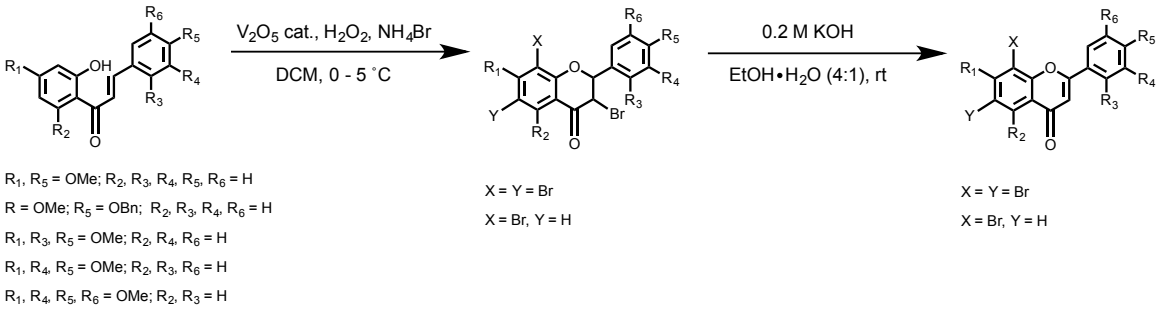

Scheme 2.3. Benign synthesis of several biologically relevant bromoflavones

preparation of a series of brominated aurones and flavones using the environmentally conscious reagents (Scheme 2.3).[4] Flavones are known for their biological activities such as anti-oxidant, anti-inflammatory, anti-viral, and anti-cancer bioactivities making them desired pharmaceutical candidates for targeted synthesis.[4,5]

2.1.3.2 α-Bromination of β-keto esters and 1,3-diketones

The Khan group also developed the chemoselective monobromination of β-keto esters and 1,3-diketones at the α-position using V_2O_5 and H_2O_2 (Scheme 2.4).[4,40] Common reagents for the monobromination of these substrates include molecular bromine (Br_2),[41] Br_2 and sodium hydride (NaH),[42] N-bromosuccinimide (NBS) and triethylamine (NEt_3) or NaH.[43-45] Some of these protocols require dry

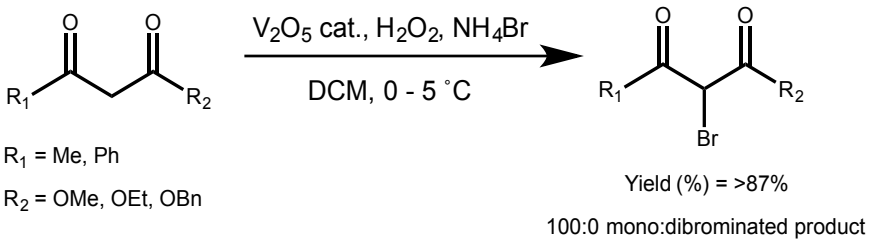

Scheme 2.4. α-Bromination of β-ketoesters

solvents or employ expensive, designer solvents like ionic liquids.[46-48] The use of molecular bromine presents operational challenges at large scale. Similarly, employing the potentially pyrophoric sodium hydride can also present operational difficulties at larger scales. Additionally, some of these processes suffer from reduced yield of the desired mono-bromo product due to disproportionation of the α-monobrominated β-keto esters to a mixture of dibrominated and debrominated products.[49,50] The V_2O_5-H_2O_2 mediated oxidation of halides for the halogenation of these substrates represented a comparatively milder process for the transformation.

The study by Khan *et. al* indicated that the V_2O_5 catalyst served as promoter for the catalytic cycle in two aspects. First, the complex acts as a Lewis acid for chelation with the two carbonyls of the β-keto ester or 1,3-diketone, thus promoting enol formation for chemoselective monobromination.[51] Second, the V_2O_5 also promotes the oxidation of NH_4Br by H_2O_2. The major limitation of this protocol is the requirement for a catalytic loading of 50 mol% V_2O_5 to efficiently promote the transformation.[51]

2.1.3.3 Sulfoxidation and thiocyanate oxidation

Starting in 2001 Khan and co-workers established dethiolization protocol for thioacetal and thioketal protecting groups, thus revealing the corresponding carbonyl functionalities (Scheme 2.5).[52,53] Common methods for deprotection include heavy metals,[54,55] iron(III) salts,[56] oxides of nitrogen,[57] and some

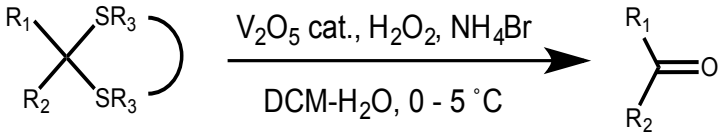

R_1 = aryl, alkyl, sugar residue

R_2 = H, aryl

R_3 = Et

Yield (%) = >75%

isolated yield

Scheme 2.5. Thioacetal and ketal cleavage using V_2O_5 catalyzed oxidation of ammonium bromide by H_2O_2

halenium ion sources.[58-60] Methods involving halenium ion sources often require hazardous reagents (Br_2, HBr, pyridine, *etc.*) and harsh reaction conditions.[58,60] Conversely, the V_2O_5 mediated process features mild reaction conditions and tolerates other reactive functionalities such as olefins, aromatic rings, as well as other carbonyl protecting groups without deprotection or side reactions.[52,53,61] Thioacetals and thioketals are used as carbonyl protecting groups due to their relative recalcitrance towards hydrolytic cleavage in both acid and basic conditions. Diethyldithioacetal is used as a protecting group in carbohydrate chemistry in the preparation of open chain aldosugars.[62]

They later extended this method to include the the hydrolysis of thioglycosides in order to address limitations in other methods for the same transformation..[52,61] The methodology for both the dethiolization of thioacetals and thioketals and the hydrolysis of thioglycosides proceeds without any side bromination reactions.[52,53,61] Direct oxidation of sulfur by hydrogen peroxide is not possible as reported by Olah in 1980.[63] The sequence of thioacetal cleavage begins with the peroxovanadium(V) intermediate formed from V_2O_5-H_2O_2 coordination oxidizing the bromide in solution to a bromenium equivalent that

reacts with the dithioacetal to form a bromosulonium complex that then undergoes hydrolysis to give the carobonyl parent compound.[53,61,64]

2.2 Results and Discussion

Haloperoxidase-like reactivity can be achieved in conventional organic methodology by employing catalytic loadings of V_2O_5 in the presence of hydrogen peroxide and a halide source. This strategy for the halogenation of organic substrates is appealing when compared to more traditional methods for bromination that rely on the use of potentially dangerous and toxic sources such as molecular bromine, Br_2. We set out to investigate a V_2O_5 mediated process as a possible route for the bromolactonization of varying alkenoic acids.

2.2.1 Initial exploratory experiments: halide investigation and catalyst equivalency

Initial investigations began by pursuing a series of exploratory grounding experiments targeting the bromolactonization of 4-phenylpentanoic acid **II-1** mediated by the V_2O_5 catalyzed oxidation of bromide (Table 2.1). We were encouraged by our initial experiment whereby the desired bromolactonization of **II-1** was achieved in a reasonable 73% yield via the oxidation of ammonium bromide (15 equiv) catalyzed by 0.5 equiv of V_2O_5 with 30% aq. H_2O_2 in an acetonitrile:water (6:1) solvent system (entry 1). A brief survey of other bromide salts, including sodium bromide, cesium bromide, lithium bromide, and potassium

Table 2.1. Exploratory halolactonization reactions with various halide sources

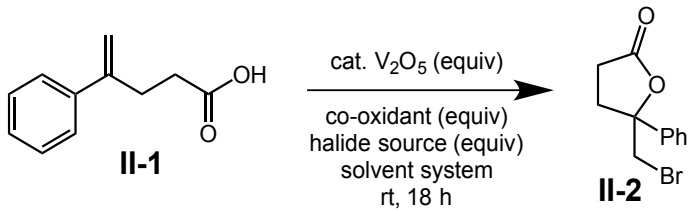

Entry	V_2O_5 (equiv)	Solvent System	Co-oxidant (equiv)[a]	Halide Source (equiv)	Yield (%)[b]
1	0.5	ACN:H_2O (6:1)	H_2O_2 (aq)	NH_4Br (15)	73
2	0.5	ACN:H_2O (6:1)	H_2O_2 (aq)	NaBr (15)	84
3	0.5	ACN:H_2O (6:1)	H_2O_2 (aq)	CsBr (15)	66
4	0.5	ACN:H_2O (6:1)	H_2O_2 (aq)	LiBr (15)	76
5	0.5	ACN:H_2O (6:1)	H_2O_2 (aq)	KBr (15)	74
6	0.5	ACN:H_2O (6:1)	H_2O_2 (aq)	NH_4Br (5)	84
7	0.5	ACN:H_2O (6:1)	H_2O_2 (aq)	NaBr (5)	73
8	0.2	ACN:H_2O (6:1)	H_2O_2 (aq)	NH_4Br (5)	65
9	0.2	ACN:H_2O (6:1)	H_2O_2 (aq)	NaBr (5)	75
10	0.2	ACN:H_2O (6:1)	H_2O_2 (aq)	NH_4Br (5)	89[c]
11	0.2	ACN:H_2O (6:1)	H_2O_2 (aq)	NH_4Cl (5)	36[d]
12	0.2	ACN:H_2O (6:1)	H_2O_2 (aq)	NaCl (5)	28[d]
13	0.1	ACN:H_2O (6:1)	H_2O_2 (aq)	NaBr (5)	59
14	0.1	ACN:H_2O (6:1)	H_2O_2 (aq)	NH_4Br (5)	54
15	0.1	ACN:H_2O (6:1)	H_2O_2 (aq)	CsBr (5)	42
16	0.1	ACN:H_2O (6:1)	H_2O_2 (aq)	LiBr (5)	40
17	0.1	ACN:H_2O (6:1)	H_2O_2 (aq)	NaI (5)	58[e]
18	0	ACN:H_2O (6:1)	H_2O_2 (aq)	NaI (5)	56[e]

[a] H_2O_2 (aq) denotes a 30% aqueous solution of hydrogen peroxide. [b] Yields are isolated yields after acid/base extraction. [c] Reactions warmed to 65 °C. [d] Corresponding chlorolactone product was isolated. [e] Corresponding iodolactone product was isolated.

bromide returned lactone **II-2** in yields ranging from 66 to 84% (entries 2-5) revealing several agreeable bromide sources for bromolactonization. Reducing the loading of halide salt from 15 equiv to 5 equiv resulted in comparable yields for ammonium bromide (84% yield, entry 6) and sodium bromide (73% yield, entry 7). Next, we attempted to reduce the catalyst loading to more reasonable levels. A 20 mol% loading of V_2O_5 resulted in comparable yields of bromolactone **II-2** as compared to the 0.5 equiv catalyst loading (entries 8 and 9). The 20 mol%

V_2O_5 loading returned an acceptable 89% yield of **II-2** when the reaction mixture was warmed to 65 ˚C (entry 10). Two experiments with chloride salts (*i.e.*, NH_4Cl and NaCl, entries 11-12) returned the corresponding chlorolactone product (not shown) in poor yields ranging from 28 to 36% yield, indicating limited reactivity of our system with chloride salts. Further reduction of the catalyst loading to 10 mol% V_2O_5 returned bromolactone **II-2** in poor yields ranging from 40 to 59% yield, regardless of the bromine source (entries 13-16). Sodium iodide was used in the corresponding iodolactonization (product not shown, entries 17 and 18). In the case of iodide oxidation, however, halolactonization occurs with our without the V_2O_5 acting as a promoter. Hence, hydrogen peroxide is a strong enough oxidant to promote iodide oxidation even in the absence of V_2O_5.

This initial effort confirmed our hypothesis that V_2O_5 and H_2O_2 could serve as a viable haloperoxidase-like catalyst for the bromolactonization of alkenoic acids by means of an active peroxovanadium(V) species. Subsequent investigations of solvent and co-oxidant screening, detailed below, were geared toward optimizing the protocol to one of reasonable synthetic utility.

2.2.2 Further optimization: solvent and co-oxidant screening

Increasing the water portion of the solvent system from 6:1 (*cf.* Table 2.1, entry 6; 84%) to 1:1 (Table 2.2, entry 1) and 1:6 (entry 2) resulted in reduced yields of 71 and 51%, respectively. Conducting the reaction in the absence of solvent aside from 30% aqueous H_2O_2 returned **II-2** in a 68% yield (entry 3).

Based on our initial screening efforts, a combination of 0.2 equiv V_2O_5 in the presence of 5 equiv NH_4Br as the halide source, in a 6:1:1 ratio of acetonitrile, water, and 30% aq. hydrogen peroxide as the starting point for a second round of optimization (entry 4) seemed appropriate despite its disappointing 65% yield of **II-2** due to the reaction returning a clean sample of the product, free from vicinal

Table 2.2. Focused screening of co-oxidant and solvent conditions for bromolactonization

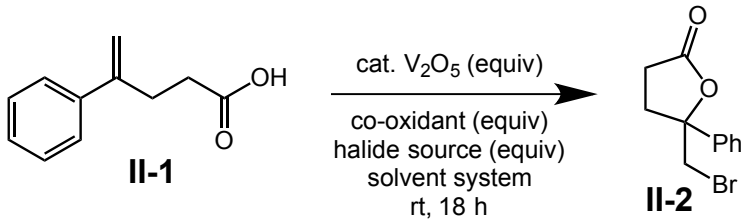

Entry	V_2O_5 (equiv)	Solvent System	Co-oxidant (equiv)[a]	Halide Source (equiv)	Yield (%)[b]
1	0.5	ACN:H_2O (1:1)	H_2O_2 (aq)	NH_4Br (15)	71
2	0.5	ACN:H_2O (1:6)	H_2O_2 (aq)	NH_4Br (15)	51
3	0.5	30% aq H_2O_2		NH_4Br (15)	68
4	0.2	ACN:H_2O (6:1)	H_2O_2 (aq)	NH_4Br (5)	65
5	0.2	PhMe:H_2O (6:1)	H_2O_2 (aq)	NH_4Br (5)	66
6	0.2	EtOAc:H_2O (6:1)	H_2O_2 (aq)	NH_4Br (5)	67
7	0.2	acetone:H_2O (6:1)	H_2O_2 (aq)	NH_4Br (5)	67
8	0.2	ACN:H_2O (6:1)	UHP[c] (5)	NH_4Br (5)	67
9	0.2	acetone:H_2O (6:1)	UHP (5)	NH_4Br (5)	87
10	0.2	acetone:H_2O (6:1)	UHP (5)	NH_4Br (5)	91[d]
11	0.2	acetone:H_2O (6:1)	UHP (3)	NH_4Br (3)	92
12	0.1	acetone:H_2O (6:1)	UHP (5)	NH_4Br (5)	96[e]
13	0.1	acetone:H_2O (12:1)	UHP (5)	NH_4Br (5)	87
14	0.1	acetone:H_2O (30:1)	UHP (5)	NH_4Br (5)	36
15	0.1	acetone:H_2O (1:1)	UHP (5)	NH_4Br (5)	29
16	0.1	acetone:H_2O (6:1)	UHP (3)	NH_4Br (3)	93
17	0.1	acetone:H_2O (6:1)	UHP (2.5)	NH_4Br (2.5)	84
18	0.1	acetone:H_2O (6:1)	UHP (2.5)	NH_4Br (2.5)	93[d]
19	0.05	acetone:H_2O (6:1)	UHP (3)	NH_4Br (3)	90
20	0.01	acetone:H_2O (6:1)	UHP (3)	NH_4Br (3)	12

[a] H_2O_2 (aq) denotes a 30% aqueous solution of hydrogen peroxide. [b] Yields are isolated yields after acid/base extraction. [c] UHP = urea-hydrogen peroxide complex. [d] Reactions warmed to 65 ˚C. [e] Identical yield observed at rt and 65 ˚C.

dibrominated by-product at room temperature. Changing the organic component of the solvent system from acetonitrile to toluene, ethyl acetate, and acetone resulted in comparable yields of **II-2** ranging from 66 to 67% (Table 2, entries 5-7). A key breakthrough was the observation of an increase in yield of bromolactone **II-2** when the co-oxidant was changed to the commercially available urea-hydrogen peroxide complex (UHP) in acetone/water (6:1) solvent system (entry 9). In the event, employing 5 equiv of UHP as the co-oxidant returned **2** in 87% yield with 0.2 equiv of catalyst (entry 9). Unfortunately, the new co-oxidant did not perform as well in acetonitrile/H_2O returning lactone **II-2** in a moderate 67% yield (entry 8). Identical conditions at 65 ˚C (entry 10) returned **II-2** in an improved yield of 91%. Finally, having an established co-oxidant and solvent system, reducing the loading of both UHP and NH_4Br to 3 equiv each returned **II-2** in 92% in the presence of 20 mol% V_2O_5 (entry 11).

A systematic screen of reaction conditions with the overall goal of reducing the loadings of the catalyst, co-oxidant, and terminal halide source to more reasonable levels ensued. The loading of V_2O_5 could be reduced to 0.1 equiv while still returning the desired product **II-2** in excellent yield at both room temperature and 65 ˚C (entry 12). Decreasing the aqueous component of the solvent system from 6:1 acetone/water to 12:1 and 30:1 and using equal ratios of the solvent mixture resulted in a dramatic decline in the yield of **II-2** (entries 13-15) As compared to the 93% yield of **II-2** obtained from using 3 equiv of both UHP and NH_4Br (entry 16), further reduction of the loading of these reagents to

2.5 equiv each relative to substrate resulted in a reduced yield of 84% (entry 17) unless the reaction was warmed to 65 ˚C, whereby the yield rose again to 93% (entry 18). Nonetheless, lowering the catalyst loading to 0.05 equiv while maintaining the co-oxidant and halide source loading at 3 equiv each afforded the recovery of bromolactone **II-2** in only a slightly reduced 90% isolated yield (entry 19). Unfortunately, further lowering the catalyst loading to 1 mol% resulted in a very poor 12% isolated yield of **II-2** (entry 20).

2.2.3 Reinvestigation of halide salts for halolactonization with established reaction conditions

Using the otherwise optimal conditions, employing sodium bromide in lieu of ammonium bromide resulted a significantly reduced 43% yield of desired

Table 2.3. Screening of halide salts for halolactonization using established reaction conditions

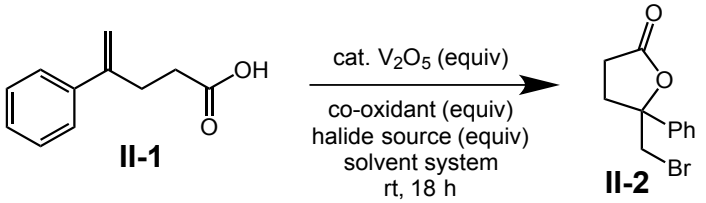

Entry	V_2O_5 (equiv)	Solvent System	Co-oxidant (equiv)[a]	Halide Source (equiv)	Yield (%)[b]
1	0.1	acetone:H_2O (6:1)	UHP (3)	NaBr (3)	43
2	0.1	acetone:H_2O (6:1)	UHP (3)	NaCl (3)	25
3	0.1	acetone:H_2O (6:1)	UHP (3)	NH_4Cl (3)	21
4	0.2	acetone:H_2O (6:1)	H_2O_2 (aq)	NaBr (5)	66
5	0.1	acetone:H_2O (6:1)	H_2O_2 (aq)	NaBr (5)	61
6	0.2	acetone:H_2O (6:1)	UHP (5)	NaBr (5)	53
7	0.1	acetone:H_2O (6:1)	UHP (5)	NaBr (5)	34

[a] H_2O_2 (aq) denotes a 30% aqueous solution of hydrogen peroxide. [b] Yields are isolated yields after acid/base extraction. [c] UHP = urea-hydrogen peroxide complex.

bromolactone product **II-2** (Table 2.3, entry 1). A significant portion of the vicinal dibromination product resulting from trapping of the initial bromonium intermediate with bromide was observed. Employing chloride salts such as sodium chloride and ammonium chloride resulted in even more drastic reduction in yields (entries 2 and 3); however, no dichlorinated product was observed. Interestingly, moderate yields were isolated when hydrogen peroxide was used in excess with either 0.2 or 0.1 equiv of catalyst (entries 4 and 5). When using UHP as the co-oxidant reduced yields were again observed with both 0.2 and 0.1 equiv of catalysts used as compared to the hydrogen peroxide (entries 6 and 7).

2.2.4 Optimal conditions

Having conducted an extensive screening process described in the previous three sections, optimal reaction conditions for the desired transformation are shown in Scheme 2.6. In detail, urea-hydrogen peroxide complex (3.0 equiv) and V_2O_5 (0.05 equiv) were dissolved in acetone/H_2O (6:1) (0.08 M relative to substrate) and stirred at 0 ˚C for 30 min. Ammonium bromide

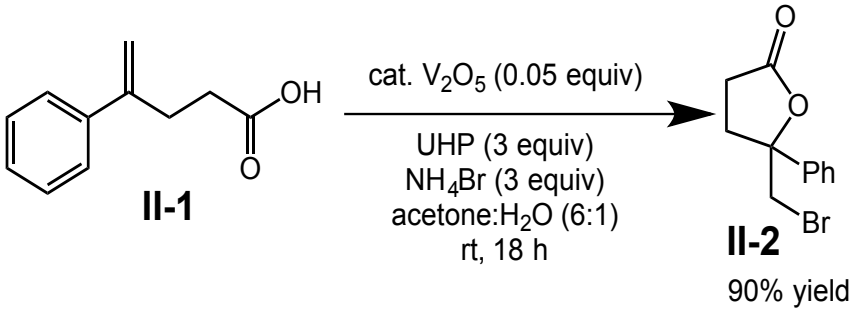

Scheme 2.6. Optimal conditions for our established bromolactonization reaction

(3.0 equiv) was added and stirred for an additional 30 min. Once the substrate (1.0 equiv) was added, the mixture was stirred for an additional 15 min at 0 ˚C before slowly warming to room temperature overnight. The major advantage of this methodology is the acceptable isolation of the desired bromolactone product after simple acid/base extraction without recourse to column chromatography. With these optimized conditions in hand, we set out to evaluate the substrate scope of the transformation.

2.2.5 Substrate scope for the bromolactonization of various alkenoic acids

Figure 2.4 depicts the substrate scope of the bromolactonization method described above. Cyclization of **II-1** returned bromolactone **II-2** in 90% isolated yield after the extensive optimization process. The method was effective for the lactonization of several related *para*-substituted 4-phenylpentenoic acid substrates in good to excellent yields ranging from 82% to 96% regardless of the electronics associated with the *para*-substituent (compounds **II-3** - **II-7**). The success of the *p*-ethyl substrate (returning lactone **II-7**) is noteworthy given that we did not observe any bromination of the relatively activated 2˚ benzylic position, suggesting that bromine radicals may not be operative in the reaction. Next, we investigated the effect of extending the carbon liker between the carboxylate nucleophile and the alkene. The disappointing yield of the corresponding δ-lactone arising from cyclization of 5-phenyl-5-hexenoic acid (**II-8a**) was improved by increasing the catalyst loading to 0.1 equiv. This

modification resulted in an improved yield of 50% (**II-8b**). In both cases, a significant amount of the undesired 5,6-dibrominated uncyclized product was isolated. In an attempt to promote the desired intramolecular cyclization, diluting the reaction in an effort to inhibit the bimolecular dibromination pathway failed to improve on the initially observed yields for this substrate. Nevertheless, the

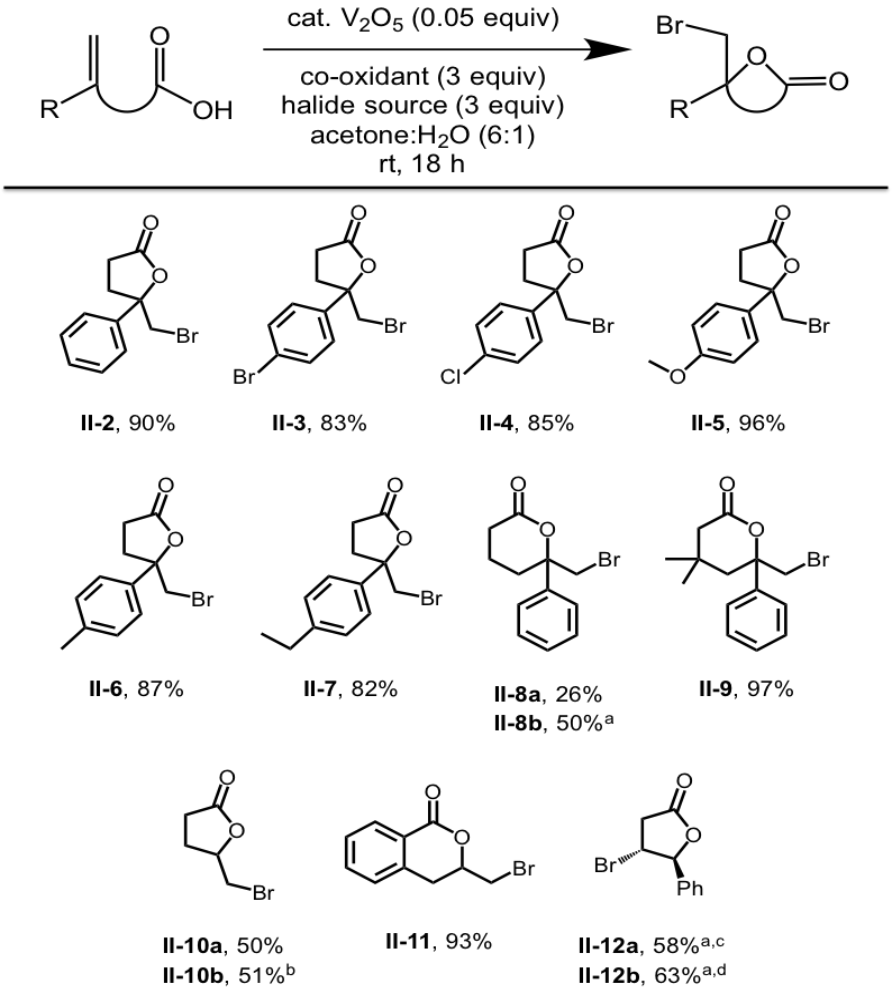

[a] Reaction conducted with 0.1 equiv. V_2O_5. [b] Reaction diluted to 0.04M. [c] A 1:1 mixture of bromolactone **12** and the corresponding α,β–unsaturated lactone was isolated. [d] 3.0 equiv *p*-toluenesulfonic acid was used as an additive.

Figure 2.4. Substrate scope for the bromolactonization of alkenoic acids using catalytic V_2O_5 and NH_4Br

incorporation of a gem-dimethyl substituent in the backbone returned the analogous 3,3-dimethyl δ-lactone **II-9** in an excellent 97% yield, taking advantage of the well-known Thorpe-Ingold effect.[65] Regardless of catalyst loading, cyclization of 4-pentenoic acid returned the corresponding unsubstituted γ-lactone in 50 to 51% yields (**II-10a** and **II-10b**). Additionally, this method provides easy access to benzolactones as highlighted by the example of the cyclization of 2-allylbenzoic acid providing **II-11** in an excellent 93% isolated yield. Finally, investigating the cyclization of *trans*-styrylacetic acid held particular interest due to the predictable lability of the initially formed bromolactone product **II-12**, which we surmised might rapidly eliminate H-Br to form the corresponding unsaturated butenolide. The optimal conditions with 0.05 equiv of V_2O_5 proved impractically sluggish. Lactonization in the presence of 0.1 equiv V_2O_5, however, returned a 58% isolated yield of a 1:1 mixture of bromolactone **II-12** and the α,β-unsaturated lactone resulting from bromide elimination (entry **II-12a**). Conducting the reaction in the presence of 3 equiv of *p*-toluenesulfonic acid somewhat attenuated the formation of the elimination product, thus returning an acceptable 63% yield of the bromolactone product. Presumably, the additive sufficiently acidifies the reaction medium so as to prevent the elimination of HBr from the initially formed bromolactone **II-12**. Attempts to locate conditions that would promote the elimination in order to favor the exclusive formation of the butenolide product were unsuccessful.

2.2.6 Control reactions for the role of urea in the transformation

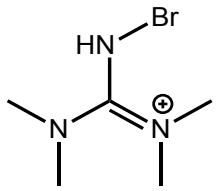

II-13

Figure 2.5. Braddock's intermediate

Since our established bromolactonization conditions employ the urea complex of hydrogen peroxide in lieu of aqueous H_2O_2, the significant concentration of urea in the system (*i.e.*, 3 equiv relative to substrate) may play an activating role in the reaction. Braddock and co-workers have highlighted the ability of electron-rich nitrogen containing nucleophiles to accelerate the *N*-bromosuccinimide (NBS) promoted bromolactonization of alkenoic acids.[66] In their work, bromolactonization of various alkenoic acids was significantly accelerated in the presence of N,N,N',N'-tetramethylguanidine through the formation of active species **II-13** (Figure 2.5).[66] Similar rate enhancements were realized with other additives including amides like N,N-dimethylformamide and N,N-dimethylacetamide.[66] Independently, the Tang and Denmark groups have detailed significant rate acceleration in halocyclization reactions in the presence of exogenous nucleophiles and Lewis bases.[67,68] In the context of our methodology, we wondered whether a similar activation of the bromenium equivalent by urea could be operative (*cf.* Braddock's intermediate **II-13**, Figure 2.5).

To probe this question, we ran reactions in parallel to determine if urea acts as a potential activating agent in our system. Thus we evaluated the synthesis of bromolactone **II-2** employing 30% aqueous H_2O_2 as the terminal

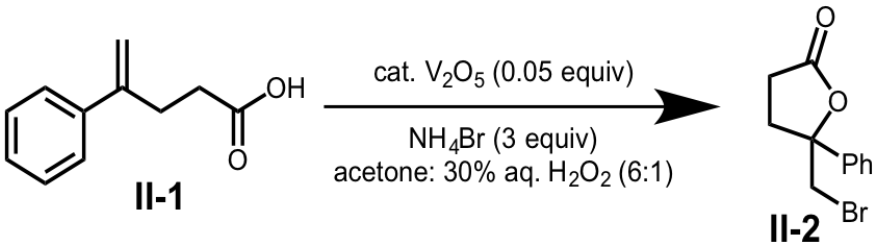

Scheme 2.7. Probing role of urea in the presence of V_2O_5 and co-oxidant, H_2O_2

oxidant instead of urea-H_2O_2 complex in the presence or absence of added urea. Comparing the yield of this transformation in the presence or absence of 3 equiv of added urea (Scheme 2.7) showed lactonization of **II-1** under these modified conditions proceeded in a comparable yield with or without added urea (cf. 40% vs 41% yield respectively). These results suggest that urea does not play a catalytic role in our system.

2.2.7 Metal oxide screening

Evaluating several other commercially available metal oxides ensured that V_2O_5 was indeed the catalyst of choice for the desired transformation. The screening of various metal oxides in a 0.1 equiv catalyst loading in the presence of 3 equiv of urea-H_2O_2 and 3 equiv NH_4Br in a 6:1 acetone/H_2O solvent system at room temperature for 18 h is presented in Table 2.4. Without the metal oxide catalyst (entry 1), no desired bromolactone was isolated or detected by ^{1}H-NMR analysis, verifying that the uncatalyzed oxidation of NH_4Br by UHP alone is not operative in our system. Entry 2 reiterates the observed 93% yield of the target

Table 2.4. Optimal conditions for the established bromolactonization reaction

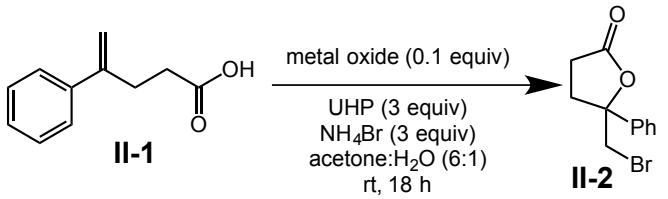

Entry	Metal oxide	Yield (%)
1	No catalyst	0
2	V_2O_5	93
3	Nb_2O_5	Trace
4	NbO_2	Trace
5	WO_3	0
6	WO_2	32
7	CrO_3	29
8	$LiTaO_3$	Trace
9	Ta_2O_5	0
10	MoO_3	78
11	MoO_2	78

bromolactone in the presence of 0.1 equiv of V_2O_5. Other commercially available metal oxides were chosen to determine whether V_2O_5 was uniquely effective at promoting the *in situ* oxidation of bromide or if there is an observable trend between oxides. Oxides of niobium, including niobium pentoxide and niobium dioxide returned trace amounts of the product along with mostly recovered starting material (entries 3-4). Interestingly, tungsten trioxide catalysis (entry 5) gave pristine starting material recovery indicating no reaction, while the use of

tungsten dioxide resulted in 32% yield of bromolactone **II-2** (entry 6). Chromium trioxide catalysis also returned bromolactone **II-2** in a 29% isolated yield (entry 7). Oxides of tantalum including lithium tantalate (entry 8) and tantalum pentoxide (entry 9) yielded minimal product.. Intriguingly, molybdenum trioxide and molybdenum dioxide returned the desired bromolactone **II-2** in acceptable yields of 78% (entries 10-11). While the reactivity of molybdenum oxides is of significance, this brief evaluation of other commercially available transition metal oxides confirmed V_2O_5 as the catalyst of choice for the desired transformation.

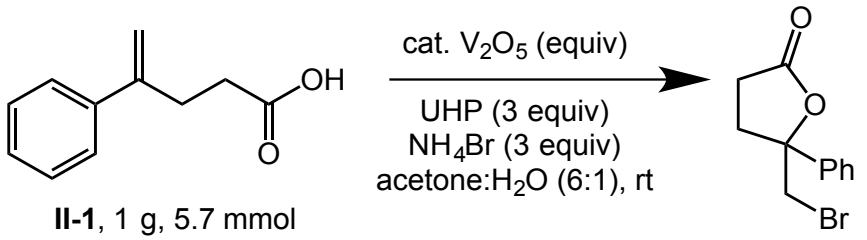

II-1, 1 g, 5.7 mmol

II-2a, 0.1 equiv V_2O_5 : 1.4 g (95%)
II-2b, 0.05 equiv V_2O_5 : 1.3 g (90%)

Scheme 2.8. Gram scale synthesis of bromolactone **II-2**

2.2.8 Scaled experiments

The ability of the method to perform at larger scale is crucial in its extension as a common method for bromination. A one gram portion (5.7 mmol) of 4-phenylpentenoic acid **II-1** was cyclized in excellent yield employing either 0.1 or 0.05 equiv of catalyst V_2O_5. Bromolactone **II-2** was isolated in acceptable purity in a 95% or 90% yield respectively by means of a simple acid/base extraction without requiring chromatographic purification (Scheme 2.8). Similarly,

trans-styrylacetic acid **II-15** was converted to bromolactone **II-12** in a 66% yield on a 5.7 mmol scale indicating that the modified protocol in the presence of *p*-toluenesulfonic acid additive is also reasonably scalable (Scheme 2.9). The versatility of both the optimized and the modified methodology for easy, safe and efficient bromolactonization helps establish our protocol as a viable process for organic bromination.

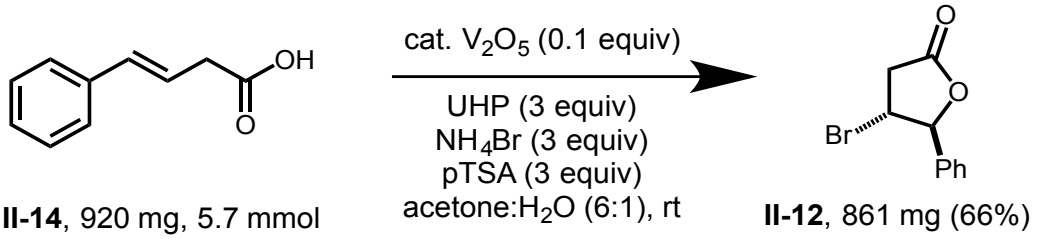

II-14, 920 mg, 5.7 mmol

II-12, 861 mg (66%)

Scheme 2.9. Near gram-scale synthesis of I**I-12**

2.2.9 α-Halogenation of β-diketone compounds

Extending on the versatility of the methodology discussed above, the idea that our optimal conditions might also represent a convenient means to effect other useful transformations including the α-halogenation of activated methylene moieties became our final endeavor. To probe this option as an extension of methodology, a brief investigation for the α-bromination of two β-diketone substrates was conducted (Scheme 2.10). Diketones **II-15** and **II-16** were mono-brominated in 92% (**II-17**) and 94% (**II-18**) yield, in the presence of 0.05 equiv V_2O_5 using identical conditions to our optimized bromolactonization protocol.

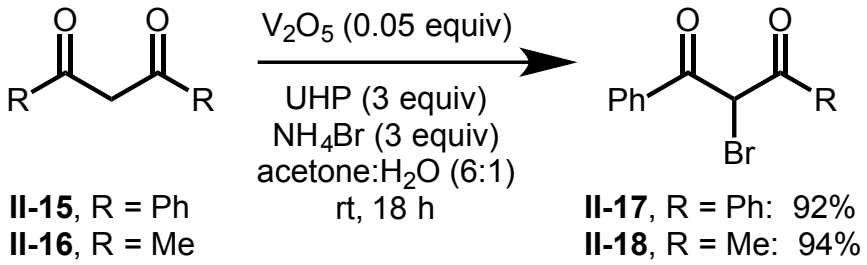

II-15, R = Ph
II-16, R = Me

II-17, R = Ph: 92%
II-18, R = Me: 94%

Scheme 2.10. α-Monobromination of 1,3-β-diketones

These results indicate that our optimal protocol for the *in situ* oxidation of bromide to bromenium may provide a convenient route for other related transformations.

2.3 Conclusions

Presented in this chapter was a full account of the development of a novel method for the bromolactonization of alkenoic acids catalyzed by vanadium (V) oxide in the presence of a 3 equiv each of UHP and NH_4Br. The method hinges on the *in situ* oxidation of bromide to bromenium equivalent as discussed early in the chapter, and inspired by early work devoted to understanding haloperoxidase-mediated halide oxidation in marine organisms. The methodology presented herein allows for facile access to bromolactone products in acceptable purity without subjection to column chromatography. The role of urea in the transformation was probed, and results indicate no competitive reactivity through Braddock-type intermediate (*c.f.* Figure 2.5, compound **II-13**). Preliminary data indicates that other transition metal oxides, most notably oxides of molybdenum, can promote similar reactivity under our established protocol. Preliminary investigation of our reaction conditions for the α-bromination of β-

diketones suggests that this bromination strategy may be more broadly applicable to other related reactions.

2.4 Experimental Section

2.4.1 General Information

All reagents were purchased from commercial sources and used without purification. Vanadium(V) oxide was purchased from Sigma Aldrich in a 99.99% purity. Preparation of the alkenoic acid substrates followed an established protocol that included Wittig methylenation followed by saponification of the terminal ester to the carboxylic acid.[69] All known substrates had ^{1}H-NMR in agreement with previous reports. ^{1}H and ^{13}C NMR spectra were collected on 300 and 500 MHz NMR spectrometers (Bruker) using $CDCl_3$. Chemical shifts are reported in parts per million (ppm) and were referenced to the residual solvent peak. All known lactone products were characterized by ^{1}H and ^{13}C NMR and were in agreement with samples reported elsewhere. Compound **II-3** was a new compound, and was characterized with ^{1}H and ^{13}C NMR, IR, and HRMS.

2.4.2 General procedure for synthesis of halolactonization products II-2 - II-12

Urea-hydrogen peroxide complex (80.1 mg, 0.851 mmol, 3.0 equiv) and vanadium pentoxide (5.20 mg, 0.028 mmol, 0.1 equiv) were dissolved in acetone/H_2O (6:1) and stirred at 0 ˚C for 30 minutes. To this ice-cold solution,

ammonium bromide (0.0803 g, 0.851 mmol, 3.0 equiv) was added and stirred for an additional 30 minutes. After addition of the substrate (50.0 mg, 0.284 mmol, 1.0 equiv), the mixture was allowed to stir for an additional 15 minutes at 0 ˚C before gradually warming to room temperature overnight.

2.4.3 Work-up procedure for organic soluble products (II-2 - II-8, II-10 - II-12)

The reaction mixture was diluted with water (15 mL) and extracted with DCM (3 X 15mL). The combined organics were washed with saturated aqueous sodium bicarbonate. The combined aqueous layers were back-extracted with DCM (15 mL).

Finally, all organic extracts were combined (60 mL total volume), dried over anhydrous sodium sulfate, concentrated by rotary evaporation, and dried *in vacuo*.

2.4.4 Work-up procedure for aqueous soluble product II-9

For the preparation of lactone **II-9**, the crude reaction mixture was concentrated by rotary evaporation in the presence of a small amount of silica gel. This silica gel plug was then subjected to column chromatography (20% EtOAc in hexanes to 40% EtOAc in hexanes).

2.4.5 Scale-up procedure for gram scale synthesis of II-2

Urea-hydrogen peroxide complex (0.160 g, 17.1 mmol, 3.0 equiv) and V_2O_5 (0.103 g, 0.570 mmol, 0.1 equiv) were stirred in acetone/H_2O (6:1) at 0 ˚C for 30 min. Ammonium bromide (0.167 g, 17.1 mmol, 3.0 eq) was added and allowed to stir for an additional 30 min at 0 ˚C. Alkenoic acid **II-1** (1.0 g, 5.7 mmol, 1 equiv) was added and stirred for 15 minutes at 0 ˚C. The flask was sealed with septum and purged with N_2. The reaction was allowed to warm to room temperature while stirring overnight.

The reaction mixture was diluted with water (100 mL) and extracted with DCM (4 x 100 mL). The combined organics were washed with saturated aqueous sodium bicarbonate (200 mL). The combined aqueous layers were back-extracted with DCM (100 mL). Finally, all organic extracts were combined (500 mL total volume), dried over anhydrous sodium sulfate, concentrated by rotary evaporation, and dried *in vacuo*. Lactone **II-2** was isolated in a 95% yield (1.4 g).

2.4.6 Scale-up procedure for gram scale synthesis of II-10

Urea-hydrogen peroxide complex (1.601 g, 17.02 mmol, 3.0 equiv) and V_2O_5 (0.206 g, 1.135 mmol, 0.2 equiv) were stirred in acetone/H_2O (6:1) at 0 ˚C for 30 min. Ammonium bromide (1.667 g, 17.02 mmol, 3.0 eq) was added and allowed to stir for an additional 30 min at 0 ˚C. Alkenoic acid **II-15** (0.9202 g, 5.67 mmol, 1.0 equiv) was added followed by *para*-toluenesulfonic acid (3.24 g, 17.02 mmol, 3.0 equiv) and stirred for 15 minutes at 0 ˚C. The flask was sealed with a

septum and purged with N_2. The reaction was allowed to warm to room temperature while stirring overnight.

The reaction mixture was diluted with water (100 mL) and extracted with DCM (4 x 100 mL). The combined organics were washed with saturated aqueous sodium bicarbonate (200 mL) twice. The combined aqueous layers were back-extracted with DCM (100 mL). Finally, all organic extracts were combined (500 mL total volume), dried over anhydrous sodium sulfate, concentrated by rotary evaporation, and dried *in vacuo*. Lactone **II-12** was isolated in a 66% yield (861 mg).

2.4.7 General procedure and work-up for synthesis of α-brominated products II-17 - II-18

Urea-hydrogen peroxide complex (80.1 mg, 0.851 mmol, 3.0 equiv) and vanadium pentoxide (5.20 mg, 0.028 mmol, 0.1 equiv) were dissolved in acetone/H_2O (6:1) and stirred at 0 ˚C for 30 minutes. To this ice-cold solution, ammonium bromide (, 0.0803 g, 0.851 mmol, 3.0 equiv) was added and stirred for an additional 30 minutes. After addition of the substrate (50.0 mg, 0.3 mmol, 1.0 equiv), the mixture was allowed to stir for an additional 15 minutes at 0 ˚C before gradually warming to room temperature overnight.

The reaction mixture was diluted with water (15 mL) and extracted with DCM (3 X 15mL). The combined organics were washed with saturated aqueous

sodium bicarbonate. The combined aqueous layers were back-extracted with DCM (15 mL).

Finally, all organic extracts were combined (60 mL total volume), dried over anhydrous sodium sulfate, concentrated by rotary evaporation, and dried *in vacuo*.

2.4.8 Analytical data for halolactonization products II-2 - II-13

5-(bromomethyl)-5-phenyloxolane-2-one, **II-2**[70]

^{1}H NMR (300 MHz, $CDCl_3$): δ 7.44-7.37 (m, 5H), 3.78-3.70 (dd, *J* = 10.2, 18.3 Hz, 2H), 2.88-2.79 (m, 2H), 2.62-2.52 (m, 2H); ^{13}C NMR (90 MHz, $CDCl_3$): δ 175.4, 140.8, 128.9, 128.7, 124.9, 86.4, 41.0, 32.4, 29.1

5-(bromomethyl)-5-(4-bromophenyl)dihydrofuran-2-(3*H*)-one, **II-3**

^{1}H NMR (300 MHz, $CDCl_3$): δ 7.57-7.52 (dt, *J* = 2.4, 4.5, 9.3, 11.1, 13.1 Hz, 2H), 7.32-7.28 (dt, *J* = 2.7, 4.5, 9.3, 11.4, 14.4 Hz, 2H), 3.73-3.64 (dd, *J* = 11.4, 13.5 Hz, 2H), 2.85-2.73 (m, 2H), 2.62-2.50 (m, 2H); ^{13}C NMR (90 MHz, $CDCl_3$): δ 174.9, 139.8, 132.0, 126.7, 122.8, 85.9, 40.4, 32.3, 28.9; IR (DCM): 1784 cm^{-1}; HRMS (ESI-TOF, positive mode): $C_{11}C_{10}O_2Br_2$; Calculated (M+H): 332.9126; Found: 332.9138.

5-(bromomethyl)-5-(4-chlorophenyl)dihydrofuran-2-(3*H*)-one, **II-4**[71]

^{1}H NMR (300 MHz, $CDCl_3$): δ 7.41-7.34 (m, 4H), 3.74-3.64 (dd, *J* = 11.4, 16.8 Hz, 2H), 2.86-2.73 (m, 2H), 2.63-2.50 (m, 2H); ^{13}C NMR (90 MHz, $CDCl_3$): δ 175.1, 139.2, 134.7, 129.0, 126.4, 85.9, 40.6, 32.4, 28.9

5-(bromomethyl)-5-(4-methoxyphenyl)dihydrofuran-2(3*H*)-one, **II-5**[71]

^{1}H NMR (300 MHz, $CDCl_3$): δ 7.36-7.31 (dt, *J* = 3.0, 5.1, 9.9, 12.0, 15.0 Hz, 2H), 6.95-6.90 (dt, *J* = 3.0, 5.1, 9.9, 12.0, 15.0 Hz, 2H), 3.82 (s, 3H), 3.75-3.64 (dd, *J* = 11.1, 20.7 Hz, 2H), 2.86-2.70 (m, 2H), 2.61-2.48 (m, 2H); ^{13}C NMR (90 MHz, $CDCl_3$): δ 175.4, 159.8, 132.6, 126.2, 114.2, 86.3, 55.3, 41.0, 32.2, 29.1

5-(bromomethyl)-5-(4-methylphenyl)dihydrofuran-2(3*H*)-one, **II-6**[71]

^{1}H NMR (300 MHz, $CDCl_3$): δ 7.31 (d, *J* = 8.4 Hz, 2H), 7.22 (d, *J* = 8.1 Hz, 2H), 3.76-3.67 (dd, *J* = 11.4, 17.4 Hz, 2H), 2.87-2.75 (m, 2H), 2.61-2.49 (m, 2H), 2.37 (s, 3H); ^{13}C NMR (90 MHz, $CDCl_3$): δ 175.5, 138.6, 137.7, 129.5, 124.8, 86.4, 41.0, 32.3, 29.0, 21.0

6-(bromomethyl)-6-phenyloxan-2-one, **II-7**[70]

^{1}H NMR (300 MHz, $CDCl_3$): δ 7.58-7.30 (m, 5H), 3.72-3.63 (dd, *J* = 11.1, 15.9 Hz, 1.65H), 2.85-2.32 (m, 3.77), 1.90-1.79 (m, 1H), 1.66-1.52 (m, 1H); ^{13}C NMR (90 MHz, $CDCl_3$): δ 170.5, 140.2, 129.0, 128.5,125.39, 85.1, 41.5, 30.0, 29.1, 16.2

3-(bromomethyl)-3,4-dihydro-1*H*-2-benzopyran-1-one, **II-8**[70]

^{1}H NMR (300 MHz, $CDCl_3$): δ 8.10 (dd, *J* = 0.9, 7.8 Hz, 1H), 7.58 (td, *J* = 1.5, 7.5 Hz, 1H), 7.40 (t, *J* = 7.5 Hz, 1H), 7.30 (d, *J* = 7.8 Hz, 1H), 4.79-4.70 (m, 1.0), 3.71-3.57 (m, 1H), 3.25-3.13 (m, 1.0); ^{13}C NMR (90 MHz, $CDCl_3$): δ 164.3, 137.9, 134.2, 130.4, 128.0, 127.7, 124.5, 76.7, 32.5, 31.5

5-(bromomethyl)oxolan-2-one, **II-9**[70]

^{1}H NMR (300 MHz, $CDCl_3$) δ 4.80-4.72 (m, 1H), 3.61-3.51 (m, 2H), 2.74-2.58 (m, 2H), 2.54-2.40 (m, 1H), 2.19-2.07 (m, 1H); ^{13}C NMR (90 MHz, $CDCl_3$) δ 176.1, 77.8, 34.0, 28.3, 26.2

4-(bromodihydro)-5-phenyl-2-(*3H*)-furanone, **II-10**[72]

^{1}H NMR (300 MHz, $CDCl_3$): δ 7.48-7.36 (m, 5H), 5.68 (d, *J* = 5.1 Hz, 1H), 4.42-4.36 (ddd, *J* = 5.4, 6.3, 7.5 Hz, 1H), 3.30-3.21 (dd, *J* = 7.2, 18.0 Hz, 1H), 3.03-2.95 (dd, *J* = 6.3, 18.0 Hz, 1H); ^{13}C NMR (90 MHz, $CDCl_3$): δ 173.0, 135.8, 129.3, 129.0, 125.4, 87.8, 45.5, 38.8

5-(bromomethyl)-5-(4-ethylphenyl)dihydrofuran-2(3*H*)-one, **II-11**

^{1}H NMR (300 MHz, $CDCl_3$): δ 7.36-7.24 (m, 4H), 3.78-3.67 (dd, *J* = 9.3 Hz, 17.4 Hz, 2H), 2.86-2.76 (m, 2H), 2.72-2.51 (m, 4H), 1.25 (t, *J* = 7.5 Hz, 3H); ^{13}C NMR

(90 MHz, $CDCl_3$): δ 175.6, 144.9, 137.9, 128.3, 124.9, 86.5, 41.1, 32.3, 29.1, 28.4, 15.4

2-bromo-1-phenyl-1,3-butanedione, **II-12**[73]

^{1}H NMR (300 MHz, $CDCl_3$): δ 8.04 (d, *J* = 17.4 Hz, 2H), 7.65 (t, *J* = 9.3, 1H), 7.50 (t, *J* = 9.0 Hz, 2H), 5.64 (s, 1H), 2.47 (s, 3H); ^{13}C NMR (90 MHz, $CDCl_3$): δ 198.2, 189.9, 134.5, 133.7, 129.3, 129.0, 52.9, 27.1

2-bromo-1,3-diphenylpropan-1,3-dione, **II-13**[73]

^{1}H NMR (300 MHz, $CDCl_3$): δ 8.01 (d, *J* = 9.0 Hz, 4H), 7.62 (tt, *J* = 3.0 Hz, 6.0 Hz, 2H), 7.48 (t, *J* = 15.0 Hz, 4H), 6.60 (s, 1H); ^{13}C NMR (90 MHz, $CDCl_3$): δ 189.0, 134.3, 133.8, 129.1, 129.0, 52.6

2.4.9 ^{1}H and ^{13}C NMR for compounds II-2 - II-13

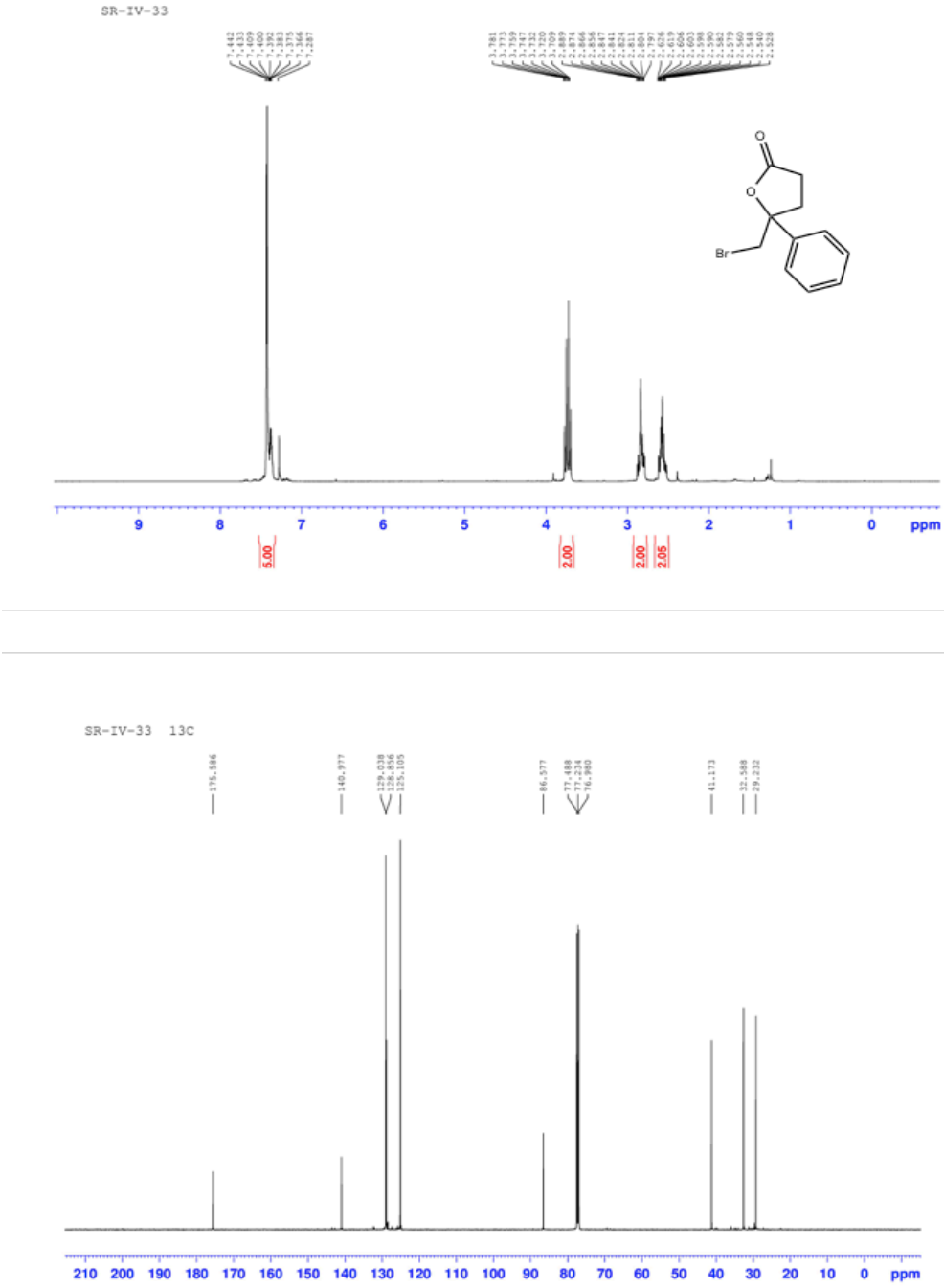

Figure 2.6. ^{1}H and ^{13}C NMR of **II-2** in $CDCl_3$

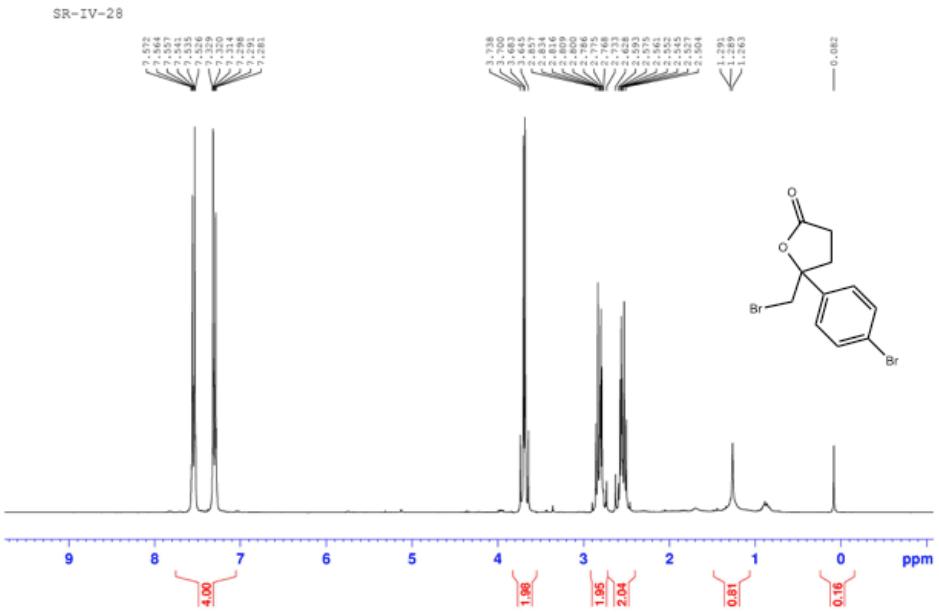

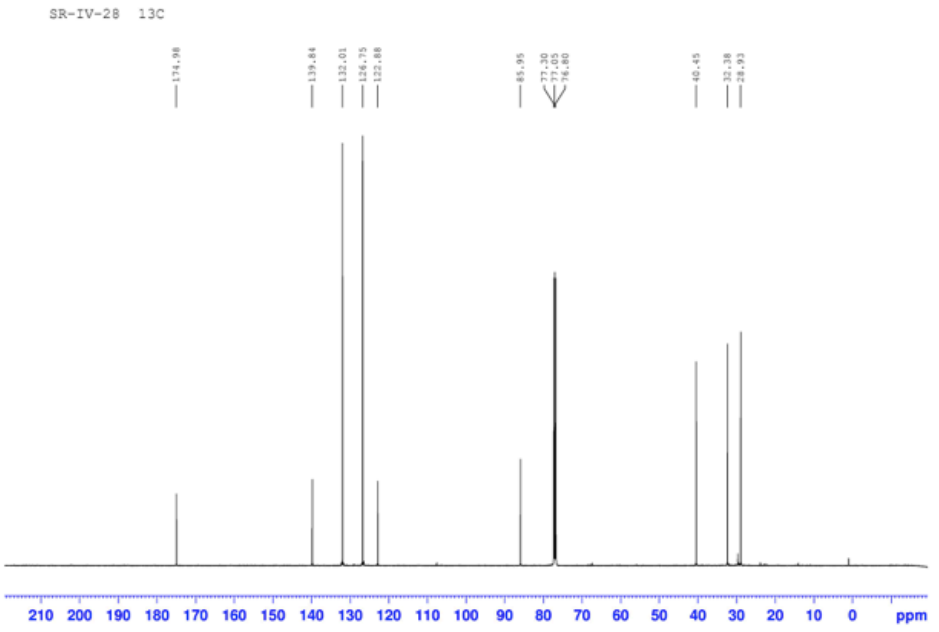

Figure 2.7. ^{1}H and ^{13}C NMR of **II-3** in $CDCl_3$

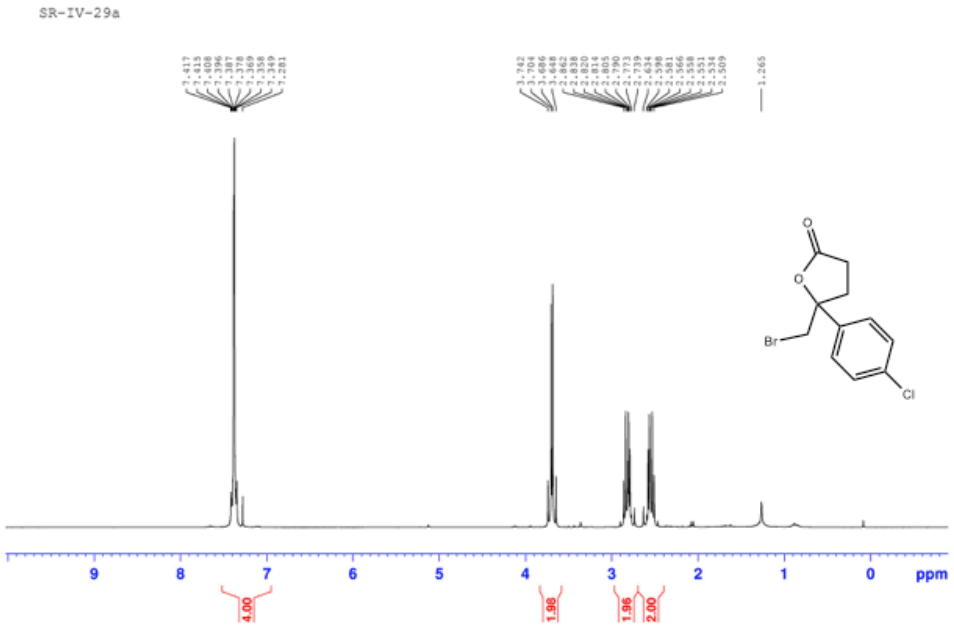

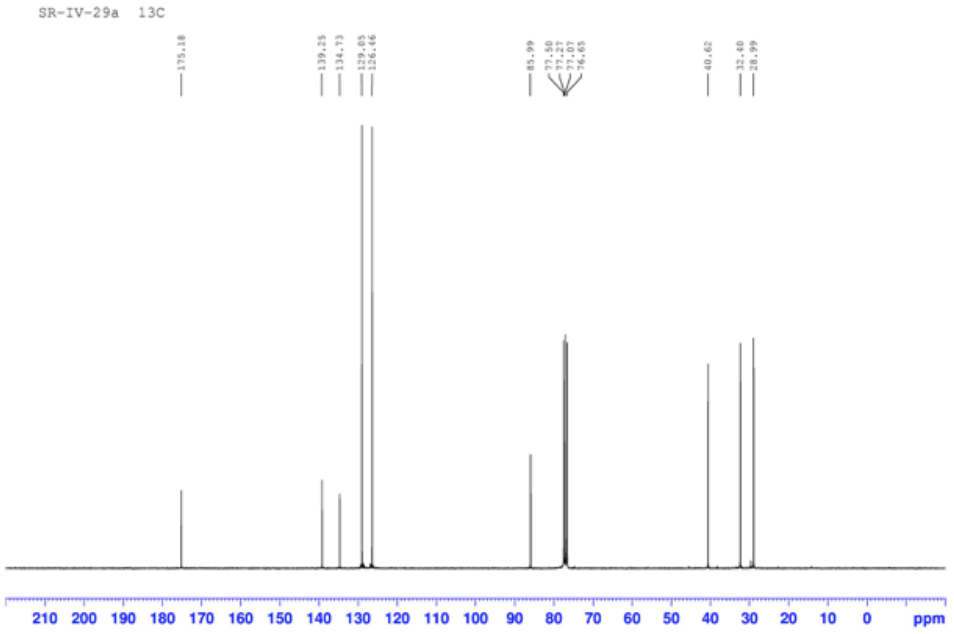

Figure 2.8. ^{1}H and ^{13}C NMR of **II-4** in $CDCl_3$

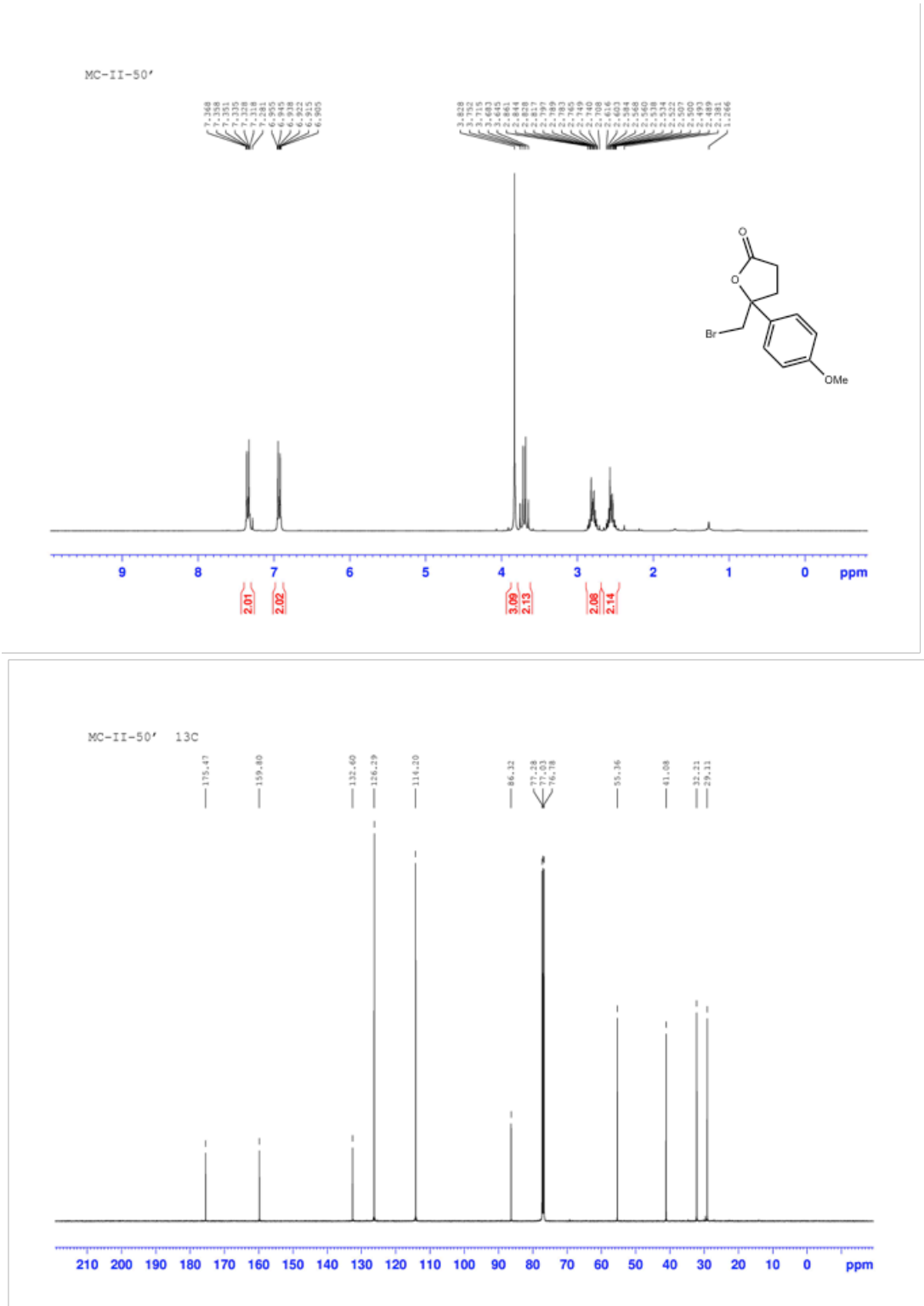

Figure 2.9. ^{1}H and ^{13}C NMR of **II-5** in $CDCl_3$

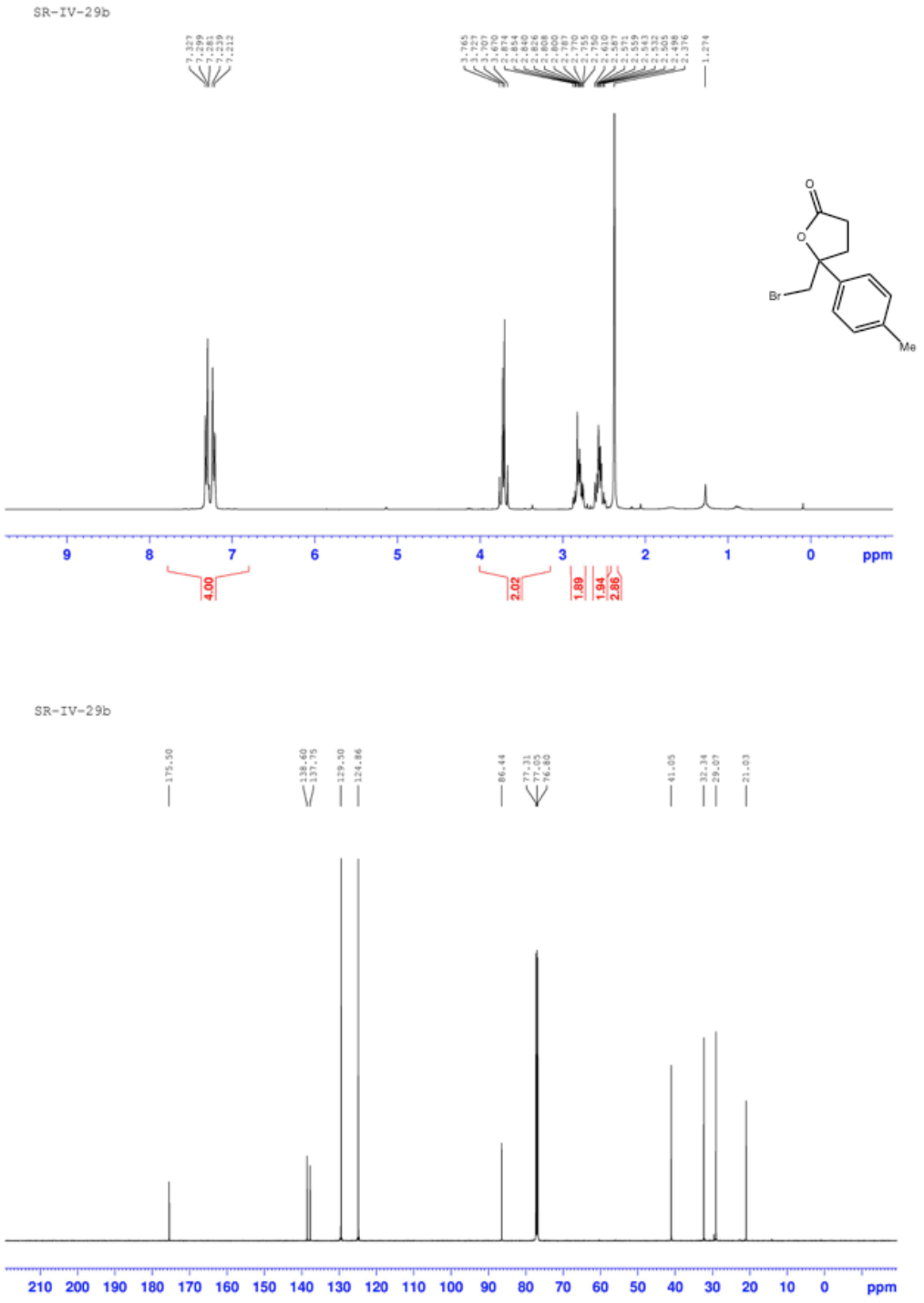

Figure 2.10. ^{1}H and ^{13}C NMR of **II-6** in $CDCl_3$

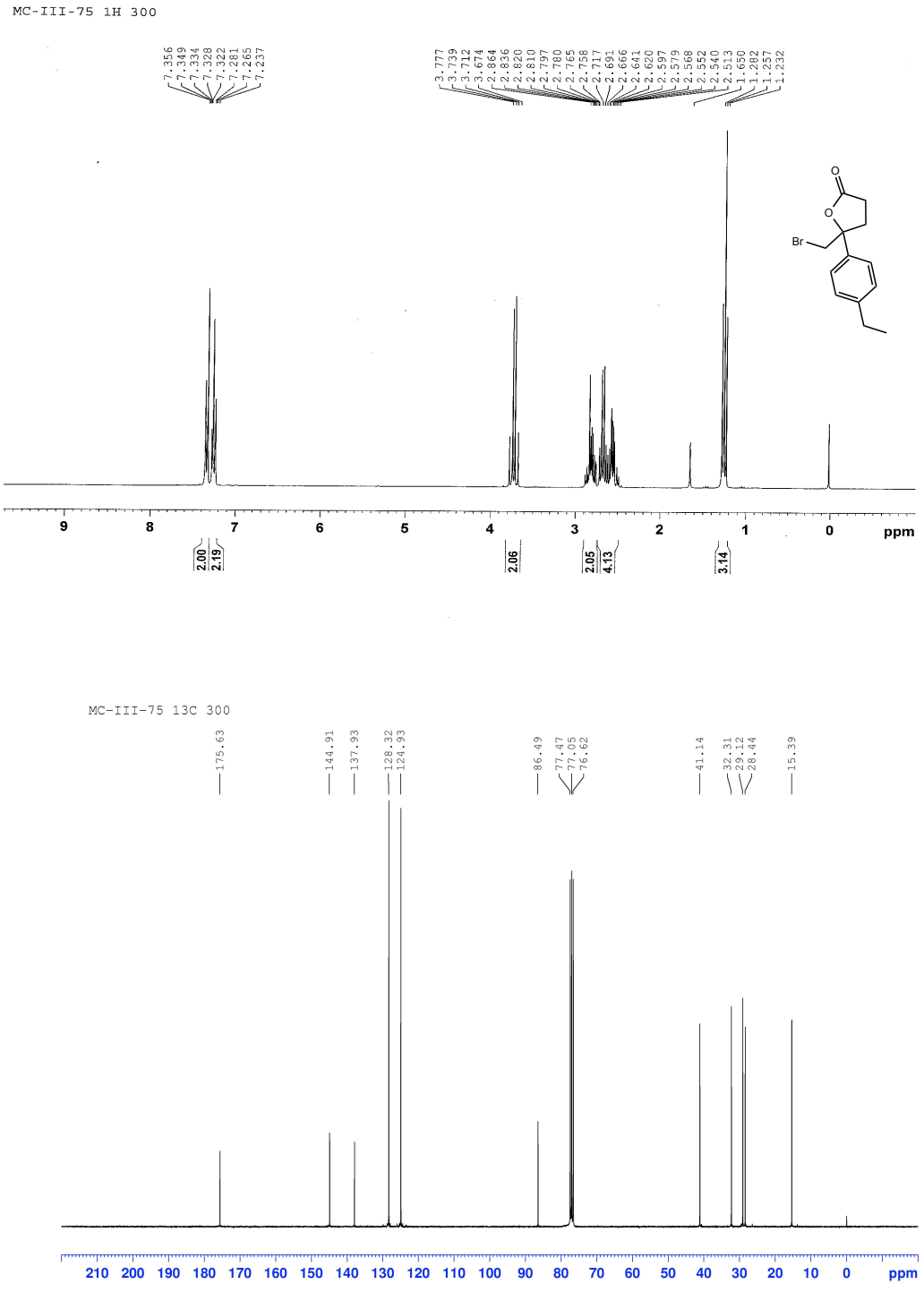

Figure 2.11. ^{1}H and ^{13}C NMR of **II-7** in $CDCl_3$

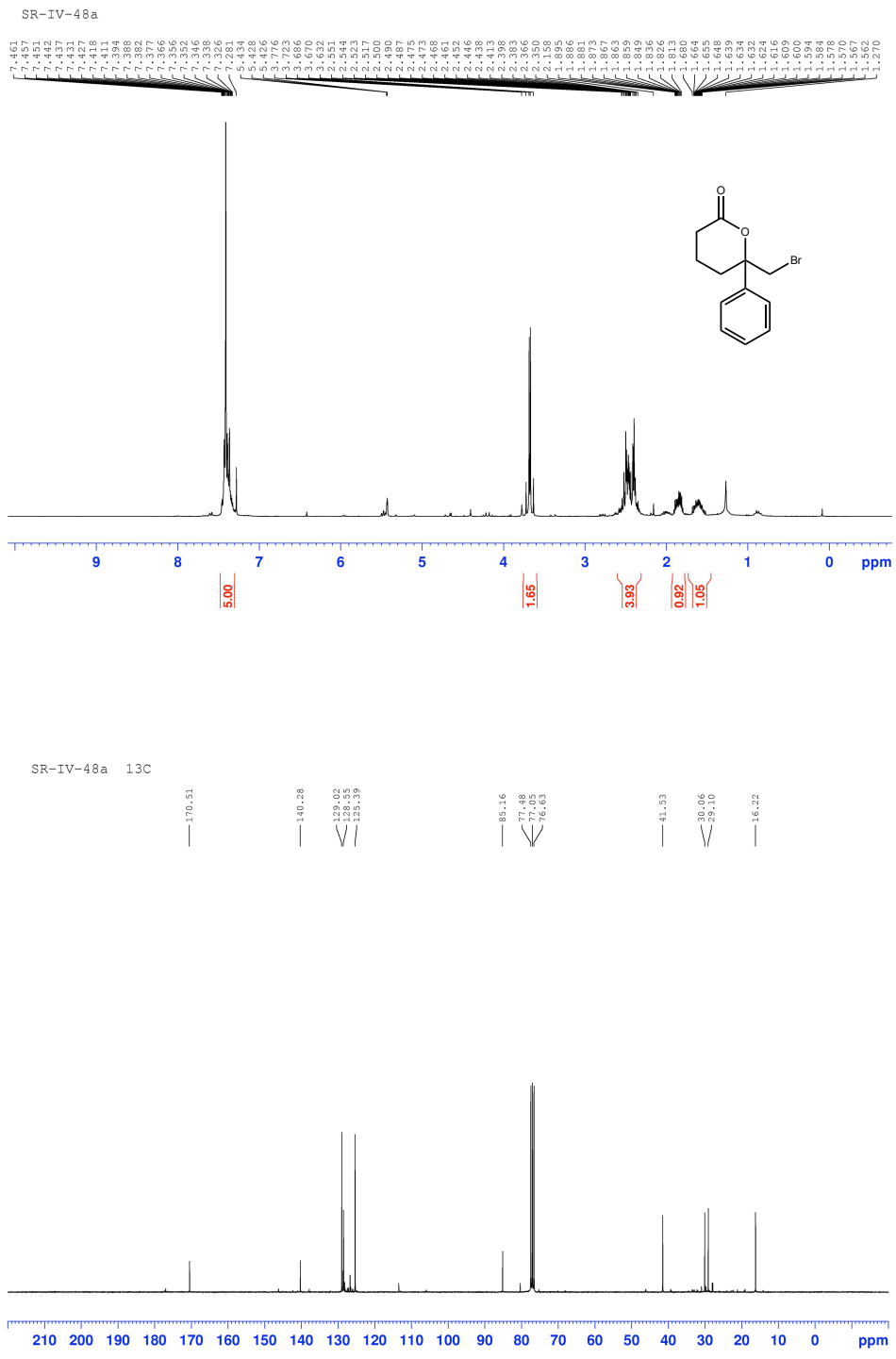

Figure 2.12. ^{1}H and ^{13}C NMR of **II-8** in $CDCl_3$

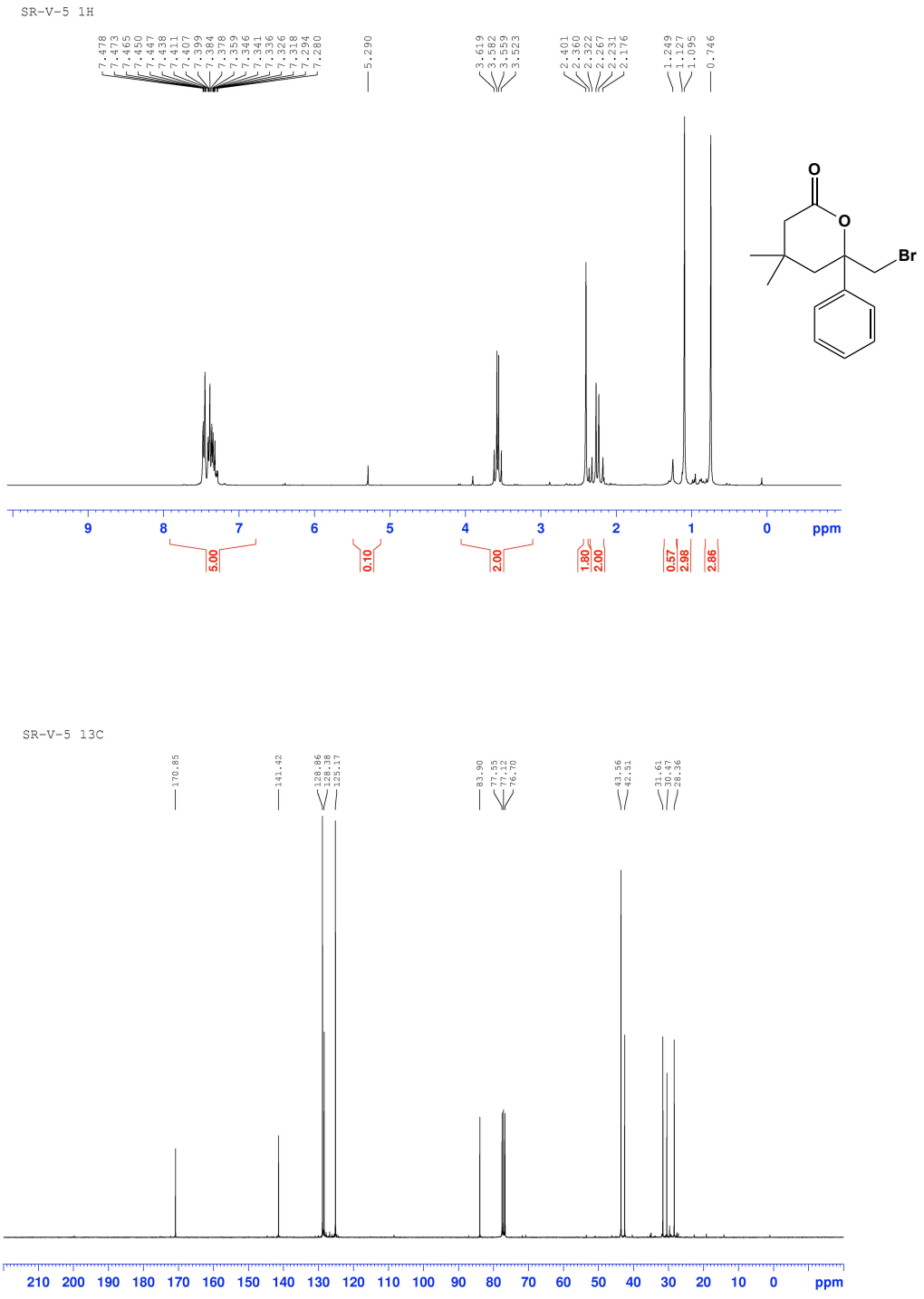

Figure 2.13. ^{1}H and ^{13}C NMR of **II-9** in $CDCl_3$

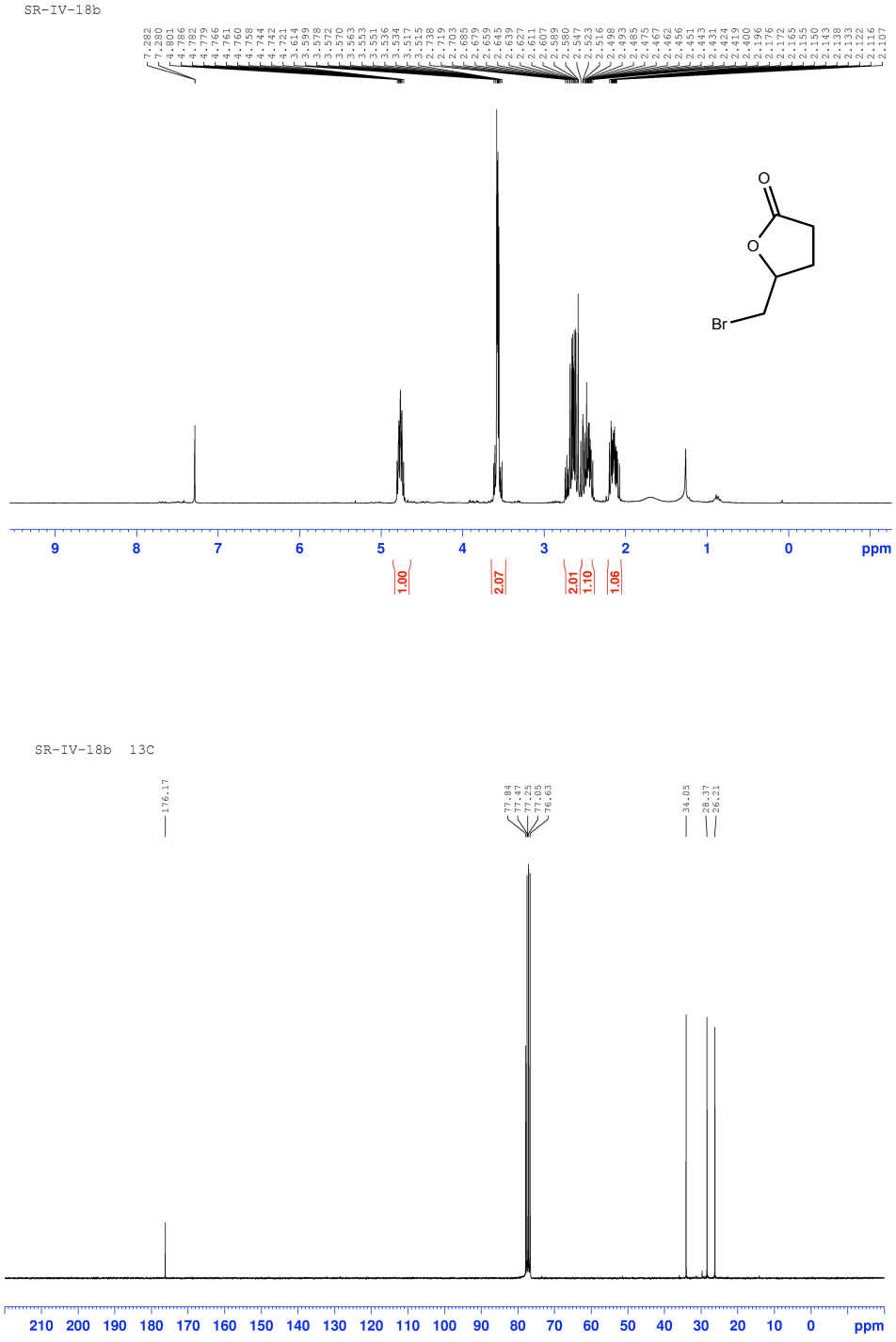

Figure 2.14. ^{1}H and ^{13}C NMR of **II-10** in $CDCl_3$

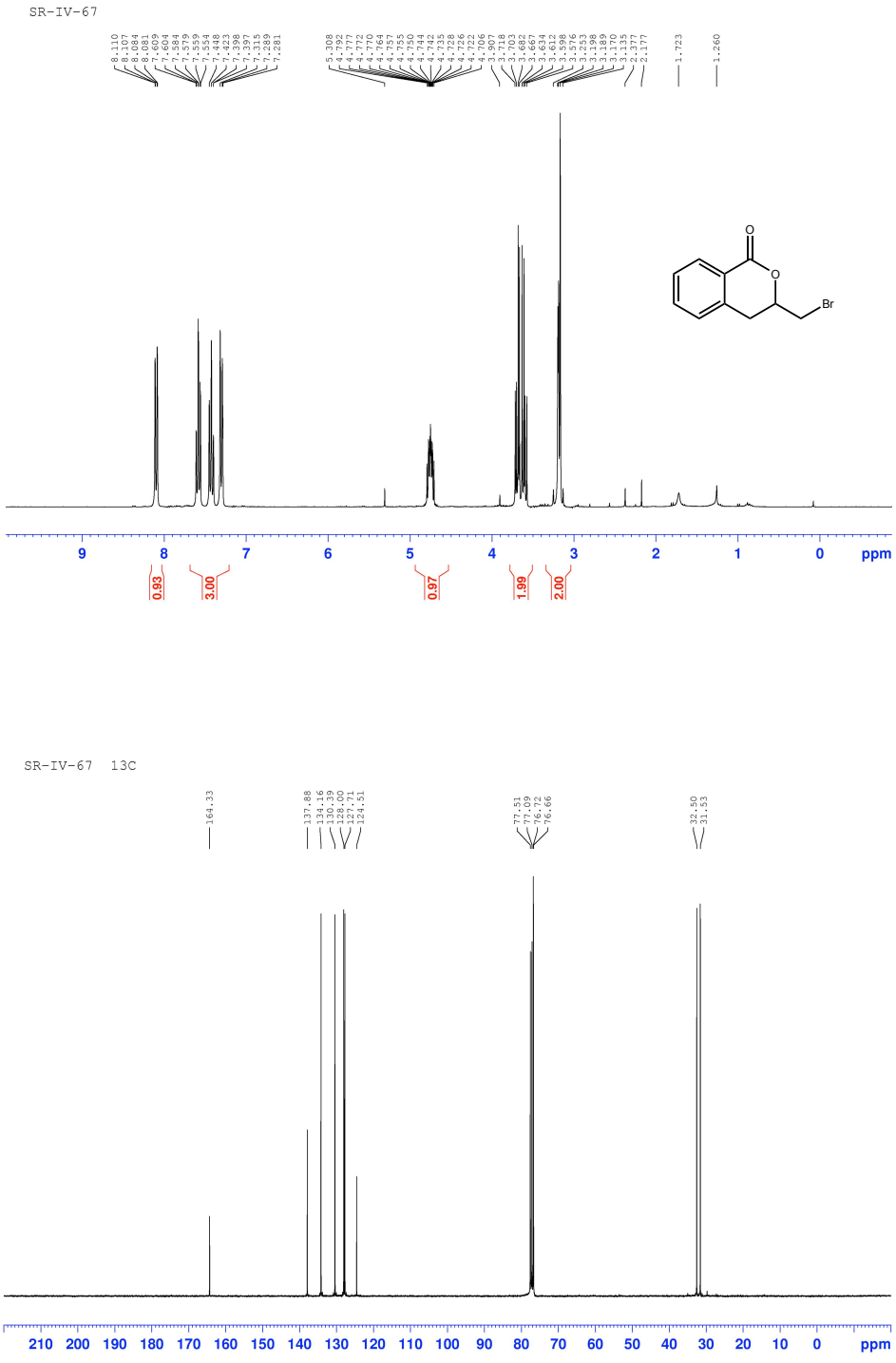

Figure 2.15. ^{1}H and ^{13}C NMR of **II-11** in $CDCl_3$

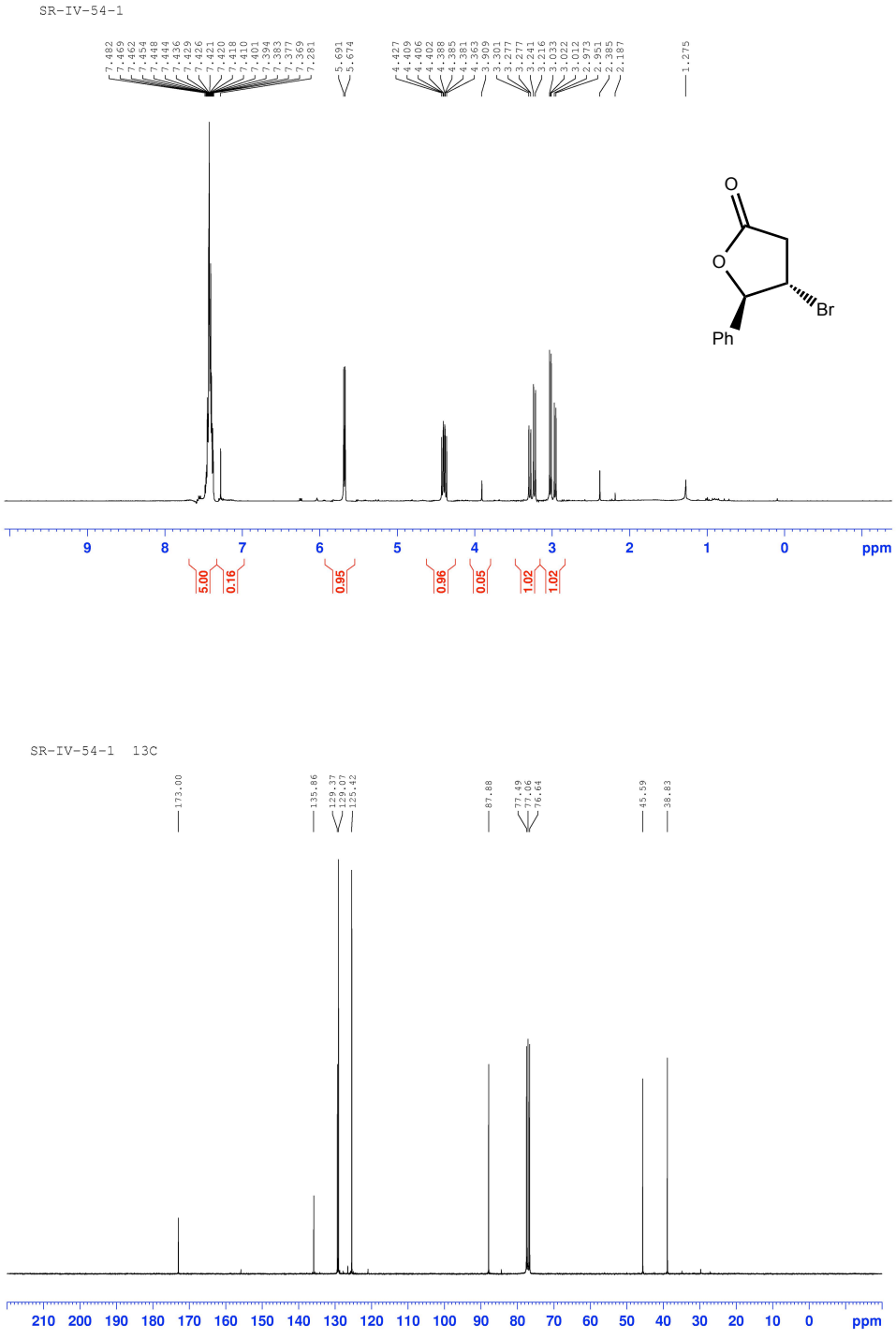

Figure 2.16. ^{1}H and ^{13}C NMR of **II-12** in $CDCl_3$

2.5 References and Notes

(1) Campbell, M. L.; Rackley, S. A.; Giambalvo, L. N.; Whitehead, D. C. *Tetrahedron* **2015**, *71*, 4888.

(2) Campbell, M. L.; Rackley, S. A.; Giambalvo, L. N.; Whitehead, D. C. *Tetrahedron Lett.* **2014**, *55*, 5680-5682.

(3) Everett, R. R.; Butler, A. *Inorg. Chem.* **1989**, *28*, 393-395.

(4) Khan, A. T.; Goswami, P. *Tetrahedron Lett.* **2005**, *46*, 4937-4940.

(5) Bora, U.; Bose, G.; Chaudhuri, M. K.; Dhar, S. S.; Gopinath, R.; Khan, A. T.; Patel, B. K. *Org. Lett.* **2000**, *2*, 247-249.

(6) Wever, R.; van der Horst, M. A. *Dalton Trans.* **2013**, *42*, 11778-11786.

(7) Gribble, G. W. *Chemosphere* **2003**, *52*, 289-297.

(8) Butler, A.; Walker, J. V. *Chem. Rev.* **1993**, *93*, 1937-1944.

(9) Butler, A. *Coord. Chem. Rev.* **1999**, *187*, 17-35.

(10) Nieder, M.; Hager, L. *Arch. Biochem. Biophys.* **1985**, *240*, 121-127.

(11) James, D. M.; Kunze, H. B.; Faulkner, D. J. *J. Nat. Prod.* **1991**, *54*, 1137-1140.

(12) Gschwend, P. M.; MacFarlane, J. K.; Newman, K. A. *Science (Washington, D. C., 1883-)* **1985**, *227*, 1033-1035.

(13) Leblanc, C.; Vilter, H.; Fournier, J. B.; Delage, L.; Potin, P.; Rebuffet, E.; Michel, G.; Solari, P. L.; Feiters, M. C.; Czjzek, M. *Coord. Chem. Rev.* **2015**, *301-302*, 134-146.

(14) Fernandez-Fueyo, E.; van Wingerden, M.; Renirie, R.; Wever, R.; Ni, Y.; Holtmann, D.; Hollmann, F. *ChemCatChem* **2015**, *7*, 4035-4038.

(15) But, A.; Le Notre, J.; Scott, E. L.; Wever, R.; Sanders, J. P. M. *ChemSusChem* **2012**, *5*, 1199-1202.

(16) Renirie, R.; Pierlot, C.; Wever, R.; Aubry, J.-M. *J. Mol. Catal. B: Enzym.* **2009**, *56*, 259-264.

(17) Wever, R.; Hartog, A. F.; Renirie, R. *Prepr. Ext. Abstr. ACS Natl. Meet., Am. Chem. Soc., Div. Environ. Chem.* **2005**, *45*, 483-485.

(18) ten Brink, H. B.; Dekker, H. L.; Schoemaker, H. E.; Wever, R. *J. Inorg. Biochem.* **2000**, *80*, 91-98.

(19) van Schijndel, J. W. P. M.; Vollenbroek, E. G. M.; Wever, R. *Biochim. Biophys. Acta, Protein Struct. Mol. Enzymol.* **1993**, *1161*, 249-256.

(20) Drew, E. T.; Yang, Y.; Russo, J. A.; Campbell, M. L.; Rackley, S. A.; Hudson, J.; Schmuki, P.; Whitehead, D. C. *Catal. Sci. Technol.* **2013**, *3*, 2610-2613.

(21) Vilter, H. *Phytochemistry* **1984**, *23*, 1387-1390.

(22) Colpas, G. J.; Hamstra, B. J.; Kampf, J. W.; Pecoraro, V. L. *J. Am. Chem. Soc.* **1996**, *118*, 3469-3478.

(23) De Boer, E.; Wever, R. *J. Biol. Chem.* **1988**, *263*, 12326-12332.

(24) Wischang, D.; Radlow, M.; Hartung, J. *Dalton Trans.* **2013**, *42*, 11926-11940.

(25) Butler, A.; Sandy, M. *Nature* **2009**, *460*, 848-854.

(26) Geibig, D.; Wilcken, R.; Bangesh, M.; Plass, W. In *NIC Symposium* 2008, p 71-78.

(27) Everett, R. R.; Soedjak, H. S.; Butler, A. *J. Biol. Chem.* **1990**, *265*, 15671-15679.

(28) De la Rosa, R. I.; Clague, M. J.; Butler, A. *J. Am. Chem. Soc.* **1992**, *114*, 760-761.

(29) Soedjak, H. S.; Butler, A. *Biochemistry* **1990**, *29*, 7974-7981.

(30) Clague, M. J.; Butler, A. *J. Am. Chem. Soc.* **1995**, *117*, 3475-3484.

(31) Clague, M. J.; Keder, N. L.; Butler, A. *Inorg. Chem.* **1993**, *32*, 4754-4761.

(32) Butler, A.; Clague, M. J. *Adv. Chem. Ser.* **1995**, *246*, 329-349.

(33) Pecoraro, V. L.; Slebodnick, C.; Hamstra, B. *ACS Symp. Ser.* **1998**, *711*, 157-167.

(34) Colpas, G. J.; Hamstra, B. J.; Kampf, J. W.; Pecoraro, V. L. *J. Am. Chem. Soc.* **1994**, *116*, 3627-3628.

(35) Yudenfreund Kravitz, J.; Pecoraro, V. L. *Pure Appl. Chem.* **2005**, *77*, 1595-1605.

(36) Schneider, C. J.; Penner-Hahn, J. E.; Pecoraro, V. L. *J. Am. Chem. Soc.* **2008**, *130*, 2712-2713.

(37) Schneider, C. J.; Zampella, G.; Greco, C.; Pecoraro, V. L.; De Gioia, L. *Eur. J. Inorg. Chem.* **2007**, 515-523.

(38) Zampella, G.; Yudenfreund Kravitz, J.; Webster, C. E.; Fantucci, P.; Hall, M. B.; Carlson, H. A.; Pecoraro, V. L.; De Gioia, L. *Inorg. Chem.* **2004**, *43*, 4127-4136.

(39) Chaudhuri, M. K.; Khan, A. T.; Patel, B. K.; Dey, D.; Kharmawophlang, W.; Lakshmiprabha, T. R.; Mandal, G. C. *Tetrahedron Lett.* **1998**, *39*, 8163-8166.

(40) Khan, A. T.; Ali, M. A.; Goswami, P.; Choudhury, L. H. *J. Org. Chem.* **2006**, *71*, 8961-8963.

(41) Hakam, K.; Thielmann, M.; Thielmann, T.; Winterfeldt, E. *Tetrahedron* **1987**, *43*, 2035-2044.

(42) Stotter, P. L.; Roman, S. A.; Edwards, C. L. *Tetrahedron Lett.* **1972**, 4071-4074.

(43) Karimi, S.; Grohmann, K. G.; Todaro, L. *J. Org. Chem.* **1995**, *60*, 554-559.

(44) Bateson, J. H.; Quinn, A. M.; Southgate, R. *J. Chem. Soc., Chem. Commun.* **1986**, 1151-1152.

(45) Curran, D. P.; Bosch, E.; Kaplan, J.; Newcomb, M. *J. Org. Chem.* **1989**, *54*, 1826-1831.

(46) Coats, S. J.; Wasserman, H. H. *Tetrahedron Lett.* **1995**, *36*, 7735-7738.

(47) Das, B.; Venkateswarlu, K.; Mahender, G.; Mahender, I. *Tetrahedron Lett.* **2005**, *46*, 3041-3044.

(48) Meshram, H. M.; Reddy, P. N.; Vishnu, P.; Sadashiv, K.; Yadav, J. S. *Tetrahedron Lett.* **2006**, *47*, 991-995.

(49) Hoffman, R. V.; Weiner, W. S.; Maslouh, N. *J. Org. Chem.* **2001**, *66*, 5790-5795.

(50) Honda, Y.; Katayama, S.; Kojima, M.; Suzuki, T.; Izawa, K. *Org. Lett.* **2002**, *4*, 447-449.

(51) Khan, A. T.; Goswami, P.; Choudhury, L. H. *Tetrahedron Lett.* **2006**, *47*, 2751-2754.

(52) Mondal, E.; Barua, P. M. B.; Bose, G.; Khan, A. T. *Chem. Lett.* **2002**, 210-211.

(53) Mondal, E.; Bose, G.; Sahu, P. R.; Khan, A. T. *Chem. Lett.* **2001**, 1158-1159.

(54) Vedejs, E.; Fuchs, P. L. *J. Org. Chem.* **1971**, *36*, 366-367.

(55) Ho, T.-L.; Ho, H. C.; Wong, C. M. *J. Chem. Soc., Chem. Commun.* **1972**, 791.

(56) Kamal, A.; Laxman, E.; Reddy, P. S. M. M. *Synlett* **2000**, 1476-1478.

(57) Mehta, G.; Uma, R. *Tetrahedron Lett.* **1996**, *37*, 1897-1898.

(58) Olah, G. A.; Mehrotra, A. K.; Narang, S. C. *Synthesis* **1982**, 151-152.

(59) Corey, E. J.; Erickson, B. W. *J. Org. Chem.* **1971**, *36*, 3553-3560.

(60) Bates, G. S.; O'Doherty, J. *J. Org. Chem.* **1981**, *46*, 1745-1747.

(61) Mondal, E.; Bose, G.; Khan, A. T. *Synlett* **2001**, 785-786.

(62) Khan, A. T.; Ahmed, W.; Schmidt, R. R. *Carbohydr. Res.* **1996**, *280*, 277-286.

(63) Olah, G. A.; Narang, S. C.; Fung, A. P.; Gupta, B. G. B. *Synthesis* **1980**, 657-658.

(64) Barua, P. M. B.; Sahu, P. R.; Mondal, E.; Bose, G.; Khan, A. T. *Synlett* **2002**, 81-84.

(65) Beesley, R. M.; Ingold, C. K.; Thorpe, J. F. *Journal of the Chemical Society, Transactions* **1915**, *107*, 1080-1106.

(66) Ahmad, S. M.; Braddock, D. C.; Cansell, G.; Hermitage, S. A. *Tetrahedron Lett.* **2007**, *48*, 915-918.

(67) Zhang, W.; Xu, H.; Xu, H.; Tang, W. *Journal of the American Chemical Society* **2009**, *131*, 3832-3833.

(68) Denmark, S. E.; Burk, M. T. *Proc. Natl. Acad. Sci. U. S. A.* **2010**, *107*, 20655-20660, S20655/20651-S20655/20646.

(69) Whitehead, D. C.; Yousefi, R.; Jaganathan, A.; Borhan, B. *J. Am. Chem. Soc.* **2010**, *132*, 3298-3300.

(70) Armstrong, A.; Braddock, D. C.; Jones, A. X.; Clark, S. *Tetrahedron Lett.* **2013**, *54*, 7004-7008.

(71) Zhou, L.; Tan, C. K.; Jiang, X.; Chen, F.; Yeung, Y.-Y. *J. Am. Chem. Soc.* **2010**, *132*, 15474-15476.

(72) Mellegaard, S. R.; Tunge, J. A. *J. Org. Chem.* **2004**, *69*, 8979-8981.

(73) Jiang, X.; Tan, C. K.; Zhou, L.; Yeung, Y.-Y. *Angew. Chem., Int. Ed.* **2012**, *51*, 7771-7775.

CHAPTER THREE

ALCOHOL OXIDATIONS USING REDUCED POLYOXOVANADATES

3.1 INTRODUCTION

3.1.1 Specific Aims

This chapter provides a full account of reaction methodology published by our group describing the room temperature oxidation of alcohols using reduced polyoxovanadates (r-POVs), $Cs_{2.5}(V_5O_9)(AsO_4)_2$ (**III**-**1**),[1] $Cs_5(V_{14}As_8O_{42}Cl)$ (**III**-**2**),[2] $Cs_{11}Na_3(V_{15}O_{36}Cl)Cl_5$ (**III**-**3**).[3] Detailed descriptions for catalyst and terminal co-oxidant optimization as well as solvent system and reaction time are given. These extensive optimizations revealed optimal conditions employing 0.02 equiv of r-POV catalyst $Cs_5(V_{14}As_8O_{42}Cl)$ (**III**-**2**), 5 equiv *tert*-butyl hydrogen peroxide (*t*BuOOH) as the terminal co-oxidant, in an acetone solvent for the quantitative oxidation of aryl-substituted secondary alcohols to their ketone products.[4] The substrate scope tolerates most aryl substituted secondary alcohols in good to quantitative yields while 2˚ alkyl and 1˚ benzylic alcohols were sluggish in comparison under similar conditions. The catalyst was recyclable on a 1.0 mmol scale of starting alcohol, 1-phenylethanol. The oxidation was also successfully promoted by the V^{IV}/V^{V} mixed valent polyoxovanadate (POV) $Cs_{11}Na_3Cl_5(V_{15}O_{36}Cl)$ (**III**-**3**). Using this catalyst, oxidation of several previously investigated alcohols proceeded in moderate to quantitative yields, and this catalyst was also recyclable over four runs. Finally, a third POV,

$Cs_{2.64}(V_5O_9)(AsO_4)_2$ (**III-1**), was investigated for catalytic activity using our established reaction protocol, but proved less effective as compared to the other two r-POV catalysts.

3.1.2 Polyoxometalates as catalysts for organic transformations

Polyoxometalates (POMs) have been used rather extensively in the past few decades as catalysts in alcohol oxidations to provide aldehyde and ketone products.[5-9] Of the catalysts used in these transformations, reports employing Keggin type POMs are more prevalent,[10-19] while Wells-Dawson scaffolds are employed to a lesser extent.[20-24] Currently, heteropolyoxotungstates and heteropolyoxomolybdates are among the most frequently utilized POM catalysts due to their strongly Lewis acidic properties and rich redox capabilities.[25-34]

Zhou and co-workers describe the dilacunary silicotungstate, $K_8[\gamma\text{-}SiW_{10}O_{36}]\cdot 12H_2O$, as a precatalyst with 5.0 equiv of 30% aq. H_2O_2 as the co-oxidant for the selective oxidation of activated benzylic alcohols as well as nonactivated aliphatic alcohols in greater than 90% yields (Scheme 3.1). [35] An

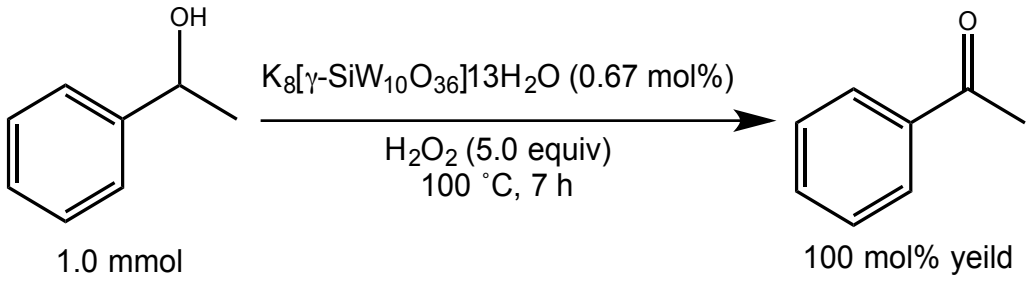

Scheme 3.1. 1-Phenylethanol oxidation to acetophenone using the silicopolyoxotungstate, $K_8[\gamma\text{-}SiW_{10}O_{36}]13H_20$

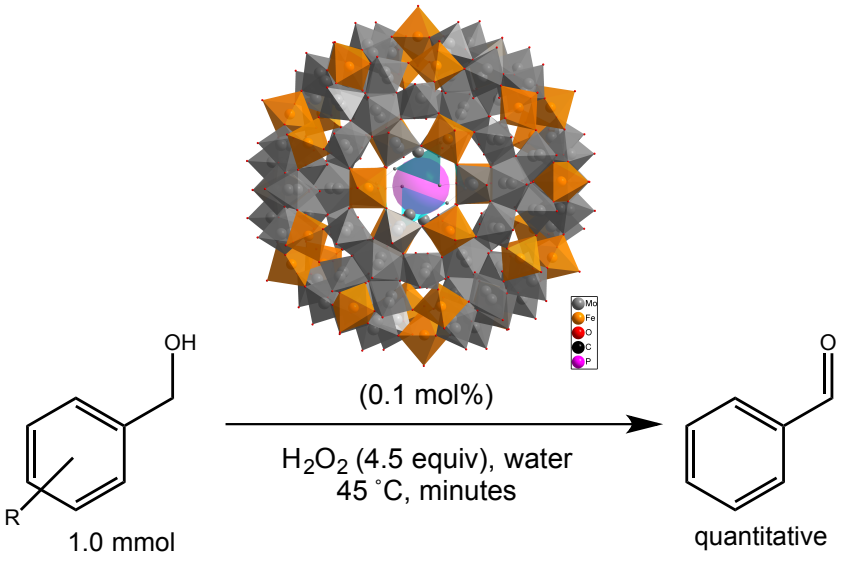

Scheme 3.2. Selective oxidation of several benzyl alcohols to their corresponding aldehydes using the featured polyoxomolybdate

elevated reaction temperature of 100 ˚C using an economically feasible 0.67 mol % catalyst loading promoted the oxidation of most substrates, although the more hydrophobic aliphatic alcohols required the use of a phase-transfer catalyst.[35] A related Keggin type polyoxomolybdate, $H_xPMo_{12}O_{40}$ ⊂ $H_4Mo_{72}Fe_{30}(CH_3COO)_{15}O_{245}$ behaves as a water soluble nanocapsule in the selective oxidation of alcohols to their corresponding aldehydes and ketones using 0.1 mol% of the POM catalyst at 45 ˚C (Scheme 3.2).[36] Again, this transformation employed approximately 5.0 equiv of 30% aq. H_2O_2 as the co-oxidant. Benzylic alcohols containing *para*-, *meta*-, and *ortho*- substituted electron withdrawing and donating groups returned quantitative yields after varied reaction times as determined by GC analysis. Non-activated cyclic and

aliphatic primary alcohols also gave quantitative yields under assorted reaction times.

Work showing increased catalytic efficiency and oxidative selectivity with incorporation of vanadium-metal ions (n= 0, 1, 2, 3) into the molybdophosphoric acid (MPA) Keggin structure Cs_2MPAV_n/TiO_2 displayed selective formation of benzaldehyde with increased vanadium substitution.[37] The authors suggest this oxidative selectivity is due to a shift in catalytic activation from acid-controlled to a redox-dominated oxidative process. A major limitation of these catalyst systems is the decreased conversion of the benzyl alcohol starting material with increasing vanadium incorporation.[37]

Extending the idea of enhanced redox-capable POM catalysts through increased vanadium substitution, a recent literature review cites vanadium-substituted POMs, *i.e. hetero-transition-metal POMs*,[38,39] as the most extensively explored transition metal POM in the oxidation of alcohols to aldehydes and ketones.[40] Unlike the commonly explored Keggin and Dawson POMs, including vanadium-substituted POMs, POVs featuring vanadium exclusively as the transition-metal cations in the POM framework are largely unexplored for catalytic reactions.[41] This untapped area of POM-catalyst design sparked our interest in the study described below.

3.1.3 Vanadium-substituted POM catalysts for organic transformations

Molybdenum and tungsten polyoxometalates (POMs) featuring vanadium-substituted anionic frameworks, *i.e.* hetero-transition-metal POMs, are important catalysts in oxidative reactions.[25-34] Yet little focus has been given to synthesizing POMs with vanadium as the sole transition metal cation in the polyoxo-core structure (*i.e.* polyoxovanadates (POVs)).[41]

A few notable examples of vanadium-substituted POM catalysts do exist in selective aerobic oxidations, such as the oxidation of benzyl alcohol to benzaldehyde promoted by $H_5PV_2Mo_{10}O_{40}$ in a reaction medium comprised of either polyethylene glycol or supercritical carbon dioxide (Scheme 3.3).[42,43] While many of these reactions feature high selectivity, acceptable yields, and utilize environmentally benign co-oxidants, reports of POVs requiring co-catalysts for reaction activation reduces their practical utility.[11,44] POVs were reported to participate in the catalytic oxidation of alcohols through oxygen transfer from sulfoxides, but only in the presence of DMSO as the solvent.[45,46] The most striking limitations of current oxidation methods promoted by POVs include high catalyst loadings (*e.g.* 40 mol %)[37,47] and reaction temperatures ranging from 90 to 135 ˚C.[20,48,49] Such high temperatures may lead to the catalyst overheating,

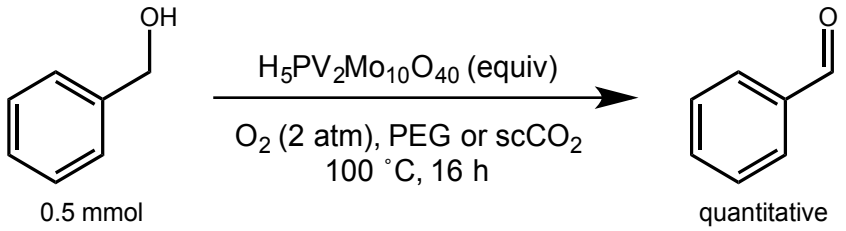

Scheme 3.3. Selective aerobic oxidation of benzyl alcohol to benzaldehyde using vanadium-substituted polyoxomolybdate

termed cooking, which results in concomitant catalyst deactivation.[40,49,50] These considerations somewhat reduce the overall synthetic utility of the resulting methods. Conversely, our method proceeds under comparatively much milder conditions at room temperature with only 2 mol% catalyst loading.[4] Unlike other anionic POM clusters, our materials described herein are highly water-soluble and feature fully reduced vanadium metal centers.

3.1.4 Salt-inclusion chemistry for synthesis of reduced polyoxovanadates (r-POV)

Numerous studies have shown Salt-Inclusion Chemistry (*SIC*) to be an alternative method for the creation of new porous materials *via* salt-inclusion, solid-state methods. The salt, like the organic cation in their zeolite and zeolite-like counterparts, serves as a template, and due to the weak interactions at the interface between these two chemically dissimilar lattices, the incorporated salt can be removed by washing with water.[51,52] While the utility of *SIC* has been demonstrated in the synthesis of unusually large porous frameworks (~2 nm in pore dimension) using molten-salt synthesis, it has been reiterated recently in the synthesis of reduced water-soluble salt-inclusion solids containing polyoxometalate clusters.[1-3] These polyoxometalate salts are soluble in water, and generate finely dispersed nanoclusters featuring a covalent metal oxide framework with counter cations surrounding the cluster.

The unique incorporation of exclusively vanadium atoms into the anionic POM framework is facilitated by the use of *SIC*.[53-56] Employing *SIC*, where molten halide salts can act as a high temperature solvent (*i.e*. > 500 ˚C), a new family of reduced POVs (r-POVs) are accessible. Two dissimilar lattices, ionic and covalent, now coexist which results in soluble r-POV-containing species. Over the years, some researchers have used salt-inclusion chemistry for the synthesis of otherwise unattainable materials featuring novel magnetic nanostructures,[57-60] mesoporous materials with permanent porosity,[3,61-63] and water-soluble polyoxometalate-containing salt-inclusion solids.[1-3]

Structrually, the POVs presented in this chapter as catalysts are overall 5- and 9- net anionic charges. While the utilization of anionic POMs as catalysts for organic oxidations is known to date back over the last two decades,[64,65] using r-POMs for alcohol oxidation with non-photocatalytic activation has not been reported to our knowledge.

3.1.5 Reduced-polyoxometalates in organic transformations

The current applications for reduced polyoxometalates (r-POM) as catalysts for alcohol oxidations is largely unexplored in comparison to their oxidized counterparts.[25-34,41] Of the few r-POM examples found in literature, there is a reported series of reduced catalysts that undergo photocatalytic reductive degradation of Acid Orange 7 (AO) (Figure 3.1), a common dye used at an industrial scale.[66] These catalytic materials must first be activated through photo-

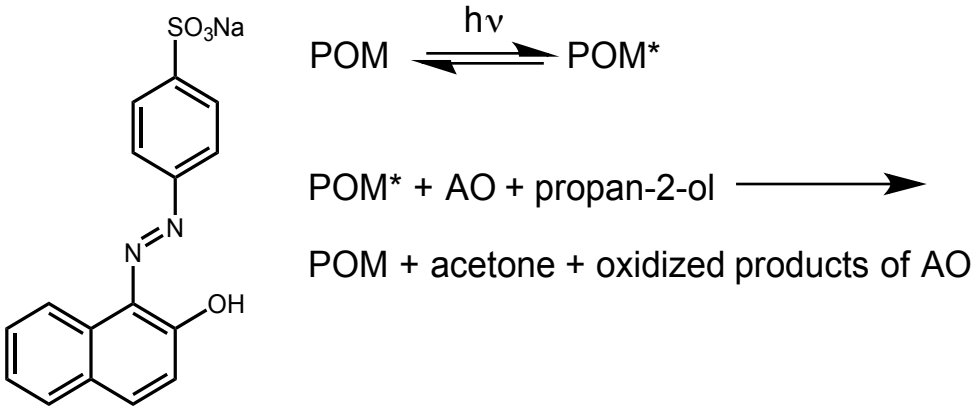

Acid Orange 7 (AO)

Figure 3.1. Photocatalytic degradation of Acid Orange (AO) using reduced-POM in the presence of 2-propanol

absorption to excite the r-POM towards oxidation of a sacrificial reducing agent, usually a low molecular weight alcohol. The activated r-POM, now being available for reoxidation-recycling, reduces the azo dye resulting in aromatic amine derivatives.[66] Several other photocatalytic transformations using r-POMs require the sacrificial reducing agent 2-propanol through similar mechanisms as discussed previously.[66,67]

The necessity for both light excitation (*i.e.* UV irradiation) and sacrificial reagents to activate the presented catalytic transformations allows for uncontrollable side reactions and therefore, reduced yield of the desired product. The previously discussed photocatalytic reduction of AO has a competing process of photocatalytic oxidative degradation of the AO substrate after continued UV exposure.[66]

Our interest in exploring the catalytic properties of the reduced POVs described herein (*i.e.* catalysts **III-1 – III-3**) was sparked by the significantly

different features of these materials compared to the commonly used POM catalysts. Given their unique electronic state (*i.e.* V^{4+}) and substantial negative charge, these POVs are more basic than their fully oxidized counterparts, and as such would likely be efficient at proton abstraction from organic alcohol substrates, which could for instance accelerate association of the substrate with the catalyst. Specifically, the composition of the reduced POV that was the major focus of the present study, $Cs_5(V_{14}As_8O_{42}Cl)$ (**III-2**), features $(V_{14}As_8O_{42}Cl)^{5-}$ clusters in which fourteen square pyramidal vanadium sites are reduced, *i.e.* V^{4+}. The crystal structure of $Cs_5(V_{14}As_8O_{42}Cl)$ is illustrated through the artwork shown in Figure 3.2, where the mixed arsenic(III)-POV cluster $[V^{4+}{}_{14}As^{3+}{}_8O_{42}Cl]^{5-}$ is residing in the Cs^+-based half sodalite (SOD) β-cage (Figure 3.2). The compound is soluble in water, due to the ionic interaction at the interface of this composite framework, and it forms micron-size $(V_{14}As_8O_{42}Cl)^{5-}$ aggregates in aqueous solution (*vide infra*). Each of the catalytically active vanadium atomic sites

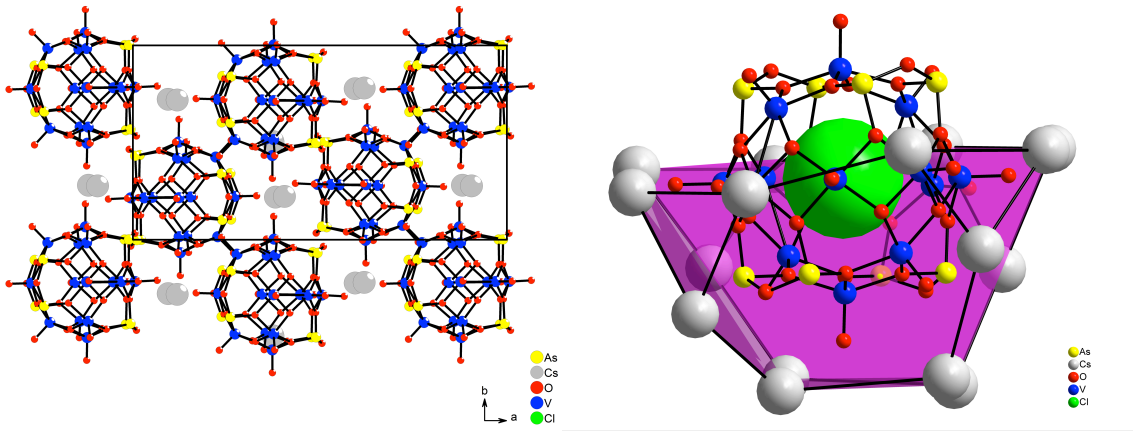

Figure 3.2. A) Unit cell representation of the $Cs_5(V_{14}As_8O_{42}Cl)$ crystal structure and B) Structure of the$(V_{14}As_8O_{42}Cl)^{5-}$ clusters

features apical vanadyl (V^{4+}=O) short oxygen bonds pointing away from the center of the cluster.

The study presented herein details the exploration of several water-soluble, reduced POV salts synthesized by means of *SIC* as catalysts for the selective oxidation of 2˚ alcohols. Ultimately, we discovered that catalytic loadings of the polyoxovanadate $Cs_5(V_{14}As_8O_{42}Cl)$ (**III-2**) efficiently promotes the oxidation of 2˚ alcohols in the presence of *tert*-butyl hydrogen peroxide (*t*BuOOH) as the terminal co-oxidant.[4] Our optimal conditions proceed at room temperature thus obviating possible thermal degradation of the r-POV catalyst. The transformation proceeds with good to excellent yields over the course of 12 to 48 h depending upon the particular substrate.

3.2 RESULTS AND DISCUSSION

Herein, we describe the details of the investigation of the catalytic aptitude of r-POV catalysts $Cs_{2.5}(V_5O_9)(AsO_4)_2$ (**III-1**), $Cs_5(V_{14}As_8O_{42}Cl)$ (**III-2**), and $Cs_{11}Na_3Cl_5(V_{15}O_{36}Cl)$ (**III-3**) for the oxidation of alcohols. These efforts culminated in a process that proceeds at room temperature using only 2 mol % of catalyst **III-2** and *t*BuOOH as the terminal co-oxidant. The utility of Salt-Inclusion Chemistry has been demonstrated in which three different reduced POVs were realized (compounds **III-1** through **III-3**).[1-3] With ready access to these unprecedented POV materials, we set out to investigate their utility as catalysts for organic transformations.

3.2.1 Exploratory Experiments and Optimization

Synthesis and full characterization for the POVs discussed herein are presented in their respective manuscripts referenced below. Briefly, molar ratios of mineralizers and inorganic salts under pressure and high temperature (*SIC*-method) afford transition metal oxide frameworks with inorganic salts intercalated within the primary structure. These salts are soluble after washing with aqueous solution leaving behind porous metal-oxide frameworks, a property suitable for possible catalytic application. Structures of the potential catalysts, $Cs_{3.5}Na_{1.47}(V_5O_9)(AsO_4)Cl_{2.33}$ (**III-1**) (Figure 3.3A),[1] $Cs_5(V_{14}As_8O_{42}Cl)$ (**III-2**)

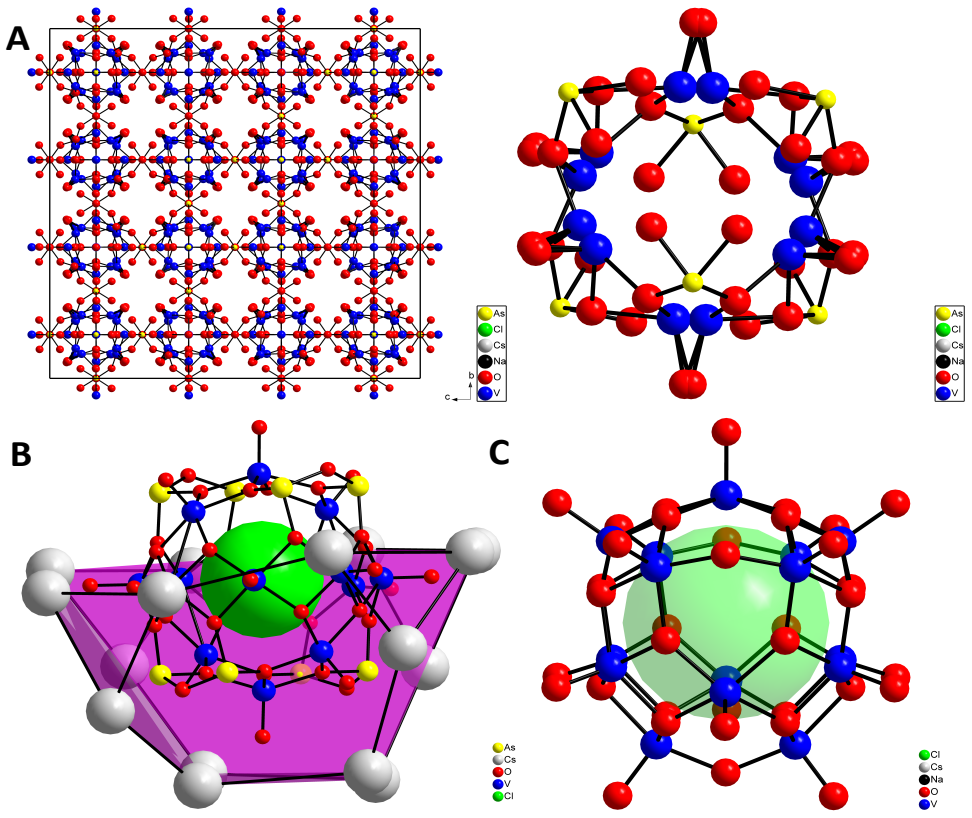

Figure 3.3. A) Structure of $Cs_{3.5}Na_{1.47}(V_5O_9)(AsO_4)Cl_{2.33}$; B) Structure of $Cs_5(V_{14}As_8O_{42}Cl)$; A) Structure of $Cs_{11}Na_3Cl_5(V_{15}O_{36}Cl)$

(Figure 3.3B),[2] and $Cs_{11}Na_3Cl_5(V_{15}O_{36}Cl)$ (**III-3**) (Figure 3.3C),[3] were verified using powder X-ray diffraction prior to synthetic use .

The initial focus of this study was to analyze the efficiency of polyoxovanadates **III-1**-**3** (Table 3.1, entries 1-3) in the catalytic oxidation of 1-phenylethanol **III-4** to acetophenone **III-5** using the terminal co-oxidant *t*BuOOH in aqueous media. Our initial investigation of the oxidation of **III-4** to **III-5** was conducted using an extraction protocol prior to GC analysis (see GC Work-Up A in Experimental Section). Product concentration values obtained in triplicate via Gas Chromatography (GC) standard curves showed catalyst **III-2** having the most activity towards product formation (entry 2) with the other POVs (entries 1 and 3) exceeding the non-catalyzed reaction (entry 4). Concentrating on catalyst **III-2**, simultaneous studies including terminal co-oxidant influence and optimal solvent system conditions were conducted. Increasing the equivalents of *t*BuOOH from 1.5 to 5 equiv. increased the yield of acetophenone **III-5** to 64% (entry 5). Aqueous hydrogen peroxide (H_2O_2) was investigated as the terminal co-oxidant but returned only trace amounts of product (entries 6 and 7). Similarly, Oxone®, returned only 15 and 13% yields of **III-5** at 1.5 and 5 equiv. loadings (*i.e.* entries 8 and 9, respectively). Having benefited from the use of urea-hydrogen peroxide complex (UHP) for the oxidative bromolactonization of alkenoic acids promoted by V_2O_5 (see Chapter 2),[68,69] we investigated the use of this reagent as the co-oxidant under our current reaction conditions. Yet, when applied in the present study, only trace amounts of product **III-5** were observed

Table 3.1. Oxidation of 1-phenylethanol to acetophenone using POVs **III-1**, **III-2**, **III-3**

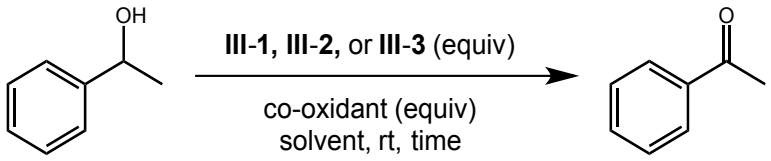

III-4, 0.1 mmol **III-5**

Entry	Catalyst (equiv.)	Co-oxidant (equiv.)	Solvent[a] [M]	Yield (%)
1	$Cs_{3.5}Na_{1.47}(V_5O_9)(AsO_4)_2\ Cl_{2.33}$ (0.05) (**1**)	TBHP (aq.)[b] (1.5)	H_2O [0.3]	28% +/- 4
2	$Cs_5(V_{14}As_8O_{42}Cl)$ (0.05) (**2**)	TBHP (aq.) (1.5)	H_2O [0.3]	56% +/- 10
3	$Cs_{11}Na_3Cl_5(V_{15}O_{36}Cl)$ (0.05) (**3**)	TBHP (aq.) (1.5)	H_2O [0.3]	22% +/- 2
4	none	TBHP (aq.) (1.5)	H_2O [0.3]	15% +/- 3
5	$Cs_5(V_{14}As_8O_{42}Cl)$ (0.05)	TBHP (aq.) (5.0)	H_2O [0.3]	64% +/- 5
6	$Cs_5(V_{14}As_8O_{42}Cl)$ (0.05)	H_2O_2 (aq.)[c] (1.5)	H_2O [0.3]	2% +/- 0
7	$Cs_5(V_{14}As_8O_{42}Cl)$ (0.05)	H_2O_2 (aq.) (5.0)	H_2O [0.3]	7% +/- 3
8	$Cs_5(V_{14}As_8O_{42}Cl)$ (0.05)	Oxone® (1.5)	H_2O [0.3]	15% +/- 3
9	$Cs_5(V_{14}As_8O_{42}Cl)$ (0.05)	Oxone® (5.0)	H_2O [0.3]	13% +/- 0
10	$Cs_5(V_{14}As_8O_{42}Cl)$ (0.05)	UHP (1.5)	H_2O [0.3]	5% +/- 0
11	$Cs_5(V_{14}As_8O_{42}Cl)$ (0.05)	UHP (5.0)	H_2O [0.3]	8% +/- 0
12	$Cs_5(V_{14}As_8O_{42}Cl)$ (0.05)	*m*CPBA (1.5)	H_2O [0.3]	29% +/- 2
13	$Cs_5(V_{14}As_8O_{42}Cl)$ (0.05)	TBHP (aq.) (1.5)	acetone [0.3]	64% +/- 11
14	$Cs_5(V_{14}As_8O_{42}Cl)$ (0.05)	TBHP (aq.) (1.5)	ACN [0.3]	57% +/- 8
15	$Cs_5(V_{14}As_8O_{42}Cl)$ (0.05)	TBHP (aq.) (1.5)	1,4-dioxane [0.3]	39% +/- 7
16	$Cs_5(V_{14}As_8O_{42}Cl)$ (0.05)	TBHP (aq.) (1.5)	Et_2O [0.3]	15% +/- 3
17	$Cs_5(V_{14}As_8O_{42}Cl)$ (0.05)	TBHP (aq.) (1.5)	acetone:H_2O (5:1) [0.3]	53% +/- 5
18	$Cs_5(V_{14}As_8O_{42}Cl)$ (0.05)	TBHP (aq.) (1.5)	acetone: H_2O (1:5) [0.3]	60% +/- 3
19	$Cs_5(V_{14}As_8O_{42}Cl)$ (0.05)	TBHP (aq.) (5.0)	none	60% +/- 8
20	**$Cs_5(V_{14}As_8O_{42}Cl)$ (0.05)**	**TBHP (aq.) (5.0)**	**acetone [0.3]**	**83% +/- 2**

[a] [M]=(0.1 mmol starting material / x mL solvent). [b] TBHP (aq.) denotes a 70% aq solution of TBHP empolyed as a co-oxidant. [c] H_2O_2 (aq.) denotes a 30% aq solution of H_2O_2 empolyed as a co-oxidant.

(entries 10 and 11). Finally, *meta*-chloroperoxybenzoic acid (*m*CPBA) did not promote appreciable turnover to **III-5** as shown in entry 12.

A solvent screen revealed acetone (entry 13) as a comparable solvent to that of the initially employed aqueous medium (entry 5). Using other polar,

aprotic solvents, such as acetonitrile (ACN), 1,4-dioxane, and diethyl ether did not improve product yields above 64% (entries 14 – 16). Next, mixtures of water and acetone were investigated, although, no further increase in yield of **III-5** was realized (entries 17 and 18).

Using 5.0 equiv of aq. *t*BuOOH as a co-oxidant (entry 5), two final preliminary investigations were run. The necessity of any additional solvent was probed by simply conducting the transformation with aq. tBuOOH as the only solvent (entry 19). Once again, comparable yields were realized to that of entry 5. Finally, acetone was employed as a co-solvent in conjunction with 5.0 equiv of aq. *t*BuOOH. Under these conditions, an approximate 20% increase in product yield was observed (83%, entry 20).

3.2.2 Further Optimization, Additive Investigation and Control Reactions

Next, we studied the effects of solvent concentration and catalyst loading in order to further optimize the transformation of alcohol **III**-**4** to its corresponding ketone **III**-**5**. First, the optimal solvent concentration was determined by screening the reaction at six concentrations ranging from 1 M to 0.1 M (Table 3.2; entries 1-6). The yield of **III**-**5** was reduced at higher concentrations (entries 1 and 2). These experiments revealed a concentration of 0.25 M to be optimal.

We then turned to an optimization of catalyst loading. Recall that the highest observed yield of **III**-**5** from the previous round of optimization was 83% while employing a 5 mol% loading of $Cs_5(V_{14}As_8O_{42}Cl)$ (**III**-**2**) (*cf.* Table 3.1, entry

Table 3.2. Oxidation of 1-phenylethanol to acetophenone catalyzed by r-POV **III-2**

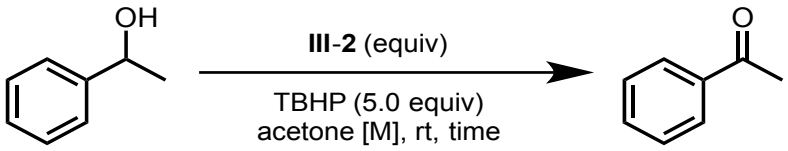

III-4, 0.1 mmol **III-5**

Entry	Catalyst (equiv.)	Acetone [M][a]	Yield (%)[b]
1	0.05	[1.00]	49% +/- 5
2	0.05	[0.50]	51% +/- 1
3	0.05	[0.33]	74% +/- 8
4	0.05	[0.25]	80% +/- 2
5	0.05	[0.20]	52% +/- 4
6	0.05	[0.10]	52% +/- 4
7	0.04	[0.25]	77% +/- 4
8	0.03	[0.25]	77% +/- 4
9	0.02	[0.25]	85% +/- 4
10	0.01	[0.25]	60% +/- 1

[a] [M]=(0.1 mmol starting material / x mL solvent). [b] Yields isolated via acid/base extraction. [c] TBHP (aq.) denotes a 70% aq solution of TBHP empolyed as a co-oxidant.

20). Reducing the catalyst loading to 4 and 3 mol% of the catalyst did not drastically affect the product yield (Table, 3.2, entries 7 and 8). The highest product yield was observed at a 2 mol % catalyst loading (entry 9). Finally, further adjusting the catalyst loading to 1 mol % resulted in a reduced 62% yield of product **III-5**.

At this point, we settled on the optimized reaction conditions for the POV-catalyzed oxidation of **III-4** to **III-5** using 2 mol % of catalyst $Cs_5(V_{14}As_8O_{42}Cl)$ (**III-2**) with 5.0 equiv of aqueous *t*BuOOH as a co-oxidant in acetone (0.25 M) for 24 hours at room temperature. These conditions reliably returned approximately 85% yields of product **III-5** (Table 2, entry 9). Next, the influence of both acidic and basic additives was investigated (Table 3.3). In this study, 3.0 equiv of *para*-toluenesulfonic acid (*p*-TSA) returned the highest yields of **III-5** (80%) (Table 3, entry 1). Other organic acid additives, *i.e.* citric acid, acetic acid, and benzoic

Table 3.3. Acidic and basic additives in the catalytic oxidation of 1-phenylethanol

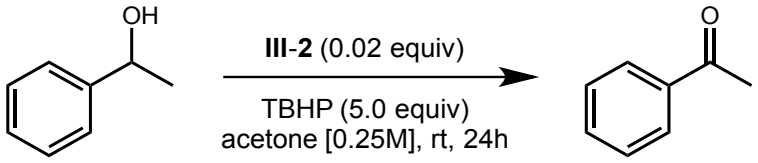

III-4, 0.1 mmol — **III-5**

Entry	Additive	% Yield[a]
1	*p*-TSA (3.0)	80% +/- 5
2	citric acid (3.0)	67% +/- 13
3	acetic acid (3.0)	68% +/- 16
4	benzoic acid (3.0)	53% +/- 12
5	K_2CO_3 (3.0)	48% +/- 0
6	$NaHCO_3$ (3.0)	38% +/- 5
7	Na_2CO_3 (3.0)	33% +/- 3

[a] Isolated via acid/base extraction.

acid did not effect an appreciable increase of acetophenone production (entries 2 through 4). Basic additives including potassium carbonate, sodium bicarbonate, and sodium carbonate gave reduced yields of **III-5** ranging from 33 to 48% (entries 5-7).

At this point in our optimization efforts, our GC work-up protocol involving an acid-base extraction prior to GC analysis (*i.e.* GC Work-Up A) was abandoned in favor of a simplified reaction work-up (GC Work-Up B). When the reaction medium was sampled directly without an intervening extraction, our optimized conditions returned a quantitative yield of **III-5** after 12 hour (Table 3.4, entry 1). Evidently, the quantitative conversion of **III-4** to **III-5** under our previously optimized conditions was obscured by product loss due to the extraction and concentration steps in our initial work-up. Employing the new work-up (*i.e.* GC Work-Up B), we next conducted a brief evaluation of the parameters of our optimal reaction conditions. Specifically, lowering the equivalents of co-oxidant resulted in reduced yields of 87% when 1.5 equiv were used (entry 2); yet the use of 3.0 equiv did not result in significant loss in yield (*i.e.* 95% yield of **III-5**, entry 3). Similar to our results with GC Work-Up A, further reduction of the catalyst loading beyond 2 mol % resulted in an unacceptable reduction in product yield (entries 4 and 5).

Next, several control reactions were conducted in order to rule out other oxidation pathways. First, to negate the possibility of the POV serving as a Lewis acid to promote an Oppenauer oxidation of **III-4** by acetone,[70,71] the

Table 3.4. Final investigations for the oxidation of 1-phenylethanol using r-POV catalyst **III-2**

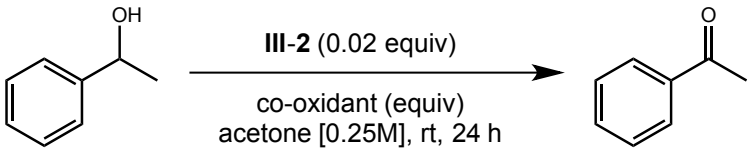

III-4, 0.1 mmol **III-5**

Entry	Catalyst (equiv.)	Co-oxidant (equiv.)	Yield (%)[b]
1	**0.02**	**TBHP[c] (aq.) (5.0)**	**100% +/- 3**
2	0.02	TBHP (aq.) (1.5)	87% +/- 5
3	0.02	TBHP (aq.) (3.0)	95% +/- 2
4	0.01	TBHP (aq.) (5.0)	62% +/- 4
5	0.005	TBHP (aq.) (5.0)	47% +/- 2
6	0.02	H_2O[d]	7% +/- 0
7	0.02	none	7% +/- 0
8[e]	0.02	TBHP (aq.) (5.0)	100% +/- 1
9[f]	0.02	none	6% +/- 2

[a] [M]=(0.1 mmol starting material / x mL solvent). [b] Yields isolated via GC. [c] TBHP (aq.) denotes a 70% aq solution of TBHP empolyed as a co-oxidant. [d] Equal volume to TBHP. [e] Ran under N_2. [f] Ran under O_2 balloon.

transformation was investigated in the absence of the *t*BuOOH co-oxidant. Under these conditions, acetophenone **III-5** was isolated in a paltry 7% yield in both acetone and acetone/water solvent systems (entries 6 and 7) indicating that the oxidation of 1-phenylethanol is not promoted by acetone in the presence of the POV **III-2** catalyst. Conducting the reaction under a dry N_2 atmosphere (anoxic conditions, entry 8) did not reduce the yield of acetophenone **III-5**, thus negating the possibility of atmospheric O_2 acting as a competing co-oxidant in

the POV-promoted oxidation of **III-4**. Further, conducting the reaction under an O_2 atmosphere (entry 9) in the absence of aq. *t*BuOOH returned only trace amounts of acetophenone.

3.2.3 Substrate Scope with Catalyst III-2

Next, the substrate scope was investigated using the optimal reaction conditions described above (GC Work-Up B). In brief, the transformation tolerates a variety of activated aryl alcohols in quantitative yields; their products are shown in Figure 3.4, compounds **III-5** – **III-7**. Substituted benzylic alcohols

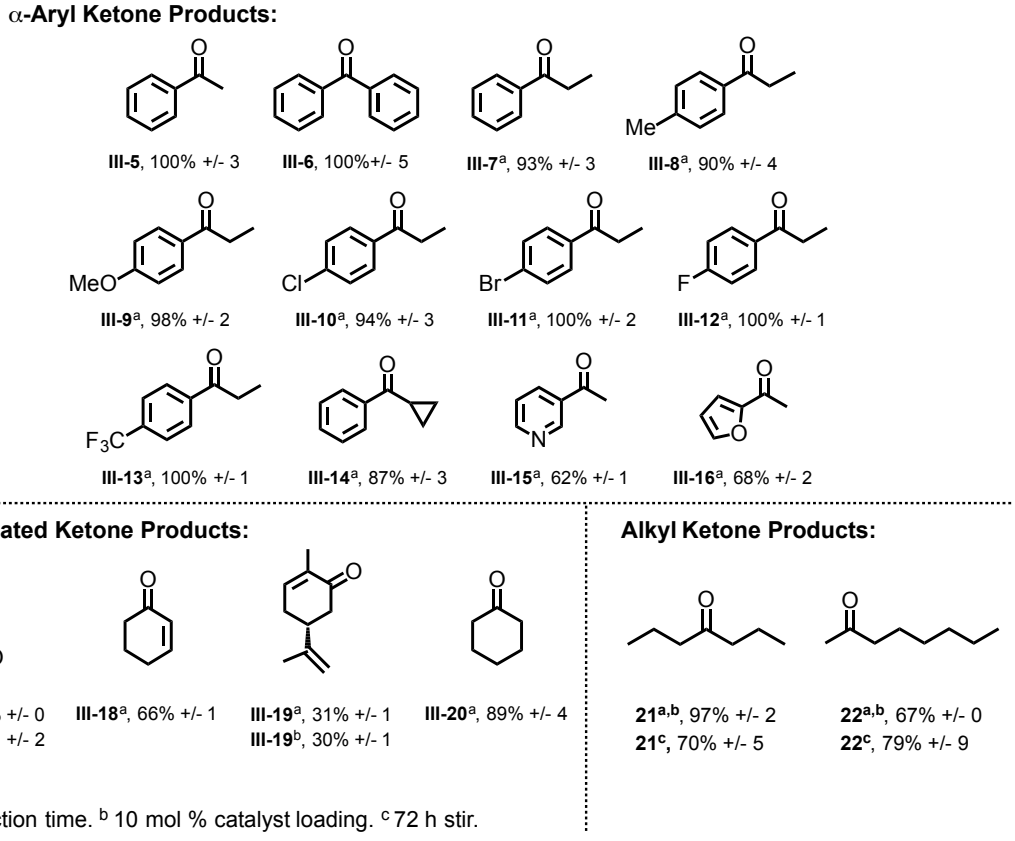

Figure 3.4. Substrate scope for the catalytic oxidation of secondary alcohols to their corresponding ketones using catalyst **III-2**

returned their ketones in 90% to quantitative yields regardless of the electronic nature of the *para*-substituted groups (compounds **III-8** - **III-13**). Isolation of compound **III-14** in an 87% yield was of particular interest due to its retention of the α-cyclopropyl moiety, suggesting that the transformation does not involve radical intermediates.

Heterocyclic products such as **III-15** and **III-16** and α,β-unsaturated ketone **III-18** were recovered in serviceable yields, while products **III-17** and **III-19** were returned in disappointing 20% and 30% yields, respectively. A non-activated secondary alcohol (cyclohexanol) was successfully oxidized in a gratifying 89% yield of **III-20**. An aliphatic secondary and symmetrical alcohol were investigated, and while good to excellent yields were observed (compounds **III-21** and **III-22**) an increased catalyst loading of 0.1 equiv. was required for successful conversion.

A series of primary alcohols were also investigated; however, their compatibility with the reaction conditions was limited to benzylic alcohols and the transformation of those substrates were inferior to that of the secondary alcohols, leading to the isolation of multiple products (Figure 3.5, compounds **III-24**, **III-25**, **III-27**, **III-28**, **III-30**, **III-31**, **III-33**, and **III-34**). Also, the potential for C-H activation of cyclohexane was investigated under the optimal conditions; however, no oxidation product was observed via GC. Therefore, our method is selective for secondary alcohol oxidation and is not readily amenable for primary alcohols or C-H oxidation. Having successfully uncovered an oxidation protocol using

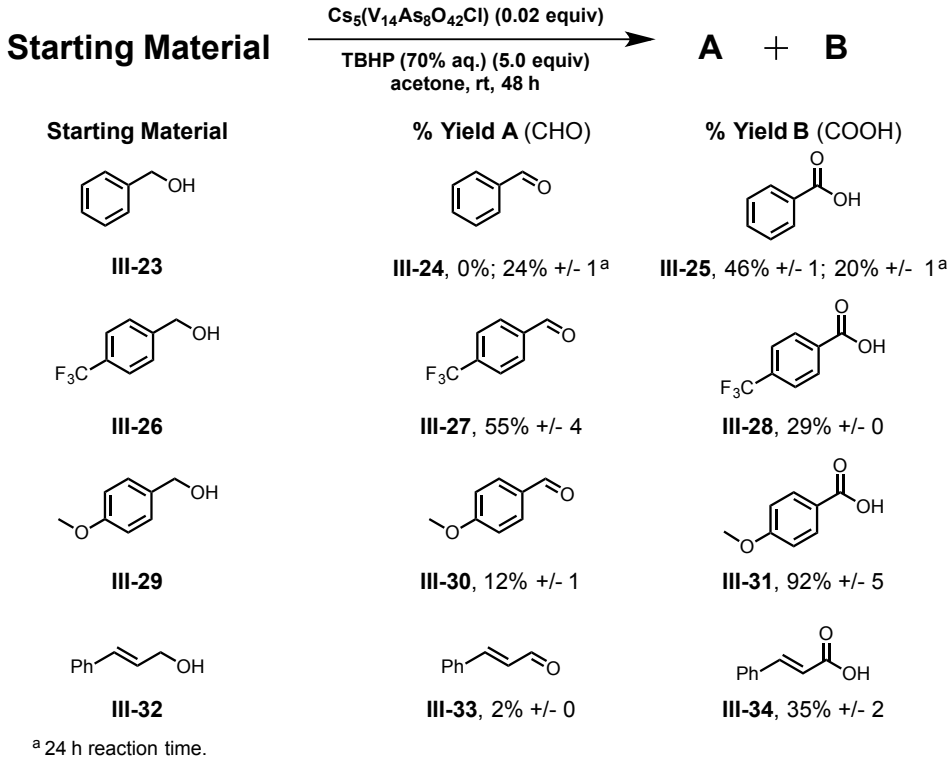

Figure 3.5. Benzylic alcohol oxidation using catalyst **III-2**

catalyst $Cs_5(V_{14}As_8O_{42}Cl)$ (**III-2**) for a variety of substituted alcohols, our efforts shifted to a more thorough investigating the other two r-POVs (*i.e.* **III-1** and **III-3**) as catalysts using our optimized conditions.

3.2.4 Investigation of Catalysts III-1 and III-3

With catalyst $Cs_{11}Na_3Cl_5(V_{15}O_{36}Cl)$ (**III-3**) (see Figure 3.3C for structure), alcohol oxidation proceeded in quantitative yields after a prolonged reaction time of 48 h at room temperature (Table 3.5, entry 1). Removal of the catalyst resulted in insignificant recovery of product **III-5** (entry 2). Similar to the reaction catalyzed by POV **III-2** (*vide supra*), the presence of acetone as a co-solvent is critical in promoting high yields of acetophenone as shown by comparing entries 3 and 4.

Table 3.5. Initial exploration of r-POV **III-3** for the catalytic oxidation of 1-phenylethanol to acetophenone

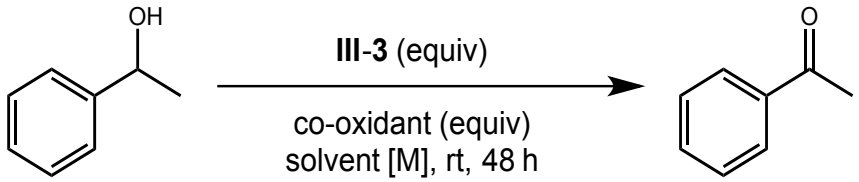

III-4, 0.1 mmol **III-5**

Entry	Catalyst (equiv)	Solvent [M][a]	Co-oxidant (equiv)	Yield (%)
1	**$Cs_{11}Na_3Cl_5(V_{15}O_{36}Cl)$ (0.02) (3)**	**acetone [0.25]**	**TBHP (aq.)[b] (5.0)**	**100% +/- 3**
2	none	acetone [0.25]	TBHP (aq.) (5.0)	15% +/- 1
3	$Cs_{11}Na_3Cl_5(V_{15}O_{36}Cl)$ (0.05)	H_2O [0.3]	TBHP (aq.) (1.5)	22% +/- 2
4	$Cs_{11}Na_3Cl_5(V_{15}O_{36}Cl)$ (0.02)	acetone [0.25]	TBHP (aq.) (1.5)	61% +/- 3
5	$Cs_{11}Na_3Cl_5(V_{15}O_{36}Cl)$ (0.01)	acetone [0.25]	TBHP (aq.) (5.0)	62% +/- 1
6	$Cs_{11}Na_3Cl_5(V_{15}O_{36}Cl)$ (0.02)	acetone [0.25]	H_2O[c]	45% +/- 3
7	$Cs_{11}Na_3Cl_5(V_{15}O_{36}Cl)$ (0.02)	acetone [0.25]	none	0%
8[d]	$Cs_{11}Na_3Cl_5(V_{15}O_{36}Cl)$ (0.02)	acetone [0.25]	TBHP (aq.) (5.0)	72% +/- 4
9[e]	$Cs_{11}Na_3Cl_5(V_{15}O_{36}Cl)$ (0.02)	acetone [0.25]	none	0%

[a] [M]=(0.1 mmol starting material / x mL solvent). [b] TBHP (aq.) denotes a 70% aq solution of TBHP empolyed as a co-oxidant. [c] Equal volume to TBHP. [d] Ran under N_2. [e] Ran under O_2 balloon.

Reducing the equivalence of the co-oxidant (entry 4) as compared to the established 5.0 equiv (entry 1) resulted in moderate product yields. Lowering the catalyst loading to 1 mol% of **III-3** also resulted in lower yields of acetophenone (entry 5).

Conducting control experiments with r-POV catalyst **III-3** yielded interesting results. In sharp contrast to the Oppenauer-like conditions investigated for catalyst **III-2** (*cf.* Table 3.2, entries 17 and 18), conversion of 1-phenylethanol to acetophenone was indeed observed in the presence of r-POV **III-3** in an acetone/water solvent system *without the inclusion of the aq. t*BuOOH

co-oxidant, albeit in a moderate 45% yield (Table 3.5, entry 6). This surprising result indicates that unlike r-POV **III-2**, catalyst **III-3** must be sufficiently Lewis acidic to allow for the acetone-promoted Oppenauer oxidation of 1-phenyl ethanol.[70,71] This result serves to highlight that structural perturbations of the r-POV scaffold, achieved by the salt-inclusion synthesis method, may allow for significant changes in organic reactivity. Interestingly, this novel Oppenauer oxidation was not observed in the absence of the water co-solvent (entry 7). In further contrast to the catalyst **III-2**, a significant, ~28% reduction in the yield of acetophenone **III-4** was observed when **III-3** was employed as the catalyst under an N_2 atmosphere (entry 8, *cf.* entry 1). The reason for this marked reduction in yield is unclear at this point, and warrants further investigation. Finally, no product formation was observed via GC analysis when using O_2 as the only oxidant source (entry 9).

3.2.5 Catalyst III-3 Substrate Scope

Next, we conducted an abbreviated evaluation of the substrate scope with the $Cs_{11}Na_3Cl_5(V_{15}O_{36}Cl)$ (**III-3**) catalyst. In the event, 0.02 equiv of **III-3** promoted quantitative oxidations of 1-phenylethanol, diphenyl methanol, and 1-phenyl propanol returning acetophenone **III-5**, benzophenone **III-6**, and 1-phenylpropanone **III-7** respectively (Figure 3.6). The *para*-substituted analogues of compound **III-7** returned only moderate yields of approximately 60% yield the desired ketone products **III-8**, **III-9**, and **III-13** regardless of electron donating or

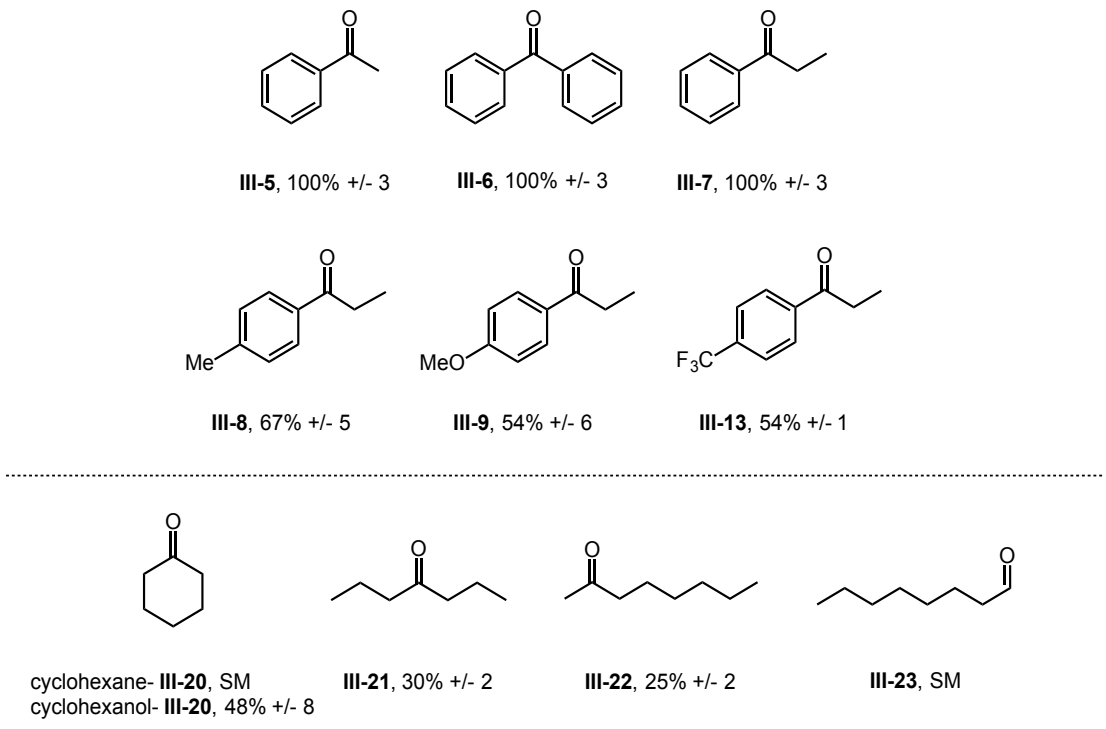

Figure 3.6. Substrate scope for the catalytic oxidation of **III-4** using 2 mol% catalyst **III-3** after a 48 h reaction time

electron withdrawing character. Secondary aliphatic alcohols reacted sluggishly, returning moderate-to-low yields of compounds **III-20**, **III-21,** and **III-22**. Further, only starting material was recovered from the attempted C-H oxidation of cyclohexane as well as the attempted oxidation of the primary alcohol, 1-octanol.

3.2.6 Catalyst III-1 Investigation

Simultaneous study investigating the catalytic efficiency of r-POV $Cs_{2.5}(V_5O_9)(AsO_4)_2$ (**III-1**) (*cf.* Figure 3.3A) revealed a reduced reactivity in the transformation of 1-phenylethanol to acetophenone (Figure 3.7, **III-5a**) returning a maximum 80% yield under our optimized conditions. This slight reduction in

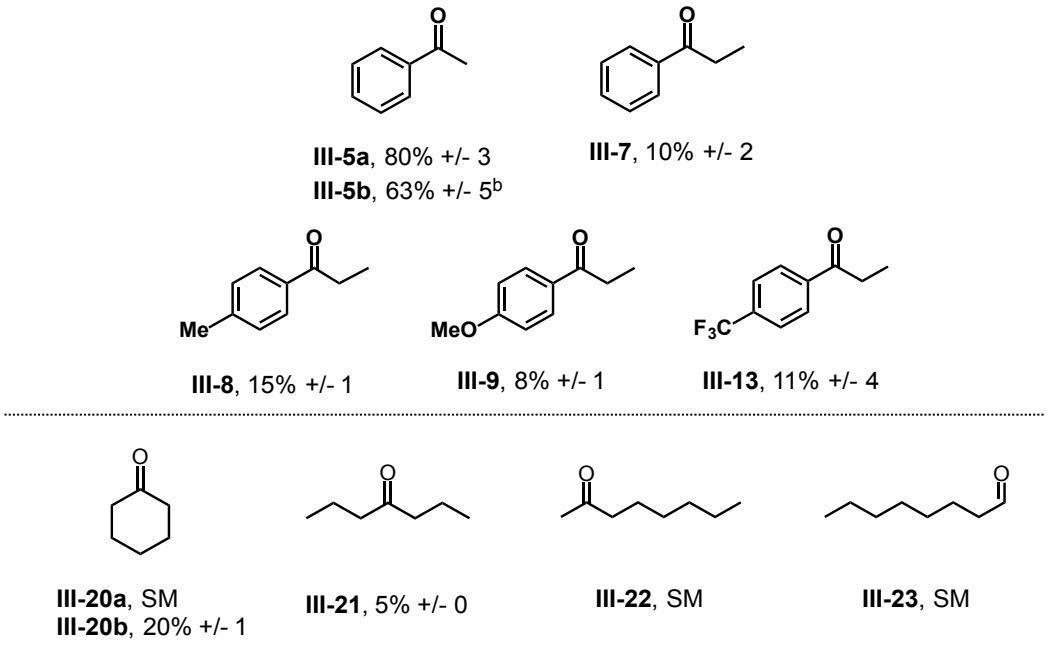

[b] 10 mol% catalyst loading.

Figure 3.7. Substrate scope using catalyst **III-1** in the oxidation of several activated and non-activated alcohols after a 48 h reaction time

reactivity may be attributed to the high degree of disorder inherent to the crystal structure for catalyst **III-1**. As highlighted in Figure 3.8, the two blue spheres boxed in orange are the same vanadium atom. Using higher catalyst loading did not afford an increase in product formation (**III**-**5b**). The most striking restriction in using catalyst **III**-**1** was is the reduced substrate tolerability with product isolation for α-ethyl aryl activated ketone **III**-**7** showing a low 10%. For other *para*-substituted aryl activated alcohols regardless of electron withdrawing or electron donating character, an insignificant product yield (compounds **III**-**8**, **III**-**9**, and **III**-**13**) was observed. Currently, it is unclear why there is such a dramatic decrease in yield when using the α-ethyl versus the α-methyl substituted aryl alcohol

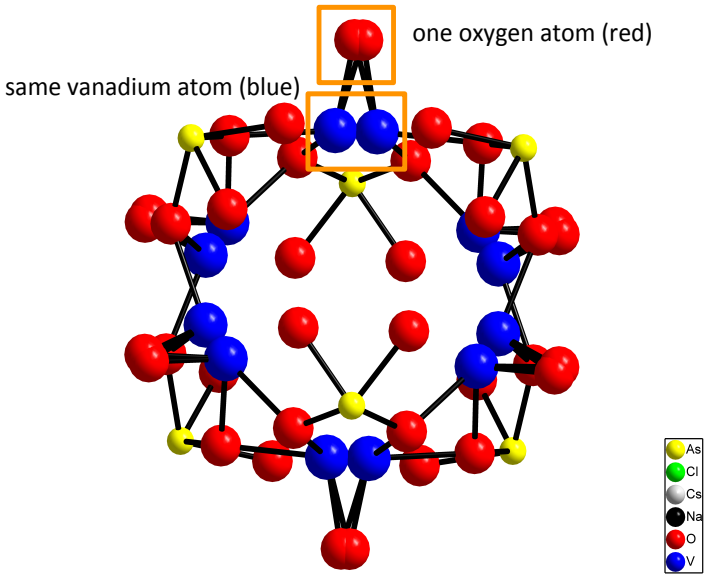

Figure 3.8. Structure for catalyst **III-1** cluster

(product **III-5a** vs **III-7**). The porous nature of catalyst **III-1** may play a larger role in the oxidative process and larger substitution at that *alpha* site may hinder reactivity needed for reaction to proceed efficiently.

The non-activated cyclic cyclohexanol was oxidized in 20% to cyclohexanone, while symmetrical, secondary, and primary alkyl alcohols returned mostly starting material comparable with the reactivity of catalyst **III-3** (*cf.* compounds **III-21**, **III-22**, and **III-23**, Figure 3.5).

3.2.7 Recyclability Study for Catalysts III-2 and III-3

To demonstrate the potential for recycling the more efficient catalysts under our optimized conditions, both $Cs_5(V_{14}As_8O_{42}Cl)$ (**III-2**) and $Cs_{11}Na_3Cl_5(V_{15}O_{36}Cl)$ (**III-3**) were impregnated on celite to aid in filtration during

the recovery process. Catalyst (**III-2**) was successfully used for three consecutive reactions in the oxidation of 1-phenylethanol to acetophenone (Figure 3.9, *scheme*). This method also highlights the ability to conduct the oxidation **III-4** to **III-5** on a 1.0 mmol scale without any reduction in isolated yield over these three catalytic cycles. For catalyst **III-3**, recyclability progressed over four oxidative cycles before showing a dramatic decrease in activity with only 17% of acetophenone **III-5** being isolated after a 48 h reaction time (Figure 3.9, *conversion graph*).

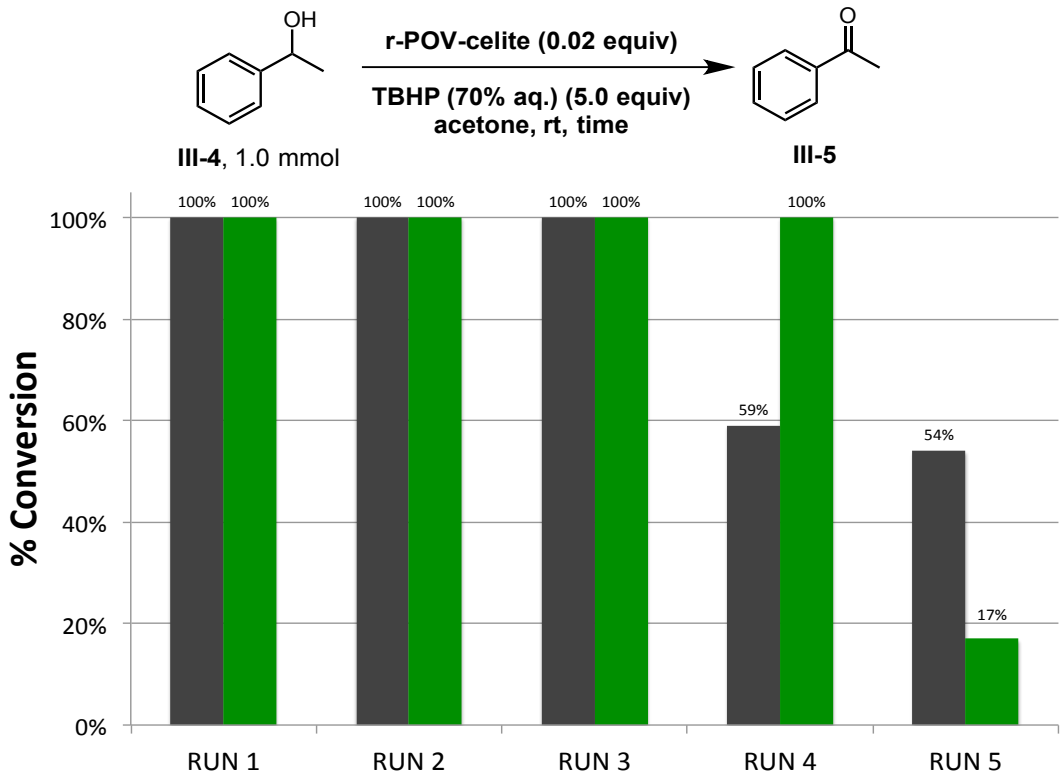

Figure 3.9. Scheme and conversion graph for 1.0 mmol scale 1-phenylethanol oxidation using catalysts **III-2** and **III-3** as catalysts over several reaction processes

3.2.8 Dynamic Light Scattering for Catalysts Under Established Conditions

A qualitative illustration for the Dynamic Light-Scattering (DLS) of the three catalysts in solution is shown in Figure 3.10. Results suggest that

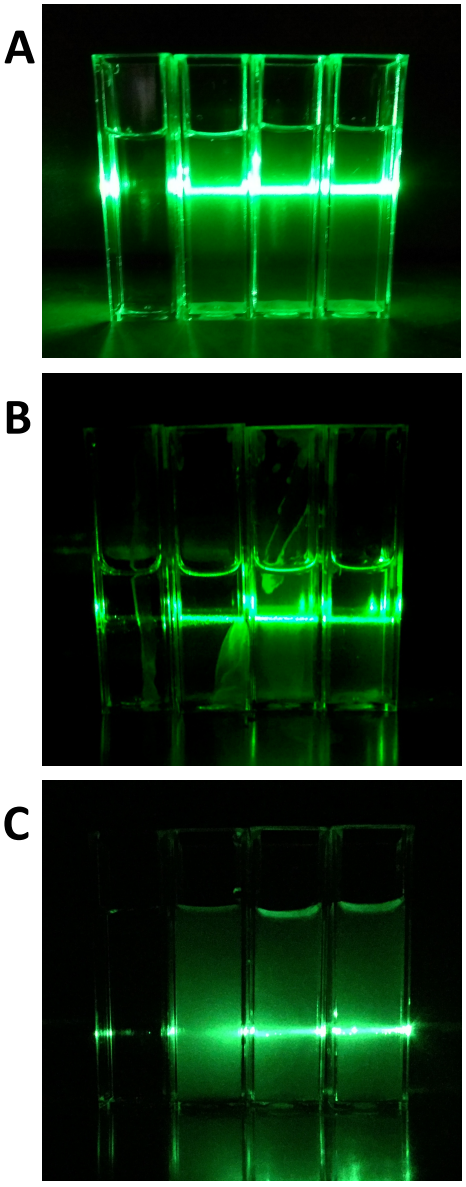

Figure 3.10. Light scattering experiment showing the aggregation of (A) $Cs_{2.5}(V_5O_9)(AsO_4)_2$ (B $Cs_5(V_{14}As_8O_{42}Cl)$ and (C) $Cs_{11}Na_3Cl_5(V_{15}O_{36}Cl)$) clusters in solution from left to right: 1. acetone 2. acetone + POV 3. acetone + POV + substrate + *t*BuOOH 4. acetone + POV + substrate + *t*BuOOH after 15 minutes

$(V_{14}As_8O_{42}Cl)^{5-}$ (Figure 3.10A) and $(V_{15}O_{36}Cl)^{9-}$ (Figure 3.10B) anions likely form suspensions including micron-sized aggregates or smaller in solution that promote the scattering of the incident green laser light, and that the r-POV may maintain its structure throughout the oxidative process. Conversely, there is reduced light transmission for the cuvettes containing catalyst **III-1** (Figure 3.10C).

3.2.9 Kinetic rates of reaction for determining the reaction order

Kinetic analysis helps elucidate the reaction order by taking in to consideration the rate of reaction for both starting alcohol and catalyst. Monitoring the oxidation of **III-4** as a function of time (Figure 3.11A) should reduce to a pseudo-first order reaction whose rate is equal to the negative slope of the linear plot for the natural logarithm of the concentration recovered as a function of time (Figure 3.11B). Reducing the rate term is allowed due to non-consumption of the catalyst material and the low catalytic loading relative to starting material (2 mol%; 0.02 mol equiv).

To experimentally confirm our hypothesis, the initial concentration of **III-4** at reaction time zero was analyzed via GC in triplicate for five initial concentrations of **III-4** (0.1 mmol, 0.05 mmol, 0.075 mmol, 0.15 mmol, and 0.125 mmol). With each concentration, the co-oxidant was introduced and the reaction was monitored via GC until the complete disappearance of 1-phenylethanol (**III-4**) (Figure 3.11, *scheme*). Repeating this process for each initial concentration

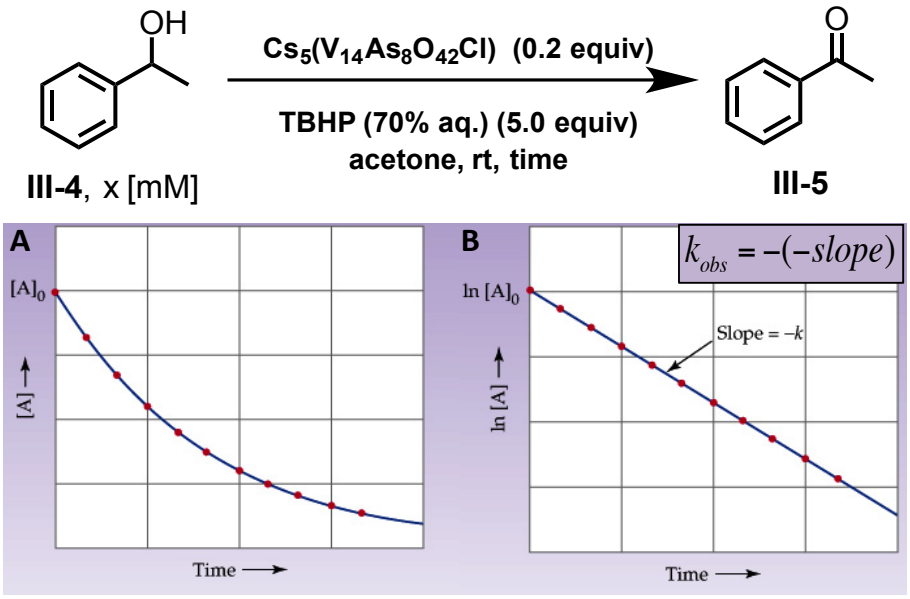

Figure 3.11. General representation for A) the consumption of starting alcohol as a function of time and B) the first order linear relationship of alcohol concentration as a function of time for the oxidation of 1-phenylethanol to acetophenone

value, data for each time point along the conversion was repeated in triplicate to ensure reproducibility before being averaged for plotting the concentration conversion over time. These averaged concentration values, when plotted as the *ln*[**III-4**] as a function of time (min), returned a linear plot for each of the five initial concentration values proposed (see Experimental Section 3.4.9). To determine the rate constant for the individual reactions, k_{obs} (Figure 3.12, *initial concentration*), the negative slope of the linear plot was extracted from the line of best-fit equation. The rate constant, k, is evaluated by plotting the measured k_{obs}

Initial Concentration, mM

0.15; k_{obs} = 0.5406 0.075; k_{obs} = 0.2531

0.125; k_{obs} = 0.4922 0.05; k_{obs} = 0.1210

0.10; k_{obs} = 0.3295

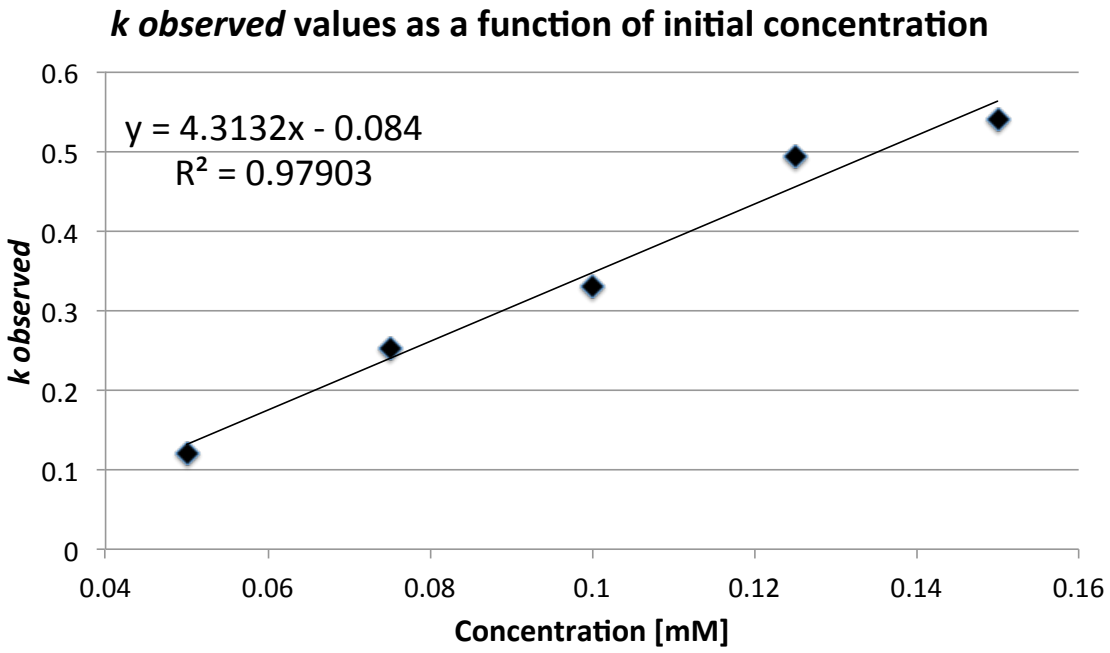

Figure 3.12. Initial 1-phenylethanol concentrations with their extracted k_{obs} constant and a graph showing their linear correlation

constants against the initial concentration values of **III-4** and extracting the slope of the plot (Figure 3.12, *graph*). Based on the initial observations for determining the reaction order and its rate constant, *k*, our predicted hypothesis for a reduced first-order transformation is reasonable returning *k* a value of 4.3132. It is appropriate to infer a rate law of r = $k[A_0]$, where $[A_0]$ is equal to the initial concentration value.

To further confirm our hypothesis of a first order transformation, we will test the order of reaction for the catalyst using the same protocol previously

described. In short, we will monitor the appearance of acetophenone **III-5** in the presence of four different catalyst loadings (0.02 eq., 0.05 eq., 0.10 eq., and 0.40 eq.). An excess of starting alcohol **III-4** is necessary in order to ensure reduced pseudo-first order kinetics in catalyst **III-2**.

3.3 CONCLUSIONS

In conclusion, our materials are the first POVs of their kind (*i.e.* fully reduced vanadium clusters) used for organic oxidations. A detailed investigation of the catalytic aptitude of reduced POV catalysts $Cs_{2.5}(V_5O_9)(AsO_4)_2$ (**III-1**), $Cs_5(V_{14}As_8O_{42}Cl)$ (**III-2**), and $Cs_{11}Na_3Cl_5(V_{15}O_{36}Cl)$ (**III-3**) for the oxidation of alcohols was conducted. Catalysts **III-2** and **III-3** showed the greatest efficiency for product formation under the optimized conditions. Unlike other previously reported POM-mediated oxidation protocols, our method proceeds at room temperature using only 2 mol% of the catalyst to facilitate the oxidation of a range of secondary alcohols. The recyclability of these materials under optimized reaction conditions was successful for scaled reactions (*i.e.* 1.0 mmol starting alcohol) using both catalyst (**III-2**) and (**III-3**). Catalyst **III-2** does act as a more efficient catalyst by promoting quantitative conversion for a larger variety of secondary alcohols and in shorter reaction times as compared to catalyst **III-3**, which only allows for quantitative conversion of certain aryl activated alcohols. Catalyst **III-3** is limited in oxidation of alkyl secondary alcohols and as with catalyst **III-2**, no activation for C-H or primary alcohol oxidation is observed.

Conversely, catalyst **III**-**1** proved to be virtually inactive as a catalyst for the oxidation of alcohols. Current efforts are focused on probing the mechanism of catalysis by r-POVs as well as investigating other organic transformations of interest. Initial investigations into our proposed hypothesis of a pseudo-first order reaction are promising with all the rate profiles exhibiting a linear first order relationship. Continuing research that focuses on the reaction order for the catalyst is underway; the results of the efforts will be reported in due course.

3.4 EXPERIMENTAL

3.4.1 General Material and Methods

All reagents were purchased from commercial suppliers and used without further purification. The synthetic protocol and requisite reagents used in the preparation of $Cs_{2.5}(V_5O_9)(AsO_4)_2$ (**III**-**1**),[1] $Cs_5(V_{14}As_8O_{42}Cl)$ (**III**-**2**),[2] and $Cs_{11}Na_3Cl_5(V_{15}O_{36}Cl)$ (**III**-**3**)[3] were reported previously. The purity of catalysts **III**-**1** - **III**-**3** was assessed by X-ray powder diffraction.

Analytical gas chromatography (GC) was performed on a SHIMADZU GC-2014 chromatograph equipped with a SHIMADZU AOC-20i autosampler, a split mode capillary injection system, a flame ionization detector and a GS-Tek stationary phase GsPB-5 GC column. GC analyses were carried out within the following parameters: inlet temperature: 200.0 ˚C; split injection with a 20:1 split ratio at 60 mL/min; injector sampling depth: 5 mm; column flow: 2.68 mL/min, constant pressure; carrier gas: helium; FID temperature: 220 ˚C; oven

temperature ramp: 100 ˚C for 1 min, 20 ˚C/min ramp to 220 ˚C, hold for 2 min. GC yields were determined using tetraglyme as the internal standard. ^{1}H and ^{13}C NMR spectra were collected on a 300 MHz Bruker NMR spectrometer using $CDCl_3$ solvent. Chemical shifts are reported in parts per million (ppm) with spectra referenced to the residual solvent peak. An isolated sample of acetophenone (**III**-**5**) was characterized by ^{1}H and ^{13}C NMR and was in complete agreement with samples reported in literature.

3.4.2 GC work-up A: Representative procedure for the catalytic oxidation of alcohols using acid-base work-up for isolation of product in triplicates

A 3 mL screw-capped vial was charged with 5.4 mg of $Cs_5(V_{14}As_8O_{42}Cl)$ catalyst (0.002 mmol; 0.02 equiv.), 12.7 µL of 1-phenylethanol (0.1 mmol; 1.0 equiv.), and 400 µL of acetone. To the stirring solution, 69 µL of 70% aqueous *tert*-butyl hydrogen peroxide (*t*BuOOH) (0.5 mmol; 5.0 equiv.) was added and allowed to stir for 12 hours at room temperature. After the 12h reaction time, the solution was first diluted with 5 mL of distilled water and 2 mL of saturated sodium meta-bisulfite solution was added to quench any remaining tBuOOH. The liquid was transferred to a 60 mL separatory funnel and the aqueous layer was extracted with 10 mL of DCM (X3). The combined organics were washed with 10 mL of saturated brine. The resulting organic layer was dried over sodium sulfate for twenty min, filtered, and concentrated *in vacuo* before being subjected to GC analysis.

Into a 1 mL volumetric flask, product residue and the internal standard tetraglyme (11 µL, 0.05 mmol) was added. The solution was diluted to 1 mL in a volumetric flask using acetone, and then the full volume of liquid was transferred to a screw-cap GC vial and analyzed by GC to determine the yield. Yields were calculated by means of product standard curves equating GC peak area to product concentration. Reported yields are triplicate averages with standard deviations.

3.4.3 GC work-up B: Representative procedure for the catalytic oxidation of alcohols ran in triplicate

A 3 mL screw-capped vial was charged with 5.4 mg of catalyst (0.002 mmol; 0.02 equiv.), 12.7 µL of 1-phenylethanol (0.1 mmol; 1.0 equiv.), and 400 µL of acetone as the solvent. To the stirring solution, 69 µL of 70% aqueous *tert*-butyl hydrogen peroxide (*t*BuOOH) (0.5 mmol; 5.0 equiv.) was added and allowed to stir for a set time at room temperature. After the allotted reaction time, the solution was transferred to a 1 mL volumetric flask and the internal standard tetraglyme (11 µL, 0.05 mmol) was added to the vial. The solution was diluted to 1 mL in a volumetric flask, and then the full volume of liquid was transferred to a screw-cap GC vial and analyzed by GC to determine the yield. Yields were calculated by means of product standard curves equating GC peak area to product concentration. Reported yields are triplicate averages with standard deviations.

3.4.4 Procedure for catalyst recyclability study

When probing the recyclability of the POV catalyst, 54 mg of $Cs_5(V_{14}As_8O_{42}Cl)$ catalyst was first impregnated on 100 mg of celite by uniform mixing of the solids in 4.0 mL of acetone before the addition of 1.0 mmol of 1-phenylethanol (121 µL; 1.0 equiv.) The co-oxidant *t*BuOOH (0.7 mL; 5.0 mmol; 5.0 equiv.) was introduced and the mixture was allowed to stir for 24 hours at room temperature. The magnetic stir bar was then removed and the heterogeneous solution was filtered through a fritted glass funnel and allowed to dry overnight. The remaining, clear liquid was concentrated *in vacuo* to approximately 5 mL before being diluted with 5 mL of water and quenched with saturated sodium meta-bisulfite. The aqueous mixture was extracted with ethyl acetate (3 x 15 mL), washed with saturated sodium bicarbonate (15 mL), and dried over anhydrous sodium sulfate. The collected aqueous layers were then back extracted with another 15 mL of ethyl acetate that was added to the drying organic layers. The organics were then filtered and concentrated *in vacuo*. Silica gel column chromatography (20% ethyl acetate/hexanes) returned the desired product.

3.4.5 General procedure for rate study using catalyst III-2

To begin, the appropriate quenching agent was determined to be sodium thiosulfate ($Na_2S_2O_3$) and the mass of material used was determined based on

the initial concentration value of 1-phenylethanol at a five times excess (*i.e.* equal equivalency to the co-oxidant added. Standard curves were plotted for each of the initial concentration of 1-phenylethanol (0.1 mmol, 0.05 mmol, 0.075 mmol, 0.15 mmol, and 0.125 mmol) (see Experimental Section 3.4.8) using the described GC method.

Reactions were monitored via GC in triplicate over the same 12 h period and were prepared according to GC work-up B. For each 12 h reaction ran in triplicate, 5.0 equiv $Na_2S_2O_3$ was added at time points zero, 0.25, 0.5, 0.75, 1, 2, 3, 4, 5, 6, 8, 10, and 12 h to quench any unreacted *t*BuOOH. The samples were prepared for GC analysis according to GC work-up A (1 µL injection) and ran immediately using the SHIMADZU AOC-20i autosampler for reaction times greater than 1 h (*I.e.* 2-12 h).

For the five remaining time points (*i.e.* 0-1 h), reactions were run individually. After quenching, the 3 mL screw-capped GC vials were prepped according to the general work-up A and immediately analyzed using manual injection for GC analysis.

3.4.6 Characterization of acetophenone (III-5)

^{1}H and ^{13}C NMR characterization of acetophenone, **III-5:** ^{1}H NMR (300 MHz, $CDCl_3$): δ 7.97-7.93 (dt, 2H, *J* = 1.5, 6.9), 7.55-7.47 (tt, 1H, *J* = 1.2, 7.2), 7.45 (t, 2H, *J* = 7.8) 2.59 (s, 3H); ^{13}C NMR (90 MHz, $CDCl_3$): δ 198.1, 137.1, 133.1,128.6, 128.3, 26.6

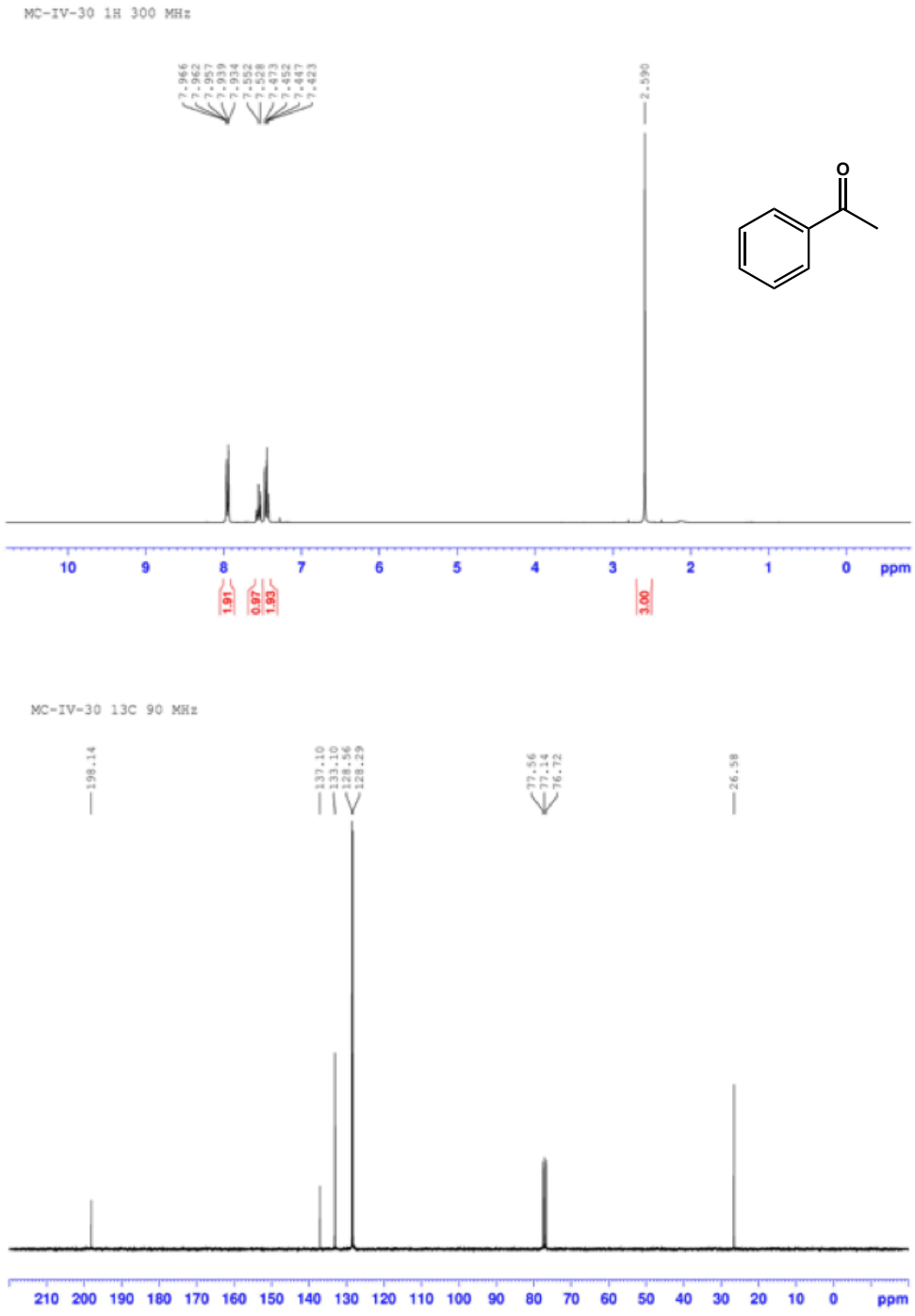

Figure 3.13. Experimental A) ^{1}H and B) ^{13}C NMR spectra

3.4.7 Standard curves for ketone products: III-5 – III-22, III-24 – III-25, III-27 – III-28, III-30 – III-31, III-33 – III-35

Acetophenone, **III-5**[72]

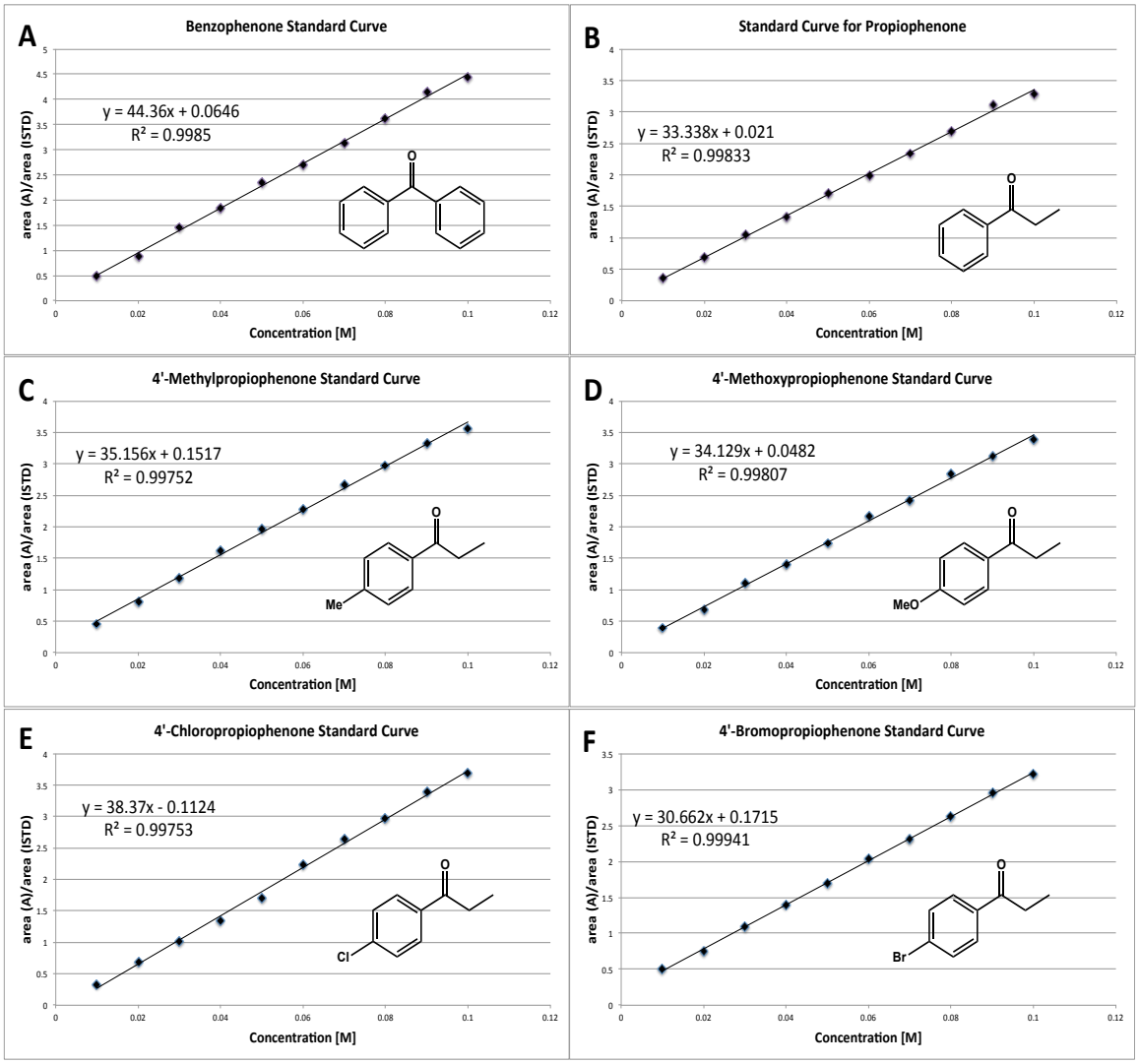

Figure 3.14. Standard curve graphs for A) Benzophenone, **III-6**; B) Propiophenone, **III-7**; C) 4'-Methylpropiophenone, **III-8**; D) 4'-Methoxypropiophenone, **III-9** E) 4'-Chloropropiophenone, **III-10**; F) 4'-Bromopropiophenone, **III-11**

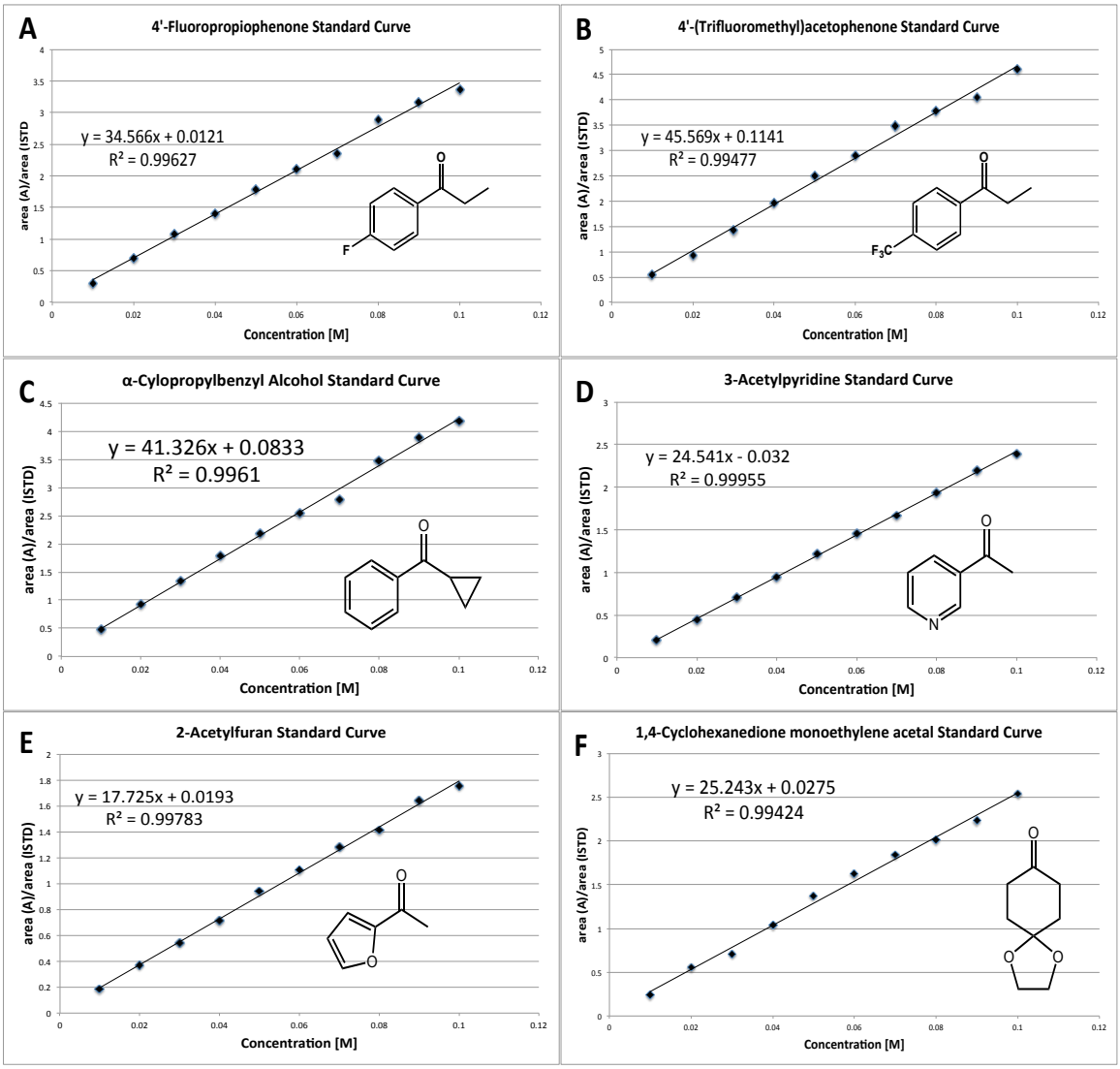

Figure 3.15 Standard curve graphs for A) 4'-Fluoropropiophenone, **III-12**; B) 4'-(Trifluoromethy)acetophenone, **III-13**; C) α-Cylopropylbenzyl Alcohol, **III-14**; D) 3-Acetylpryridine, **III-15**; E) 2-Acetylfuran, **III-16**; F) 1,4-Cyclohexanedione monoethylene acetal, **III-17**

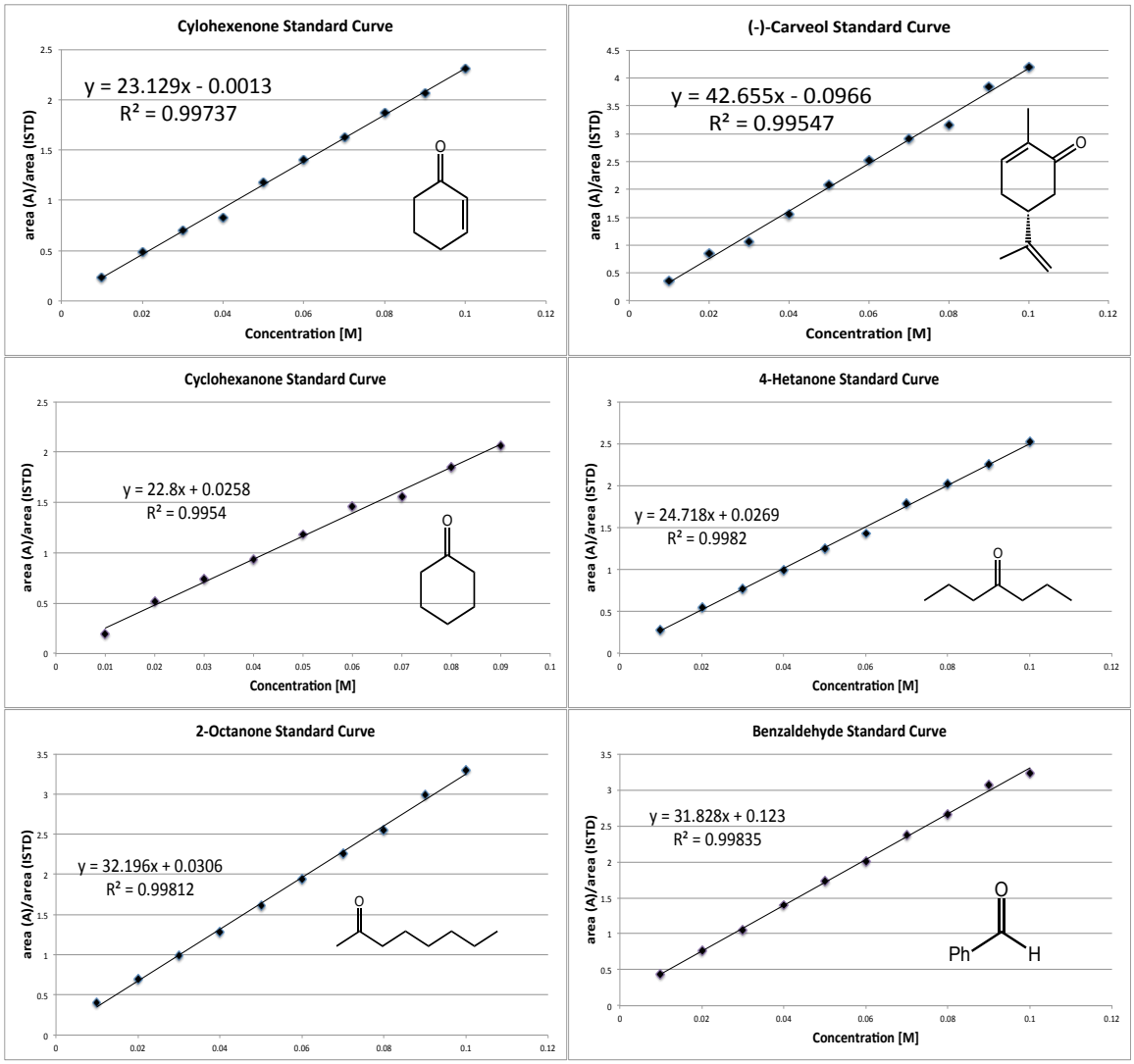

Figure 3.16. Standard curve graphs for A) Cyclohexenone, **III-18**; B) (-)-Carveol, **III-19**; C) Cyclohexanone, **III-20**; D) 4-Heptanone, **III-21**; E) 2-Octanone, **III-22B**; F) Benzaldehyde, **III-24**

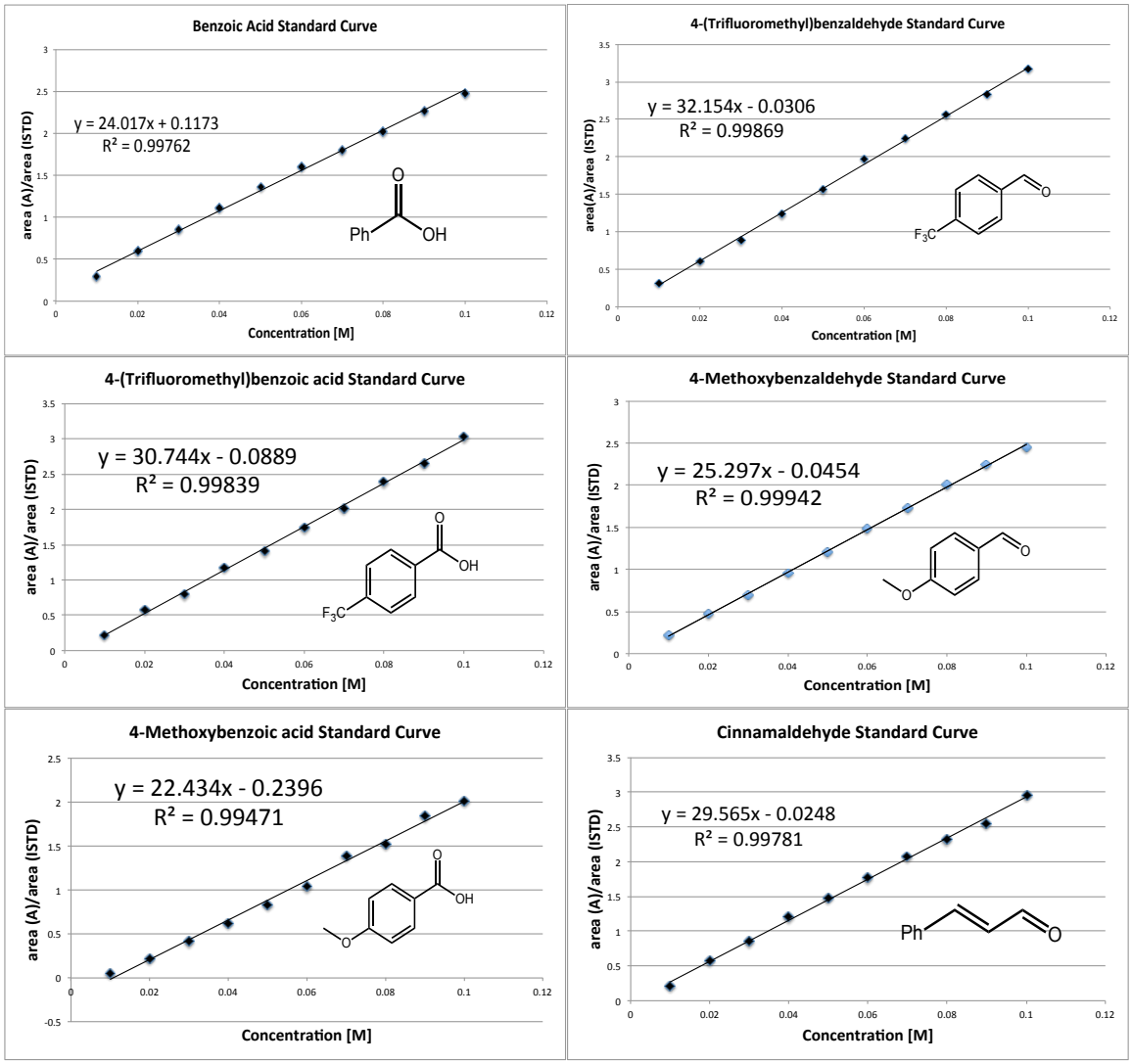

Figure 3.17. Standard curve graphs for A) Benzoic Acid, **III-25**; B) 4-(Trifluoromethyl)benzaldehyde, **III-27**; C) 4-(Trifluoromethyl)benzoic acid, **III-28**; D) 4-Methoxybenzaldehyde, **III-30**; E) 4-Methoxybenzoic acid, **III-32**; F) Cinnamaldehyde, **III-33**

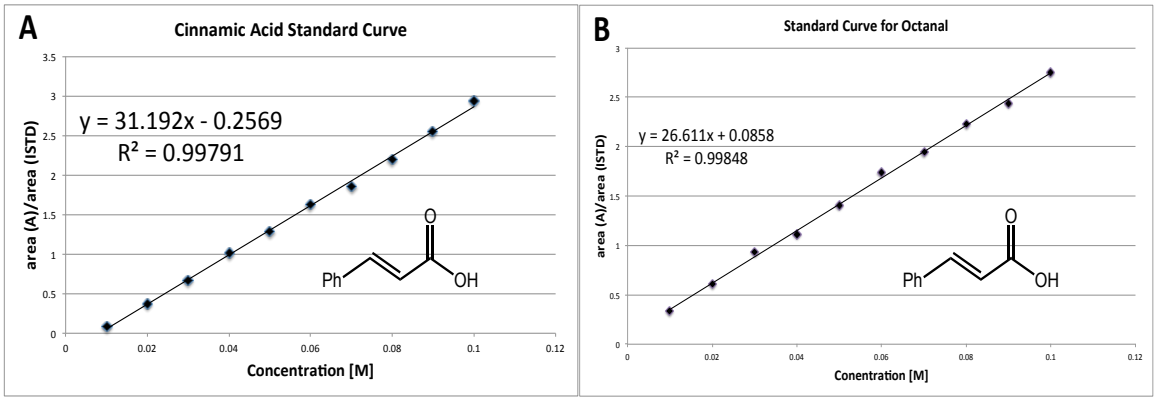

Figure 3.18. Standard curve graphs for A) Cinnamic Acid, **III-**34; B) Octanal, **III-35**

3.4.8 Standard curves for 1-phenylethanol III-4 at increasing concentrations

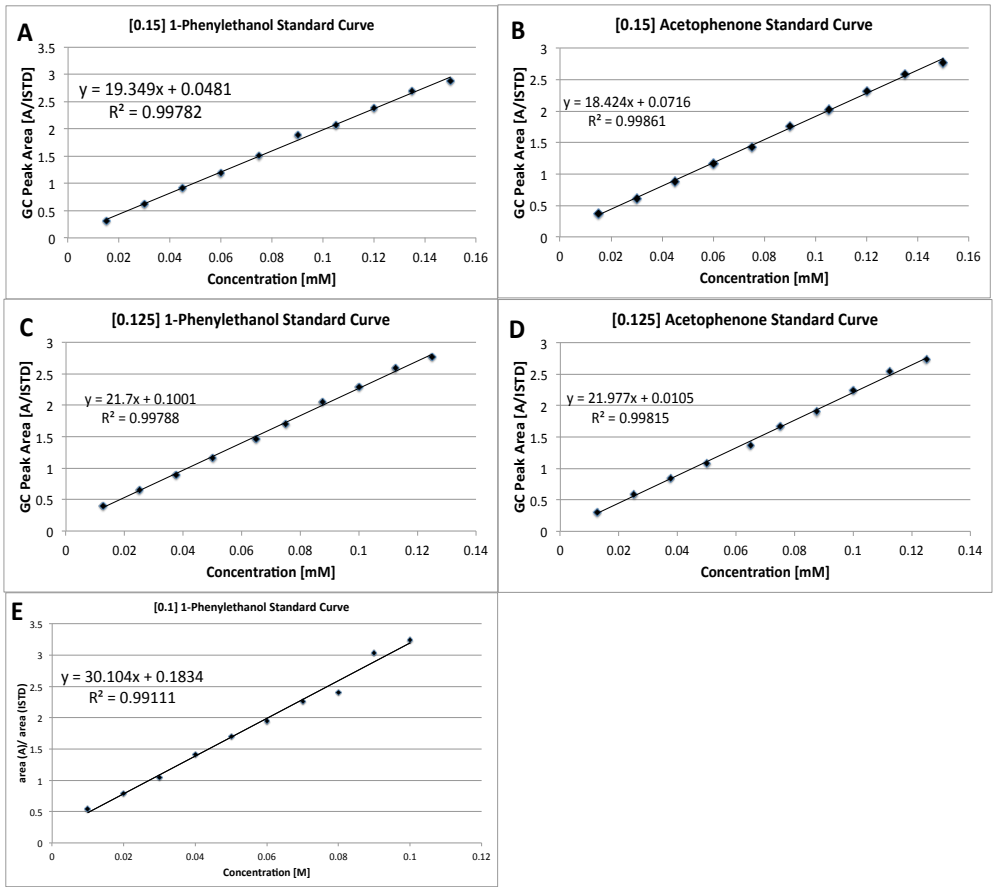

Figure 3.19. Standard curves for A) [0.15] 1-phenylethanol; B) [0.15] acetophenone; C) [0.15] 1-phenylethanol; D) [0.15] acetophenone; E) [0.1] 1-phenylethanol

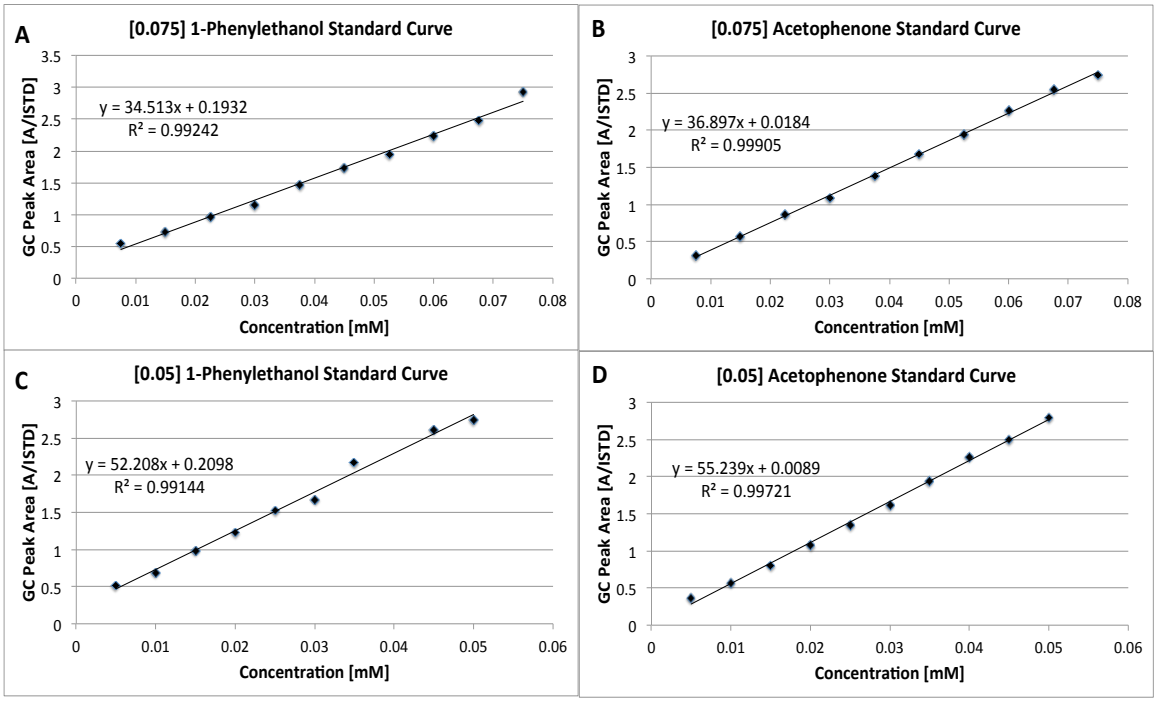

Figure 3.20. Standard curves for A) [0.075] 1-Phenylethanol; B) [0.075] Acetophenone; C) [0.05] 1-Phenylethanol; D) [0.05] Acetophenone

3.4.9 First order rate profiles for each concentration – extracting k_{obs}

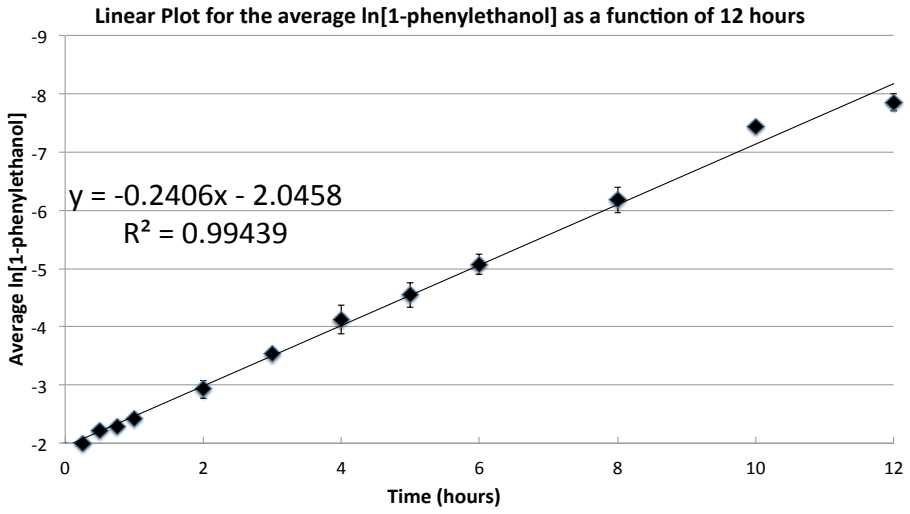

Figure 3.21. [0.15] 1-Phenylethanol linear plot

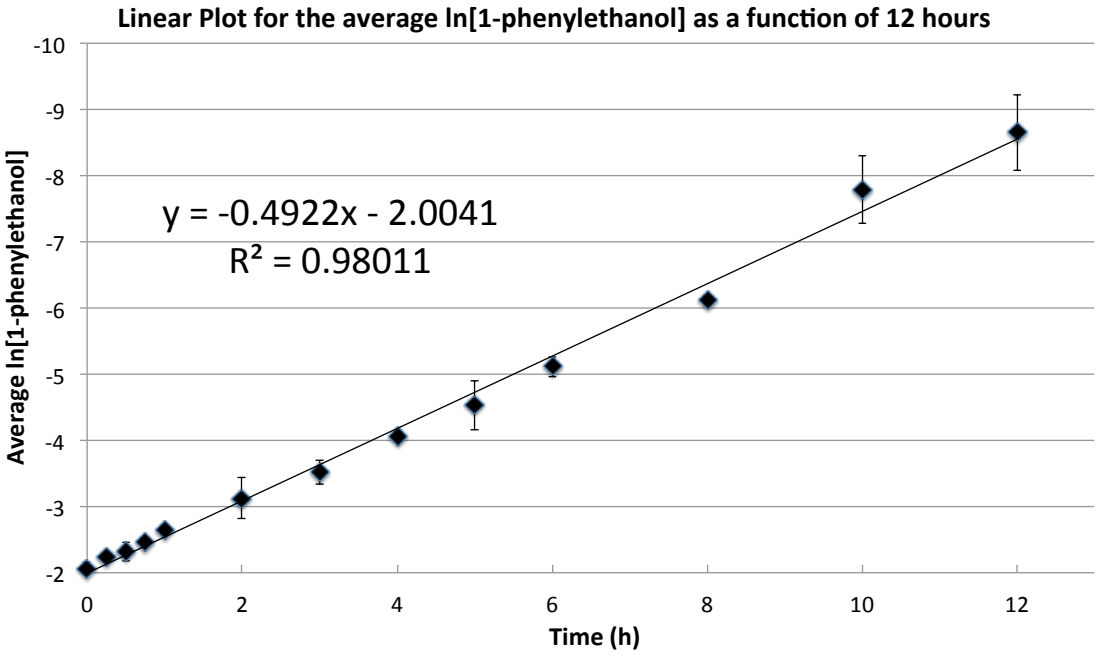

Figure 3.22. [0.125] 1-Phenylethanol linear plot

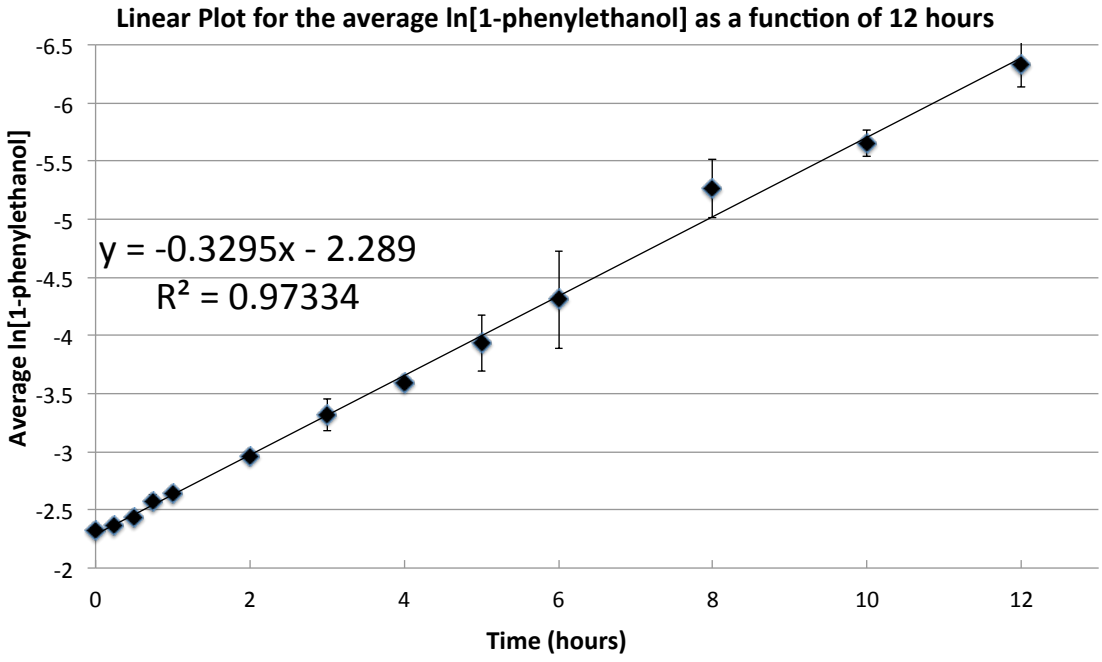

Figure 3.23. [0.1] 1-Phenylethanol linear plot

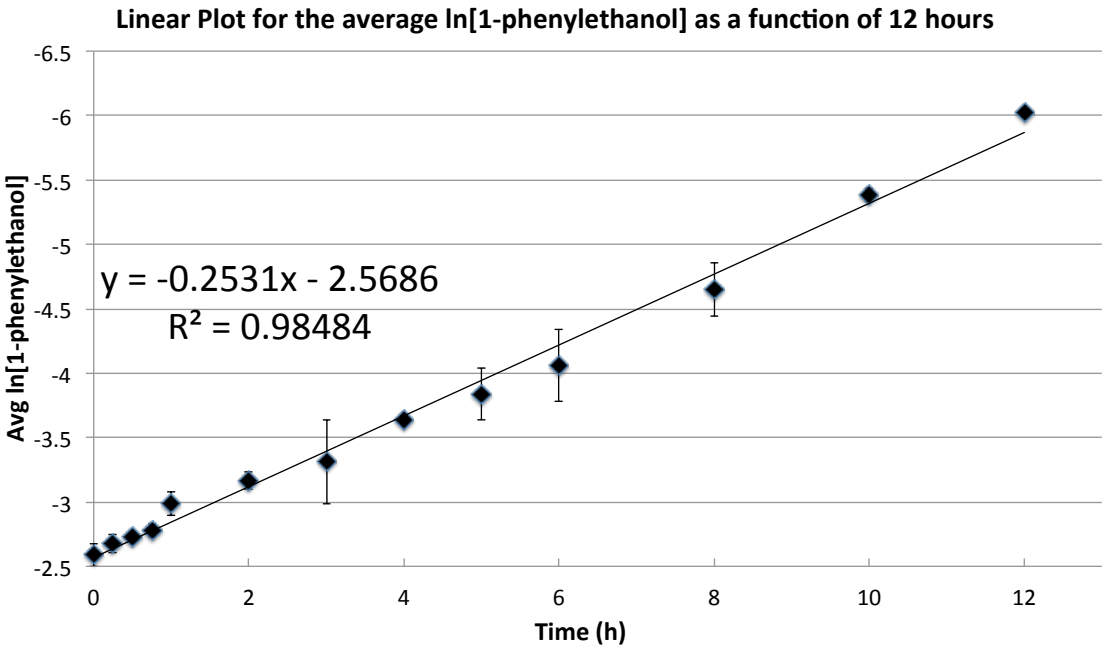

Figure 3.24. [0.075] 1-Phenylethanol linear plot

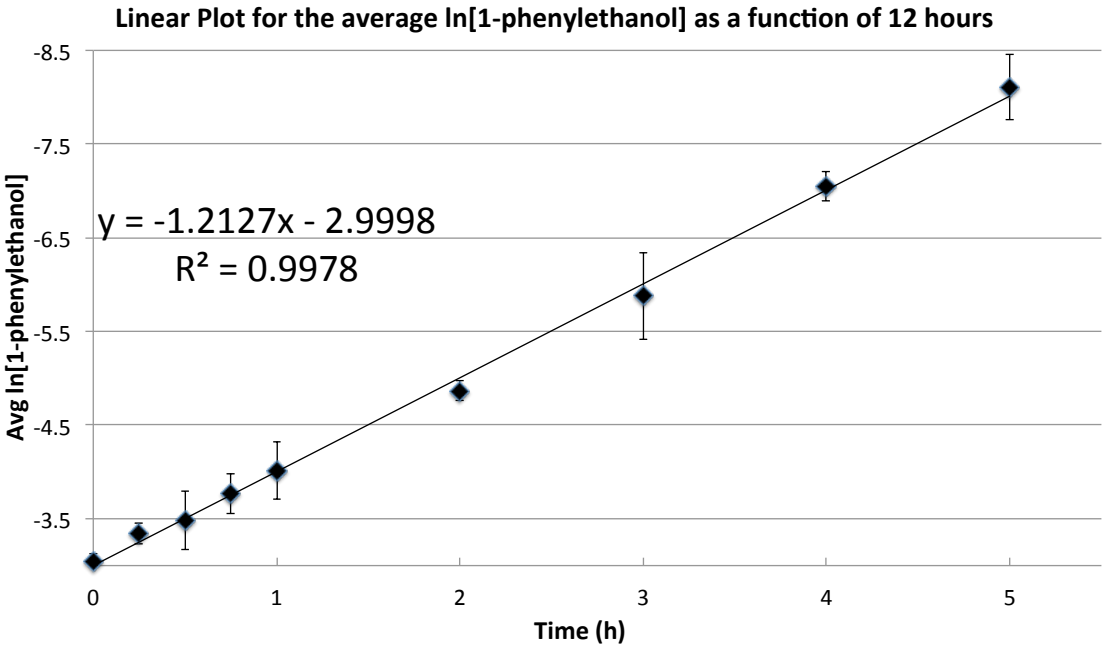

Figure 3.25. [0.05] 1-Phenylethanol linear plot

3.5 REFERENCES

(1) Queen, W. L.; Hwu, S.-J.; Reighard, S. *Inorganic Chemistry* **2010**, *49*, 1316-1318.

(2) Queen, W. L.; West, J. P.; Hwu, S.-J.; Tran, T. T.; Halasyamani, P. S.; VanDerveer, D. *Chemical Communications* **2012**, *48*, 1665-1667.

(3) Queen, W. L.; West, J. P.; Hudson, J.; Hwu, S.-J. *Inorganic Chemistry* **2011**, *50*, 11064-11068.

(4) Campbell, M. L.; Sulejmanovic, D.; Schiller, J. B.; Turner, E. M.; Hwu, S.-J.; Whitehead, D. C. *Catal. Sci. Technol.* **2016**, *6*, 3208-3213.

(5) Kozhevnikov, I. V.; Taraban'ko, V. E.; Matveev, K. I. *Dokl. Akad. Nauk SSSR* **1977**, *235*, 1347-1349 [Phys. Chem.].

(6) Nomiya, K.; Sugie, Y.; Miyazaki, T.; Miwa, M. *Polyhedron* **1986**, *5*, 1267-1271.

(7) Neumann, R.; Khenkin, A. M.; Juwiler, D.; Miller, H.; Gara, M. *Journal of Molecular Catalysis A: Chemical* **1997**, *117*, 169-183.

(8) Firouzabadi, H.; Iranpoor, N.; Amani, K. *Synthesis* **2003**, *2003*, 0408-0412.

(9) Leng, Y.; Zhao, P.; Zhang, M.; Wang, J. *Journal of Molecular Catalysis A: Chemical* **2012**, *358*, 67-72.

(10) Kikukawa, Y.; Yamaguchi, K.; Mizuno, N. *Angewandte Chemie International Edition* **2010**, *49*, 6096-6100.

(11) Wang, J.; Yan, L.; Li, G.; Wang, X.; Ding, Y.; Suo, J. *Tetrahedron Letters* **2005**, *46*, 7023-7027.

(12) Tundo, P.; Romanelli, G. P.; Vázquez, P. G.; Aricò, F. *Catalysis Communications* **2010**, *11*, 1181-1184.

(13) Zhao, W.; Zhang, Y.; Ma, B.; Ding, Y.; Qiu, W. *Catalysis Communications* **2010**, *11*, 527-531.

(14) Ding, Y.; Zhao, W. *Journal of Molecular Catalysis A: Chemical* **2011**, *337*, 45-51.

(15) N., K. C.; Akiko, T.; Satoshi, N.; Kazuhiro, G.; Kenji, N. *Chemistry Letters* **2005**, *34*, 238-239.

(16) Yokoyama, A.; Ohkubo, K.; Ishizuka, T.; Kojima, T.; Fukuzumi, S. *Dalton Transactions* **2012**, *41*, 10006-10013.

(17) Wang, J.; Yan, L.; Qian, G.; Lv, G.; Li, G.; Suo, J.; Wang, X. *Reaction Kinetics and Catalysis Letters* **2007**, *91*, 111-118.

(18) Hasannia, S.; Yadollahi, B. *Polyhedron* **2015**, *99*, 260-265.

(19) Pathan, S.; Patel, A. *Catalysis Science & Technology* **2014**, *4*, 648-656.

(20) Farsani, M. R.; Jalilian, F.; Yadollahi, B.; Rudbari, H. A. *Polyhedron* **2014**, *76*, 102-107.

(21) Choi, J. H.; Kim, J. K.; Park, S.; Song, J. H.; Song, I. K. *Applied Catalysis A: General* **2012**, *427–428*, 79-84.

(22) Park, D. R.; Kim, H.; Jung, J. C.; Lee, S. H.; Song, I. K. *Research on Chemical Intermediates* **2008**, *34*, 845-851.

(23) Choi, J. H.; Kang, T. H.; Bang, Y.; Song, J. H.; Song, I. K. *Catalysis Communications* **2014**, *55*, 29-33.

(24) Masteri-Farahani, M.; Najafi, G. R.; Modarres, M.; Taghvai-Nakhjiri, M. *J. Porous Mater.* **2016**, *23*, 285-290.

(25) Kozhevnikov, I. V. *Chemical Reviews* **1998**, *98*, 171-198.

(26) Ding, Y.; Zhao, W.; Zhang, Y.; Ma, B.; Qiu, W. *Reaction Kinetics, Mechanisms and Catalysis* **2011**, *102*, 85-92.

(27) Farsani, M. R.; Assady, E.; Jalilian, F.; Yadollahi, B.; Rudbari, H. A. *Journal of the Iranian Chemical Society* **2015**, *12*, 1207-1212.

(28) Farsani, M. R.; Yadollahi, B. *Journal of Molecular Catalysis A: Chemical* **2014**, *392*, 8-15.

(29) Chen, Y.; Tan, R.; Zheng, W.; Zhang, Y.; Zhao, G.; Yin, D. *Catal. Sci. Technol.* **2014**, *4*, 4084-4092.

(30) Misono, M. *Chemical Communications* **2001**, 1141-1152.

(31) Ben-Daniel, R.; Neumann, R. *Angewandte Chemie International Edition* **2003**, *42*, 92-95.

(32) Ben-Daniel, R.; Alsters, P.; Neumann, R. *J. Org. Chem.* **2001**, *66*, 8650-8653.

(33) Dornan, L. M.; Muldoon, M. J. *Catalysis Science & Technology* **2015**, *5*, 1428-1432.

(34) Huang, X.; Zhang, X.; Zhang, D.; Yang, S.; Feng, X.; Li, J.; Lin, Z.; Cao, J.; Pan, R.; Chi, Y.; Wang, B.; Hu, C. *Chem. - Eur. J.* **2014**, *20*, 2557-2564.

(35) Ma, B.; Zhang, Y.; Ding, Y.; Zhao, W. *Catalysis Communications* **2010**, *11*, 853-857.

(36) Nikbakht, E.; Yadollahi, B.; Farsani, M. R. *Inorganic Chemistry Communications* **2015**, *55*, 135-138.

(37) Rao, P. S. N.; Parameswaram, G.; Rao, A. V. P.; Lingaiah, N. *Journal of Molecular Catalysis A: Chemical* **2015**, *399*, 62-70.

(38) Palermo, V.; Villabrille, P. I.; Vazquez, P. G.; Caceres, C. V.; Tundo, P.; Romanelli, G. P. *J. Chem. Sci. (Bangalore, India)* **2013**, *125*, 1375-1383.

(39) Rao, P. S. N.; Venkateswara Rao, K. T.; Sai Prasad, P. S.; Lingaiah, N. *Catalysis Communications* **2010**, *11*, 547-550.

(40) Wang, S.-S.; Yang, G.-Y. *Chemical Reviews* **2015**, *115*, 4893-4962.

(41) Monakhov, K. Y.; Bensch, W.; Kogerler, P. *Chemical Society Reviews* **2015**, *44*, 8443-8483.

(42) Haimov, A.; Neumann, R. *Chemical Communications* **2002**, 876-877.

(43) Maayan, G.; Ganchegui, B.; Leitner, W.; Neumann, R. *Chemical Communications* **2006**, 2230-2232.

(44) Neumann, R.; Khenkin, A. M.; Vigdergauz, I. *Chemistry – A European Journal* **2000**, *6*, 875-882.

(45) Khenkin, A. M.; Leitus, G.; Neumann, R. *J. Am. Chem. Soc.* **2010**, *132*, 11446-11448.

(46) Khenkin, A. M.; Neumann, R. *The Journal of Organic Chemistry* **2002**, *67*, 7075-7079.

(47) Bordoloi, A.; Sahoo, S.; Lefebvre, F.; Halligudi, S. B. *Journal of Catalysis* **2008**, *259*, 232-239.

(48) Okuhara, T. *Chemical Reviews* **2002**, *102*, 3641-3666.

(49) Jing, L.; Shi, J.; Zhang, F.; Zhong, Y.; Zhu, W. *Industrial & Engineering Chemistry Research* **2013**, *52*, 10095-10104.

(50) Kozhevnikov, I. V. *Journal of Molecular Catalysis A: Chemical* **2007**, *262*, 86-92.

(51) West, J. P.; Hwu, S.-J. *Journal of Solid State Chemistry* **2012**, *195*, 101-107.

(52) Huang, Q.; Ulutagay, M.; Michener, P. A.; Hwu, S.-J. *Journal of the American Chemical Society* **1999**, *121*, 10323-10326.

(53) Wang, L.; Hwu, S.-J. *Chem. Mater.* **2007**, *19*, 6212-6221.

(54) Choudhury, A.; Dorhout, P. K. *Inorg. Chem.* **2006**, *45*, 5245-5247.

(55) Wang, L.; Hung, Y.-C.; Hwu, S.-J.; Koo, H.-J.; Whangbo, M. H. *Chem. Mater.* **2006**, *18*, 1219-1225.

(56) Hwu, S.-J. In *Inorganic Chemistry in Focus III*; Wiley-VCH Verlag GmbH & Co. KGaA: 2006, p 239-250.

(57) Ranmohotti, K. G. S.; Queen, W. L.; West, J. P.; VanDerveer, D.; Hwu, S.-J. *J. Chem. Crystallogr.* **2009**, *39*, 303-307.

(58) Hwu, S.-J.; Ulutagay-Kartin, M.; Clayhold, J. A.; Mackay, R.; Wardojo, T. A.; O'Connor, C. J.; Krawiec, M. *J. Am. Chem. Soc.* **2002**, *124*, 12404-12405.

(59) Huang, Q.; Kartin, M.; Mo, X.; Hwu, S.-J. *Mater. Res. Soc. Symp. Proc.* **2002**, *755*, 459-464.

(60) Ulutagay, M.; Schimek, G. L.; Hwu, S.-J.; Taye, H. *Inorg. Chem.* **1998**, *37*, 1507-1512.

(61) Huang, Q.; Hwu, S.-J.; Mo, X. *Angew. Chem., Int. Ed.* **2001**, *40*, 1690-1693.

(62) Huang, Q.; Ulutagay, M.; Michener, P. A.; Hwu, S.-J. *J. Am. Chem. Soc.* **1999**, *121*, 10323-10326.

(63) Etheredge, K. M. S.; Hwu, S.-J. *Inorg. Chem.* **1995**, *34*, 3123-3125.

(64) Hiskia, A.; Papaconstantinou, E. *Inorg. Chem.* **1992**, *31*, 163-167.

(65) Kim, W. B.; Voitl, T.; Rodriguez-Rivera, G. J.; Dumesic, J. A. *Science (Washington, DC, U. S.)* **2004**, *305*, 1280-1283.

(66) Troupis, A.; Triantis, T. M.; Gkika, E.; Hiskia, A.; Papaconstantinou, E. *Appl. Catal., B* **2009**, *86*, 98-107.

(67) Gkika, E.; Troupis, A.; Hiskia, A.; Papaconstantinou, E. *Environ. Sci. Technol.* **2005**, *39*, 4242-4248.

(68) Campbell, M. L.; Rackley, S. A.; Giambalvo, L. N.; Whitehead, D. C. *Tetrahedron* **2015**, *71*, 4888.

(69) Campbell, M. L.; Rackley, S. A.; Giambalvo, L. N.; Whitehead, D. C. *Tetrahedron Lett.* **2014**, *55*, 5680-5682.

(70) Oppenauer, R. V. *Recl. Trav. Chim. Pays-Bas Belg.* **1937**, *56*, 137-144.

(71) Creyghton, E. J.; Huskens, J.; Van Der Waal, J. C.; Van Bekkum, H. *Stud. Surf. Sci. Catal.* **1997**, *108*, 531-537.

(72) Drew, E. T.; Yang, Y.; Russo, J. A.; Campbell, M. L.; Rackley, S. A.; Hudson, J.; Schmuki, P.; Whitehead, D. C. *Catal. Sci. Technol.* **2013**, *3*, 2610-2613.

CHAPTER FOUR

A BRIEF OVERVIEW OF NANOMATERIALS FOR REMEDIATION OF HAZARDOUS VOLATILE ORGANIC COMPOUNDS

4.1 INTRODUCTION

4.1.1 Nanomaterials in hazardous organic compound remediation

The breadth of research focusing on nanomaterial synthesis for the remediation of environmental pollutants is extensive; therefore, the discussion in chapter four will focus on the most referenced materials reviewed in the last two decades that are capable of sequestering harmful volatile organic compounds (VOCs).[1-3] Emerging nanotechnologies hold novelty by reducing costs and improving overall effectiveness in remediating environmental pollutants. Their applications as sorbents, in high-flux membrane separation, and pollution prevention is well documented.[4,5]

Gaseous emissions from a variety of sources are a current global concern due to their potential effects on both the environment and communities in populated regions. Certain volatile organic compounds (VOCs), such as carbon dioxide (CO_2), ammonia (NH_3), formaldehyde, formic acid, *etc.*, are harmful both to the environment and to human health and are the subject of many studies (Figure 4.1).[6] A number of techniques that employ nanotechnology have been investigated for the detection or remediation of gaseous pollutants and are described in the following sections. Pollution being a worldwide concern, the

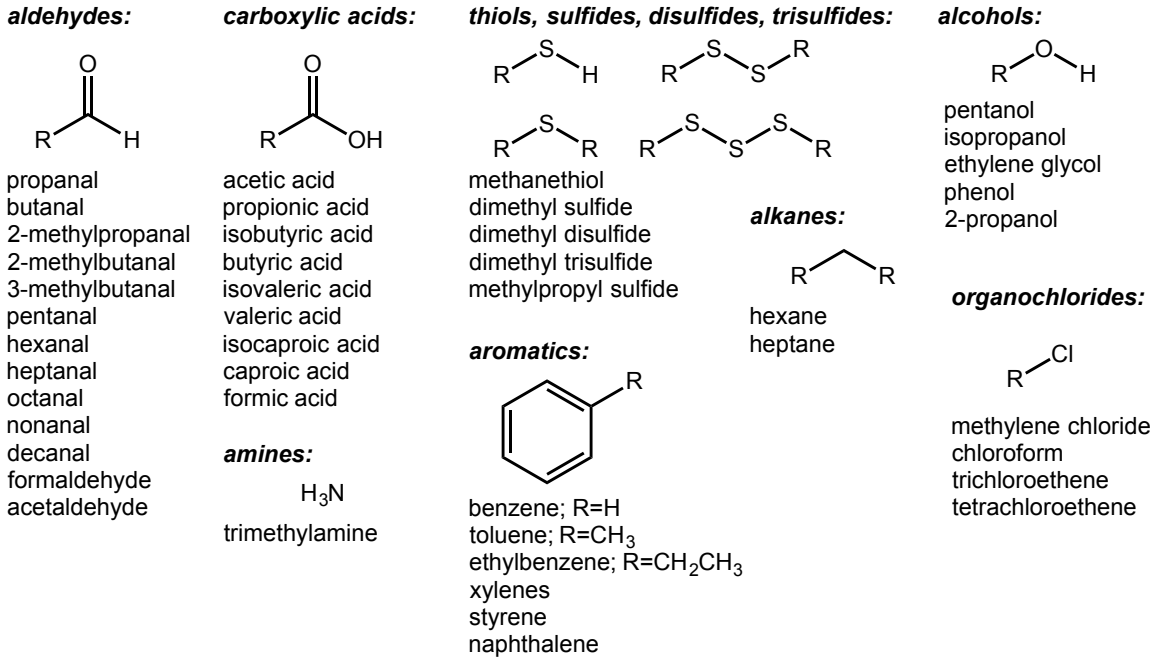

Figure 4.1. Common volatile organics that represent hazardous aerosols for human exposure

development of strategies for contaminant remediation is underway to either regulate anthropogenic emissions in order to decrease the volume of contaminants expelled or to decrease the concentration of pollutants already present in the environment.

The United States annually produces millions of tons of pollution and spends on average ten billion dollars annually for its control. Consequently new methods to reduce or prevent pollution at the source are critical.[1,7,8] Global policies have been enacted to regulate pollution emission in an effort to decrease both environmental and population exposure to these harmful compounds. Therefore, maintaining and improving air, water, and soil quality are important challenges that communities must address.

This chapter will introduce subsets of current nanomaterials used for the remediation of organic compounds from various environmental media.[2,5,9-11] The materials presented in this chapter are porous, providing increased surface area available for the liquid or gaseous pollutant to penetrate, thus leading to increased interactions with available reactive sites for targeted liquid/gaseous contaminants capture during exposure. In this overview, we present the remediation mechanisms of these nanomaterials and discuss specific methods for remediation of gaseous compounds. Selecting the best nanomaterial to mitigate pollution in a specific environmental context requires an in-depth analysis of the type of contaminant to be removed, the accessibility to the remediation site, the amount of material to be used, and whether it is advantageous to recover the remediation nanomaterial. Given that each material has its own advantages and issues related to its applicability, we provide an overall perspective on the use of several current nanomaterials in environmental remediation.

4.2 Nanomaterials: carbon-based

Carbonaceous nanomaterials (CNMs) are one of the most frequently applied sorbent materials and are used in the environment to remediate pollutants (retroactive application) while also limiting environmental impact (proactive application).[5] Carbon's ability to undergo vast structural changes based on varying synthetic protocols allows for a degree of control in the

assembly of structured carbonaceous nanomaterials. Due to carbon's ability to adopt sp^3, sp^2, or sp hybridized configurations, a large range of organic nanomaterials are allowed with a variety of bulk configurations.[5] The degree of saturation is dependent on temperature and pressure. For lower heats of formation, carbon assembles in a planar sp^2 conformation forming monolayer sheets. When subjected to higher temperatures and pressure, carbon seeks the thermodynamically stable sp^3 tetrahedral configuration.[5] Fullerene C_{60}, single-walled nanotubes (SWCNTs), multi-walled nanotubes (MWCNTs), and graphene are all notable structures used for the remediation of environmental pollutants (Figure 4.2).[5] CNMs feature a high surface area to volume ratio, an easily tailored surface chemistry, and controlled pore size distribution.[12-17] Fundamental hydrophobic and weak dipolar forces determine sorption energies required for direct sorption of organic hazardous compounds.[18,19] Higher rates for adsorption with carbonaceous nanosorbents over conventional activated carbon is due to π-π interaction in which electron-donor-acceptor reactivity with aromatic sorbates

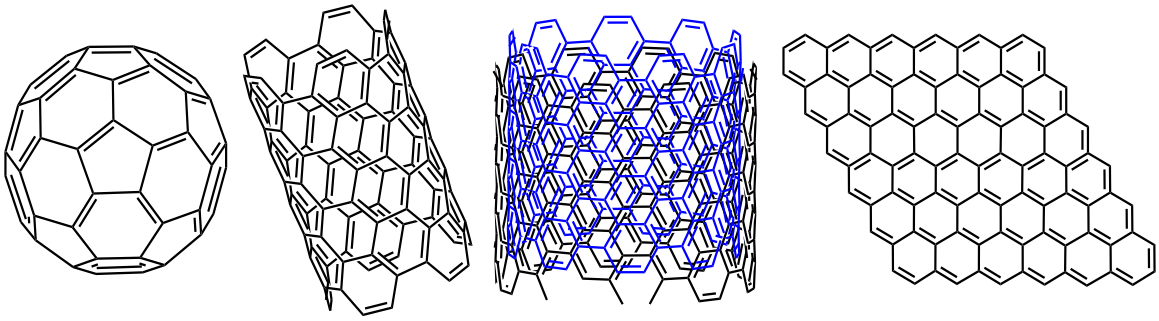

Figure 4.2. Several common carbonaceous nanomaterials used for VOC remediation

allows for organic compound remediation.[20-23] Another characteristic of CNMs which may contribute to increased rate of capture is the absence of pore diffusion as an intermediate mechanism in adsorption.[24] These factors were observed by Yang *et al.* in a study using several different CNMs (*e.g.* C-60 NPs, SWNTs, and MWNTs).[23] Of the previously mentioned CNMs, single and multi-walled carbon nanotubes and graphene-based nanomaterials are the focus of this discussion as they are the most employed CNMs for the sequestration of organic compounds such as toxic trihalomethanes, polycyclic aromatic hydrocarbons, naphthalene, *etc.* from contaminated environmental media.[13,17,23]

4.2.1 Carbon nanotubes: single- and multi-walled nanomaterials

The primary mode of adsorption for SWCNTs and MWCNTs is through nonspecific van der Waals interactions. The driving force for these interactions is induced dipole interactions between the carbon nanotubes (CNTs) and the targeted molecule for capture. Van der Waals interactions are the weakest interactions between molecules; however, the large degree of these interactions between the carbon surface and analyte increases the strength of the interactions. Mechanisms for adsorption of organic compounds to the surface of CNTs have been well documented by Yang and Xing.[25] CNT organic adsorption proceeds through electrostatic interactions, hydrophobic effect, π-π bonding, hydrogen bonding, and covalent bonding. The understanding of CNT binding mechanisms are applied to understanding adsorption of organic compounds by

graphene-based materials.[26]

SWCNTs are arranged in a hexagonal configuration (one nanotube surrounded by six others) and form bundles of aligned tubes that present a heterogeneous porous structure (Figure 4.3A). Monte Carlo simulations were used to determine the optimal pore diameter for gaseous adsorption to SWCNTs (Figure 4.3B). The use of this computational method for determining optimal pore size was applied to the adsorption of tetrafluoromethane; a known greenhouse gas with potent toxicity. Results from the Monte Carlo simulations revealed a 1.05 nm diameter for the nanotube allowed for balancing the strong binding energies (*i.e.* enthalpy of adsorption) against the total volume available for gas storage.[27]

The argument against the utility of carbonaceous nanomaterials versus

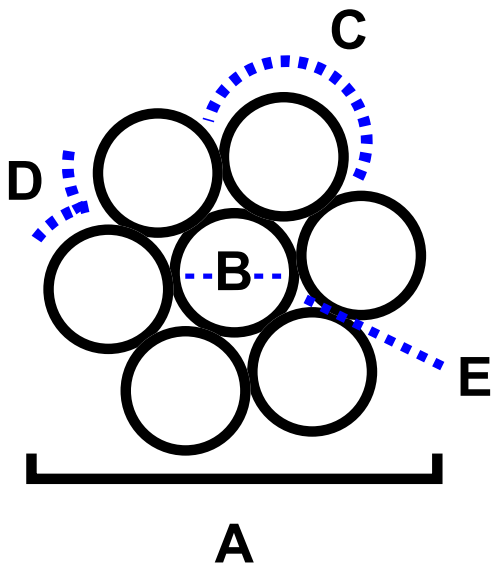

Figure 4.3. Representation of the hexagonal arrangement for SWCNTs including labeled regions common for adsorption

conventional remediation techniques is the high costs associated with their synthesis and possible toxicity concerns.[10,28] Yet, the cost effectiveness of SWCNTs and MWCNTs as replacements for traditional activated carbon was demonstrated recently in the remediation of common contaminants.[29] The use of SWCNTs and MWCNTs as adsorbents are particularly useful in the removal of organic and inorganic pollutants from gas and from large volumes of aqueous solution.[10]

Efforts to open the closed ends of pristine SWCNTs to enhance their adsorption properties are common in gaseous capture.[6] A typical open-ended SWCNT bundle exhibits four different available sites for potential contaminant adsorption. The sites may be one of two types. The first are those with lower adsorption energy that are localized on external surfaces of the outer SWCNT composing the bundle (Figure 4.3C and 4.3D). The second type includes those of higher adsorption energy localized either in between two neighboring tubes or within an individual tube (Figure 4.3E and 4.3B respectively). A substantial enhancement of the adsorption capacity is related to the availability of the adsorption sites within the inner hollow space of an individual tube (Figure 4.3B) Preparation of SWCNTs with larger diameters increases the effective pore volume, which promotes the enclosure of several layers of adsorbate species.[6]

Multi-walled carbon nanotubes (MWCNTs), which are the predecessor of SWCNTs, do not usually exist as bundles. The aggregated pores in MWCNTs, caused by SWCNT aggregation, are more responsible for adsorption properties

of these materials than other kinds of pores, like the inner cavities. In their study of nitrogen adsorption in aggregated MWCNTs, Yang *et al.* determined that the different types of pores, inner and aggregated, as shown in Figure 4.4, created a multi-stage adsorption process.[30] They also determined that the aggregated pores played a greater role in adsorption than the inner cavities, reinforcing the potential strategy that pore aggregation could be controlled during the treatment

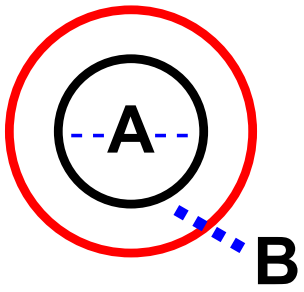

Figure 4.4. Representation of the inner (A) and aggregate (B) pores for MWCNTs

of pristine CNTs in a effort to improve adsorption capacity.[30]

Even though SWCNT and MWCNT have been studied for gas adsorption, a variety of studies suggest that treatment of the adsorbent surface with high temperatures and vacuum is necessary in order to measure high gas adsorption, which can limit the practical application of this technique.[31] The true innovative potential of nanosorbants is seen in their diverse availability for tailored functionalization of the surface chemistry, especially in nanotubes, and provide for an approach for targeting specific pollutants and removing low concentrations of contaminants.[32] When CNTs are functionalized with hydrophilic hydroxyl (-OH) or carboxylic acid (-COOH) moieties, the functional groups show excellent

capture of low molecular weight and polar compounds.[17]

4.2.2 Graphene-based nanomaterials: pristine *versus* modified

Graphene is a two-dimensional single layer of carbon atoms in a hexagonal crystalline structure. The current understanding of the mechanism for organic analyte capture is based of prior studies related to adsorption phenomena with CNTs.[26,33] Known for its unique physicochemical properties, graphene is one of the most extreme cases of high surface area given that every atom of a single-layer sheet is exposed on the top and bottom to give a total surface area of 2630 m^2 g^{-1} for adsorption. Geim and Novoselov's Nobel Prize winning research described the synthesis of graphene, the naturally found building block of graphite, by means of micromechanical exfoliation (*i.e.* Tape synthesis). Pristine graphene formed in synthetically useful quantities was allowed using micromechanical exfoliation. The resultant single layer of carbon atoms are arranged in sp^2-bonded aromatic structures (Figure 4.1).

Graphene's high surface area is ideal for adsorption chemistry and surface functionalization leading to graphene-based nanomaterials being an active area of current research.[34] Their application as adsorbents for removal of organic pollutants including dyes, antibiotics, hydrocarbons, crude oil, pesticides, and natural organic matter have been reported.[35-40] The mode/mechanism of capture between nanomaterial and organic compound varies depending on the structural properties of the material and the target analyte (*e.g.*, molecular

conformation, dipole moment, functional group compatibility, bond hybridization).[25,26] As such, the adsorption capacity is dependent on those factors as well as the presence or absence of surface functionalization with -NH_2, -OH, -COOH functional groups. Any of these factors, or more accurately a combination of them, will influence the mechanism and adsorption capacity.[25]

A common application of graphene-based nanomaterials is for gaseous pollutant capture.[41,42] Carbon dioxide (CO_2) is a common analyte of interest based on its contribution to global warming.[43] For a single layer pristine graphene sheet, Ghosh *et al.* showed a maximum uptake of 37.93 wt% CO_2.[41] Using DFT calculations, defective graphene sheets were shown to have four times higher CO_2 adsorption capacity than pristine graphene sheets. They surmised that this observation was due to an exothermic adsorption at the defect's vacant site through formation of a covalent C-O bond.[42]

Modifications to graphene decrease the aggregation of the graphene layers and in turn increase the effective surface area.[44] Specific functional groups or nanoparticles have also been used to modify the surface of graphene in order to increase the interaction between graphene and the target organic pollutant, thus increasing removal efficiency.[45] To date, modified graphene-based nanomaterials have been functionalized with amines, layered double hydroxides, and metal species to enhance gas adsorption.[46-52]

Removal of several greenhouse gases with modified graphene gives higher reduction than pristine graphene. For example, graphene sheets

decorated with polyaniline exhibited greater CO_2 capture due to covalent bond formation between the CO_2 and amine functional group available on the surface to give carbamates ($R\text{-}NHCOO^-$) (Scheme 4.1).[46] Several breenhouse gases including nitrogen dioxide (NO_2), sulfur dioxide (SO_2), and carbon monoxide (CO)

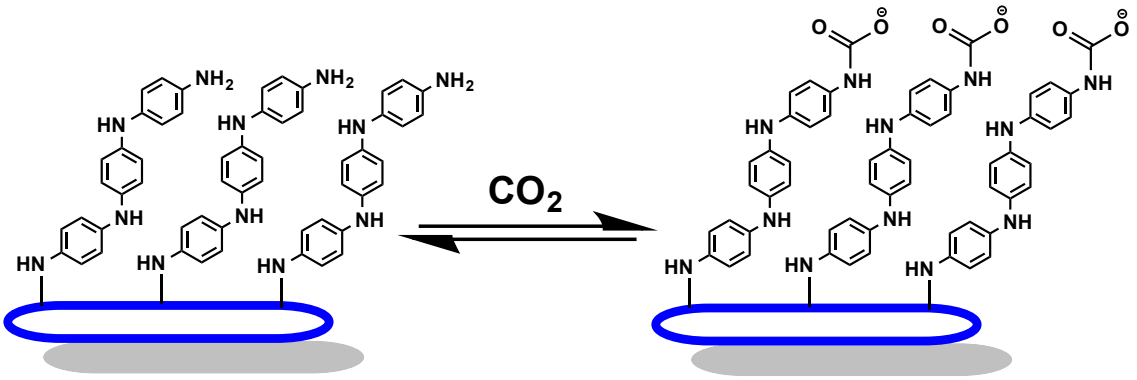

Scheme 4.1. Remediation of carbon dioxide using polyanaline functionalized graphene sheets represented by the blue support

have also been remediated using modified graphene nanomaterials.[18,19,53] Various nitrogen oxides were investigated using DFT calculations for both graphene and graphene oxide (GO).[54] Having the oxygen present allows for stronger adsorption of NO_x onto GO than graphene.[54] Additionally, both theoretical and experimental evidence highlighted the abilities of graphene-based materials to remove ammonia (NH_3).[14,16,17,55,56] Adsorption of NH_3 onto GO and layered-GO through hydroxyl and carboxyl groups, hydrogen bonding, and physical trapping into the inter layer space or pores are thought to be the primary mechanisms of capture for the gaseous analyte.[15,56]

4.3 Nanomaterials: mesoporous aminosilicate materials

In recent years, the Jones group has pioneered the use of amine laden silicate materials for CO_2 capture. These materials have demonstrated the efficiency of the amine groups for the reversible capture of CO_2 and remediation of small organic aldehydes and ketones.[5,57-61] The mechanism for CO_2 capture is possible through the reversible adsorption of CO_2 onto the amines of the aminosilicate material to form carbamates, as with the product of CO_2 adsorption to polyanaline functionalized graphene (*cf.* Scheme 4.1). Alkyl substitution at the nitrogen modulates the basicity of the amine and therefore, its ability to engage the CO_2 target analyte. Capture of aldehydes and ketones proceeds through the formation of a covalent imine bond (Scheme 4.2)[5,57-61]

In their analysis of the adsorption capacity and recyclability for a number of amino silicate derivatives, the Jones group observed material adsorption-

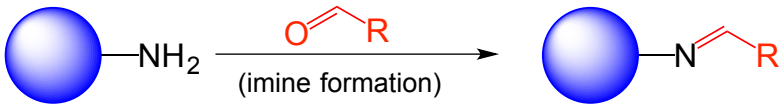

Scheme 4.2. Aminosilicates in the covalent capture of aldehydes through imine formation

desorption cycling for CO_2 capture using amino functionalized silica.[62] Rapid reactivity with up to 90% capture of CO_2 (total capacity of 7.9 mmol CO_2/g aminosilicate) was demonstrated within 90 minutes of treatment.[63] Consequently, these materials represent a viable alternative to traditional CO_2 capture methods in that they are less expensive, easier to synthesize, and exhibit greater

performance and stability when compared to other platforms.

In an extension of the method, the Jones group also used amine-functionalized porous silicates in an aldehyde abatement experiment to capture formaldehyde. The group determined that 1.4 mmol/g formaldehyde was retained in silica materials containing primary amines, 0.8 mmol/g of formaldehyde for materials containing secondary amines, and a negligible amount for tertiary amines.[62,64] While cursory, this investigation of other molecules nonetheless demonstrated the potential for capturing aldehyde molecules with a higher molecular weight. Unfortunately, the reaction time necessary to achieve equivalent performance was in excess of 10 hours, much longer compared to formaldehyde adsorption.[64]

These materials incorporate the amine functionality during the fabrication of the material, rather than a post-treatment functionalization technique applied to a scaffold material. This incorporation limits their use uniquely to target contaminants that can react with amines, whereas the materials that can be tailored to possess different functionalities may not be limited by the inherent functionality.

4.4 Nanomaterials: polymeric nanomaterials (PNMs)

Polymeric nanomaterials (PNMs) are used in the catalytic and redox degradation of contaminants, in pollutant sensing and detection, the adsorption of pollutants, and biosensing.[11] Common catalytic nanoparticles incorporated into

the polymeric host include nano-TiO_2, zero-valent metals, and bimetallic nanoparticles.[65-76] These materials are also used for the degradation polychlorinated biphenyls,[76,77] azo dyes,[78-80] halogenated herbicides[81] and organochlorine pesticides.[69,82]

PNMs exhibit specific interaction with contaminants in water, gases, and soils; however, the difficulty of separating and reusing nanoparticles as well as their associated risks to ecosystems and human health has necessitated the development of hybrid nanocomposites through the coating of fine particles onto larger solid materials.[11] The characteristics of these polymer-based nanocomposites (PNCs) are inherent to both the particles and polymer with which it is made, specifically in that they are highly stable and easily processed. The mechanical and thermal behavior, the hydrophobic/hydrophilic balance, the chemical stability, functionalities, and biocompatibility are all used to determine the specific polymeric host to be used.[11]

Most of the advantages inherent in the use of nanoparticles derive from their large surface area to volume ratios, which yield a high rate of reactivity. Adhering nanoparticles to a polymeric scaffold can increase the stability of the material when compared to the use of nanoparticles alone.[83-85] Furthermore, functionalizing the material with specific chemicals responsible for targeting contaminant molecules of interest can increase the selectivity and efficiency of the material.[86]

4.4.1 Polymer-supported nanocomposites

Porous polymeric adsorbents represent an ideal alternative for targeted pollutant removal due to their mechanical strength, potential for long-term use, and adjustable surface chemistry. Polymer-supported nanocomposites consist of materials that utilize a polymer as a host material that serves as the medium through which nanoparticles are either included within or coated on top. This material combines the desirable properties of both polymers (*i.e.* exquisite mechanical strength) with those of nanoparticles (*i.e.* high reactivity, arising from their large surface to volume ratio). Many direct compounding or *in situ* synthesis techniques are available for the preparation of polymer nanocomposites (PNCs).[11,87-92]

These materials are used in the purification of both water and gas, specifically by means of the catalytic and redox reaction of contaminants and via the adsorption of pollutants. Zhao, X. *et al.*[10] used TiO_2 nanoparticles to decolorize a methylene blue solution, by 96%, after a one-hour solar illumination on a polymer polyhydroxylbutyrate matrix.[10] The group also used Fe^0 nanoparticles to reduce, by 94%, the presence of Cr(VI) using TiO_2 nanoparticles on a carboxylmethyl cellulose matrix.

4.5 CONCLUSIONS

Various nanomaterials and their applicability in environmental remediation of VOCs were discussed emphasizing their unique chemical and physical

properties due to their small size and large surface area relative to their volume. The challenges preventing the global use of nanomaterials are formidable, specifically in synthetic expense, limited scale-up procedures, potential toxicity, and the low off-targeting specificity. Nevertheless, this brief discussion of current nanotechnologies highlights the continued effort towards understanding their adsorption mechanisms and their application for the remediation of organic compounds from various environmental media.

Recently, our group has published research describing the use of polymeric nanomaterials for the remediation of volatile organic compounds (VOCs).[93] The incorporation of amine groups from poly(ethyleneimine) onto the polymeric nanomaterial PDDLA-PEG-COOH allowed for the targeted capture of VOCs of the aldehyde and carboxylic acid functional group classes. The next chapter will focus on our development of a Gas Chromatography headspace analysis method, which was then used to demonstrate that the amine-functionalized nanoparticles synthesized by our collaborators of the Alexis group were able to reduce aldehydes (from 69% and up reductions) and carboxylic acid vapors (from 76% and up reductions).

4.6 REFERENCES

(1) Karn, B.; Kuiken, T.; Otto, M. *Environmental health perspectives* **2009**, 1823-1831.

(2) Shan, G.; Yan, S.; Tyagi, R.; Surampalli, R. Y.; Zhang, T. C. *Practice Periodical of Hazardous, Toxic, and Radioactive Waste Management* **2009**, *13*, 110-119.

(3) Klefenz, H. *Engineering in life sciences* **2004**, *4*, 211-218.

(4) Savage, N.; Diallo, M. S. *Journal of Nanoparticle research* **2005**, *7*, 331-342.

(5) Mauter, M. S.; Elimelech, M. *Environmental Science & Technology* **2008**, *42*, 5843-5859.

(6) Lithoxoos, G. P.; Labropoulos, A.; Peristeras, L. D.; Kanellopoulos, N.; Samios, J.; Economou, I. G. *The Journal of Supercritical Fluids* **2010**, *55*, 510-523.

(7) Congress, U. *Public Law* **1990**, 13101-13109.

(8) Masciangioli, T.; Zhang, W.-X. *Environmental science & technology* **2003**, *37*, 102A-108A.

(9) Li, X.-q.; Elliott, D. W.; Zhang, W.-x. *Critical reviews in solid state and materials sciences* **2006**, *31*, 111-122.

(10) Ren, X.; Chen, C.; Nagatsu, M.; Wang, X. *Chemical Engineering Journal* **2011**, *170*, 395-410.

(11) Zhao, X.; Lv, L.; Pan, B.; Zhang, W.; Zhang, S.; Zhang, Q. *Chemical engineering journal* **2011**, *170*, 381-394.

(12) Ravelli, D.; Dondi, D.; Fagnoni, M.; Albini, A. *Chem. Soc. Rev.* **2009**, *38*, 1999-2011.

(13) Chong, M. N.; Jin, B.; Chow, C. W. K.; Saint, C. *Water Res.* **2010**, *44*, 2997-3027.

(14) Seredych, M.; Rossin, J. A.; Bandosz, T. J. *Carbon* **2011**, *49*, 4392-4402.

(15) Seredych, M.; Bandosz, T. J. *J. Phys. Chem. C* **2007**, *111*, 15596-15604.

(16) Petit, C.; Bandosz, T. J. *Adv. Funct. Mater.* **2011**, *21*, 2108-2117.

(17) Tang, S.; Cao, Z. *J. Phys. Chem. C* **2012**, *116*, 8778-8791.

(18) Leenaerts, O.; Partoens, B.; Peeters, F. M. *Phys. Rev. B: Condens. Matter Mater. Phys.* **2008**, *77*, 125416/125411-125416/125416.

(19) Seredych, M.; Bandosz, T. J. *J. Phys. Chem. C* **2010**, *114*, 14552-14560.

(20) Yang, S.-T.; Chen, S.; Chang, Y.; Cao, A.; Liu, Y.; Wang, H. *J. Colloid Interface Sci.* **2011**, *359*, 24-29.

(21) An, X.; Yu, J. C. *RSC Adv.* **2011**, *1*, 1426-1434.

(22) Fujishima, A.; Honda, K. *Nature (London)* **1972**, *238*, 37-38.

(23) Khan, Z.; Chetia, T. R.; Vardhaman, A. K.; Barpuzary, D.; Sastri, C. V.; Qureshi, M. *RSC Adv.* **2012**, *2*, 12122-12128.

(24) Linsebigler, A. L.; Lu, G.; Yates, J. T., Jr. *Chem. Rev. (Washington, D. C.)* **1995**, *95*, 735-758.

(25) Yang, K.; Xing, B. *Chem. Rev. (Washington, DC, U. S.)* **2010**, *110*, 5989-6008.

(26) Zhao, J.; Wang, Z.; White, J. C.; Xing, B. *Environ. Sci. Technol.* **2014**, *48*, 9995-10009.

(27) Zhang, Y.; Tang, Z.-R.; Fu, X.; Xu, Y.-J. *ACS Nano* **2011**, *5*, 7426-7435.

(28) Perreault, F.; Fonseca de Faria, A.; Elimelech, M. *Chem. Soc. Rev.* **2015**, *44*, 5861-5896.

(29) Zhang, Y.; Tang, Z.-R.; Fu, X.; Xu, Y.-J. *ACS Nano* **2010**, *4*, 7303-7314.

(30) Yang, Q. H.; Hou, P. X.; Bai, S.; Wang, M. Z.; Cheng, H. M. *Chem. Phys. Lett.* **2001**, *345*, 18-24.

(31) Darkrim, F. L.; Malbrunot, P.; Tartaglia, G. *International Journal of Hydrogen Energy* **2002**, *27*, 193-202.

(32) Lambert, T. N.; Chavez, C. A.; Hernandez-Sanchez, B.; Lu, P.; Bell, N. S.; Ambrosini, A.; Friedman, T.; Boyle, T. J.; Wheeler, D. R.; Huber, D. L. *J. Phys. Chem. C* **2009**, *113*, 19812-19823.

(33) Geim, A. K. *Science (Washington, DC, U. S.)* **2009**, *324*, 1530-1534.

(34) Compton, O. C.; Nguyen, S. T. *Small* **2010**, *6*, 711-723.

(35) Yan, H.; Tao, X.; Yang, Z.; Li, K.; Yang, H.; Li, A.; Cheng, R. *J. Hazard. Mater.* **2014**, *268*, 191-198.

(36) Gao, Y.; Li, Y.; Zhang, L.; Huang, H.; Hu, J.; Shah, S. M.; Su, X. *J. Colloid Interface Sci.* **2012**, *368*, 540-546.

(37) Zhang, C.; Wu, L.; Cai, D.; Zhang, C.; Wang, N.; Zhang, J.; Wu, Z. *ACS Appl. Mater. Interfaces* **2013**, *5*, 4783-4790.

(38) Li, J.; Wang, F.; Liu, C.-y. *J. Colloid Interface Sci.* **2012**, *382*, 13-16.

(39) Liu, X.; Zhang, H.; Ma, Y.; Wu, X.; Meng, L.; Guo, Y.; Yu, G.; Liu, Y. *J. Mater. Chem. A* **2013**, *1*, 1875-1884.

(40) Chowdhury, I.; Duch, M. C.; Mansukhani, N. D.; Hersam, M. C.; Bouchard, D. *Environ. Sci. Technol.* **2014**, *48*, 9382-9390.

(41) Ghosh, A.; Subrahmanyam, K. S.; Krishna, K. S.; Datta, S.; Govindaraj, A.; Pati, S. K.; Rao, C. N. R. *J. Phys. Chem. C* **2008**, *112*, 15704-15707.

(42) Ning, G.; Xu, C.; Mu, L.; Chen, G.; Wang, G.; Gao, J.; Fan, Z.; Qian, W.; Wei, F. *Chem. Commun. (Cambridge, U. K.)* **2012**, *48*, 6815-6817.

(43) Solomon, S.; Plattner, G.-K.; Knutti, R.; Friedlingstein, P. *Proc. Natl. Acad. Sci. U. S. A.* **2009**, *106*, 1704-1709.

(44) Zhang, N.; Yang, M.-Q.; Tang, Z.-R.; Xu, Y.-J. *J. Catal.* **2013**, *303*, 60-69.

(45) Lue, K.; Zhao, G. X.; Wang, X. K. *Chin. Sci. Bull.* **2012**, *57*, 1223-1234.

(46) Mishra, A. K.; Ramaprabhu, S. *J. Mater. Chem.* **2012**, *22*, 3708-3712.

(47) Zhao, Y.; Ding, H.; Zhong, Q. *Appl. Surf. Sci.* **2012**, *258*, 4301-4307.

(48) Hong, S.-M.; Kim, S. H.; Lee, K. B. *Energy Fuels* **2013**, *27*, 3358-3363.

(49) Chandra, V.; Yu, S. U.; Kim, S. H.; Yoon, Y. S.; Kim, D. Y.; Kwon, A. H.; Meyyappan, M.; Kim, K. S. *Chem. Commun. (Cambridge, U. K.)* **2012**, *48*, 735-737.

(50) Garcia-Gallastegui, A.; Iruretagoyena, D.; Gouvea, V.; Mokhtar, M.; Asiri, A. M.; Basahel, S. N.; Al-Thabaiti, S. A.; Alyoubi, A. O.; Chadwick, D.; Shaffer, M. S. P. *Chem. Mater.* **2012**, *24*, 4531-4539.

(51) Carrillo, I.; Rangel, E.; Magana, L. F. *Carbon* **2009**, *47*, 2758-2760.

(52) Wang, L.; Zhao, J.; Wang, L.; Yan, T.; Sun, Y.-Y.; Zhang, S. B. *Phys. Chem. Chem. Phys.* **2011**, *13*, 21126-21131.

(53) Chen, C.; Xu, K.; Ji, X.; Miao, L.; Jiang, J. *Phys. Chem. Chem. Phys.* **2014**, *16*, 11031-11036.

(54) Tang, S.; Cao, Z. *J. Chem. Phys.* **2011**, *134*, 044710/044711-044710/044714.

(55) Petit, C.; Mendoza, B.; Bandosz, T. J. *Langmuir* **2010**, *26*, 15302-15309.

(56) Deliyanni, E.; Seredych, M.; Bandosz, T. J. *Langmuir* **2009**, *25*, 9302-9312.

(57) Nomura, A.; Jones, C. W. *Chemistry–A European Journal* **2014**, *20*, 6381-6390.

(58) Drese, J. H.; Talley, A. D.; Jones, C. W. *ChemSusChem* **2011**, *4*, 379-385.

(59) Choi, S.; Gray, M. L.; Jones, C. W. *ChemSusChem* **2011**, *4*, 628-635.

(60) Kuwahara, Y.; Kang, D.-Y.; Copeland, J. R.; Brunelli, N. A.; Didas, S. A.; Bollini, P.; Sievers, C.; Kamegawa, T.; Yamashita, H.; Jones, C. W. *Journal of the American Chemical Society* **2012**, *134*, 10757-10760.

(61) Nomura, A.; Jones, C. W. *ACS applied materials & interfaces* **2013**, *5*, 5569-5577.

(62) Alkhabbaz, M. A.; Bollini, P.; Foo, G. S.; Sievers, C.; Jones, C. W. *J. Am. Chem. Soc.* **2014**, *136*, 13170-13173.

(63) Sakwa-Novak, M. A.; Jones, C. W. *ACS Appl. Mater. Interfaces* **2014**, *6*, 9245-9255.

(64) Bollini, P.; Didas, S. A.; Jones, C. W. *J. Mater. Chem.* **2011**, *21*, 15100-15120.

(65) Trivedi, P.; Axe, L. *Environmental science & technology* **2000**, *34*, 2215-2223.

(66) Xiong, Z.; Zhao, D.; Pan, G. *Water research* **2007**, *41*, 3497-3505.

(67) Ponder, S. M.; Darab, J. G.; Mallouk, T. E. *Environmental Science & Technology* **2000**, *34*, 2564-2569.

(68) Lin, C. J.; Lo, S.-L.; Liou, Y. H. *Chemosphere* **2005**, *59*, 1299-1307.

(69) Wang, Z.; Huang, W.; Fennell, D. E.; Peng, P. a. *Chemosphere* **2008**, *71*, 360-368.

(70) Guczi, L. *Catalysis Today* **2005**, *101*, 53-64.

(71) Zhang, W.-x.; Wang, C.-B.; Lien, H.-L. *Catalysis today* **1998**, *40*, 387-395.

(72) Elliott, D. W.; Zhang, W.-X. *Environmental Science & Technology* **2001**, *35*, 4922-4926.

(73) Schrick, B.; Blough, J. L.; Jones, A. D.; Mallouk, T. E. *Chemistry of Materials* **2002**, *14*, 5140-5147.

(74) Chen, L.-H.; Huang, C.-C.; Lien, H.-L. *Chemosphere* **2008**, *73*, 692-697.

(75) Rivero-Huguet, M.; Marshall, W. D. *Journal of hazardous materials* **2009**, *169*, 1081-1087.

(76) Liu, Z.; Zhang, F.-S. *Bioresource technology* **2010**, *101*, 2562-2564.

(77) Varanasi, P.; Fullana, A.; Sidhu, S. *Chemosphere* **2007**, *66*, 1031-1038.

(78) Zhu, H.; Jiang, R.; Xiao, L.; Chang, Y.; Guan, Y.; Li, X.; Zeng, G. *Journal of Hazardous Materials* **2009**, *169*, 933-940.

(79) Konstantinou, I. K.; Albanis, T. A. *Applied Catalysis B: Environmental* **2004**, *49*, 1-14.

(80) Daneshvar, N.; Salari, D.; Khataee, A. *Journal of photochemistry and photobiology A: chemistry* **2004**, *162*, 317-322.

(81) Konstantinou, I. K.; Sakellarides, T. M.; Sakkas, V. A.; Albanis, T. A. *Environmental science & technology* **2001**, *35*, 398-405.

(82) Song, H.; Carraway, E. R.; Kim, Y. H.; Batchelor, B.; Jeon, B.-H.; Kim, J.-g. *Chemosphere* **2008**, *73*, 1420-1427.

(83) Trujillo-Reyes, J.; Peralta-Videa, J.; Gardea-Torresdey, J. *Journal of hazardous materials* **2014**, *280*, 487-503.

(84) Allabashi, R.; Arkas, M.; Hörmann, G.; Tsiourvas, D. *Water Research* **2007**, *41*, 476-486.

(85) Sun, Y.; Ding, C.; Cheng, W.; Wang, X. *Journal of hazardous materials* **2014**, *280*, 399-408.

(86) Liu, Y.; Su, G.; Zhang, B.; Jiang, G.; Yan, B. *Analyst* **2011**, *136*, 872-877.

(87) Yang, D.; Li, J.; Jiang, Z.; Lu, L.; Chen, X. *Chemical Engineering Science* **2009**, *64*, 3130-3137.

(88) Tong, Y.; Li, Y.; Xie, F.; Ding, M. *Polymer international* **2000**, *49*, 1543-1547.

(89) Ahmad, S.; Ahmad, S.; Agnihotry, S. *Bulletin of Materials Science* **2007**, *30*, 31-35.

(90) Luo, Y.-B.; Li, W.-D.; Wang, X.-L.; Xu, D.-Y.; Wang, Y.-Z. *Acta Materialia* **2009**, *57*, 3182-3191.

(91) Sanz, R.; Luna, C.; Hernández-Vélez, M.; Vázquez, M.; López, D.; Mijangos, C. *Nanotechnology* **2005**, *16*, S278.

(92) Wu, W.; He, T.; Chen, J.-f.; Zhang, X.; Chen, Y. *Materials Letters* **2006**, *60*, 2410-2415.

(93) Campbell, M. L.; Guerra, F. D.; Dhulekar, J.; Alexis, F.; Whitehead, D. C. *Chem. - Eur. J.* **2015**, *21*, 14834-14842.

CHAPTER FIVE

APPLICATION OF FUNCTIONALIZED PDDLA-PEG-PEI NANOPARTICLES AND NATURAL CLAYS FOR VOLATILE ORGANIC COMPOUND REMEDIATION

5.1 INTRODUCTION

5.1.1 Specific Aims

Aldehyde and carboxylic acid volatile organic compounds (VOCs) cause significant concern for the environment due to their increasing prevalence in the atmosphere and potential toxicity towards humans. Joint work with the Alexis group in Clemson University's Bioengineering Department has allowed us access to biodegradable functionalized nanoparticles (NPs) comprised of Poly(D,L-lactic acid)-poly(ethylene glycol)-poly(ethyleneimine) (*i.e.* PDLLA-PEG-PEI) block copolymers that capture the aforementioned VOCs via chemical reaction. NP preparation involved nanoprecipitation and surface functionalization with branched PEI. The PDLLA-PEG-PEI NPs were characterized using TGA, IR, ^{1}H-NMR, elemental analysis, and TEM. The materials feature 1˚, 2˚, and 3˚ amines on their surface, capable of capturing aldehydes and carboxylic acids from gaseous mixtures. The focus of chapter five will describe the remediation of several VOCs in the gas phase analyzed by a unique Gas Chromatography (GC) headspace technique developed by our lab.[1] Analytes included aldehydes, which are captured via a condensation reaction forming imines, and carboxylic acids

that are captured via acid-base reaction. These NP materials react selectively with target contaminants obviating off-target binding when challenged by other VOCs with orthogonal reactivity.

Kaolinite and montmorillonite (MMT) are well established sorbents for the removal of organic pollutants, including pesticides, dyes, and small organic molecules, from aqueous solutions.[2-5] After observing successful VOC remediation using biodegradable PDDLA-PEG-PEI NPs, we investigated the comparatively inexpensive clays as an inorganic platform for amine functionalization. These materials were considered an attractive alternative material due to their mesoporous channels for possible electrostatic capture of contaminants along with surface functionalized amine groups available for chemical capture by means of chemical reaction. Using wet impregnation techniques, both kaolinite and MMT clays were successfully functionalized with PEI. These novel materials were then characterized using FTIR, TGA, and elemental analysis. While unmodified clays were moderately effective at remediating VOCs using the same experimental protocol as was implemented for the PDDLA-PEG-PEI NPs vapor assays, the amine functionalized kaolinite and MMT were extremely successful at selectively capturing organics in the vapor phase.

5.1.2 Biodegradable nanomaterials for capture of volatile organic compounds (VOCs)

The environment has been greatly affected by the rapid pace of industrialization and the increasing concentration of volatile organic compounds that are released. Volatile organic compounds (VOCs) are examples of compounds with low vapor pressures that are emitted into the atmosphere from sources divided into 2 categories: biogenic (*i.e.* mainly vegetative processes), and anthropogenic.[6,7] Although biogenic sources emit approximately ten times more VOCs than anthropogenic sources anthropogenic VOCs often dominate in urban areas and therefore are of concern to the human population.[8] VOCs include a variety of reactive functional groups, such as aldehydes, carboxylic acids, alcohols, amines, amides, aromatic compounds, *etc*.; Several examples are shown in Figure 5.1.[8]

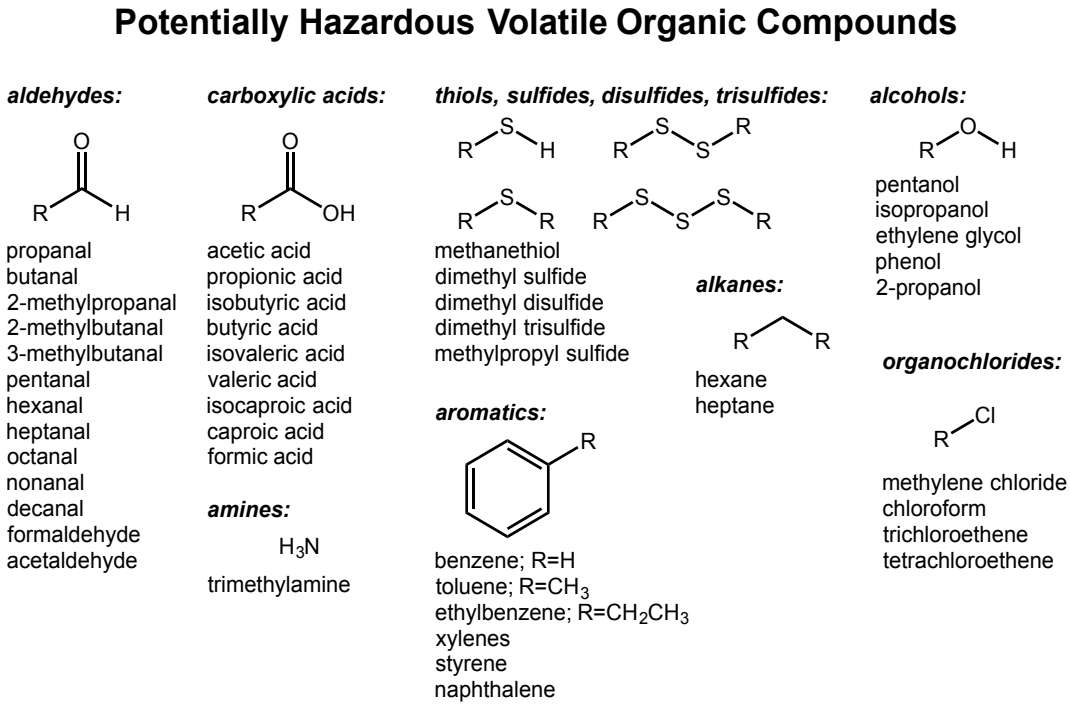

Figure 5.1. A sampling of VOCs listed according to their functional groups

VOC emissions comprising short-chain, carboxylic acids and aldehydes are emitted from both vehicular exhaust and the atmospheric photochemical oxidation of olefin and hydrocarbon emissions (Figure 5.1).[9-12] Further, the global daily use of cookstoves, fireplaces, and certain industrial operations contribute to the emission of carbonyl compounds along with other compounds resulting from incomplete combustion of biomass and fossil fuels (Figure 5.1), which can in turn undergo atmospheric oxidation to aldehydes and ketones.[13-15] Additionally, some aldehydes and carboxylic acid contaminants are also observed in enclosed environments, such as homes and apartments, due to various sources including paints, aerosols, and wood products.[16] High concentrations of these VOCs are known irritants with the Environmental Protection Agency listing thirteen carboxylic acids and aldehydes/ketones as hazardous air pollutants under the 1990 Clean Air Act Amendments.[17-19] Additionally, the EPA lists three of those aldehydes/ketones as priority pollutants.[20] Aldehydes are potent mucosal membrane, eye, skin, and respiratory irritants, even causing bronchial asthma symptoms including several reports of full asthma attacks.[13,16,17,21] Additionally, volatile carbonyl compounds are known for their low, often unpleasant, odor thresholds below 1 parts per billion (ppb) in some cases.[18] As previously discussed, atmospheric reactions of primary emissions can form newly hazardous compounds. For example the reaction of formaldehyde with atmospheric hydrochloric acid (HCl) generates bis(chloromethyl)ether, a suspected carcinogen.[14,22,23] Both volatile organic aldehydes and carboxylic

acids are also implicated in the atmospheric generation of light-scattering aerosols, which contribute to increasing smog problems in urbanized areas.[10,12,13]

Environmental pollution has become a global concern and providing clean air and water remains a challenge. Conventional technologies that have been used to treat organic and toxic waste include adsorption, biological oxidation, chemical oxidation and incineration. With the growth of nanotechnology, there is excellent potential for the fabrication of nanomaterials with large surface-to-volume ratios, high chemical reactivity, and unique functionalities to treat pollutants.[24]

Nanomaterials play a large role in environmental remediation and have been used for various applications such as the treatment of natural waters, soils, sediments, industrial and domestic wastewater, mine tailings, and polluted air as discussed previously in chapter four.[8] Nanomaterials are extremely versatile; they have been employed previously as adsorbents,[25,26] catalysts,[27] and sensors[28] owing to their unique properties. Our interest in nanomaterials is motivated by the facile ability to functionalize them by coating techniques or chemical modification to improve surface and optical properties as well as aid in avoiding aggregation.[24]

A variety of studies have exploited the use of nanomaterials for the remediation of VOCs in an effort to decrease air pollution.[24,29,30] As discussed in greater detail in chapter four, examples of sorbents include metal and metal

oxide nanomaterials,[29] dendrimers,[24] carbon nanomaterials,[30] and polymer nanocomposites.[31] The target-specific capturing of compounds from gaseous mixtures is a significant and difficult problem since off-target fouling of sorbents might limit their utility. Therefore, a broad impact might be achieved with the development of a method that can selectively capture compounds of different functionalities from complex gaseous mixtures of various concentrations. Here in chapter five, the use of a versatile and modular platform for NP functionalization is described that provides functional nanomaterials capable of selectively targeting and capturing aldehyde and carboxylic acid functional group classes in the gas phase. Specifically, our collaborators in the Alexis group designed functional nanoparticles comprised of Poly(D,L-lactic acid)-poly(ethylene glycol)-poly(ethyleneimine) (*i.e.* PDLLA-PEG-PEI) block copolymers that present a branched polyamine functionality on their surface (Figure 5.2). Recent work involving the selective capture of aldehydes and CO_2 using amino-functionalized mesoporous silicates highlights the impact amine containing nanomaterials afford on targeting gases.[32-37] The Jones group has disclosed elegant studies utilizing poly(ethylenimine)-capped mesoporous silicates for CO_2 adsorption in direct capture from ambient air and flue gas with reversible CO_2 desorption capabilities as discussed in detail in chapter 4.[38,39] By installing a branched amine on the surface of our self-assembled NPs, we surmised that aldehydes might be captured by means of a condensation reaction to form an imine (Scheme 5.1,

equation 1), whereas the carboxylic acids might form ammonium carboxylates via acid-base reaction (Scheme 5.1, equation 2).

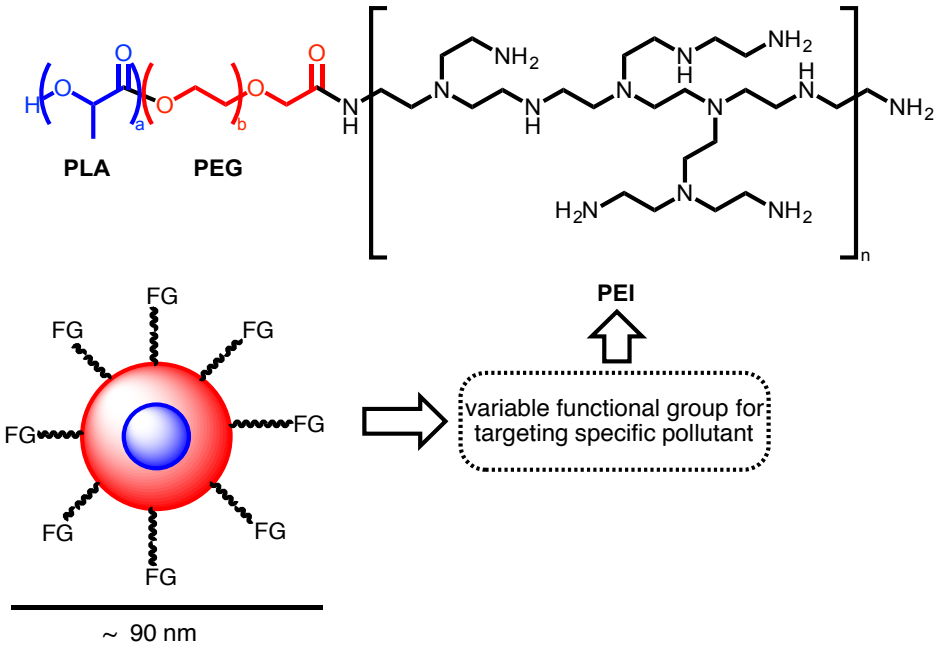

Figure 5.2. Functionalization of PDDLA-PEG NPs with polyethyleneimine

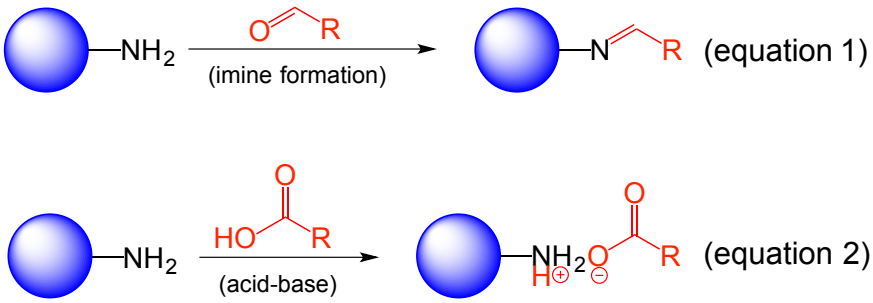

Scheme 5.1. (Equation 1) Aldehyde capture through imine bond formation with primary amines of the PDDLA-PEG-PEI NPs. (equation 2) Ionic capture of carboxylic acid vapors using primary amines decorating the PDDLA-PEG-PEI NPs

5.1.3 Clay minerals for remediation of hazardous organic substances

Just as nanoparticles are known for their high surface areas, clays and modified-clays have been used as raw materials for numerous industrial applications due to their abundant availability, inexpensive cost, and large degree of surface area available for sorption. Most natural clays are porous which also contributes to their high degree of surface area. Clay minerals are usually classified according to their structure and layer type and they are divided into four main groups: kaolinite group, illite group, smectite group, and vermiculite.[2,40] Due to extensive literature on the subject,[2,3,40] special attention will be given to the klaolinite and smectite (*e.g.* montmorillonite) groups for the purpose of our research focus.

Classified under the phyllosilicate family (*i.e.* sheet silicate), clay minerals are layered structures of polymeric SiO_4 sheets linked into sheets of aluminum, manganese, or iron oxides/hydroxides with an octahedral geometry. They are layer-type aluminosilicates formed from chemical weathering of other silicate minerals at the earth's surface.[41] The most common classifications of clay minerals used by chemists are based on the layer type and charge per formula unit. A 1:1 layer structure consists of a unit made up of one octahedral and one tetrahedral sheet (Figure 5.3A), with the apical O^{2-} ions of the tetrahedral sheets being shared with the octahedral sheet. A 2:1 layer structure consists of two tetrahedral sheets with one bound to each side of an octahedral sheet (Figure 5.3B).

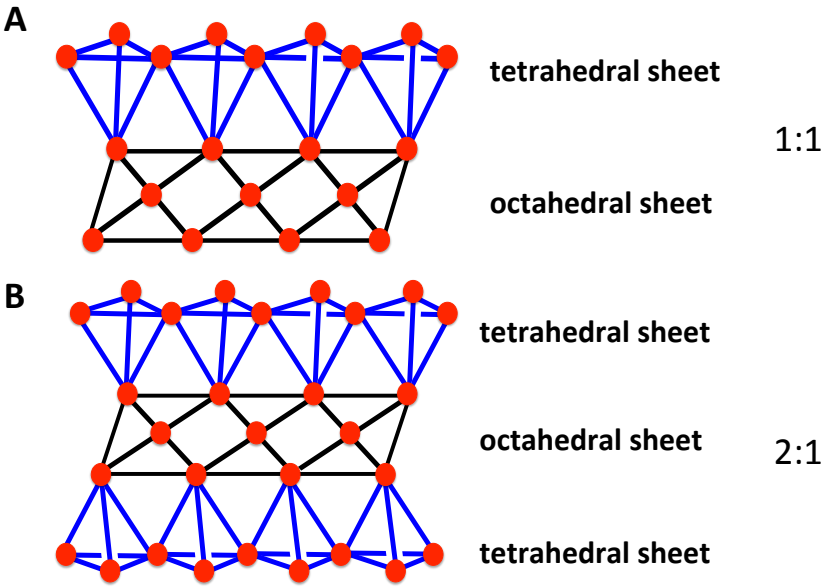

Figure 5.3. A) 1:1 crystal layer structure representation B) 2:1 crystal layer structure representation

The usage of clay minerals is vital in environmental protection through disposing and storing hazardous chemicals.[2,3] They aid in sequestering harmful substances including heavy metals, dyes, antibiotics, biocide compounds, and other organic chemicals.[2-5] Remediation of pollutants in water has been the largest application of these materials thus far.[3] A brief survey of clay minerals used by researchers to sequester organics in the vapor phase is highlighted in this chapter.

5.1.3.1 Selective pollutant gas adsorption by clay minerals

Many investigations have been made for the sorption of non-polar and polar gases using clay minerals due to extensive industrial activities releasing a

number of toxic VOCs as pollutants into the environment. The abatement of VOCs using efficient adsorption technology has been developed to improve on other methods for gaseous removal such as thermal or catalytic oxidation.[42]

Hydrogen sulfide is classified as a noxious, gaseous pollutant and is responsible for the "rotten eggs" odor most people associate with sulfur compounds. It is very corrosive, flammable, poisonous, and explosive. A number of studies utilized clay minerals for the removal of hydrogen sulfide (H_2S) from systems that mimic environment conditions.[43-47] Adsorption of ammonia and H_2S onto activated carbon-sepiolite pellets was studied by Molina-Sabio *et al.* using sepiolite, which acts as a binder for the pellet and as the adsorbent.[43] The modification of MMT with iron (Fe) in order to introduce active centers for hydrogen sulfide adsorption was conducted by Thanh *et al*.[48] Iron-doped samples showed a significant improvement in the capacity for H_2S removal despite an obvious decrease in microporosity compared to the initial pillared clay. Variations in adsorption capacity are likely due to differences in the chemistry of iron species, the degree of their dispersion on the surface, and accessibility of small pores for the H_2S molecule.[48] Considerations for the adsorption of ammonia gas (NH_3), also classified as a dangerous gaseous pollutant, was addressed by Molina-Sabio'n *et al.* where strong interactions between sepiolite and NH_3 were observed.[43] Sepiolite has special affinity towards NH_3 with the ammonia and the acid groups of the sepiolite surface producing strong ionic interactions.[43,49]

The chemical nature and pore structure of clay minerals commonly

influence their adsorption capability. In order to increase adsorption capacity, modifications to the pores of the clay material have been investigated. Successful functionalization leads to an increase in surface area, pore volume, and the number of active sites. Additionally, increased hydrophobicity is observed when the clay surface is modified with nonionic organic substrates , thus reversing the natural clays' solubility in aqueous media.

Recently Guegan *et al.* reported the synthesis of a nonionic organoclay capable of adsorbing organic pollutants from aqueous solutions.[50] Sodium montmorillonite (Na-MMT) was employed as the starting clay material and triethylene glycol monodecyl ether (*i.e.* C10E3) as the nonionic organic reactant. The adsorption performance of the nonionic organoclay was tested to remove three organic micro-pollutants (benzene, dimethylphthalate, and paraquat) and the results were compared to adsorption using pristine MMT. The adsorption results indicate that the chemical nature of the micro-pollutants play a critical role in the performance of nonionic organoclay.[50]

Surface functionalization of polymeric nanoparticles (PNPs) and clay minerals improves the adsorption capacity for both systems. In the project, we have successfully prepared functionalized adsorbents that are either biodegradable (*e.g.* PDDLA-PEG-PEI PNPs) or environmentally benign (*e.g.* kaolinite and MMT). Further, these materials were successful for the remediation of volatile small organic molecules.

5.2 RESULTS AND DISCUSSION

Polymeric nanoparticles (PNPs) were synthesized and functionalized by the Alexis laboratory for capturing target gaseous molecules of the aldehyde and carboxylic acid functional group classes. The group began by synthesizing Poly(D,L-lactic acid)-poly(ethylene glycol)-carboxylic acid (PDLLA-PEG-COOH) block copolymer and subsequently generating PDLLA-PEG-COOH NPs employing the solvent evaporation technique.[51] PDLLA-PEG-COOH NPs were reacted with branched poly(ethyleneimine) (PEI) to obtain PDLLA-PEG-PEI NPs, through an amide conjugation reaction with 1-ethyl-3-(3-dimethylaminopropyl)carbodiimide (EDC). The PEI polymer was chosen to functionalize PDLLA-PEG-COOH NPs based on the presence of a suite of primary, secondary, and tertiary amines in its structure. The two features that distinguish our NPs from the materials developed during the course of the pioneering work of Jones and coworkers[32-39,51] are both results of our design strategy: 1.) our materials are based upon a biodegradable and environmentally friendly PDLLA polymer platform, and 2.) our EDC-mediated NP capping strategy is modular and tunable, opening the door for the development of a suite of functionalized NPs for a variety of environmental applications.

After successfully observing VOC remediation using biodegradable PDDLA-PEG-PEI NPs, interest in inexpensive clay minerals as an inorganic, environmentally benign platform for amine functionalization was considered as an attractive alternative. Kaolinite and MMT were selected as parent minerals for

functionalization and the investigation of VOC reduction. Moderate vapor reduction primarily through electrostatics of the inorganic crystalline lattice was observed. Functionalization of both kaolinite and MMT with PEI was successfully realized on a multi-gram scale using wet impregnation technique and were then subjected to the same vapor assays returning excellent reduction of both carboxylic acids and aldehydes.

5.2.1 Vapor assays using PDDLA-PEG-PEI NPs

After a thorough characterization of the synthesized PDLLA-PEG-PEI NPs was executed in collaboration by the Alexis laboratory, we set out to evaluate the ability of the materials to capture gaseous vapors comprised of aldehyde and carboxylic acid functional groups. For full synthetic protocol and characterization analysis for the PDDLA-PEG-PEI NPs please refer to our manuscript in *Chemistry a European Journal*.[1]

A unique protocol for analyzing vapor reduction was developed by our group. In a standard assay, 10 mg of freshly prepared PDLLA-PEG-PEI NPs were suspended on a tissue paper barrier above a 1 µL aliquot of target analyte in a GC vial (Figure 5.4) and the NPs were allowed to interact with the vapor portion of the analyte sample for 30 minutes. Headspace analysis was conducted by gas chromatography (FID detection). The GC headspace concentration of the analyte was compared between samples treated with PDLLA-PEG-PEI NPs for 30 minutes and untreated control headspace samples. Data was collected in

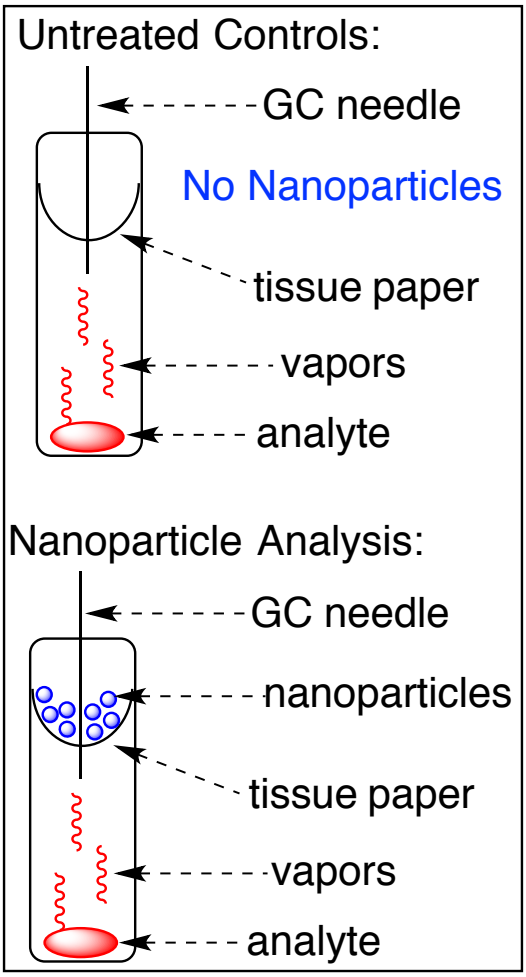

Figure 5.4. Cartoon representation of vapor assay sampling method

sextuplicate and evaluated for statistical significance using a one-tailed Student's T test.

5.2.1.1 Single vapor assays using PDDLA-PEG-PEI NPs

We first investigated the capture of hexanal and hexanoic acid (Figure 5.5; compounds **V-1** and **V-2**). The PDLLA-PEG-PEI NPs effected a 98% reduction

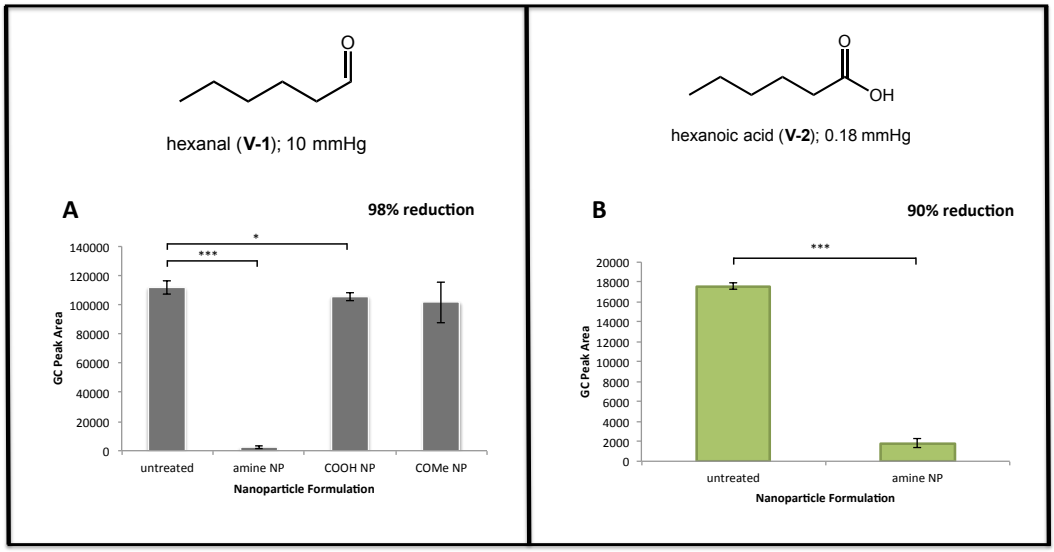

Figure 5.5. A) Average GC peak area reduction for hexanal after exposure to PDDLA-PEG-PEI NPs, PDDLA-PEG-COOH NPs, and PDDLA-PEG-OMe NPs. B) Average GC peak area reduction for hexanoic acid after exposure to PDDLA-PEG-PEI Ps; $P < 0.05$, *; $P < 0.005$, **; $P < 0.0005$, ***

($P < 0.0005$) of the headspace vapors of hexanal samples as compared to untreated hexanal controls (Figure 5.5A). PDLLA-PEG-COOH (*i.e.* carboxylic acid capped) and PDLLA-PEG-OCH_3 (*i.e.* methoxy capped) NPs were evaluated as controls. We expected that these materials, presenting non-compatible surface functional groups, would fail to significantly reduce the headspace vapor of the target analytes. In the event, these control NPs exhibited only slight reduction (6% ($P < 0.05$) and 9% (statistically insignificant) respectively) in hexanal headspace vapors, possibly due to weak electrostatic adsorption phenomena. However, hexanoic acid vapors were reduced by 90% ($P < 0.0005$) when exposed to the PDLLA-PEG-PEI NPs (Figure 5.5B)

Next branched molecules, 2-methylbutyraldehyde (Figure 5.6A, compound **V-3**) and 3-methylbutanoic acid (Figure 5.6B, compound **V-4**), were investigated

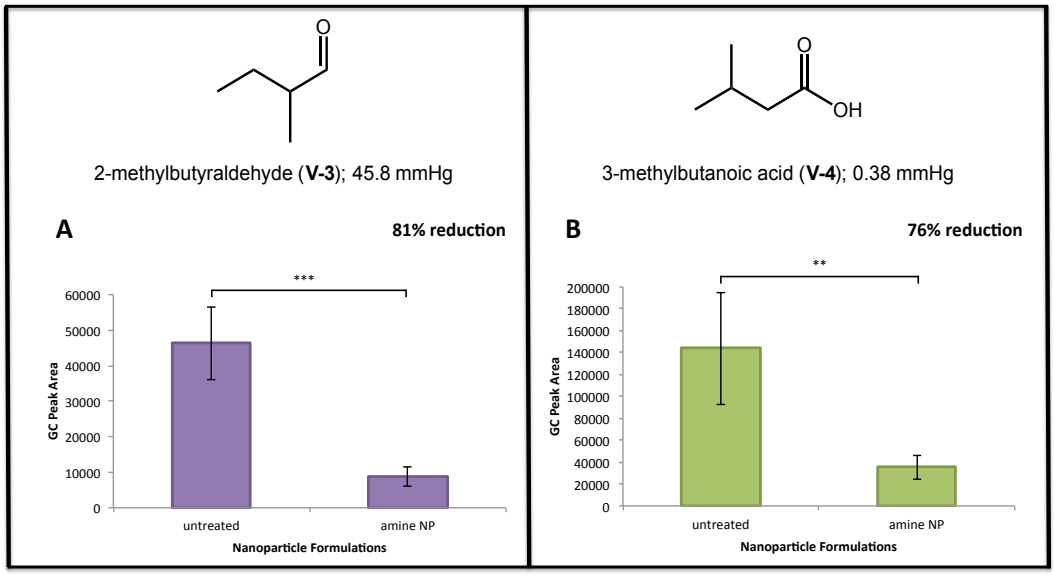

Figure 5.6. A) Average GC peak area reduction for 2-methylbutyraldehyde after exposure to PDDLA-PEG-PEI NPs. B) Average GC peak area reduction for 3-methylbutanoic acid after exposure to PDDLA-PEG-PEI NPs; $P < 0.05$, *; $P < 0.005$, **; $P < 0.0005$, ***

to assess whether steric factors within the substrate would hinder capture by the PDLLA-PEG-PEI NPs. Exposure to the PDLLA-PEG-PEI NPs afforded an 81% reduction ($P < 0.0005$) of the 2-methylbutyraldehyde (Figure 5.6A) and a 76% reduction ($P < 0.005$) of the 3-methylbutanoic acid (Figure 5.6B).

Smaller molecular weight aldehyde and carboxylic acid congeners with higher vapor pressures were used to illustrate the ability of the PDLLA-PEG-PEI NPs to capture more volatile compounds with similar efficiency to the less volatile hexanal and hexanoic acid. Butyraldehyde (Figure 5.7A, **V-5**) has a vapor pressure of 83.1 mmHg at 20 ˚C, which is approximately eight times that of hexanal (10 mmHg at 20 ˚C). When exposed to the PDLLA-PEG-PEI NPs, an 86% reduction ($P < 0.0005$) in butyraldehyde vapor was observed (Figure 5.7A). Butyric acid (Figure 5.7B, **V-6**) was used as the smaller acid analogue with a

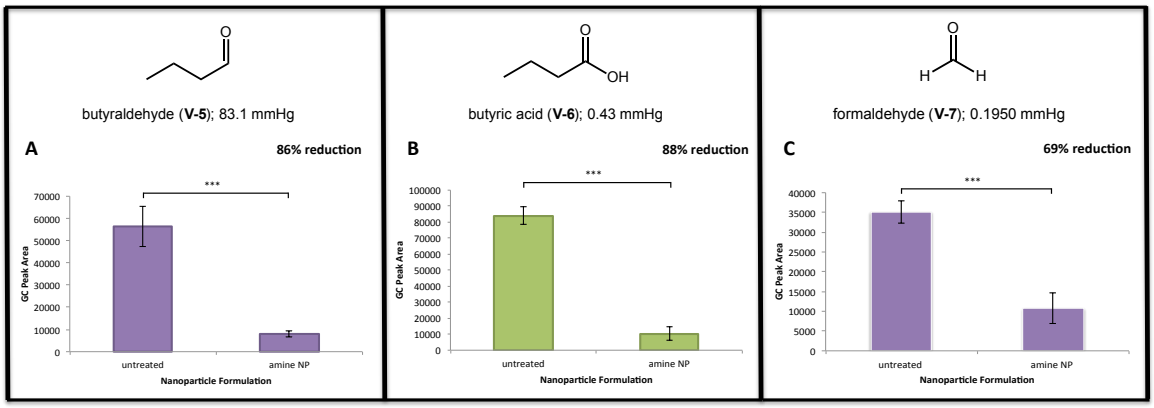

Figure 5.7. A) Average GC peak area reduction for butyraldehyde after exposure to PDDLA-PEG-PEI NPs. B) Average GC peak area reduction for butyric acid after exposure to PDDLA-PEG-PEI NPs. C) Average GC peak area reduction for formaldehyde after exposure to PDDLA-PEG-PEI NPs; $P < 0.05$, *; $P < 0.005$, **; $P < 0.0005$, ***

vapor pressure of 0.43 mmHg in comparison to 0.18 mmHg at 20 ˚C for hexanoic acid. Treatment with the functionalized nanoparticles afforded an 88% reduction ($P < 0.0005$) of the butyric acid vapor (Figure 5.7B). Trace formaldehyde (Figure 5.7C, **V-7**) vapors were also consumed at 69% ($P < 0.0005$) as shown in Figure 5.7C, highlighting our materials scope for the sequestration of highly volatile small molecules.

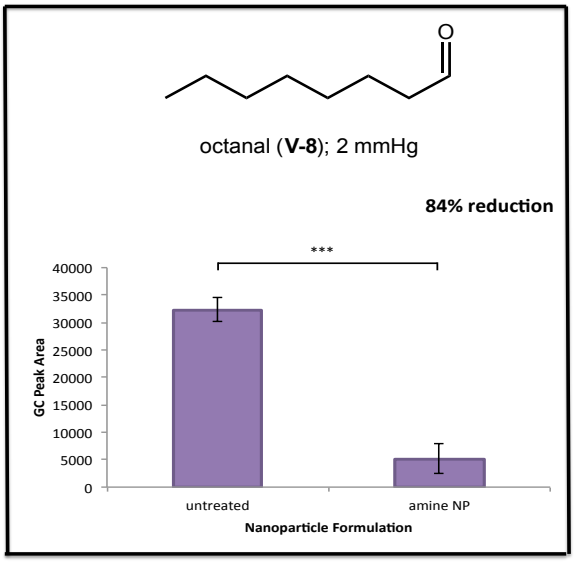

Figure 5.8. Average GC peak area reduction for 1-octanal after exposure to PDDLA-PEG-PEI NPs; $P < 0.05$, *; $P < 0.005$, **; $P < 0.0005$, ***

In contrast to the more volatile aldehydes tested, octanal (Figure 5.8, **V-8**; 2 mmHg at 20 ˚C) was investigated to probe the capability for our materials to capture a less volatile aldehyde contaminant. When exposed to the PDLLA-PEG-PEI NPs,

the octanal vapor concentration was reduced by 84% ($P < 0.0005$) (Figure 5.8).

The final two single vapor assays sought a proof of concept for the chemoselectivity of our PDLLA-PEG-PEI NPs. We challenged our PDLLA-PEG-PEI NPs with 1-nonene (Figure 5.9A, **V-9**), a linear 9-carbon molecule bearing an alkene functional group. We surmised that our amine-functionalized PDLLA-PEG-PEI NPs would fail to capture 1-nonene to an appreciable extent, owing to the lack of compatible reactivity between the amine functionality on the NPs and the alkene functional group on the target analyte. Figure 5.9A shows an overall retention of the nonene vapor after exposure to the PDLLA-PEG-PEI NPs with only a statistically insignificant reduction of 14%, presumably due to non-reactive adsorption mediated by electrostatic interactions of the target analyte with the surface of the PDLLA-PEG-PEI NPs. Further, the concept was extended to a

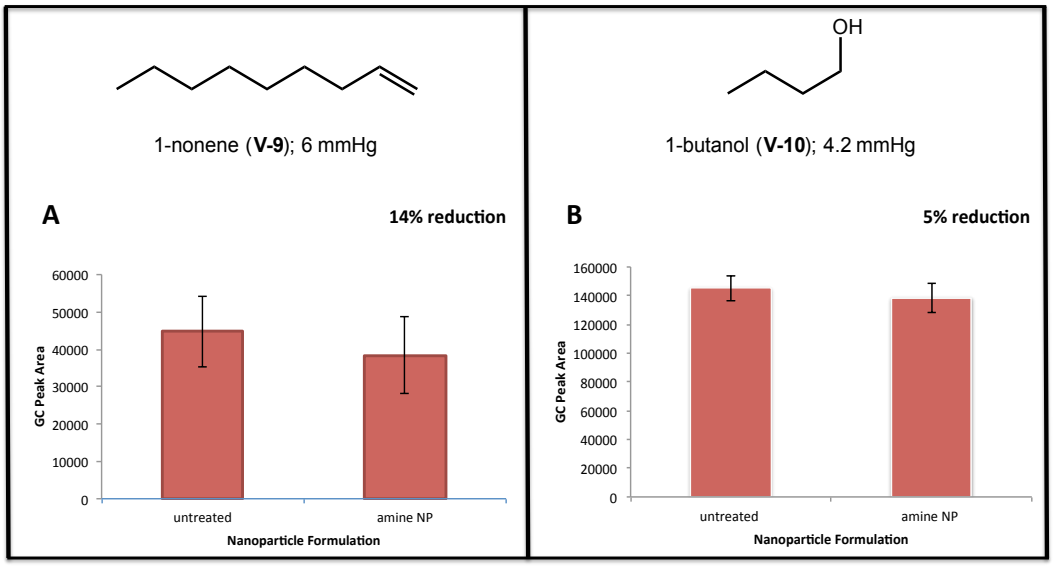

Figure 5.9. A) Average GC peak area reduction for 1-nonene after exposure to PDDLA-PEG-PEI NPs. B) Average GC peak area reduction for 1-butanol after exposure to PDDLA-PEG-PEI NPs; $P < 0.05$, *; $P < 0.005$, **; $P < 0.0005$, ***

more polar substrate, 1-butanol (Figure 5.9B, **V-10),** which returned a statistically insignificant 5% reduction after exposure to our material. These results are important for two reasons. First, it lends credence to our proposed mechanisms for the capture of the targeted aldehyde and carboxylic acid analytes. Secondly, it demonstrates that our PDLLA-PEG-PEI NPs are avoiding off-target binding.

5.2.1.2 Competition assays using PDDLA-PEG-PEI NPs

To further illustrate the chemoselectivity of our PDLLA-PEG-PEI NPs, a competition assay was conducted in which both hexanal and 1-nonene were introduced to the reaction chamber simultaneously (Figure 5.10), and then given 30 minutes to vaporize and react with the PDLLA-PEG-PEI NPs. In this experiment, we expected to see preferential binding of the aldehyde, hexanal, via our predicted reactivity. Further, we expected that 1-nonene, containing an incompatible alkene functional group, would fail to react with the PDLLA-PEG-PEI NPs and thus would not be captured.

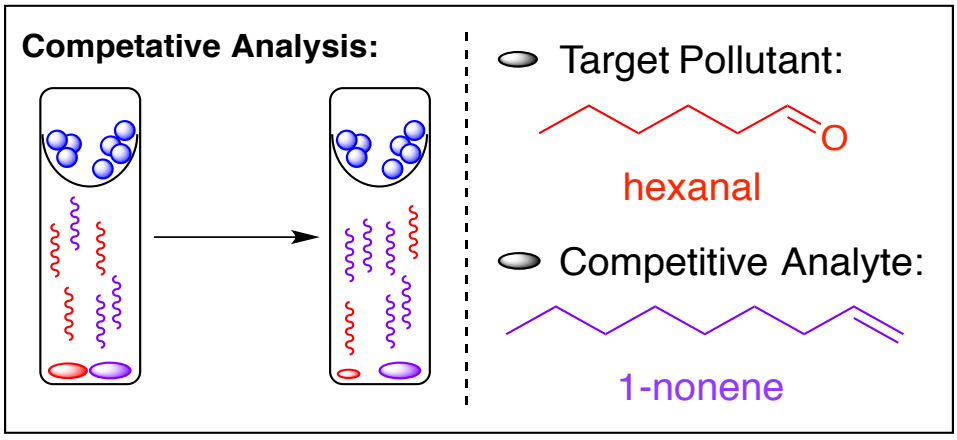

Figure 5.10. Cartoon representation of the competition assay sampling method

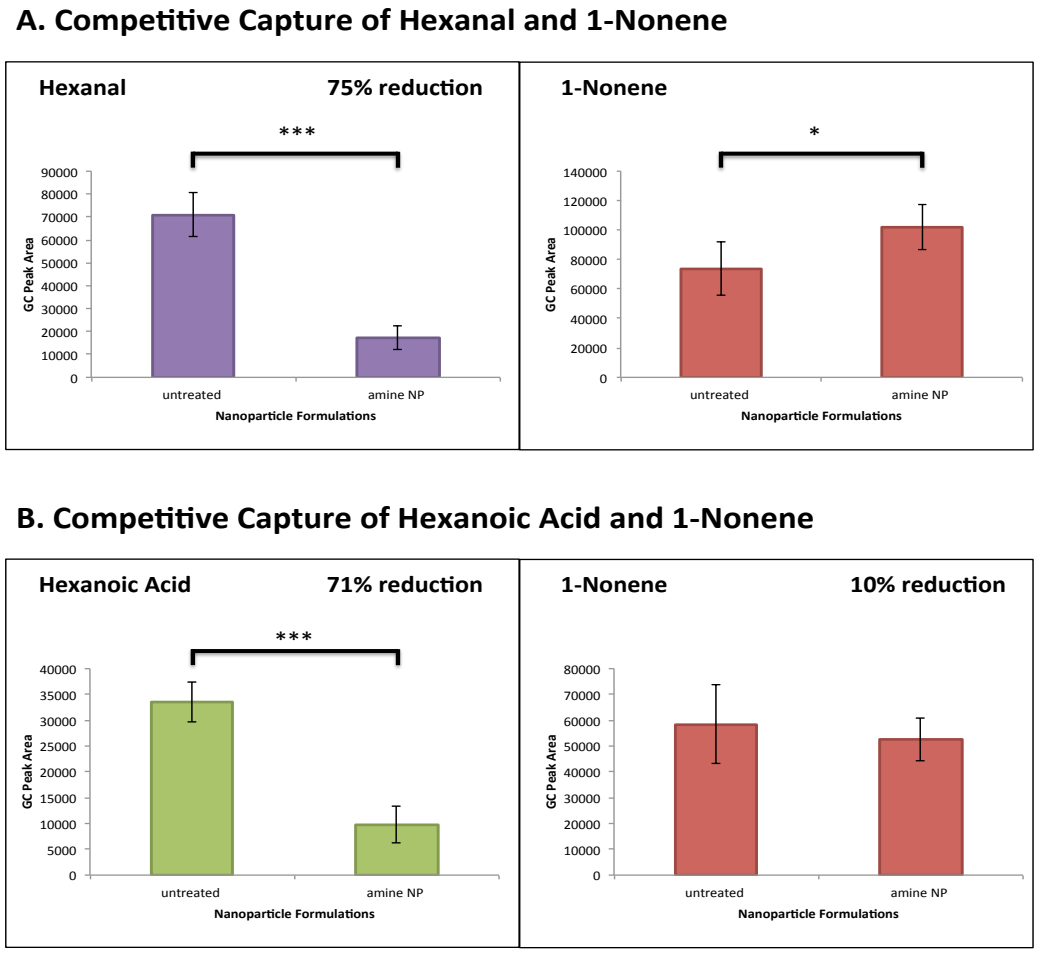

Figure 5.11. A) Average GC peak area reduction for hexanal and 1-nonene after exposure to PDDLA-PEG-PEI NPs. B) Average GC peak area reduction for hexanoic acid and 1-nonene after exposure to PDDLA-PEG-PEI NPs; $P < 0.05$, *; $P < 0.005$, **; $P < 0.0005$, ***

Analysis revealed a 75% reduction ($P < 0.0005$) of the hexanal vapor concentration along with a ~1.4X increase ($P < 0.05$) in the gas-phase portion of 1-nonene present after treatment (Figure 5.11A). These phenomena arise from the selective reduction of the hexanal vapor in the sample chamber by selective adsorption onto the PDLLA-PEG-PEI NPs. Re-equilibration of the closed system results in a larger vapor concentration of 1-nonene after hexanal capture,

accounting for the enhanced 1-nonene signal after NP treatment. Next, we probed the reactivity of hexanoic acid in a competitive system with 1-nonene. The PDLLA-PEG-PEI NPs afforded a 71% reduction ($P < 0.0005$) of the hexanoic acid with a statistically insignificant 10% reduction of the 1-nonene (Figure 5.11B). This result is particularly compelling given that 1-nonene is approximately 33 times more volatile than hexanoic acid.

Lastly, hexanal and hexanoic acid were treated simultaneously to demonstrate the concurrent capture of aldehyde and carboxylic acid analytes. Treatment with PDLLA-PEG-PEI NPs effected a simultaneous 90% ($P < 0.0005$) and 69% ($P < 0.0005$) reduction of headspace vapors for hexanal and hexanoic acid, respectively (Figure 5.12A). The comparatively inferior capture of the hexanoic acid is likely due to the lower vapor pressure of hexanoic acid (0.18 mmHg at 20 ˚C) as compared to hexanal (10 mmHg at 20 ˚C). Additionally, hexanal and octanal vapors were exposed concurrently, and the observed reductions (hexanal, 87% ($P < 0.0005$); octanal, 52% ($P < 0.0005$) for the two vapors followed similar trends to previous competition results: the less volatile octanal had a lower percent reduction compared to the more volatile hexanal shown (Figure 5.12B).

5.2.1.3 Aldehyde capture mediated by imine formation

Finally, ^{1}H-NMR spectroscopy studies were conducted in order to probe the mechanism of aldehyde capture. Specifically, we wished to confirm the

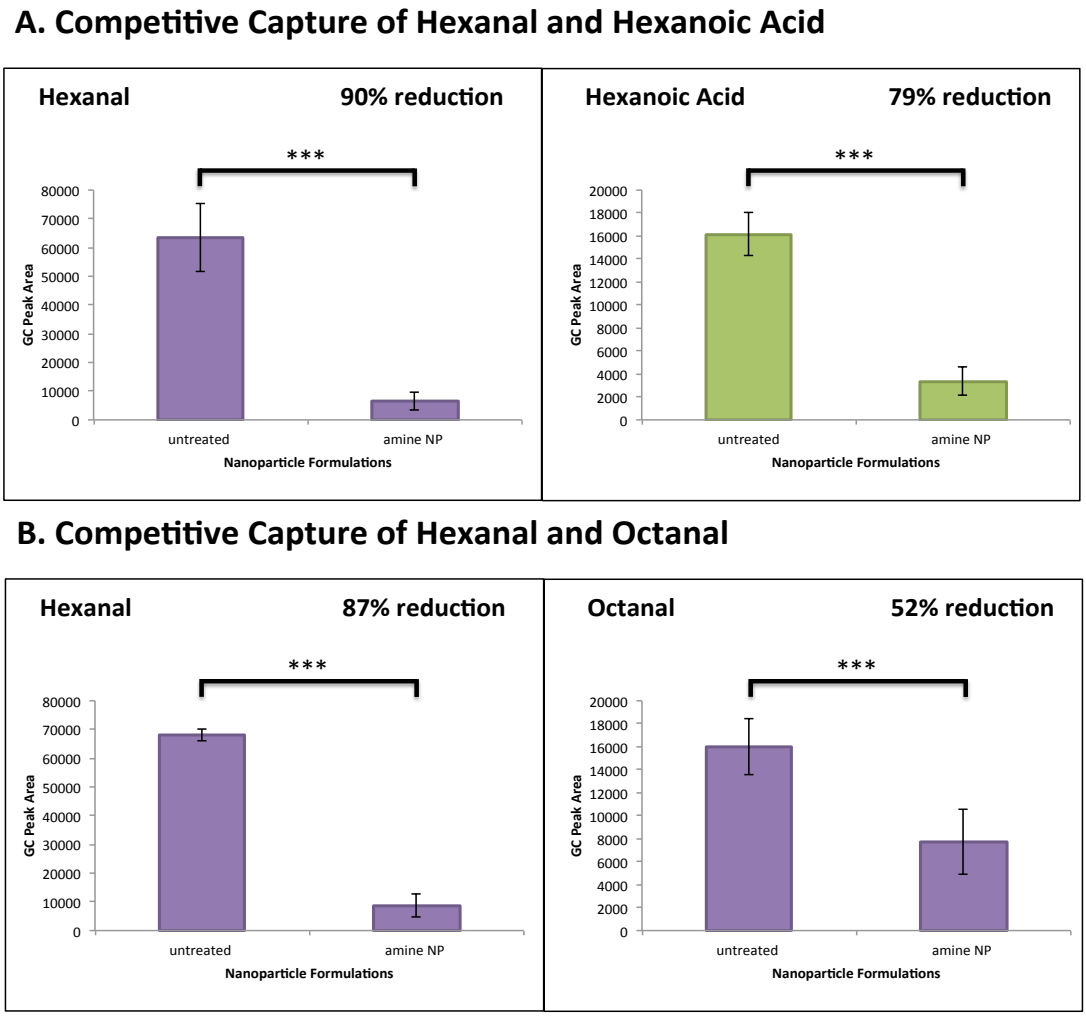

Figure 5.12. A) Average GC peak area reduction for hexanal and hexanoic acid after exposure to PDDLA-PEG-PEI NPs. B) Average GC peak area reduction for hexanal and 1-octanal after exposure to PDDLA-PEG-PEI NPs; $P < 0.05$, *; $P < 0.005$, **; $P < 0.0005$, ***

formation of the putative imine bond in order to further rule out any non-specific adsorption of the target analyte by electrostatic interactions. In this experiment, we treated PDLLA-PEG-PEI NPs with a spectroscopically simple aldehyde analyte, pivaldehyde. A partial ^{1}H NMR spectrum resulting from the interaction between the PDLLA-PEG-PEI NPs and pivaldehyde is shown in Figure 5.13B. The diagnostic appearance of a new singlet at 7.5 ppm suggests the presence of

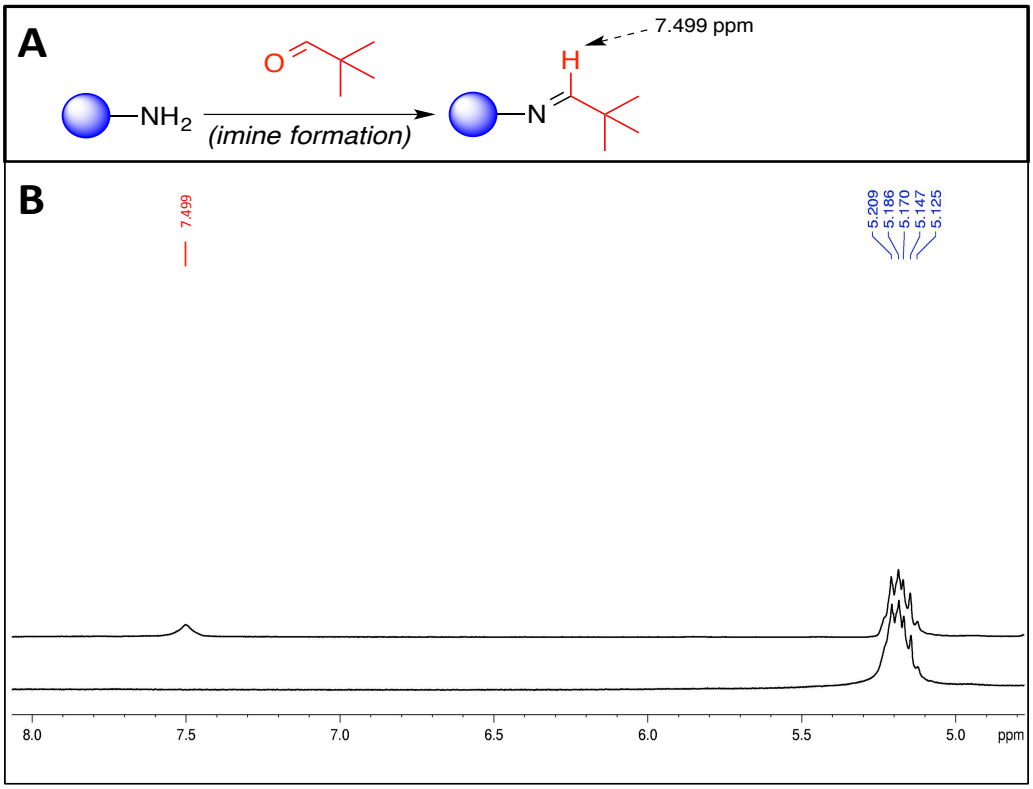

Figure 5.13. A) Scheme of pivaldehyde reacting with the PDDLA-PEG-PEI NPs resulting in an imine bond with an imine methine proton resonance of 7.5 ppm. B) ^{1}H NMR evidence for imine bond formation indicating capture of aldehyde functionality with the PDDLA-PEG-PEI NPs

an imine proton within the aldehyde-treated PDLLA-PEG-PEI NP sample (Figure 5.13A).[52] Any contribution of the possible hemi-aminal tetrahedral intermediate was ruled out by D_2O treatment of the NMR sample, which failed to induce loss of the new singlet at 7.5 ppm by means of proton-deuteron exchange.

5.2.2 Synthesis and characterization for modified kaolinite and MMT with poly(ethyleneimine) (PEI)

From our previous report on PDDLA-PEG-PEI NPs as efficient sorbents in the selective sequestering of aldehyde and carboxylic acid vapors,[1] we knew

amines present in the PEI corona were vital for the chemical capture of these gases through covalent bond formation and ionic interactions respectively. Applying this information, we set out to combine the efficient and selective reactivity of PEI with the attractive adsorption properties and thermal stability intrinsic to clay minerals. Kaolinte-PEI and MMT-PEI clays were synthesized by embedding PEI into the pores of the clay lattice using the wet impregnation method by which the clay is first suspended in an organic or aqueous solvent and a solution of PEI in the appropriate solvent is added slowly to achieve amino-functionalized microporous clay minerals. For evidence of successful modification, FTIR spectroscopy, thermogravimetric analysis (TGA) and elemental analysis (EA) techniques were performed.

FTIR spectroscopy was used to qualitatively confirm PEI impregnation into the kaolinite pores. In Figure 5.14A, three intense bands at approximately 3650 cm^{-1} are attributed to the kaolinite's hydroxyl stretching vibrations and can be observed in both the kaolinite and kaolinite-PEI spectra. Strong overlapping bands at approximately 1000 cm^{-1} include vibrations credited to the silicon-oxygen bonds and the bending vibration of the hydroxyl groups for kaolinite. When comparing the polymeric PEI reagent to the amine-modified kaolinite, the appearance of new bands in the kaolinite-PEI spectra corresponding to the impregnated PEI were diagnostic of successful modification. Specifically, we observed bending vibrations of NH_2 resulting in bands **(5)** at 1600 cm^{-1} and **(6)** at 1470 cm^{-1}, respectively (Figure 5.14A). The broad nitrogen-hydrogen stretching

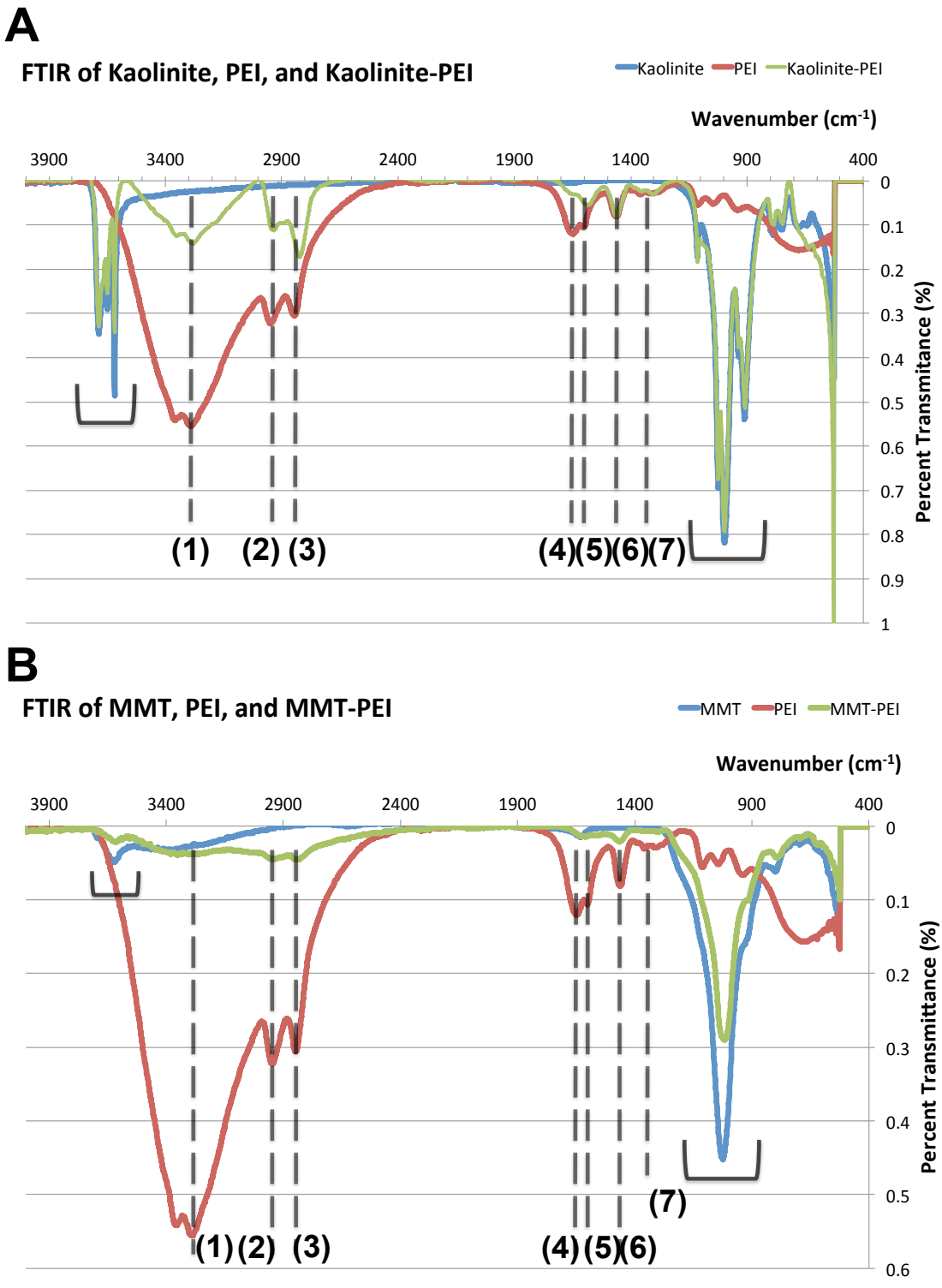

Figure 5.14. FTIR spectra for qualitative comparison of the natural clay vs. the PEI-modified A) kaolinite and B) montmorillonite

bands at 3280 cm^{-1} **(1)** and 1650 cm^{-1} **(4)**, the stretching vibrations for CH_2 at 2871 cm^{-1} **(2)** and 2943 cm^{-1} **(3)** and the bending mode of the carbon-nitrogen bond at 1330 cm^{-1} **(7)** are all qualitative matches for PEI's experimental vibrational bands (Figure 5.14). Coupling is presumed to proceed through ionic interactions between the hydroxyl of the silicate and the lone pair of amines of the PEI. Montmorillonite (MMT) modification results are shown in Figure 5.14B and based on qualitative comparison between bands present in the pre- and post- treated clays, there is evidence of PEI impregnation into the 2:1 MMT lattice.

TGA profiles for the treated kaolinite and MMT also give support for effective modification of the minerals (Figure 5.15). Both the non-modified clays showed little thermal degradation up to 1000 ˚C with kaolinite maintaining 88% of its original mass under inert N_2 atmosphere (Figure 5.15A). Similarly, MMT retained 94% of its mass over the temperature ramp (Figure 5.15B). After decorating the kaolinite and MMT porous structures with organoamines, a different temperature degradation profile is observed. A thermal degradation is observed for both PEI-modified aluminosilicate clays at approximately 300 ˚C resulting in 25% mass loss for each until the amine is fully desorbed from the clay surface at approximately 400 ˚C. The addition of PEI into the crystal structure of kaolinite and MMT results in the disruption of their lattices and a lower temperature requirement for degrading the material. Simultaneously, the temperature needed to begin degrading the PEI is raised due to tightly bound

ionic interactions with the clay minerals. The thermal limit for both modified clays is approximated at 300 ˚C where full degradation of the PEI functionalization occurs thereafter resulting in an overall mass loss of approximately 63% for both

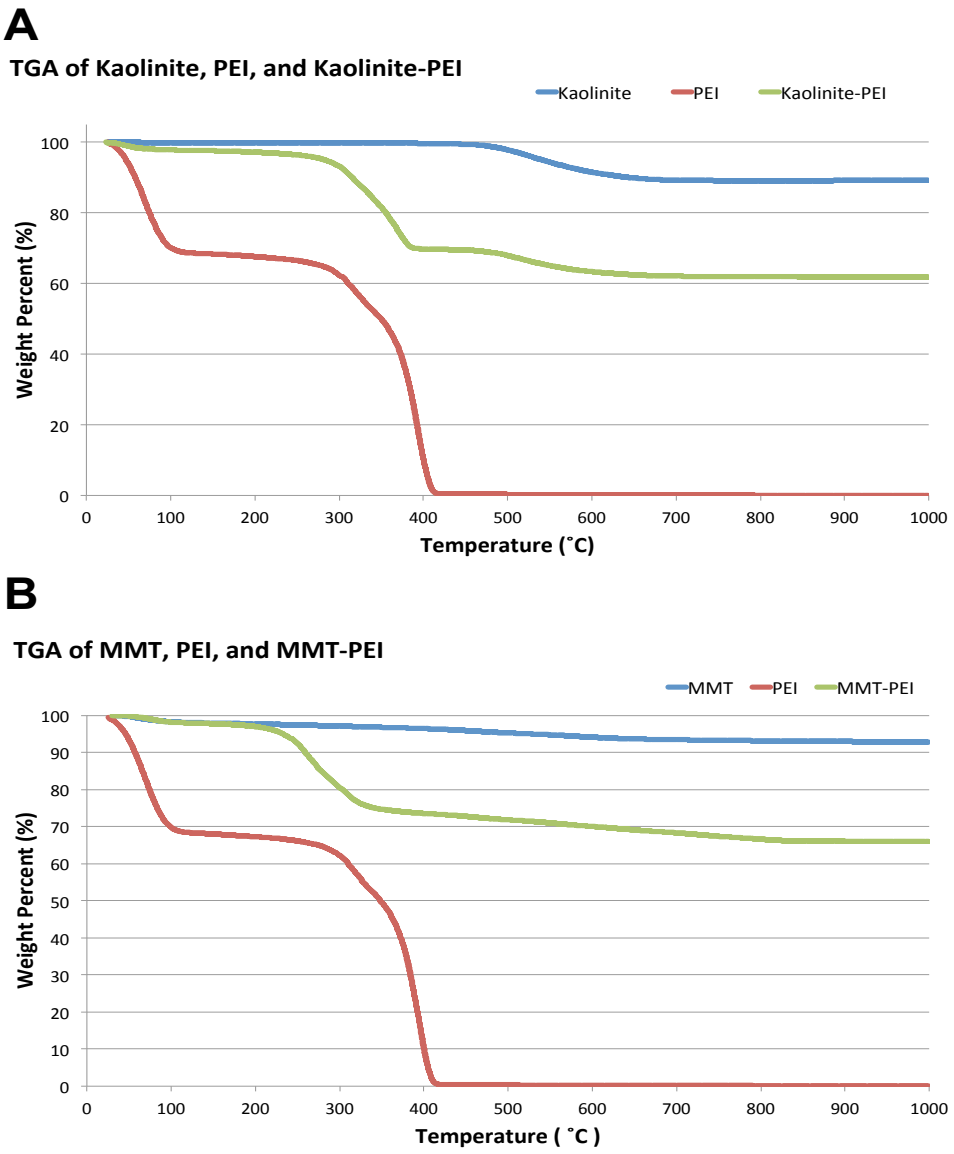

Figure 5.15. TGA profiles for qualitative comparison of the natural clay vs. the PEI-modified A) kaolinite and B) montmorillonite

aminoclays. Currently, EA and energy-dispersive X-ray analysis (EDX) are being conducted on all materials for relative atomic distribution.

5.2.2.1 Vapor assays using kaolinite and kaolinite-PEI

Next, initial investigations into the application of both kaolinite and kaolinite-PEI in remediating VOCs were conducted as previously tested using the PDDLA-PEG-PEI NPs. Several small, volatile compounds were investigated including aldehydes, carboxylic acids, and organosulfides. Treatment of each VOC with kaolinite and kaolinite-PEI was completed in sextuplicate, and vapor reduction percentages were calculated using our GC headspace analysis protocol discussed previously.

Figure 5.16 highlights the percent reduction for each VOC after a 30 minute exposure to kaolinite and kaolinite-PEI. Butyraldehyde vapors were partially remediated in the presence of kaolinite with 33% ($P < 0.0005$) vapor reduction observed (Figure 5.16A). When treated with our amine-modified kaolinite, butyraldehyde was completely reduced with 100% ($P < 0.0005$) vapor consumption after 30 minutes (Figure 5.16A). Kaolinite in the presence of butyric acid vapors was somewhat effective at sequestering the carboxylic acid; most likely due to diffusion into the clay pores (18% ($P < 0.0005$), Figure 5.16B). The kaolinite-PEI clays were successful in reducing 90% ($P < 0.0005$) of the butyric acid vapors (Figure 5.16B) through ionic bonding between the COOH and NH_2 (*cf.* equation 2, Scheme 5.2).

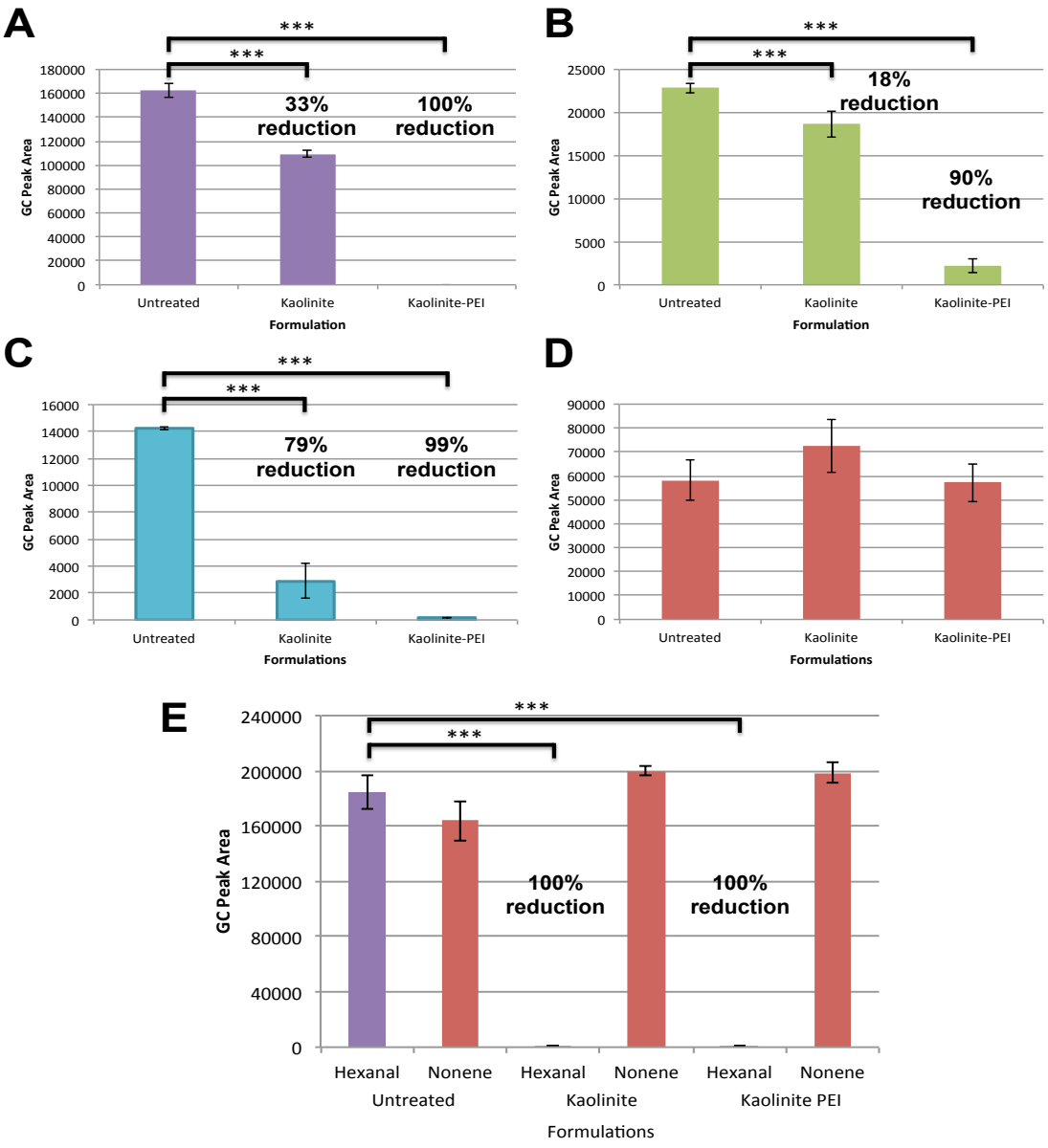

Figure 5.16. A) Average GC peak area reduction for butyric acid after exposure to kaolinite and kaolinite-PEI; B) Average GC peak area reduction for hexanoic acid after exposure to kaolinite and kaolinite-PEI; C) Average GC peak area reduction for dimethyl disulfide (DMDS) after exposure to kaolinite and kaolinite-PEI; D) Average GC peak area for 1-nonene after exposure to kaolinite and kaolinite-PEI; E) A) Average GC peak area reduction for hexanal and 1-nonene after exposure to kaolinite and kaolinite-PEI; $P < 0.05$, *; $P < 0.005$, **; $P < 0.0005$, ***

Sulfur compounds being exceptionally pungent to the human olfactory senses are often targeted for remediation. Dimethyl disulfide (DMDS) was treated with both kaolinite and kaolinite-PEI, and both were promising adsorbents. Treatment of DMDS with kaolinite resulted in 79% ($P < 0.0005$) reduction of DMDS vapors and the amine-modified kaolinite was 99% ($P < 0.0005$) effective (Figure 5.16C). While covalent capture of the sulfur compounds does not occur, it was concluded that possible electrostatic or ionic capture is feasible due to the large surface area and pores available within the clay materials for capture.

5.2.2.2 Kaolinite and kaolinite-PEI sorbent capabilities after one-month ageing cycle

Our final investigation using kaolinite and kaolinite-PEI probed the adsorbent efficiency of the materials during one-month of storing at ambient temperature and at a 35 ˚C. Briefly, 10 mg of the appropriate clay was loaded into the GC screw-capped sampling system in sextet for all eleven assays. All samples were prepped on day zero and the two and four week vials were divided accordingly for treatment at room temperature and 35 ˚C. The standard vials were absent of any sorbent material and returned an approximate 90,000 area units for hexanal after 30 minutes to establish vapor equilibrium (Figure 5.17). Treatment of hexanal vapors with kaolinite and kaolinite-PEI were conducted on day zero to establish the adsorbent function of the modified clay directly after

synthesis. Kaolinite reduced hexanal up to a statistically significant 69% (P < 0.0005) while the kaolinite-PEI was 100% (P < 0.0005) successful at capturing the vapors (Figure 5.17).

After two weeks storage under the two temperature conditions, the hexanal assay was repeated for each material. The kaolinite-PEI clay material was again 100% (P < 0.0005) effective at reducing the hexanal vapor after sitting at 25 and 35 ˚C for two weeks. The kaolinite samples that were kept at 35 ˚C returned comparable results to day zero taking into consideration their error factors returning 83% (P < 0.0005) and 62% (P < 0.0005) reduction at 25 and 35 ˚C respectively. Finally, the four-week samples for both clays were tested with hexanal vapors to see if the longer storage time results in any loss in efficiency

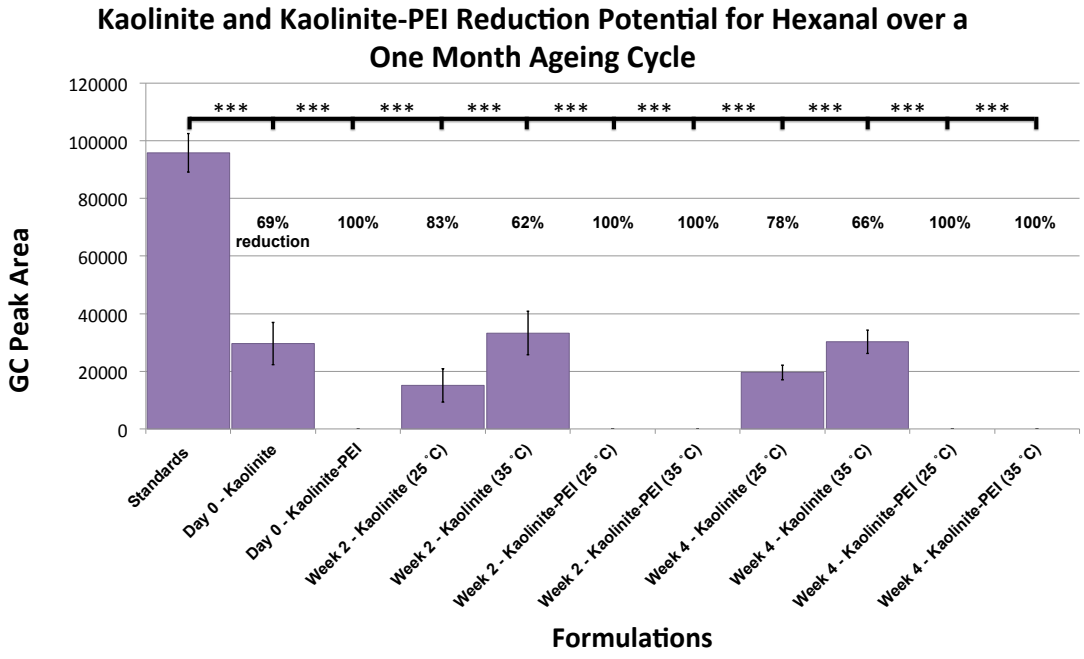

Figure 5.17. Graph showing the percent reduction for hexanal vapors after treatment with kaolinite and kaolinite-PEI stored for one month at 25 and 35˚C

for adsorbing vapor. For both temperature treatments, the kaolinite was again moderately successful at remediating the hexanal vapors with percent reductions of 76% ($P < 0.0005$) and 66% ($P < 0.0005$) for the 25 and 35 ˚C treatments respectively. The kaolinite-PEI stored for one month under both temperature conditions again effected a 100% reduction ($P < 0.0005$) of the hexanal vapors.

After the one-month study, it was conclusive that our modified kaolinite clay was extremely successful in maintaining its efficiency over a prolonged storage time at both room temperature and at a slightly elevated 35 ˚C. Kaolinite was moderately successful over this time and returned an approximate 70% reduction for material exposed to both temperature treatments.

5.3 CONCLUSIONS

Through a collaborative effort by the Alexis and Whitehead groups, we presented the preparation, characterization, and evaluation of PDLLA-PEG-PEI NPs capable of selectively capturing environmental contaminants of broad concern bearing aldehyde and carboxylic acid functional groups in the gas phase.[1] Our material showed reduction of aldehyde and carboxylic acid vapors greater than 80% and 76%, respectively, with reductions of up to 98% in some cases. Further, we demonstrated that our NPs were capable of effecting the simultaneous capture of mixtures of aldehydes and carboxylic acids as well as mixtures of two different aldehydes. Additionally, our NPs were capable of selectively capturing target aldehyde and carboxylic acid contaminants even

when challenged by comparably or more volatile non-targeted vapors. The significant advantage of our strategy over current methods arises from the potential ability to tailor the surface functionality of the nanomaterials for a specific target analyte from vapor mixtures. Future efforts will focus on the evaluation of subsequent generations of these promising NPs for the remediation of other environmental contaminants of broad concern by taking advantage of the uniquely modular nature of our functional nanomaterials.

The functionalization of kaolinite and montmorillonite clays with poly(ethyleneimine) showed initial success according to TGA and FTIR analysis. With the EA and EDX images, we should be able to determine the atomic distribution for the modified clays as compared to their natural precursors. The synthesized kaolinite-PEI has shown significant efficiency in capturing aldehydes, carboxylic acids and sulfides with most of these assays showing 100% reduction ($P < 0.0005$) of these vapors. Currently, the same vapor assays are underway with the MMT and MMT-PEI clay minerals, and initial evidence is promising for the reduction of hexanal vapors up to 100% ($P < 0.0005$). These efforts will be reported soon.

5.4 EXPERIMENTAL SECTION

5.4.1 General Materials and Methods

Solvents, reagents, starting materials, and product GC standards were purchased from commercial sources and used without purification. Gas

Chromatography (GC) analyses were conducted using a Shimadzu GC-2014 Gas Chromatograph equipped with a Shimadzu AOC-20i Auto Injector and a Flame Ionization Detector (FID). The GC was equipped with a 30 m x 0.25 mm x 0.25 μm Zebron ZB-WAX Plus capillary GC column. Agilent Technologies Gas Chromatography vials with septum screw-caps, 1.5 mL in total volume, were used in the analysis assays. ^{1}H NMR spectra were collected on a Bruker 300 MHz NMR using DMSO-d_6 as the solvent. Chemical shifts are reported in parts per million (ppm) and are referenced to the residual solvent peak. Thermal gravimetric analysis was performed on a TA Intruments Hi-Res TGA 2950 analyzer. Analysis was conducted under nitrogen from 25 to 1000˚C at 10˚C/min. Fourier Transform Infrared analysis was performed with a Nicolet Magna 500 with NicPlan FT-IR Microscope and Mapping Stage.

5.4.2 Splitless Method Temperature Profile for Vapor Assays

GC analyses were carried out within the following parameters: inlet temperature: 250.0 ˚C; splitless injection at 30.9 mL/min; injector sampling depth: 10 mm; column flow: 1.33 mL/min, constant pressure; carrier gas: helium; FID temperature: 225 ˚C; temperature program: 40 ˚C for 5 min, 50 ˚C/min ramp to 200 ˚C, hold for 5 min.

5.4.3 Methodology for Vapor Assay Analysis Via Gas Chromatography

General Gas Chromatography procedure for vapor assays including 1) standard vapor areas for each substrate followed by 2) functionalized nanoparticle formulation reactivity with each individual vapor substrate.

1) General procedure for standard vapor area assay by GC analysis:

The opening of a 1.5 mL GC vial was covered with a 5 x 5 cm piece of Kimwipe tissue paper. Using a glass stir rod, a small sample well was made with the Kimwipe by gently applying pressure with the tip of the glass stir rod. A vial cap was secured on the vial and a 1 μL injection of the volatile liquid substrate was introduced into the vial. After a 30-minute vaporization equilibrium time, the vial was subjected to GC analysis as described above.

2) General procedure for functionalized nanoparticle assays by GC analysis:

Using the previously described process for formation of a well within the GC vial, 10 mg of the functionalized nanoparticle was added into the Kimwipe sample well and then secured with a vial cap. A 1 μL injection of the designated volatile substrate was introduced into the vial and allowed to vaporize and subsequently react with the solid nanoparticles for 30 minutes. Upon completion of the 30-minute reaction time, the vial was subjected to GC analysis.

5.4.4 Protocol for pivaldehyde capture using PDDLA-PEG-PEI NPs observed via ^{1}H NMR

To evaluate the formation of a putative imine bond, a 1.5 mL screw-capped GC vial was charged with 0.3 mL of pivaldehyde before suspension of 10 mg PDDLA-PEG-PEI NPs in the Kimwipe well above the liquid as described in the previous section. The liquid was given the allotted 30 minutes to vaporize in the sealed system. The nanoparticles were then collected and dissolved in 1 mL of DMSO-d_6 and the ^{1}H NMR spectrum was collected on a 500 MHz NMR spectrometer (Bruker). Chemical shifts are reported in parts per million (ppm) and are referenced to the residual solvent peak.

When testing for possible hemi-aminal intermediate formation, 0.5 µL of D_2O was added to the test tube and a subsequent ^{1}H NMR spectrum was collected using the 500 MHz NMR spectrometer (Bruker). Again, chemical shifts are reported in parts per million (ppm) and are referenced to the residual solvent peak.

5.5 REFERENCES

(1) Campbell, M. L.; Guerra, F. D.; Dhulekar, J.; Alexis, F.; Whitehead, D. C. *Chem. - Eur. J.* **2015**, *21*, 14834-14842.

(2) Ismadji, S.; Soetaredjo, F. E.; Ayucitra, A. *Clay materials for environmental remediation*; Springer, 2015; Vol. 25.

(3) Arief, V. O.; Trilestari, K.; Sunarso, J.; Indraswati, N.; Ismadji, S. *CLEAN–Soil, Air, Water* **2008**, *36*, 937-962.

(4) Febrianto, J.; Kosasih, A. N.; Sunarso, J.; Ju, Y.-H.; Indraswati, N.; Ismadji, S. *Journal of Hazardous Materials* **2009**, *162*, 616-645.

(5) Järup, L. *British medical bulletin* **2003**, *68*, 167-182.

(6) Kesselmeier, J.; Staudt, M. *J. Atmos. Chem.* **1999**, *33*, 23-88.

(7) Atkinson, R.; Arey, J. *Chem. Rev. (Washington, DC, U. S.)* **2003**, *103*, 4605-4638.

(8) Vaseashta, A.; Vaclavikova, M.; Vaseashta, S.; Gallios, G.; Roy, P.; Pummakarnchana, O. *Sci. Technol. Adv. Mater.* **2007**, *8*, 47-59.

(9) Possanzini, M.; Di Palo, V.; Cecinato, A. *Atmos. Environ.* **2002**, *36*, 3195-3201.

(10) Kawamura, K.; Kaplan, I. R. *Environ. Sci. Technol.* **1987**, *21*, 105-110.

(11) Kawamura, K.; Ng, L. L.; Kaplan, I. R. *Environ. Sci. Technol.* **1985**, *19*, 1082-1086.

(12) Yokouchi, Y.; Ambe, Y. *Atmos. Environ.* **1986**, *20*, 1727-1734.

(13) Zhang, J.; Smith, K. R. *Environ. Sci. Technol.* **1999**, *33*, 2311-2320.

(14) Lipari, F.; Dasch, J. M.; Scruggs, W. F. *Environ. Sci. Technol.* **1984**, *18*, 326-330.

(15) Schauer, J. J.; Kleeman, M. J.; Cass, G. R.; Simoneit, B. R. T. *Environ. Sci. Technol.* **2001**, *35*, 1716-1728.

(16) Ranciere, F.; Dassonville, C.; Roda, C.; Laurent, A.-M.; Le Moullec, Y.; Momas, I. *Sci. Total Environ.* **2011**, *409*, 4480-4483.

(17) Marnett, L. J. In *Health effects of aldehydes and alcohols in mobile source emissions*; Health Effects Institute. National Academy: 1988.

(18) Hoshika, Y. *Anal. Chem.* **1982**, *54*, 2433-2437.

(19) Mosby, R. C. In *Proceedings of the seventieth annual convention* 1991.

(20) Kleopfer, R. *IN" TRACE SUBSTANCES IN ENVIRON. HEALTH-XIV".* **1980**, 390-398.

(21) Altshuller, A. P. *Atmos. Environ., Part A* **1993**, *27A*, 21-32.

(22) Back, K. C. *Journal of Occupational and Environmental Medicine* **1983**, *25*, 507.

(23) Yao, C.; Miller, G. C. In *Research study on bis (chloromethyl) ether, formation and detection in selected work environments*; Department of Health, Education, and Welfare. NIOSH: 1979.

(24) Khin, M. M.; Nair, A. S.; Babu, V. J.; Murugan, R.; Ramakrishna, S. *Energy Environ. Sci.* **2012**, *5*, 8075-8109.

(25) Lithoxoos, G. P.; Labropoulos, A.; Peristeras, L. D.; Kanellopoulos, N.; Samios, J.; Economou, I. G. *The Journal of Supercritical Fluids* **2010**, *55*, 510-523.

(26) Chen, W.; Duan, L.; Zhu, D. *Environ. Sci. Technol.* **2007**, *41*, 8295-8300.

(27) Di Paola, A.; Garcia-Lopez, E.; Marci, G.; Palmisano, L. *J. Hazard. Mater.* **2012**, *211-212*, 3-29.

(28) Kamat, P. V.; Meisel, D. *C. R. Chim.* **2003**, *6*, 999-1007.

(29) Shan, G.; Yan, S.; Tyagi, R. D.; Surampalli, R. Y.; Zhang, T. C. *Pract. Period. Hazard., Toxic, Radioact. Waste Manage.* **2009**, *13*, 110-119.

(30) Ren, X.; Chen, C.; Nagatsu, M.; Wang, X. *Chem. Eng. J. (Amsterdam, Neth.)* **2011**, *170*, 395-410.

(31) Nomura, A.; Jones, C. W. *ACS Appl. Mater. Interfaces* **2013**, *5*, 5569-5577.

(32) Nomura, A.; Jones, C. W. *Chem. - Eur. J.* **2014**, *20*, 6381-6390.

(33) Qi, G.; Wang, Y.; Estevez, L.; Duan, X.; Anako, N.; Park, A.-H. A.; Li, W.; Jones, C. W.; Giannelis, E. P. *Energy Environ. Sci.* **2011**, *4*, 444-452.

(34) Alkhabbaz, M. A.; Bollini, P.; Foo, G. S.; Sievers, C.; Jones, C. W. *J. Am. Chem. Soc.* **2014**, *136*, 13170-13173.

(35) Kuwahara, Y.; Kang, D.-Y.; Copeland, J. R.; Brunelli, N. A.; Didas, S. A.; Bollini, P.; Sievers, C.; Kamegawa, T.; Yamashita, H.; Jones, C. W. *J. Am. Chem. Soc.* **2012**, *134*, 10757-10760.

(36) Choi, S.; Drese, J. H.; Jones, C. W. *ChemSusChem* **2009**, *2*, 796-854.

(37) Hicks, J. C.; Drese, J. H.; Fauth, D. J.; Gray, M. L.; Qi, G.; Jones, C. W. *J. Am. Chem. Soc.* **2008**, *130*, 2902-2903.

(38) Choi, S.; Drese, J. H.; Eisenberger, P. M.; Jones, C. W. *Environ. Sci. Technol.* **2011**, *45*, 2420-2427.

(39) Bollini, P.; Choi, S.; Drese, J. H.; Jones, C. W. *Energy Fuels* **2011**, *25*, 2416-2425.

(40) Bergaya, F.; Theng, B.; Lagaly, G. *Handbook of clay science* **2006**, *1*, 10.

(41) Sposito, G.; Skipper, N. T.; Sutton, R.; Park, S.-h.; Soper, A. K.; Greathouse, J. A. *Proceedings of the National Academy of Sciences* **1999**, *96*, 3358-3364.

(42) Pires, J.; Pinto, M. In *Pillared Clays and Related Catalysts*; Springer: 2010, p 23-42.

(43) Molina-Sabio, M.; González, J.; Rodríguez-Reinoso, F. *Carbon* **2004**, *42*, 448-450.

(44) Tatarazako, N.; Ishibashi, H.; Teshima, K.; Kishi, K.; Arizono, K. *Environmental sciences: an international journal of environmental physiology and toxicology* **2003**, *11*, 133-140.

(45) Stepova, K. V.; Maquarrie, D. J.; Krip, I. M. *Applied Clay Science* **2009**, *42*, 625-628.

(46) Batista, L. C.; de S. Dantas, D.; de Farias, R. F. *Synthesis and Reactivity in Inorganic, Metal-Organic, and Nano-Metal Chemistry* **2014**, *44*, 1398-1400.

(47) Zhang, Q.; Yang, C.; Huang, W.; Dang, Z.; Shu, X. *Chemosphere* **2013**, *93*, 2180-2186.

(48) Nguyen-Thanh, D.; Block, K.; Bandosz, T. J. *Chemosphere* **2005**, *59*, 343-353.

(49) Dandy, A. *Journal of the Chemical Society A: Inorganic, Physical, Theoretical* **1971**, 2383-2387.

(50) Guégan, R.; Giovanela, M.; Warmont, F.; Motelica-Heino, M. *Journal of colloid and interface science* **2015**, *437*, 71-79.

(51) Rege, K.; Medintz, I. L. *Methods in Bioengineering: Nanoscale Bioengineering and Nanomedicine*; Artech House, 2009.

(52) Karabatsos, G. J.; Lande, S. S. *Tetrahedron* **1968**, *24*, 3907-3922.

CHAPTER SIX

CONCLUSION REMARKS

6.1 CONCLUSIONS

6.1.1 Methodology development using vanadium materials as catalysts

The rich chemistry of vanadium and its subsequent oxides results in numerous vanadium complexes for oxidative transformations.[1-3] Reasons for this lie in vanadium's ability to easily interconvert between its different oxidation states (*i.e.* +2, +3, +4, and +5) and easily access higher oxidation states with the +4 and +5 states being the most stable under aerobic conditions.[3,4] The metal center also has a high affinity for oxygen and behaves as a Lewis acid.[5] All of these factors contribute to vanadium complexes being used as catalysts in redox and Lewis acid mediated oxidation reactions.[4]

Vanadium complexes that form peroxovanadium species in the oxidation of organic compounds are a widely applicable catalytic system using environmentally conscious terminal oxidant sources such as H_2O_2 and O_2 to promote selective and often quantitative organic oxidations. Vanadium pentoxide has been a valuable contributor in both the early years of its catalytic utilization and still remains an area of interest for many organic chemists owing to vanadium's unique chemical properties; specifically its redox capabilities. By producing reactive peroxovanadium complexes, organic substrates can then be oxidized to a more reactive intermediate in linear synthesis for introducing

chemical complexity without concerns for using toxic chemicals or harsh reaction conditions.

Presented in this dissertation was a full account of our development of a novel method for the bromolactonization of alkenoic acids catalyzed by vanadium (V) oxide in the presence of a 3:3 ratio of UHP and NH_4Br.[6,7] The method hinges on the *in situ* oxidation of bromide to bromenium equivalent as inspired by previous studies on marine haloperoxidase catalyzed halide oxidation. The methodology presented herein allows for facile access to bromolactone products in acceptable purity without subjection to column chromatography. The role of urea in the transformation was probed, and results indicated that no competitive reactivity through Braddock-type intermediate.[8] Data indicates that other transition metal oxides, most notably oxides of molybdenum, can promote similar reactivity under our established protocol. Preliminary investigation of our reaction conditions in the α-bromination of β-diketones suggests that this bromination strategy could be more broadly applicable to other related reactions.

More recent generations of vanadium complexes include substitution with ligands that can influence the chemo-, regio-, and stereochemical outcome in product formation. Vanadium-substituted polyoxometalates (V-POMs) have been utilized as catalysts in organic oxidation reactions most extensively over the last thirty years. Their unique redox reactivity has prompted a large volume of reactions, a selection of which has been presented in this thesis. The high regio-,

stereo-, and diastereometric selectivity that V-POMs exhibit versus other POMs is one of the contributing factors for its extended use in catalytic oxidations.

Having shown our group's interest in vanadium catalysis through several cited investigations,[6,7,9] Dr. Hwu's highly functional, anionic polyoxovanadates (POVs)[10-12] posed a particular interest as possible catalysts for organic oxidations. A detailed investigation of the catalytic aptitude of reduced POV catalysts $Cs_{2.5}(V_5O_9)(AsO_4)_2$ (**III-1**), $Cs_5(V_{14}As_8O_{42}Cl)$ (**III-2**), and $Cs_{11}Na_3Cl_5(V_{15}O_{36}Cl)$ (**III-3**) for the oxidation of alcohols was conducted.[13] Catalysts **III-2** and **III-3** showed the greatest efficiency for product formation under the optimized conditions. Unlike other previously reported POM-mediated oxidation protocols, our method proceeds at room temperature using only 2 mol% of the catalyst to facilitate the oxidation of a range of secondary alcohols. The recyclability of these materials under optimized reaction conditions was successful for scaled reactions (*i.e.* 1.0 mmol starting alcohol) using both catalyst (**III-2**) and (**III-3**). Catalyst **III-2** does act as a more efficient catalyst by promoting quantitative conversion for a larger variety of secondary alcohols and in shorter reaction times as compared to catalyst **III-3**, which only allows for quantitative conversion of certain aryl activated alcohols. The reactivity of catalyst **III-3** is limited to the oxidation of secondary alcohols, and as with catalyst **III-2**, no activation for C-H or primary alcohol oxidation was observed. Conversely, catalyst **III-1** proved to be comparatively inactive as a catalyst for the oxidation of alcohols. Current efforts are focused on probing the mechanism of catalysis by r-

POVs as well as investigating other organic transformations of interest. Initial investigations into our proposed hypothesis of a pseudo-first order reaction are promising with all the rate profiles exhibiting a linear first order relationship. Continuing research that focuses on the reaction order for the catalyst is underway as well as kinetic isotopic labeling to probe the mechanism of oxidation; results of these efforts will be reported in due course.

6.1.2 Remediation of VOCs using PNPs, natural clay minerals and their amino-functionalized analogues

The need for environmentally safe reagents in promoting organic methodology is critical in reducing hazardous wastes and byproducts associated with industrial scale chemical processes. We have demonstrated two practical methods for obviating harsh oxidative and toxic brominating reagents. Similar efforts in reducing environmental contamination by our group includes applying polymeric nanoparticles and amino-functionalized clay minerals as adsorbents for sequestering hazardous VOCs.

Several types of nanomaterials and their applicability in remediating VOCs were discussed within this dissertation. Challenges preventing the global use of nanomaterials are formidable specifically with respect to their synthetic expense, limited scale-up procedures, potential toxicity, and the low off-targeting specificity. Nevertheless, the brief sampling of current nanotechnologies presented herein highlights continued effort towards understanding the

adsorption mechanisms for these materials and their application in remediating volatile organic contaminants found in our environment.

Through a collaborative effort between the Alexis and Whitehead groups, we were successful in the preparation, characterization, and evaluation of PDLLA-PEG-PEI NPs capable of selectively capturing environmental contaminants of broad concern bearing aldehyde and carboxylic acid functional groups in the gas phase.[14] Our material showed reduction of aldehyde and carboxylic acid vapors greater than 80% and 76%, respectively, with reductions of up to 98% in some cases. Further, we demonstrated that our NPs were capable of effecting the simultaneous capture of mixtures of aldehydes and carboxylic acids as well as mixtures of two different aldehydes. Additionally, our NPs were capable of selectively capturing target aldehyde and carboxylic acid contaminants even when challenged by comparably or more volatile non-targeted vapors. The significant advantage of our strategy over current methods arises from the ability to tailor the surface functionality of the nanomaterials for a specific target analyte from vapor mixtures. Future efforts will focus on the evaluation of further generations of these promising NPs for the remediation of other environmental contaminants of broad concern by taking advantage of the uniquely modular nature of our functional nanomaterials.

Additionally, the functionalization of kaolinite and montmorillonite clays with poly(ethyleneimine) shows initial success according to TGA and FTIR analysis. Once EA and EDX images are collected, we should be able to

determine the atomic distribution for the modified clays as compared to their natural precursors. The synthesized kaolinite-PEI has shown significant efficiency in capturing aldehydes, carboxylic acids and sulfides with several of these assays showing 100% reduction ($P < 0.0005$) of vapor. Currently, the same vapor assays are underway with the MMT and MMT-PEI clay minerals.

6.2 REFERENCES

(1) Haber, J. *ACS Symp. Ser.* **1985**, *279*, 3-21.

(2) Haber, J.; Witko, M.; Tokarz, R. *Appl. Catal., A* **1997**, *157*, 3-22.

(3) Haber, J. *Catal. Today* **2009**, *142*, 100-113.

(4) Sutradhar, M.; Martins, L. M. D. R. S.; Guedes da Silva, M. F. C.; Pombeiro, A. J. L. *Coord. Chem. Rev.* **2015**, *301-302*, 200-239.

(5) da Silva, J. A. L.; da Silva, J. J. R. F.; Pombeiro, A. J. L. *Coordination Chemistry Reviews* **2011**, *255*, 2232-2248.

(6) Campbell, M. L.; Rackley, S. A.; Giambalvo, L. N.; Whitehead, D. C. *Tetrahedron* **2015**, *71*, 4888.

(7) Campbell, M. L.; Rackley, S. A.; Giambalvo, L. N.; Whitehead, D. C. *Tetrahedron Lett.* **2014**, *55*, 5680-5682.

(8) Ahmad, S. M.; Braddock, D. C.; Cansell, G.; Hermitage, S. A. *Tetrahedron Lett.* **2007**, *48*, 915-918.

(9) Drew, E. T.; Yang, Y.; Russo, J. A.; Campbell, M. L.; Rackley, S. A.; Hudson, J.; Schmuki, P.; Whitehead, D. C. *Catal. Sci. Technol.* **2013**, *3*, 2610-2613.

(10) Queen, W. L.; West, J. P.; Hwu, S.-J.; Tran, T. T.; Halasyamani, P. S.; VanDerveer, D. *Chemical Communications* **2012**, *48*, 1665-1667.

(11) Queen, W. L.; West, J. P.; Hudson, J.; Hwu, S.-J. *Inorganic Chemistry* **2011**, *50*, 11064-11068.

(12) Queen, W. L.; Hwu, S.-J.; Reighard, S. *Inorganic Chemistry* **2010**, *49*, 1316-1318.

(13) Campbell, M. L.; Sulejmanovic, D.; Schiller, J. B.; Turner, E. M.; Hwu, S.-J.; Whitehead, D. C. *Catal. Sci. Technol.* **2016**, *6*, 3208-3213.

(14) Campbell, M. L.; Guerra, F. D.; Dhulekar, J.; Alexis, F.; Whitehead, D. C. *Chem. - Eur. J.* **2015**, *21*, 14834-14842.

APPENDIX A

JOHN WILEY AND SONS LICENSE TERMS AND CONDITIONS

Aug 26, 2016

This Agreement between MCKENZIE L CAMPBELL ("You") and John Wiley and Sons ("John Wiley and Sons") consists of your license details and the terms and conditions provided by John Wiley and Sons and Copyright Clearance Center.

License Number	3936780834918
License date	Aug 26, 2016
Licensed Content Publisher	John Wiley and Sons
Licensed Content Publication	Chemistry - A European Journal
Licensed Content Title	Target-Specific Capture of Environmentally Relevant Gaseous Aldehydes and Carboxylic Acids with Functional Nanoparticles
Licensed Content Author	McKenzie L. Campbell,Fernanda D. Guerra,Jhilmil Dhulekar,Frank Alexis,Daniel C. Whitehead
Licensed Content Date	Sep 1, 2015
Licensed Content Pages	9
Type of use	Dissertation/Thesis
Requestor type	Author of this Wiley article
Format	Print and electronic
Portion	Full article
Will you be translating?	No
Title of your thesis / dissertation	INVESTIGATING MATERIALS THAT PROMOTE NEW ORGANIC METHODOLOGY AND REMEDIATION OF VOLATILE ORGANIC COMPOUNDS
Expected completion date	Jan 2017
Expected size (number of pages)	300